ELES-1984

August 1984

EXPANDED LIQUID ENGINE SIMULATION COMPUTER PROGRAM

TECHNICAL INFORMATION MANUAL

Prepared By:

Charles E. Taylor

Aerojet TechSystems Company
P.O. Box 13222
Sacramento, California 95813

ACKNOWLEDGEMENTS

The mathematical models used in ELES-1984 are the result of many analysts committing their knowledge and experience to the task of producing simplified, preliminary-design algorithms. The following is a list of contributors:

Roger Anderson
Ed Barth (AFRPL)
Randy Bickford
Kirk Christensen
Don Culver
Jack Dever
Al Epes
Fred Fischietto
Keith Hamlyn (MMDA)
Ross Hewitt
John Hidahl
Bob Holman (SEA)
Jack Ito
Joe Jellison
Craig Judd
Tom Lee
Don Lemke
Bruce Lindley
Barbara Loch/Bicknell (MMDA)
Rich Matlock (AFRPL)
Gregg Meagher
Joe Mellish
Gary Nickerson (SEA)
Charles O'Brien
Dave Perkins (AFRPL)
Bob Schwantes
Adam Siebenhaar
Jim Smith
Charles Taylor
Vic Viteri
Dick Walker

TABLE OF CONTENTS

TABLE OF CONTENTS (cont.)

TABLE OF CONTENTS (cont.)

LIST OF FIGURES

LIST OF FIGURES (cont.)

LIST OF FIGURES (cont.)

LIST OF TABLES

1.0 INTRODUCTION

The ELES-1984 computer code is a landmark development in the preliminary systems analysis of liquid rocket vehicles. It is capable of revealing subsystem interactions and design choice impacts on total vehicle performance. Its use enables very rapid determinations of optimum vehicle designs.

The liquid propulsion system models in ELES have been developed by Aerojet TechSystems Company under the auspices of AFRPL during the past few years (1980-1984). The main purpose of ELES is to find optimum vehicle designs for specified mission requirements. Toward that end it is capable of evaluating the size, weight, and performance of system components over a range of design configurations, materials of construction, and operating points. These capabilities allow the code to act as an excellent propulsion system preliminary design training tool.

The objective of this manual is to explain the algorithms, physical models, and design choices implicit in the liquid propulsion models of the ELES-1984 computer code.

Use of the non-liquid portions of ELES (solid stage design, trajectory simulation, method of multipliers optimization, etc.) are documented by other sources available through AFRPL.

There are four manuals which describe the operation of the ELES-1984 Computer Program.

Taylor, C. E.
Expanded Liquid Engine Simulation Computer Program
New Users Guide, Aerojet TechSystems Company, 1984

Taylor, C. E.
Expanded Liquid Engine Simulation Computer Program
Technical Information Manual, Aerojet TechSystems Company, 1984

Taylor, C. E.
Expanded Liquid Engine Simulation Computer Program
Programmers Manual, Aerojet TechSystems Company, 1984

Taylor, C. E.
Expanded Liquid Engine Simulation Computer Program
Advanced Users Manual, Aerojet TechSystems Company, 1984

Introduction (cont.)

Both users guides are concerned with proper formulation and input of a problem statement. The new users guide does so in a more basic manner than the advanced users guide. The technical information manual describes the mathematical algorithms used in ELES to model the various propulsion subsystems. The programmers manual deals with the internal structure of the FORTRAN code, its file structure, and internal communication.

For more information regarding the ELES-1984 computer program contact

Charles E. Taylor
Aerojet TechSystems Company
P.O. Box 13222
Sacramento, CA 95813
(916) 355-2773

2.0 ENGINE PERFORMANCE

This section documents the engine performance routine chosen by Aerojet TechSystems to best fit the needs of this preliminary design tool. The procedure is predicated on the standard JANNAF method; it begins with one-dimensional equilibrium performance and derives efficiency multipliers for the various loss mechanisms. The methods used to derive individual loss multipliers are often specific to Aerojet. The philosophy used in choosing these methods was to achieve the best accuracy possible with a fast-running routine and, where possible, to minimize the quantity of required inputs and their level of detail. The procedures thus chosen were intended to represent the best compromise between accuracy and complexity.

The following list is an overview of the engine performance routine. It is followed by an in-depth description of each step in the procedure. The two lists are cross-indexed with circled integers in the lefthand margin.

PERFORMANCE ROUTINE - OVERVIEW

① Obtain Isp_{ODE} and C^*_{ODE} for thrust chamber core and barrier stream tubes.
② Get rough estimate of delivered Isp
③ Calculate propellant weight flows
④ Obtain propellant properties
⑤ Determine pressure drop across injector
⑥ Calculate injector characteristics
⑦ Calculate propellant vaporization constants
⑧ Calculate mean drop sizes
⑨ Calculate generalized vaporization length
⑩ Calculate vaporized mixture ratio
⑪ Calculate vaporization efficiency
⑫ Calculate mixing efficiency
⑬ Calculate mixture ratio maldistribution efficiency

⑭ Calculate boundary layer efficiency
⑮ Calculate divergence efficiency
⑯ Calculate kinetic efficiency
⑰ Calculate two-phase flow efficiency
⑱ Calculate nozzle efficiency
⑲ Calculate delivered Isp
⑳ Recalculate final flowrates and engine geometry

① The one dimensional equilibrium (ODE) Isp and C* are interpolated from tables. The tables were created from data generated by the ODE computer program for each of the library propellants. The range of data for each propellant conbination is listed below. Points outside the data range are obtained by extrapolation.

ODE DATA RANGE

	MR	Pc	Area Ratio
ClF_5/MHF-3	0-5.0	50-3000	2-200
MON-25/MHF-3	0-2.8	50-3000	2-200
N_2O_4/MMH	0-2.8	50-3000	2-200
MON-25/60%MHF-3 + 40% Al	0.1-2.0	50-3000	2-200
LOX/CH_4	0.6-4.5	20-5000	1-3000
LOX/LH_2	0.1-10.	20-5000	1-3000
LOX/RP-1	.22-10.	20-5000	1-3000
LF_2/LH_2	0.1-20.	40-5000	1-3000
LF_2/N_2H4	0.1-5.	40-5000	1-3000

② Estimate the delivered Isp as 92% of ODE.

③ Calculate weight flows based on the estimated Isp and thrust inputs. The MR used to get oxidizer and fuel flowrates is the Core MR.

④ The propellant properties are calculated by the method of corresponding states for the temperature and pressure of interest.

⑤ The entire pressure schedule is driven by the pressure requirement in the combustion chamber. The plenum pressure in the chamber (Pc) is the pressure used in performance calculations. The injector face pressure is higher than the plenum pressure due to the Rayleigh line loss. Because it is the injector face pressure which must be overcome by the injected propellant, it must be calculated and used to determine the injector pressure drop.

The face pressure (Pc_{face}) is calculated as

$$Pc_{face} = [1 + 0.25/\ \varepsilon_c^{1.8}]\ P_c$$

where: ε_c = contraction ratio

The injector inlet pressure (P_{inj}) is then

$$P_{inj} = Pc_{face}\ (1 + f_{chug})$$

where f_{chug} is the fraction of the face pressure across the injector required to eliminate engine chugging. The value of f_{chug} is nominally 0.25 however existing engines fall into the range of about 0.15 to 0.40. The injector pressure drop is then

$$\Delta P_{inj} = Pc_{face}\ f_{chug}$$

⑥ Calculate velocities and areas at injection orifices.

$V_{ox} = 24 g_c\ \Delta P_{ox\ inj}/\rho_{ox}$ = ox jet velocity

$V_{fuel} = 24 g_c\ \Delta P_{fuel\ inj}/\rho_{fuel}$ = fuel jet velocity

$A_{ox} = \omega_{ox}/(\rho_{ox}\ C_{D_{ox}}\ V_{ox})$ = area of ox orifices

$A_{fuel} = \omega_{fuel}/(\rho_{fuel}\ C_{D_{fuel}}\ V_{fuel})$ = area of fuel orifices

$D_{ox} = \sqrt{4\ A_{fuel}/\pi\ N_{ox}}$ = ox jet diameter

$D_{fuel} = \sqrt{4\ A_{fuel}/\pi\ N_{fuel}}$ = fuel jet diameter

where: N_{ox} = total number of ox orifices

N_{fuel} = total number of fuel orifices

$R_{mox} = 0.05\ D_{ox}$ = approx mean radius of ox droplet size

$R_{mfuel} = 0.05\ D_{fuel}$ = approx mean radius of fuel droplet size

⑦ C1 and C2 are constants used by Aerojet to calculate the vaporization characteristics of propellants. They are calculated as follows:

$$C1_{ox} = [(.0247\ \mu_{ox}\sigma_{ox}) / (4.12 \times 10^{-9}\ \rho ox)]^{0.25}$$

$$C1_{fuel} = [(.0247\mu_{fuel}\ \rho_{fuel}) / (4.12 \times 10^{-9}\ \rho_{fuel})]^{0.25}$$

$$C2_{ox} = (\Delta H_{v\ ox} / 140)^{0.8}\ (M_{ox} / 100)^{0.35}\ (1 - T_{r\ ox})^{0.4}$$

$$C2_{fuel} = (\Delta H_{v\ fuel} / 140)^{0.8}\ (M_{fuel} / 100)^{0.35}\ (1 - T_{r\ fuel})^{0.4}$$

where: μ = viscosity
σ = surface tension
ρ = density
ΔH_v = heat of vaporization
M = molecular weight
T_r = reduced temperature

These constants are calculated internally by the ELES code using the fluid properties routines for heat of vaporization, surface tension, viscosity and density.

⑧ Correct drop mean radius

The approximate mean drop radii calculated in step 6 are based simply on the orifice diameters. These estimates are improved by including information about the propellants (C1) and information about the injector element type in the equation

$$R_{m\ ox} = R_{m\ ox}\ C1_{ox}\ F_{ox}$$

$$R_{m\ fuel} = R_{m\ fuel}\ C1_{fuel}\ F_{fuel}$$

where: F_{ox} & F_{fuel} = drop size correction factors

Recommended values for F_{ox} and F_{fuel} (based on Aerojet experience) are as follows:

$F_{ox} = F_{fuel} =$	3.0	showerhead shear co-ax (zero cup recess)
	1.0	like-doublet splash plate X doublet V doublet Pre-atomized triplet
	0.5	Vortex Swirl co-ax
	0.33	unlike-triplets unlike-doublets

⑨ The generalized vaporization length is used by Aerojet to calculate the degree of propellant vaporization in a given chamber. It and its correlated relationship to percent vaporization are calculated as follows:

chamber shape factor: $S = [1 + (1/\sqrt{\varepsilon_c}) + (1/\varepsilon_c)]/3$

$$L_{gen\ ox} = \left(\frac{XLC}{\varepsilon_c^{0.44}} + \frac{0.83\ XLN}{\varepsilon_c^{0.22}\ S^{0.33}}\right) \left(\frac{P_c}{300}\right)^{0.66} / \left[C2_{ox} \left(\frac{R_{m\ ox}}{0.003}\right)^{1.45} \left(\frac{V_{ox}}{1200}\right)^{0.75}\right]$$

$$L_{gen\ fuel} = \left(\frac{XLC}{\varepsilon_c^{0.44}} + \frac{0.83\ XLN}{\varepsilon_c^{0.22}\ S^{0.33}}\right) \left(\frac{P_c}{300}\right)^{0.66} / \left[C2_{fuel} \left(\frac{R_{m\ fuel}}{0.003}\right)^{1.45} \left(\frac{V_{fuel}}{1200}\right)^{0.75}\right]$$

where:
- XLC = cylindrical chamber length
- XLN = convergent chamber length
- ε_c = contracting ratio
- S = shape factor
- R_m = mean drop radius
- P_c = chamber pressure
- V = injection velocity
- C_2 = propellant constant

The fraction of each propellant which is vaporized is a function of L_{gen} (f) defined as:

$$f = 1.0 \left(\frac{421.8}{L_{gen} + 428.5}\right)^{45.68} \quad \text{for: } L_{gen} > 10$$

$$f = 0.25475 \ln (L_{gen}) + 0.2434 \quad \text{for: } 1 \leq L_{gen} \leq 10$$

$$f = 0.2434\ L_{gen} \quad \text{for: } L_{gen} < 1$$

⑩ Calculate performance based on vaporized MR

$$MR_{vap} = \left(\frac{\text{fraction ox vaporized}}{\text{fraction fuel vaporized}}\right) \times MR_{core}$$

Call Isp_{ODE} routine with vaporized MR = $Isp_{ODE\ vap}$

Call C^*_{ODE} routine with vaporized MR = $C^*_{ODE\ vap}$

⑪ The vaporization efficiency (η_{EREvap}) is calculated as a weighted average of the Isp at vaporized conditions vs. injected conditions.

$$\eta_{ERE\ vap} = Isp\ ODE\ vap\ (f_{ox}\ \omega_{ox} + f_{fuel}\ \omega_{fuel})/$$

$$(\omega_{total}\ Isp_{ODE\ 100\%\ vaporized})$$

$$\eta_{C^*\ vap} = C^*_{ODE\ vap} \times (f_{ox}\ \omega_{ox} + f_{fuel}\ \omega_{fuel})/(\omega_{total}\ C^*_{ODE\ 100\%\ vap})$$

where: f_{ox} and f_{fuel} = fraction of vaporized ox and fuel

⑫ Begin the mixing loss calculation

Approximate the throat diameter and chamber diameter

$$D_{t1} = \sqrt{\frac{4 \times_{n\ C^*vap} \times C^*_{ODE\ 100\%\ vap} \times \omega_{total}}{\pi\ g_c\ P_c}}$$

$$D_{c1} = D_{t1}\sqrt{\varepsilon_c}$$

average element diameter (D_{ave}) = $D_{c1}\sqrt{\frac{\pi}{4\ Nelem}}$

average orifice diameter ($D_{orifice}$) = $(D_{ox} + D_{fuel})/2$

The mixing loss is now calculated a fraction of the distance between orifices in adjacent elements and the chamber length.

$$\text{Mixing angle } \beta_{mix} = \tan^{-1}\left[(Dave - Dorifice)/(XLC + XLN)\right]$$

$$\eta_{ERE\ MIX} = 1.0 - 0.01\ (57.3 * \beta_{mix}/2)^2$$

Note that β_{mix} is normally about .0125 radians (2 to 2.5 degrees) for most design purposes. This approach to mixing loss is an Aerojet preliminary design estimate.

⑬ Barrier Cooling Loss

The simplified barrier cooling loss routine chosen by Aerojet is a stream tube analysis which flow-averages the performance of the core stream tube with that of the barrier stream tube. The mixture ratio (MR) of each stream tube is chosen by the user. The core MR is chosen for performance and the barrier MR for cooling compatibility. The procedure for calculating stream tube flow areas, flow rates, and the overall barrier cooling loss is as follows:

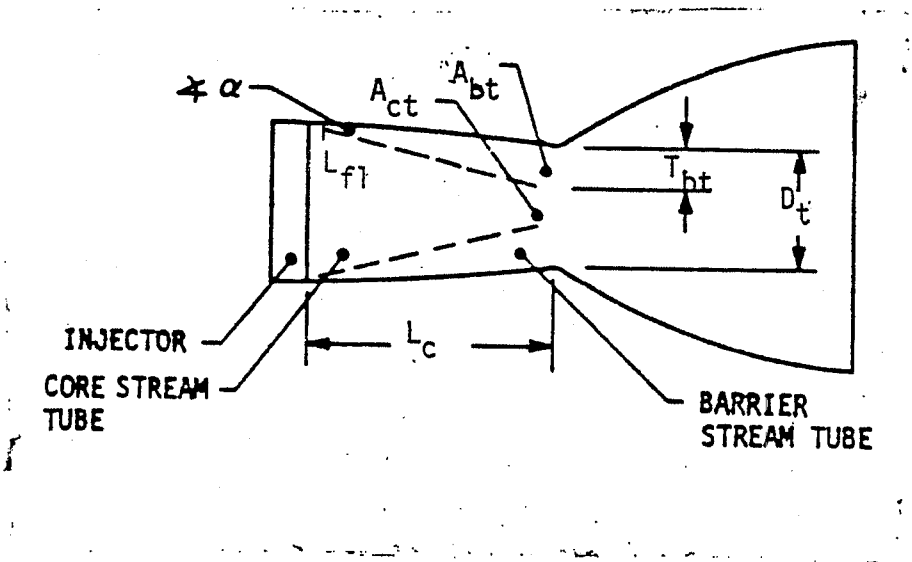

Chamber length = XLC + XLN = L_c

Input a mixing angle α , and liquid film length L_{FL}

Barrier thickness at throat (t_{bt}) = $\alpha\ (L_C - L_{FL})$

To generate a better estimate of the throat size, start with an estimate of the mass flux through the core and barrier stream tubes

$$\text{barrier mass flux at throat } (f_{bt}) = \frac{P_c g_c}{C^*_{\substack{\text{barrier} \\ \text{ODE}}}\ \eta_{\text{barrier}}} = \frac{\omega_{\text{barrier}}}{A_{bt}}$$

$$\text{Core mass flux at throat } (f_{ct}) = \frac{P_c\ g_c}{C^*_{\text{core}}\ \eta_{\text{mix}}\ \eta_{C^*\text{vap}}}$$

The throat diameter (D_t) can be expressed as

$$D_t = 2\sqrt{[f_{bt}t_{bt}^{\ 2}\ (\frac{f_{bt}}{f_{ct}} - 1) + \frac{\omega}{\pi}]/f_{ct}} \quad - 2\ (\frac{f_{bt}}{f_{ct}} - 1)\ t\ bt$$

which is a function of the barrier flux (f_b), the core flux (f_c), the barrier thickness at the throat (t_{bt}), and the estimated propellant flowrate (ω).

The above equation is derived from the equations

$$\omega = f_{bt}A_{bt} + f_{ct}A_{ct}$$

which defines total flow rate as the sum of barrier flux times barrier area and core flux times core area

$$A_t = A_{bt} + A_{ct} = \pi\ D_t^{\ 2}/4$$

which defines throat area as the sum of core and barrier throat areas. The standard equation for the area of a circle is also used

$$A_{bt} = \pi \; t_{bt} \; (D_t - t_{bt})$$

defines the barrier area at the throat as the area of the ring around the inside of the throat which is t_{bt} thick.

Combining the above equations yields

$$\frac{\pi}{4} D_t^2 + \left(\frac{f_{bt}}{f_{ct}} - 1\right) \pi \; t_{bt} \; D_t - \left[\left(\frac{f_{bt}}{f_{ct}} - 1\right) \pi \; t_{bt}^2 + \frac{\omega}{f_{ct}}\right] = 0$$

Solving for D_t using the quadratic formula and simplifying yields the solution for D_t already shown. Once D_t is known, the same equations may be used to calculate the various areas at the throat (A_t, A_{bt}, A_{ct}).

Weight flows are calculated from the known mixture ratios, mass fluxes, and flow areas

ω barrier $= f_{bt} \; A_{bt}$

ω tot core $= \omega$ total $- \omega$ barrier

ω fuel core $= \omega$ tot core$/(1 + MR_{core})$

ω ox core $= MR_{core} \times \omega$ fuel core

ω fuel barrier $= \omega$ tot barrier$/(1 + MR_{barrier})$

ω ox barrier $= MR_{barrier} \times \omega$ fuel barrier

The fraction of fuel used for film cooling (FFFC) is calculated as the difference of the total fuel in the barrier and the fuel which migrated into the barrier from the core divided by the total fuel flowrate.

$$FFFC = \frac{(\omega_{\text{fuel barrier}} - \omega_{\text{ox barrier}} / MR_{\text{core}})}{(\omega_{\text{fuel core}} + \omega_{\text{fuel barrier}})}$$

The overall mixture ratio is the total oxidizer flowrate divided by the total fuel flowrate.

$$MR_{TCA} = (\omega_{\text{ox core}} + \omega_{\text{ox barrier}}) / (\omega_{\text{fuel core}} + \omega_{\text{fuel barrier}})$$

The predicted characteristic velocity (c*) is a weight averaged value, which includes the previously calculated mixing and vaporization losses.

Predicted c* =

$$(c^*_{\text{core ODE}}\ \omega_{\text{core}}\ \eta_{\text{mix}}\ \eta_{\text{vap}} + c^*_{\text{barrier ODE}}\ \omega_{\text{barrier}}\ \eta_{\text{barrier}}) / \omega_{\text{total}}$$

The barrier loss (η_{barrier}) in the above equation is calculated as

$$\eta_{\text{barrier}} = 0.95\ \eta_{\text{mix}}\ \eta_{\text{vap}}$$

The mixture ratio maldistribution loss (η_{MRD}) is calculated as the weighted average of the core and barrier performances.

$$\eta_{MRD} = \frac{(Isp_{\text{core ODE}}\ \omega_{\text{core}}\ \eta_{\text{vap}}\ \eta_{\text{mix}} + Isp_{\text{barrier ODE}}\ \omega_{\text{barrier}}\ \eta_{\text{barrier}})}{Isp_{\text{core ODE}}\ \omega_{\text{total}}\ \eta_{\text{vap}}\ \eta_{\text{mix}}}$$

(14) Boundary Layer Loss (η_{bl})

The following boundary layer loss correlation is a result of Aerojet experience in defining this loss. It is calculated with the following equation.

$$\eta_{bl} = .997 - (\ln(\varepsilon)/100) \times [1 - 0.065 \ln(0.01\ P_c\ F_{vac}) + .001 (\ln(0.01\ P_c\ F_{vac}))^2\ ]$$

Although area ratio is normally the most influential variable in the above equation, it should be noted that P_c and F_{vac} can also change delivered Isp by a second or more, due to η_{bl} alone.

⑮ Divergence loss (η_{div})

The equations which describe divergence loss were derived as curve-fits from the information presented in Appendix A of the CPIA document No. 178, "ICRPG Liquid Propellant Thrust Chamber Performance Evaluation Manual," by J. L. Pieper, September 1968. These curve-fits are as follows:

For conical nozzle:

$$\eta_{div} = 0.5 + \frac{\cos \alpha}{2}$$ where α = half angle, degrees

For RAO Nozzle:

$$\eta_{div} = 1 - (1-C)[(1.75 - RATMLR)/0.75]^{1.7}$$

for: RATMLR $\leq$ 1.75

or

$$\eta_{div} = 1.0$$

for: RATMLR > 1.75

where: C = Const = $0.945 + 0.01 \ln(\varepsilon)$ for: $\varepsilon \leq 20$

= $0.958 + 0.00566 \ln(\varepsilon)$ for: $\varepsilon > 20$

RATMLR = ratio of nozzle length to the length of a minimum length RAO nozzle

⑯ Kinetic Loss Routine (η_{KL})

Because of the development history of ELES-1984, there are two different approaches to determining kinetic loss. The first method is to apply an Aerojet correlation for kinetic loss, the second is to run the computer

program ODK (one-dimensional kinetics) for a matrix of operating points and tabulate the results for interpolation.

The first four storable propellants use the first method, the remainder of the propellants use the tabulated approach.

The nozzle kinetic efficiency has been correlated by Aerojet based on the major chemical species present in the combustion gas. To use these correlations, the chamber pressure is input in units of psia, thrust is input in units of lbf. The mixture ratio is a weight flowrate ratio of oxidizer to fuel. All logarithms refer to natural logs. The recommended correlation agrees with the ODK data within ± 0.5% Isp.

Simplified expressions to estimate nozzle kinetic efficienties η_{KL} for the following propellant combinations

(1) N_2O_4/MMF (IPROP = 1)
(2) MON-25/MHF-3 (IPROP = 2)
(3) ClF_5/MHF-3 (IPROP = 3)
(4) MON-25/.60 MHF-3 + .40 Al (IPROP = 4)

are as follows:

$$\eta_{KL}^{(1)} = 1.0 - [.187 + .0016\ (\ln P_c)^2 - .03\ \text{Ln}\ P_c - .0041\ \text{Ln}F_{vac}] \times \frac{[9.5\ MR_{core})^{-2}\ (R_{core})^2 - 8.9\ ]}{2.1} \times \frac{[.08 + .50\ \text{Ln}\varepsilon - .007\ (\text{Ln}\varepsilon)^3]}{1.7}$$

$$\eta_{KL}(3) = 1.0 - [.256 - .066\ \text{Ln}\ P_c + .0043\ (\text{Ln}\ P_c)^2] \times \left[\frac{100 \times Pc}{F_{vac}}\right]$$

$$(.04 + .035 \text{Ln}\ (.1 \times P_c)) \times [.045 + .255\ \text{Ln}\ \varepsilon\ - .0023\ (\text{Ln}\ \varepsilon\ )^3]$$

$$\times \frac{[2.6-5.5\ (MR_{core}-2.8)^2 - 3.8\ (MR_{core}-2.8)^3]}{1.44}$$

$$\eta_{KL}(4) = 1.0 - [.0212 - .013\ \text{Ln}\ (P_c/200) + .0022\ [\text{LN}\ (\frac{P_c}{200})]^2$$

$$\times [\frac{25 \times Pc}{F_{vac}}]^{(.095-.036\ \text{Ln}(Pc/50)}$$

$$\times [1. + 2\ (MR_{core} - 1.2)^2] \times [.187\ \text{Ln}\varepsilon + .0065\ \text{Ln}\varepsilon)^2]$$

CHECK: If $\eta_{KL}\ (i) \geq 1.00$, Set $\eta_{KL} = 1.0$

The ODK (One-Dimensional Kinetics) computer program was run for the following propellant combinations

(5) LO_2 / LH_2
(6) LO_2 / RP-1
(7) LO_2 / CH_4
(8) LF_2 / LH_2
(9) LF_2 / N_2H_4

To minimize the amount of computer runs and data storage requirements, the ODK specific impulse was evaluated at a reference throat radius, and a correlation was developed to account for the effect of engine size on the ODK specific impulse. The correlation relates the change in kinetic loss to the change in throat radius:

$$\frac{\Delta KL}{\Delta R_t} = \frac{KL_{R_{t_1}} - KL_{R_{T_{Ref}}}}{R_{t_1} - R_{t_{Ref}}}$$

The ratio of the difference in kinetic loss to the difference in throat radius was correlated for each of the new propellant combinations. A typical correlation is illustrated in Figure 2.0.1 for LF_2/N_2N_4. In all cases, a logarithmic correlation curve fit was generated and the appropriate coefficients supplied for each of the new propellant combinations. The ODK specific impulse for a specified throat radius is calculated by the equation

$$\text{ODK Isp}_{R_t} = \text{ODK Isp}_{R_{t_{Ref}}} - [(R_t - R_{t_{Ref}}) (A + b \ln KL_{R_{T_{Ref}}})]$$

Characteristic velocity and combustion temperature data were compiled from the ODE output. Therefore, the same ODE chamber pressure and mixture ratio arrays used to tabulate specific impulse are also used for the C* and Tc data.

(17) Two-Phase Flow Loss Correlation

The two-phase flow efficiency model is that developed by N. Cohen and used as a simplified procedure in the Solid Performance Program, SPP (Ref. 1). The particle size, D_p, is calculated using a correlation developed by R. Hermsen (Ref. 2).

The form of the correlations and the values of the constants used in the correlation were obtained by fitting solutions obtained from detailed parametric calculations of two-phase flow through rocket nozzles.

Ref. 1. Coats, D.E., et al, "A Computer Program for the Prediction of Solid Propellant Rocket Motor Performance," Vol. I, AFRPL-TR-75-36 Ultrasystems, Inc., July 1975.

Ref. 2. Nickerson, G.R., et al, "A Computer Program for the Prediction of Solid Propellant Rocket Motor Performance, "Vol. I, AFRPL-TR-79-to be issued, SEA, Inc., May 1980.

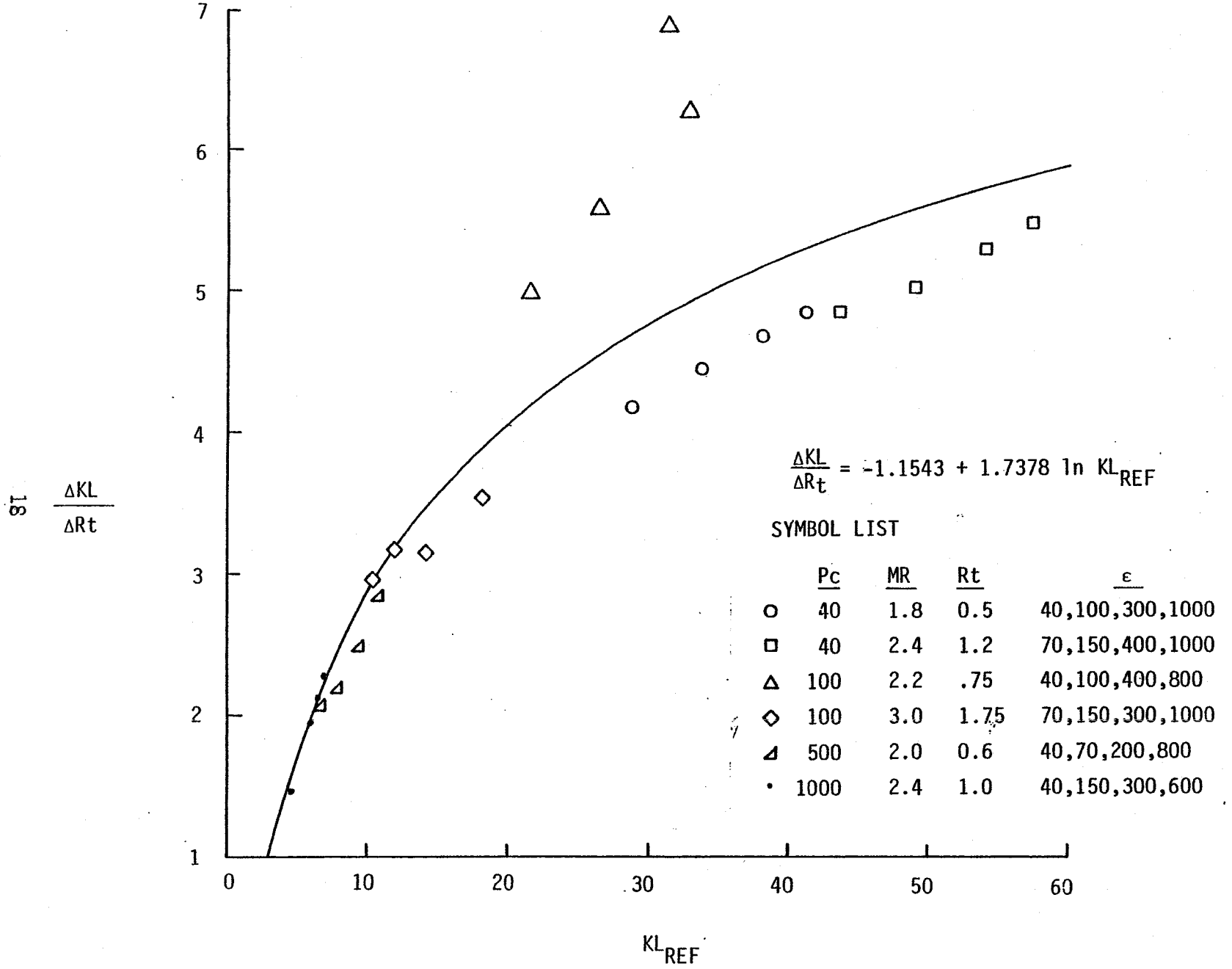

Figure 2.0.1. Throat Radius Correction Correlation for LF_2/N_2H_4

The two-phase flow efficiency is given by:

$$\eta_{TP} = \frac{C_3 \xi^{C_4} D_p^{C_5}}{P_C^{.15} \varepsilon^{.08} D_t^{C_6}}$$

where

ξ = concentration of condensed phase, g-mole/100 gm
D_p = particle size, microns
P_C = chamber pressure, psi
ε = expansion ratio
D_t = throat diameter, in.

If $\varepsilon \geq 0.09$,	C_4	= 0.5
$D_t < 1$:	C_3	= 9.0, C_5 = 1.0, C_6 = 1.0
$1 \leq D_t \leq 2$	C_3	= 9.0, C_5 = 1.0, C_6 = 0.8
$D_t \geq 2$: and $D_p < 4$:	C_3	= 13.4, C_5 = 0.8, C_6 = 0.8
$4 \leq D_p \leq 8$:	C_3	= 10.2, C_5 = 0.8, C_6 = 0.8
$D_p > 8$:	C_3	= 7.58, C_5 = 0.8, C_6 = 0.33
If $\xi < 0.09$,	C_4	= 1.0
$D_t < 1$:	C_3	= 80.0, C_5 = 1.0, C_6 = 1.0
$1 \leq D_t \leq 2$:	C_3	= 30.0, C_5 = 1.0, C_6 = 0.8
$D_t > 2$ and $D_p < 4$:	C_3	= 44.6, C_5 = 0.8, C_6 = 0.8
$4 \leq D_p \leq 8$	C_3	= 34.0, C_5 = 0.8, C_6 = 0.4
$D_p > 8$:	C_3	= 25.2, C_5 = 0.8, C_6 = 0.33

and

$$D_p = 3.6304\, D_t^{0.2932} \left(1 - e^{-0.0008163 \xi_c P_c \tau}\right)$$

where:

D_p = mass-weighted average diameter, microns
D_t = nozzle throat diameter, in.
ξ_c = Al_2O_3 concentration in chamber, g-mole/100g
P_c = chamber pressure, psia
τ = average chamber residence time, msec

The correlation is based on results obtained from the TD2P module of the SPP. Thus, results obtained from the correlation are in general agreement with results obtained from TD2P after an adjustment is made for divergence loss. The fraction of the condensed phase, ξ , expressed in gm-atoms/100 gm is nearly the same as the mass fraction of alumina, since

$$\xi = \frac{100}{M_w} c \quad \text{gm-atoms/100 gm}$$

where:

M_w = the molecular wt of alumina = 102

c = the mass fraction of alumina present in chemical equilibrium

Values of c for 6 very different SRM's and for the "bulls eye" MON-25/alumizine case are presented in Table 2.0.1. It can be seen that the alumina mass fraction for the alumizine propellant is similar to that occurring in SRM's. Thus, the particle size correlation should be applicable to metalized liquid propellants (MLP's) provided the mixture ratio is not too low.

A parametric study was carried out on the MON-25/Alumizine system using the ODE computer program. Results obtained for condensed phase are summarized in Table 2.0.2. It is found that at mixture ratios lower than .6, the solid phase species A ℓ N(S) is formed in large concentrations. For example, at a mixture ratio of .1, 60% of the mass is contained in this species. This is because the very limited amount of oxygen available will form CO before forming $A\ell_2O_3$. Thus, if the vapor phase mixture ratio is less than .6, the range of the η_{TP} correlation is exceeded.

The particle size correlation that gives the value of D_p used in the η_{TP} correlation is not applicable to alumizine propellants. The combustion process in a SRM differs significantly from that occurring in an engine operating with an MLP. Thus, it is not possible to assume that a particle size correlation based on particle size data obtained from SRM firings can be used for MLP systems.

TABLE 2.0.1

ALUMINA MASS FRACTIONS FOR THE "BULLS EYE" CASE AND FOR SIX SOLID ROCKET MOTORS

Motor	Chamber	Throat	Solidification Point		Solidification Area Ratio
Bulls Eye" Case MON-25/Alumizine MR=1.2	.3233	.3307	.3435	at	17.
Extended Delta	.2842	.2910	.3020	at	3.85
Titan IIIC Stage 0	.2886	.2950	.3040	at	3.24
C4 STage 3 (SDP)	.3132	.3219	.3398	at	5.28
IUS Large Motor	.3131	.3217	.3382	at	4.33
AIM	.3252	.3343	.3639	at	6.93
MM II Stage 2 Wing 6	.3019	.3076	.3182	at	5.86

TABLE 2.0.2

MON-25/ALUMIZINE, P_C = 500 : SUMMARY OF CONDENSIBLES

O/F	Chamber Mole Frac. $A\ell_2O_3(l)$	Chamber Mole Frac. A&N(S)	Chamber Mass Frac. Total Condensibles	T_c°R
.1	0	.2103	.6020	4542
.4	.0181	.1190	.3677	4944
.6	.0451	.0199	.2525	5084
.8	.0742	0	.3526	6224
1.0	.0782	0	.3515	6655
1.2	.0755	0	.3233	6836
1.6	.0691	0	.2753	6932
2.0	.0635	0	.2409	6852

There is not much data on particle size for MLP systems. A literature survey for particle size measurements conducted for the SPP contract listed one Aerojet source (Ref. 3). In this reference particle size measurements are given that were obtained from 13 engine firings. These results are for motors operating at approximately 2K lbs. thrust. Chamber pressure varied from 500 psia to 1500 psia, the initial throat diameter varied from 1.024" to 1.874", and the mixture ratio varied from .417 to .766. The propellant was N_2O_4/-Alumizine in which the aluminum content was varied. Measured mass median particle sizes were

$$1.08 \leq D_p \leq 2.51$$

The Hermsen particle size correlation has been used to calculate D_p for these 13 motors. In general, the correlation predicts a smaller size than measured. The error exceeds 50% in some cases. The particle size correlation of N. Cohen which is used in Ref. 1 predicts particle sizes that are low by approximately a factor of 3. The data itself is open to question since on Page 72, Ref. 3 states "significant error may be present in these reported particle sizes". The correct particle size to be used for MLP systems can only be roughly estimated at this time.

⑱ The overall nozzle efficiency (PCTCF) is calculated as the product of the divergence, kinetic, boundary layer, and two-phase flow efficiencies.

$$PCTCF = \eta_{div}\ \eta_{KL}\ \eta_{bl}\ \eta_{TPF}$$

⑲ Similarly, the delivered Isp is calculated as the product of the one-dimensional equilibrium Isp and all of the efficiency multipliers.

Ref 3. Aerojet General Corporation, Final Report, Contract AF04(611) 11205, AFRPL-TR-66-231, September 1966.

$$\text{Isp predicted} = \text{Isp}_{\text{ODE core}}\ \eta_{MRD}\ \eta_{vap}\ \eta_{mix}\ \eta_{div}\ \eta_{KL}\ \eta_{bl}\ \eta_{TPF}$$

(20) The final step in the engine performance routine is to recalculate flowrates and geometry based on the final performance results.

$$\omega_{total} = F_{vac}/\text{Isp predicted}$$

$$\omega_{fuel} = \omega_{total}/(1 + MR_{TCA})$$

$$\omega_{ox} = MR_{TCA}\ \omega_{fuel}$$

$$c^*_{delivered} = \text{predicted c* from step 13.}$$

$$D_{throat} = \sqrt{\frac{4\ c^*_{delivered}\ \omega_{total}}{P_c\ \pi\ g_c}}$$

$$D_{chamber} = D_{throat}\ \sqrt{\varepsilon_c}$$

$$D_{exit} = D_{throat}\ \sqrt{\varepsilon}$$

2.1 NON-LIBRARY PROPELLANTS PERFORMANCE

For propellant combinations which are not in the propellant library, the preceding Isp calculations can still apply if the equivalence ratio procedure is employed to obtain ideal Isp_{ODE} and C^*_{ODE}. The equivalence ratio (ER) method is outlined below.

a) For the propellants of interest, run the one dimensional equilibrium (ODE) computer program at Pc = 500, Area Ratio = 20, over a range of mixture ratios.

b) Locate the mixture ratio (MR) at which maximum Isp occurs and convert MR to ER. (ER is listed on ODE and the product of ER and MR is a constant so that ER = MR/C).

c) Use the peak Isp vs ER point of the new propellant to scale from the peak Isp vs ER of a library propellant with a similar chemical composition (see figure below).

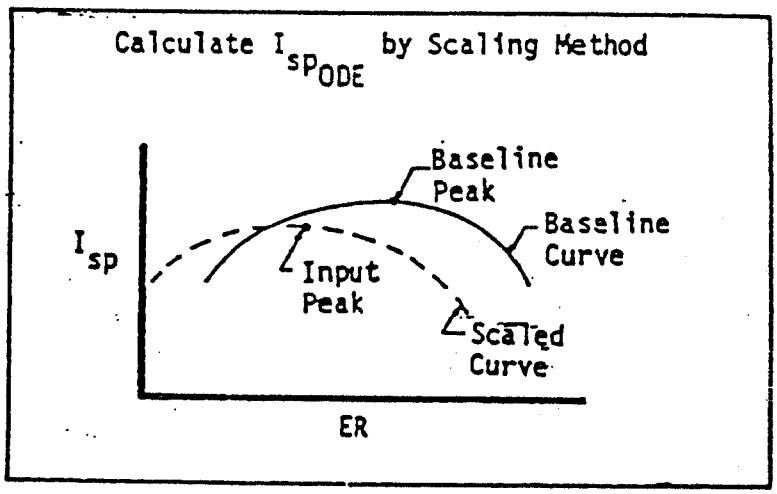

Using this method allows the ELES optimizer or the user to change any parameters which effect the calculated Isp, while still obtaining a good performance estimate. The enhancement facilitates the investigation of new propellant combinations.

3.0 ENGINE COOLING

3.1 TCA COOLING

There are four basic TCA cooling options in ELES: 1) ablative, 2) regenerative, 3) trans-regen, 4) radiation. The ablative model is concerned with providing a sufficient thickness of ablative material in the chamber to withstand the chamber temperature for the burn time of the engine. The regenerative model is concerned with determining the pressure drop across the regen jacket. That pressure dictates the coolant velocities and therefore heat transfer coefficients available to accept heat flux through the chamber wall. The trans-regen model is like the regenerative model with the added responsibility of determining the transpiration flowrate required to cool designated portions of the chamber. The radiation model calculates the maximum combustion gas barrier temperature which allows the chamber material operating temperature to be maintained by radiation to the ambient environment.

3.1.1 Ablative Cooling

The ablative cooling model calculates ablative thickness by three different equations depending on the location within the chamber. The equations assume the ablative material to be operating at its nominal temperature (silica phenolic operates up to 3900°R) and the required thickness is calculated as a function of chamber pressure and burn time. The form of the equation for the ablative thickness at the throat and in the chamber is:

$$t = cP_c^{\,a}\, t_b^{\,b}$$

where: t = ablative thickness (in)
a, b, c = empirical constants
P_c = chamber pressure (psia)
t_b = burn time (sec)

Ordinarily the value of the empirical constant c is calculated within ELES from the actual ablative thicknesses of a baseline engine. At the throat the values of a and b are 0.2 and 0.77 respectively. In the combustion chamber a and b are 0.4 and 0.5. The ablative thickness is more sensitive to chamber pressure in the chamber itself and more sensitive to burn time at the throat.

Ablative thickness downstream of the throat is relatively insensitive to chamber pressure. It is calculated as:

$$t = ct_b^{0.5}\ EXP(-0.0247\varepsilon)$$

where: t = ablative thickness (in)
c = empirical constant
t_b = burn time (sec)
EXP( ) = irrational number e raised to the power of the expression in parentheses
ε = area ratio

3.1.2 Regenerative Cooling (See Nomenclature List, Pgs. 34 & 35)

The purpose of the regenerative cooling model is to predict the pressure drop and bulk temperature rise of a regeneratively cooled thrust chamber. The routine uses a simplified model of a thrust chamber made up of three sections (cylindrical, convergent, and nozzle). Each section can be divided into any number of segments although more than five (5) segments per section appears to have little effect on the accuracy of the result.

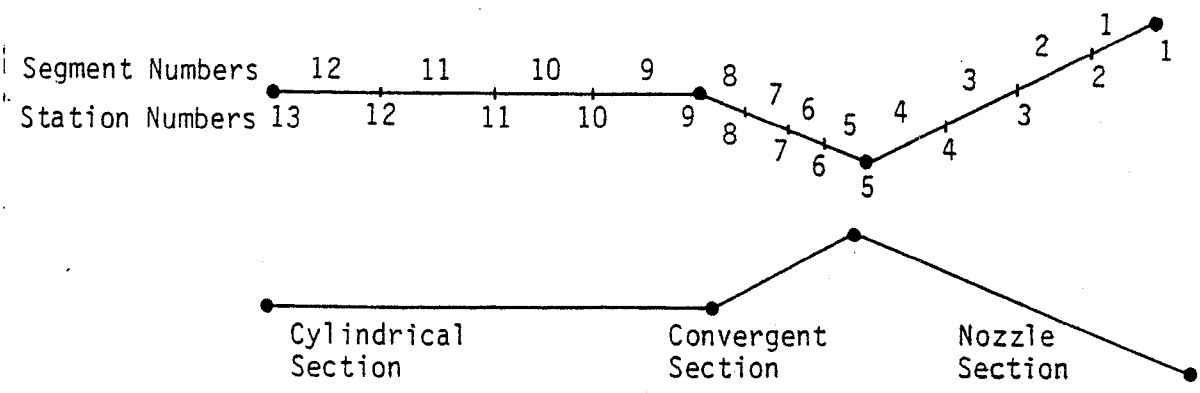

The point of intersection (called a station) between two segments is represented as a series thermal resistance circuit between the combustion gas and the coolant. The maximum gas wall temperature is specified by the material of construction. This wall temperature (along with gas temperature and heat transfer coefficient) allows the heat flux to be calculated and ultimately the coolant heat transfer coefficient required to cool the chamber. (See Nomenclature at the end of this section)

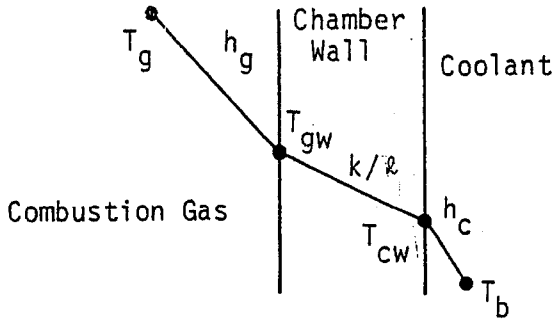

$$q = h_g(T_g - T_{gw}) = (k/\ell)\ (T_{gw} - T_{cw}) = h_c(T_{cw} - T_b)$$

The number of cooling channels is calculated from the known land and channel widths at the throat. ELES assumes that the land width is constant throughout the chamber. Channel widths are calculated from the geometry assuming a constant number of coolant channels. The height of the channels is calculated at the intersection of each segment based on the velocity required to give the needed heat transfer coefficient at those points.

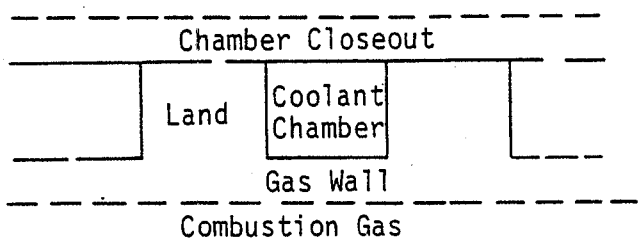

ELES assumes a counter current heat exchanger with coolant entering a manifold on the nozzle and flowing towards the injector. Since the chamber pressure is specified, the regen jacket outlet pressure can be determined by

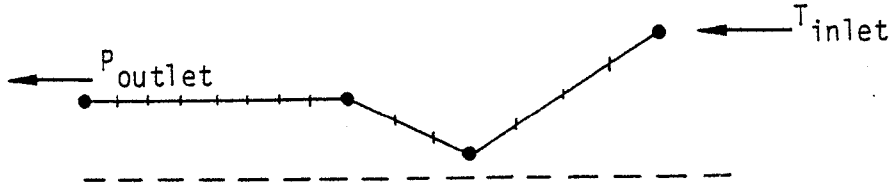

knowing the injector inlet pressure required to obtain that chamber pressure. The coolant inlet temperature can be determined from the propellant operating temperature range.

Because it is required to know both temperature and pressure of the coolant at either the inlet or the outlet in order to step through the calculation, and because the coolant temperature can be easily estimated at the outlet from the preliminary estimate of the heat flux at each station; the regen model begins at the outlet with desired pressure and estimated temperature and steps towards the inlet calculating the pressure drop and temperature rise occurring across each segment. If the gas wall temperature is held exactly to the maximum allowable all along the chamber then the initial estimate of coolant temperature rise should be very good and the answer is obtained immediately. However, if the gas wall is overcooled at any location due to nucleate boiling or high coolant velocities, then the overall heat flux will be higher than the initial guess and an iteration through the stepwise jacket calculation will be required using a new, better estimate of coolant outlet temperature.

The stepwise calculation itself is as follows: Begin at the outlet station with temperature and pressure of the coolant. Using the maximum allowable gas wall temperature, combustion gas temperature, and gas side heat transfer coefficient calculate the heat flux at that station.

$$q = h_g(T_g - T_{gw})$$

Use this heat flux to calculate the coolant side wall temperature

$$q = (k/\ell)\ (T_{gw} - T_{cw})$$

Use this coolant wall temperature to calculate the coolant heat transfer coefficient required

$$q = h_c (T_{cw} - T_b)$$

To use this required heat transfer coefficient in calculating a coolant velocity, the coolant properties (density, viscosity, thermal conductivity, heat capacity) must be determined. The coolant temperature and pressure are the input to the properties routines which provide the properties information. It is now possible to determine the required coolant velocity from the equation

$$Nu = K\ Re^a\ Pr^b$$

where K, a, and b are taken from the Dittus Boelter, McAdams, Hines correlations, or an empirical equation depending on the coolant in question. Given a velocity, the channel height which provides that velocity (and therefore sufficient cooling) can be calculated. This calculated channel geometry is then converted into a hydraulic diameter to provide pressure drop across the segment by

$$\Delta P_{seg} = \left(\frac{4f\ L_{seg}}{D_h}\right)\left(\frac{\nu^2 \rho}{2\ g_c}\right)$$

The actual temperature rise can also be determined by

$$\Delta T_{seg} = \frac{q_{seg} A_{seg}}{C_p\ \omega}$$

When continued, the procedure generates a channel geometry which can look similar to the one below. Total ΔP and ΔT are obtained by summing those of each segment.

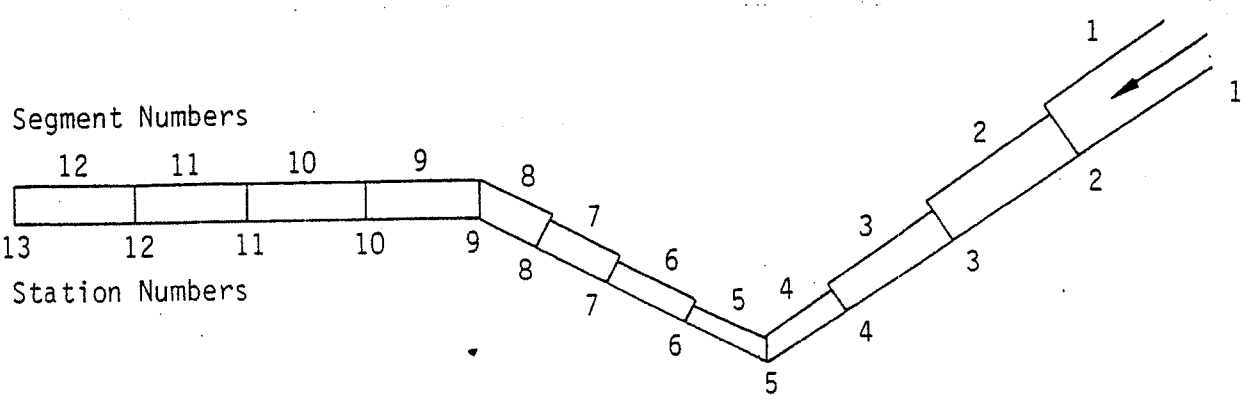

$$\Delta P \text{ chamber} = \Sigma \Delta P_{seg}$$
$$\Delta T \text{ chamber} = \Sigma \Delta T_{seg}$$

The previous discussion neglected the effects of nucleate boiling and unreasonable channel geometries which result from low coolant velocity requirements.

Nucleate boiling occurs when the coolant side wall temperature is 50 to 100 degrees Rankine above the saturation temperature of the coolant. (A vapor pressure routine is included which returns saturation temperature as a function of pressure). When it is determined that nucleate boiling is occurring it is assumed that the coolant wall temperature (T_{cw}) is held at T_{sat} + 75. On this basis the heat flux can be recalculated as

$$q = (T_g - T_{cw})/(1/h_g + \ell/k)$$

With this heat flux the channel can be sized from the equation

$$q_{ult} = C_1 + C_2 \, v \, \Delta T_{sub}$$

where C_1 and C_2 are unique to the coolant in use.

It is possible that the channel geometry will have to be determined by manufacturing limits rather than by coolant velocity requirements. For this purpose there is a maximum height to width ratio for coolant channels. When this limit is reached in the nucleate boiling case, it causes ΔP to be increased but has no effect on heat flux. In the non-nucleate boiling regime, however, the increased velocities caused by this limit will increase coolant heat transfer coefficients. Therefore, ΔP and heat flux will both be increased.

Both nucleate boiling and channel height to width limits will cause the

chamber wall to be overcooled and the coolant bulk temperature rise to be higher than that predicted by the nominal gas wall temperature. When this occurs the program typically requires only one iteration to converge on a result for total ΔP, ΔT.

When the coolant within the regen jacket experiences two-phase flow, warning messages are output to that effect. If the bulk temperature of the coolant is pushed above the required coolant wall temperature, then sufficient cooling cannot take place and again a warning message results. In both cases the stepwise calculation ends and the pressure drop is set to a very high value.

The gas side heat transfer coefficient is calculated from a Bartz-type equation

$$h_g = \left[\frac{.026}{D_t^{.2}} \left(\frac{\mu^{.2}\, C_p}{Pr^{.6}}\right) \left(\frac{P_c\, g_c}{C^*}\right)^{.8}\right] \left(\frac{1}{\varepsilon}\right)^{.9} \sigma$$

$$\text{Where } \sigma = \frac{1}{\left[\frac{1}{2}\frac{T_{gw}}{T_{cm}}\left(1 + \frac{\gamma - 1}{2} M^2\right) + \frac{1}{2}\right]^{.68} \left[1 + \frac{\gamma - 1}{2} M^2\right]^{.12}}$$

The gas properties T_{cm}, C^*, and M are available from ELES performance subroutines; however, combustion gas μ, C_p, and Pr are not calculated and at present are considered constants.

The gas temperature upstream of the throat is considered to be that of the barrier stream which is returned from the I_{sp} calculating routine. Downstream of the throat the gas temperature is calculated from

$$T_g = T_{cm} \left(\frac{P}{Pc}\right)^{\frac{\gamma-1}{\gamma}}$$

where: the local pressure (P) is calculated from the empirical curve-

fit equation

$$P = P_{cm} \,/\, EXP\left[\frac{\ln \varepsilon}{.80065} - .87203\ EXP\left\{-[(\varepsilon - 1)\ 1.11252]^{.43032} + 1.56518\right\}\right]$$

Variation of coolant properties (density, thermal conductivity, viscosity, heat capacity, and vapor pressure) are calculated by corresponding state methods (i.e. a generalized method based on critical properties, normal boiling point, etc.) The value of each property is forced through a reference point so that both the trend and the value are accurate. This approach allows investigation of coolants for which extensive property data is not available or, if available, does not require the very time-consuming task of finding data and creating data files.

For all properties except heat capacity, reference values and critical properties are sufficient input to obtain property values. Heat capacity requires some additional input.

Liquid heat capacities have been correlated as the sum of two components, that of the ideal gas, and that of the non-ideal liquid. For many gases the ideal heat capacity variation with temperature is given in equation form.

$$C_p^{\,o} = A + BT + CT^2 + DT^3$$

Where the constants A, B, C, and D have been derived based on the molecular structure of the gas. REGEN uses this equation in the form

$$C_p^{\,o} = A' + B'T_r + C'T_r^{\,2} + D'T_r^{\,3}$$

Where $A' = A$

$B' = BT_c$

$C' = CT_c^{\,2}$

$D = DT_c^{\,3}$

and $C_p^{\,o}$ [=] BTU/lb mole ^oR

These constants must therefore be found in the literature. They can be approximated, if not found in the literature, by subtracting the non-ideal portion from actual heat capacity data and fitting it with the above equation form for the ideal gas. The non-ideal portion is calculated by the method of corresponding states (see Section 11.0).

REGEN MODEL NOMENCLATURE

A_{seg}	Chamber area available for heat transfer in a segment
a	Dimensionless heat transfer exponent
b	Dimensionless heat transfer exponent
C_1, C_2	Burnout heat flux constants
C*	Characteristic exhaust velocity
C_p	Heat capacity
C_p^o	Ideal gas heat capacity
D_h	Hydraulic diameter
D_t	Throat diameter
f	Friction factor
g_c	Gravitational conversion factor
h_c	Coolant side heat transfer coefficient
h_g	Gas side heat transfer coefficient
k	Thermal conductivity
K	Dimensionless heat transfer constant
ℓ	Wall thickness
L_{seg}	Segment length
M	Mach number
Nu	Nusselt number ($h D_h / k$)
P	Pressure
Pr	Prandtl number ($C_p \mu / k$)
ΔP_{seg}	Pressure drop across a segment
q	Heat flux
q_{ult}	Maximum heat flux for nucleate boiling
R	Ideal gas constant
Re	Reynolds number ($\rho v D_h / \mu$)
T_b	Bulk temperature of coolant
T_c	Critical temperature
T_{cm}	Combustion temperature
T_{cw}	Coolant side wall temperature

T_g	Gas temperature
T_{gw}	Gas side wall temperature
T_r	Reduced temperature (T/T_c)
T_{sat}	Saturation temperature
ΔT_{seg}	Temperature change across a segment
ΔT_{sub}	Degree to which coolant is subcooled ($T_{sat} - T_b$)
v	Velocity
ω	Mass flow rate
γ	Ratio of specific heats
ε	Local area ratio
μ	Viscosity
ρ	Density

3.1.3 Heat Transfer Coefficients (See Nomenclature List, Pgs, 34 & 35)

The regenerative cooling model needs to calculate heat transfer coefficients for the propellant in the regen jacket cooling channels. The method used by ELES is intended to work in the regime of turbulent forced convection; however, nucleate boiling and ultimate heat flux are also included.

Forced convection heat transfer coefficients can be shown to depend only on Nusselt number, Reynolds number, Prandtl number, and a geometry factor (L/D) when applied to a fluid with constant properties. A typical plot for real fluids of Nusselt number vs Reynolds number over a range of Prandtl numbers is shown in Figure 3.1.3.1 with the entrance effect L/D neglected.

Except for the case of very low Prandtl numbers, the curves are nearly straight lines and therefore, behave as simple power functions. A simple power function equation which has proven itself very useful in describing the relationship between Nusselt, Reynolds, and Prandtl numbers is shown below.

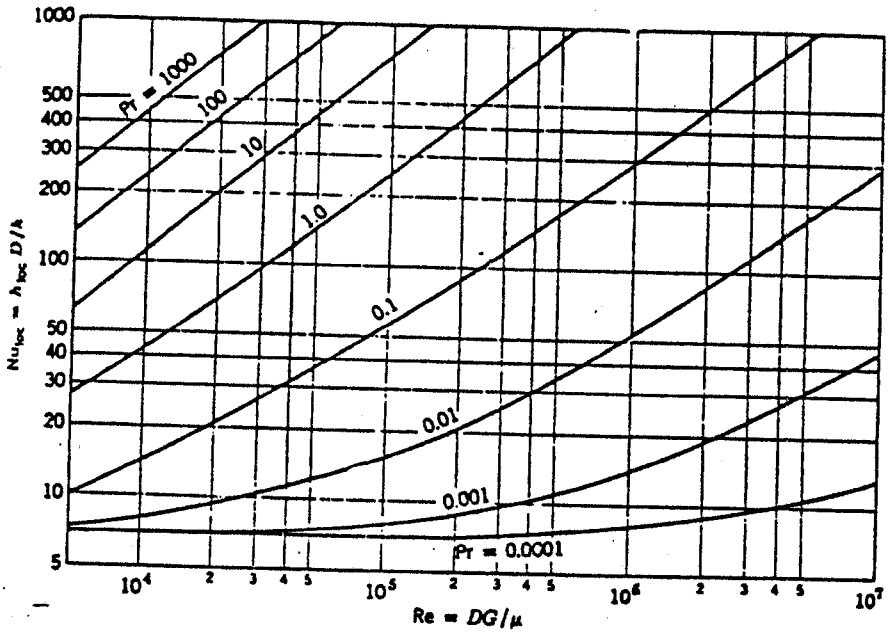

Predicted Nusselt Numbers for Developed Turbulent Flow with Constant Wall Heat Flux. [Results for Pr ≥ 1 are From R. G. Deissler, NACA Report 1210 (1955); Others are From R. C. Martinelli, Trans. ASME, 69, 947-959 (1947).]

Figure 3.1.3.1. Heat Transfer Coefficients for Regen Cooling

$$Nu_b = K\ Re_b^{\alpha}\ Pr_b^{\beta}$$

where: Nu = Nusselt number $= \frac{hD}{k}$

Re = Reynolds number $= \frac{\rho D \bar{v}}{\mu}$

Pr = Prandtl number $= \frac{Cp\mu}{k}$

h = heat transfer coeff.
D = characteristic dimension
k = thermal conductivity
ρ = density
$\bar{v}$ = mean velocity
μ = viscosity
Cp = heat capacity
α, β, K = empirical constants
b = subscript denoting bulk properties

The storable propellants in ELES are well described by the above equation. Fluid properties are evaluated at the bulk temperature and the values of α, β, and K are constant. Some of the cryogenic propellants, however, require more consideration to the variability of fluid properties. Empirical correlations which describe the cryogenic propellants which do not fit the more simple model are:

Hydrogen: $$Nu_f = .0208\ Re_f^{.8}\ Pr_f^{.4}\ (1 + 0.01457\ \frac{\nu_w}{\nu_b})$$

Oxygen: $$Nu_b = .0025\ Re_b^{1.0}\ Pr_b^{.4}\ (\frac{\rho_b}{\rho_w})^{-\frac{1}{2}}\ (\frac{k_b}{k_w})^{-\frac{1}{2}}\ (\frac{\overline{Cp}}{Cp_b})^{2/3}\ (\frac{P}{Pc})^{-1/5}$$

Methane $$Nu_b = .00545\ Re_b^{.9}\ Pr_b^{.4}\ (\frac{\rho_b}{\rho_w})^{-.11}\ (\frac{\mu_b}{\mu_w})^{.23}\ (\frac{k_b}{k_w})^{.27}\ (\frac{\overline{Cp}}{Cp_b})^{.53}$$

where: ν = kinetic viscosity = $\frac{\mu}{\rho}$

and subscripts f = film temp = (Tw + Tb)/2
w = wall temp = Tw
b = bulk temp = Tb

If fluid property variations are lumped into a calculation of the constant (K) in the simple equation form, a table of constants can be compiled for all of the library propellants in ELES (see Table 3.1.3.1)

TABLE 3.1.3.1

HEAT TRANSFER COEFFICIENT EMPIRICAL CONSTANTS

$$Nu = K\, Re^{\alpha}\, Pr^{\beta}$$

Propellant	K	α	β
MMH	.005	.95	.4
N_2O_4	.0305	.85	.4
N_2H_4	.005	.95	.4
MHF-3	.005	.95	.4
ClF_5	.005	.95	.4
MON-25	.0305	.85	.4
LO_2	$.0025 \left(\frac{\rho_b}{\rho_w}\right)^{-\frac{1}{2}} \left(\frac{k_b}{k_w}\right)^{\frac{1}{2}} \left(\frac{\overline{Cp}}{Cp_b}\right)^{2/3} \left(\frac{P}{Pc}\right)^{-1/5}$	1.0	.4
LH_2*	$.0208 \left(1 + .01457 \frac{\nu_w}{\nu_b}\right)$	.8	.4
RP-1	.005	.95	.4
CH_4	$.00545 \left(\frac{\rho_b}{\rho_w}\right)^{-.11} \left(\frac{\mu_b}{\mu_w}\right)^{.23} \left(\frac{k_b}{k_w}\right)^{.27} \left(\frac{\overline{Cp}}{Cp_b}\right)^{.53}$	.9	.4
LF_2	.005	.95	.4

*evaluated at film temperature

As the heat flux into a subcritical coolant increases it eventually passes the saturation temperature of the fluid by a sufficient amount to cause nucleate boiling. The heat transfer coefficient of a fluid undergoing nucleate boiling is very high as small bubbles form at the chamber wall and move into the bulk coolant where they collapse. ELES senses this condition and calculates the wall temperatures which result.

If the heat flux is much higher than that required for nucleate boiling it can pass into the transition regime between nucleate boiling and film boiling. The highly desirable nucleate boiling condition of using the heat of vaporization to "pump" heat into the bulk fluid becomes a very undesirable condition in the transition zone. The movement of gas bubbles away from the wall can begin to impede the movement of coolant to the wall. The heat flux at which this becomes a problem is called the critical or ultimate heat flux.

The ultimate heat flux is dependent on the propellant in question and the flow conditions. A simplified model for ultimate heat flux is:

$$q_{ult} = C_1 + C_2 \, v \, (T_{sat} - T)$$

where:

q_{ult}	= ultimate heat flux (Btu/in.^{2} sec)
C_1 & C_2	= constants
v	= velocity (in/sec)
T_{sat}	= saturation temperature (°R)
T	= fluid temperature (°R)

The coolant velocity in the regenerative cooling channels is kept at sufficient velocity to meet this ultimate heat flux criteria. ELES uses the following values for C_1 and C_2 and constricts the coolant channel if necessary to raise the allowable heat flux.

Propellant	C_1	C_2
MMH	4.2	1.67E-5
N_2O_4	2.6	3.17E-5
N_2H_4	4.55	4.77E-5
MHF-3	4.2	1.67E-5
CLF_5	2.6	3.17E-5
MON-25	2.6	3.17E-5
LO_2	10.0	1.
LH_2	10.0	1.
RP-1	0.5	2.26E-5
CH_4	0.5	2.26E-5
LF_2	10.0	1.

3.1.4 Trans-Regen Cooling

The regenerative cooling model was modified to include transpiration cooling effects. Sections of the chamber which are regeneratively cooled are calculated as before. When a transpiration section is encountered, the required transpiration coolant is calculated and subtracted from the regenerative coolant flow. The remainder of the regen flow is routed around the transpiration section without gaining any heat. If transpiration sections continue to be encountered, the same procedure is followed; otherwise, normal regen cooling is performed.

On completion of each regen segment, the total transpiration coolant flowrate is available. That flowrate is used in the engine performance routine to calculate performance loss from transpiration cooling. Because the performance is required prior to performing the cooling analysis, an iterative approach was taken (i.e., it is necessary to assume a performance in order to calculate engine geometry, and therefore transpiration flowrate). The iterative loop for transpiration coolant was combined with the existing iterative loop for propellant temperature schedule. The run time impact of iteration is therefore mitigated.

The region of the trans-regen chamber which is transpiration cooled can be controlled by either of two methods. The area ratios of the chamber at the upstream and downstream locations where transpiration cooling begins and ends may be specified directly. Alternatively, transpiration cooling can be flagged to occur at all chamber locations which are above a specified heat flux.

Given gas side conditions, the transpiration cooling model calculates the transpiration flowrate required to limit the chamber material temperature to a maximum allowable design temperature. Two cooling mechanisms are included in this model: (1) a heat flux blockage model which reduces convective heating of the gas wall by altering the boundary-layer properties; and (2) an internal cooling model which transfers heat from the chamber material

to the coolant inside the transpiration channels. The transpiration chamber geometry is assumed to be of platelet design. Rigimesh or sintered chamber designs can be modeled by reducing the values of S, h, 1, and w (see Figure 3.1.4.1) to those appropriate for the design in question.

The blockage equation is

$$q/_{qo} = 1/[1 + (0.3 + .14 \text{ EXP } (-2.8\ (h + 2S)/h))\ (\frac{C_{pc}}{C_{pg}})_{T_g}\ (\frac{C_{pg}}{h_g})_{T_g}\ \dot{m}]^3$$

where	h	= coolant channel height (in.)
	s	= spacer width (in.)
	C_p	= heat capacity (Btu/lb-°R)
	h_g	= heat transfer coefficient (Btu/in.^{2}sec °R)
	$\dot{m}$	= coolant mass flux (lb/sec)
subscripts	c	= coolant
	g	= combustion gas
	T_g	= evaluated at combustion gas temperature

The internal cooling model is developed from the differential equations describing conduction in the material and the coolant temperature.

$$k_m\ (h/2 + S)\ \frac{d^2T}{dx^2} = h_1\ (T-T_c)$$

$$G\ C_{p,c}\ (h/2 + S)\ \frac{dTc}{dx} = h_L\ (T-T_c)$$

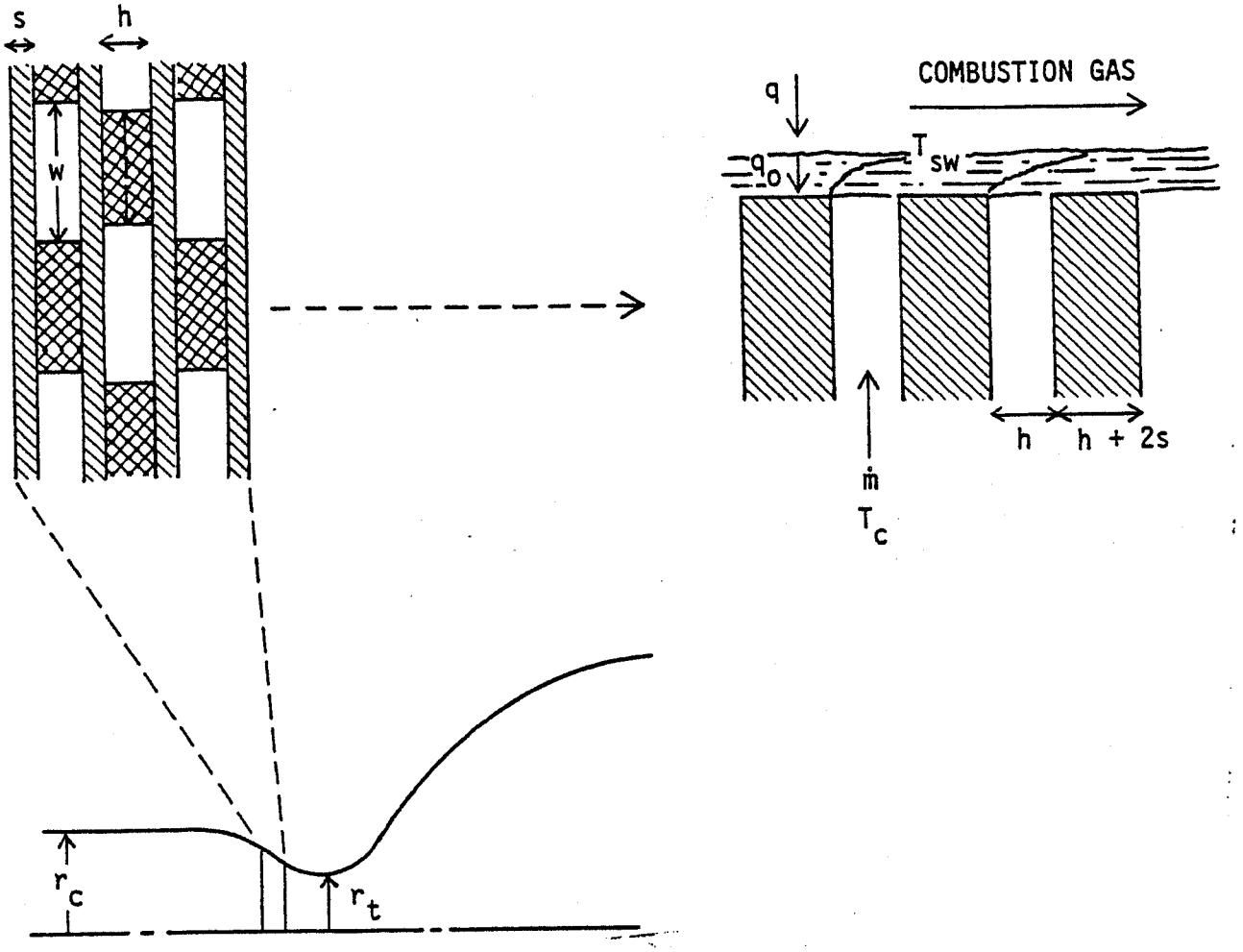

Figure 3.1.4.1. Trans-Regen Cooling Model

where

k_m = material conductivity

T = material temperature at location x

x = distance from coolant inlet

h_L = coolant heat transfer coefficient

T_c = coolant temperature at x

G = coolant weight flow per unit of cooled wall surface area

$C_{p,c}$ = coolant specific heat

Substitution yields

$$\frac{d^3T}{dx^3} + \frac{h_L}{G\,C_{p,c}\,(h + 2S)/2}\,\frac{d^2T}{dx^2} + \frac{h_L}{k_m\,(h + 2S)/2}\,\frac{dT}{dx} = 0$$

Applying boundary conditions

(1) $h_g\,(T_g - T) = k_m\,\frac{dT}{dx}$ at side wall (x=L)

(2) $\frac{dT}{dx} = 0$ at x = 0

(3) $k_m\,(h + 2S)/2\,\frac{d^2T}{dx^2} = h_L\,(T - T_{ci})$ at x = 0

and making assumptions about the relative magnitudes of the results yields

$$T_{gw} = T_{ci} + q/km\,\left[\frac{-h_L}{2G\,C_{p,c}\,(h - 2S)/2} + \sqrt{\left(\frac{h_L}{G\,C_{p,c}\,(h + 2S)/2}\right)^2/4 + \left(\frac{h_L}{k_m\,(h + 2S)/2}\right)}\right]$$

The above internal cooling model and the blockage equation are solved iteratively in order to calculate the mass flowrate required to cool the chamber

3.1.5 Transpiration Cooling Performance Loss Model

The performance loss model due to transpiration cooling is a stream tube analysis similar to the barrier cooling model in ELES (see figure below). The two models are in fact combined to give a single mixture ratio maldistribution loss multiplier. The effect of transpiration cooling is to change the mixture ratio of the barrier stream tube. ELES then performs a stream tube analysis which flow-averages the performance of the core stream tube with that of the barrier stream tube. The mixture ratio (MR) of each stream tube is chosen by the user. The core MR is chosen for performance and the barrier MR for cooling ability.

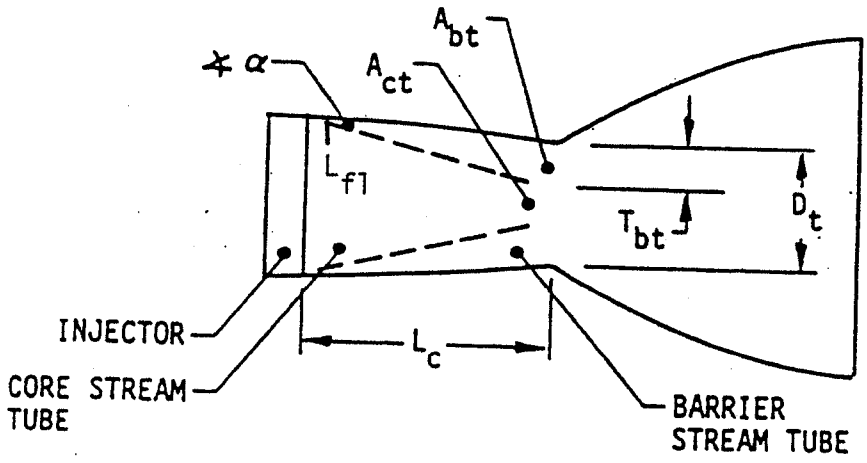

3.1.6 TCA Radiation Cooling Model

The radiation cooling model calculates the maximum allowable gas temperature at the gas side wall of the thrust chamber assembly (TCA). The radiation model calculates the heat flux from the TCA to the vehicle, other TCA's, and the ambient environment. The following model is used to represent the heat conduction path from the combustion gas barrier in the TCA to the ambient environment (see figure below.)

T_a - ambient temperature (°R)
T_b - barrier temperature (°R)
T_e - exterior wall temperature (°R)
T_{gw} - gas wall temperature (°R)
T_v - vehicle temperature (°R)
h_g - gas side heat transfer coeff. (Btu/sec-in.^{2}-°R)
k - thermal conductivity (Btu/sec-in.-°R)
ℓ wall thickness (in.)

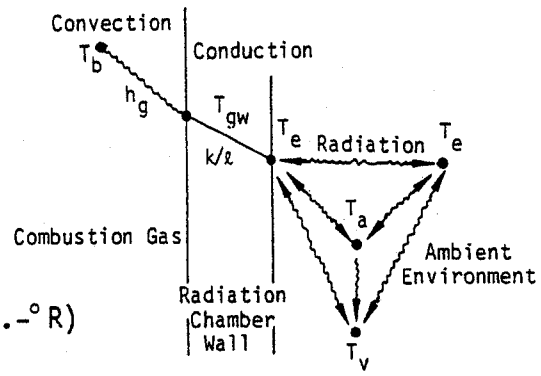

In ELES the gas wall temperature (T_{gw}) is known from material of construction limits. The ambient temperature is input by the user based on mission constraints. With this information and with the appropriate view factors and emissivities of the TCA's, vehicle, and ambient environment, it is possible to solve for T_e in terms of T_{gw}. The heat flux through the wall is then a simple conduction problem. Given the heat flux and heat transfer coefficient on the gas side, the barrier temperature is calculated. This yields the corresponding barrier mixture ratio and ultimately the engine performance.

The solution for T_e in terms of T_{gw} is simplified by assuming that radiation exchange between TCA's can be analyzed as a single TCA's view of itself. Under this assumption, the following equations are solved simultaneously:

$$B_e = \varepsilon_e \sigma T_e^4 + \rho_e [B_e F_{ee} + B_a F_{ea} + B_v F_{ev}]$$

$$B_a = \varepsilon_a \sigma T_a^4 + \rho_a [B_e F_{ae} + B_a F_{aa} + B_v F_{av}]$$

$$B_v = \varepsilon_v \sigma T_v^4 + \rho_v [B_e F_{ve} + B_a F_{va} + B_v F_{vv}]$$

$$q = \left(\frac{\varepsilon_e}{1-\varepsilon_e}\right) (\sigma T_e^4 - B_e) = \left(\frac{k}{\ell}\right) (T_{gw} - T_e)$$

Substitution into the above equations yields a 4th order equation for T_e.

$$\varepsilon_e \sigma T_e^4 \left[1 - F_{ee} - \frac{F_{ev} F_{ve}}{1-F_{vv}}\right] + T_e \left(\frac{k}{\ell}\right) \left[1 - \rho_e F_{ee} - \frac{\rho_e \varepsilon_e F_{ev} F_{ve}}{(1-F_{vv}) \varepsilon_a}\right]$$

$$= T_{gw} \left(\frac{k}{\ell}\right) \left[1 - \rho_e F_{ee} - \frac{F_{ve} \rho_e \varepsilon_e F_{ev}}{(1-F_{vv}) \varepsilon_a}\right] + \varepsilon_a T_a^4 \left[\varepsilon_a \sigma F_{ea} + \frac{F_{va} F_{ev} \varepsilon_a \sigma}{(1-F_{vv})}\right]$$

Where:

T	= Temperature
q	= Heat flux
B	= defined equations
ε	= emissivity
σ	= Stefan-Boltxmann Constant
ρ	= reflectance = $(1-\varepsilon)$
F_{ij}	= view factor of i to j
k	= thermal conductivity
ℓ	= chamber wall thickness

Subscripts:

e	= engine
a	= ambient
v	= vehicle

Solving for T_e and then q, the barrier temperature is calculated from

$$q = h_g (T_b - T_{gw})$$

The value of T_b thus obtained is used to obtain the barrier mixture ratio which corresponds. That mixture ratio for the barrier stream tube dictates the amount of film cooling the engine must use in order to cool by radiation.

The view factors are obtained through simple geometric models of the engine and vehicle. Engine geometry is estimated by assuming 92% of theoretical performance and a simple cylinder/cone construction. This is done prior to calculating performance more accurately, in order to avoid an iteration loop which yields little improvement to the final answer.

3.2 NOZZLE COOLING

There are four nozzle cooling options in ELES: 1) ablative, 2) radiation, 3) regenerative, 4) film. The main objective of the ablative model is to calculate the ablative thickness in the nozzle required to withstand the thermal environment. The radiation model calculates the barrier stream tube temperature consistent with the radiation heat flux to the environment and the maximum nozzle material temperature. The regenerative model calculates the pressure drop across the cooling jacket consistent with the maximum operating temperature of the nozzle material. The film cooling model uses the gas generator bleed flow to cool the nozzle. At present ELES does not do a thermal analysis of the film cooled nozzle but assumes that the low mixture ratio turbine exhaust will be cool enough to protect the nozzle.

The ablative and radiation models both calculate a barrier stream tube mixture ratio (MR) requirement. This mixture ratio is compared with the mixture ratio required in the combustion chamber and the lower temperature MR is used. It is therefore possible for either the chamber or the nozzle to dictate the barrier mixture ratio in a given engine design.

The nozzle regenerative model assumes that the chamber is also cooled regeneratively or trans-regeneratively. There is no mechanism in ELES for cooling only the nozzle regeneratively (to do so is contrary to good engineering judgement).

3.2.1 Ablative Nozzle

The equation used in ELES to calculate ablative thickness requirements in the nozzle is:

$$t = ct_b^{0.5} \text{ EXP } (-0.0247\varepsilon)$$

where:

t	= ablative thickness (in)
c	= empirical constant
t_b	= burn time (sec)
EXP( )	= irrational number e raised to the power of the expression in parenthesis
ε	= area ratio

The thickness calculation is area averaged over the ablative cooled nozzle for weight calculations.

The attach area ratio of the ablative nozzle can have an effect on engine performance since the ablative material should not be exposed to combustion gas at a temperature above its maximum operating temperature (for silica phenolic the maximum is 3900°R) If the attach point is at a small enough area ratio, the combustion gas may not have expanded enough to have cooled below the maximum operating point. In that case, ELES will add film cooling to the barrier stream tube in order to lower its temperature and will therefore lower the engine performance.

3.2.2 Radiation Cooled Nozzle

The radiation model described for the TCA is the same model used for nozzle radiation cooling. The difference in the implementation of the model is the method for calculating radiation view factors. It is the view factors

of a radiation cooled component which dictate how much radiation is exchanged with itself and with the ambient environment. The view factors are calculated from simple geometric representations of the engine, nozzle, vehicle, and space.

As with the ablative nozzle, it is possible for the barrier mixture ratio to be determined by the attach area ratio and operating temperature of the radiation cooled nozzle.

3.2.3 Regeneratively Cooled Nozzle

The model used to analyze regeneratively cooled nozzles is described in the section on TCA cooling. Because regenerative nozzles are required by ELES to be used only with regenerative or trans-regenerative chambers, there is no special model for nozzles alone.

The engine weight model, however, does have provision for changing the nozzle configuration from milled channel to tubes. The milled channel construction would be much too heavy if carried out to the exit of a large expansion area ratio nozzle.

3.2.4 Film Cooled Nozzle

The film cooled nozzle is used with gas generator bleed cycles. The gas generator exhaust is ducted through a manifold to the nozzle of the main TCA where it is injected downstream of the throat. A moderately low area ratio is normally chosen for the attach area ratio, however the choice depends on weight, exhaust Isp, and turbine pressure drop being traded.

A typical geometry for a film cooled nozzle is shown in Figure 3.2.4.1 The manifolding consists of a tapered ring around the nozzle and a constant cross section from the turbine exhaust to the ring inlet. The size and weight of the manifolding is calculated in the TPA hot gas manifolding section.

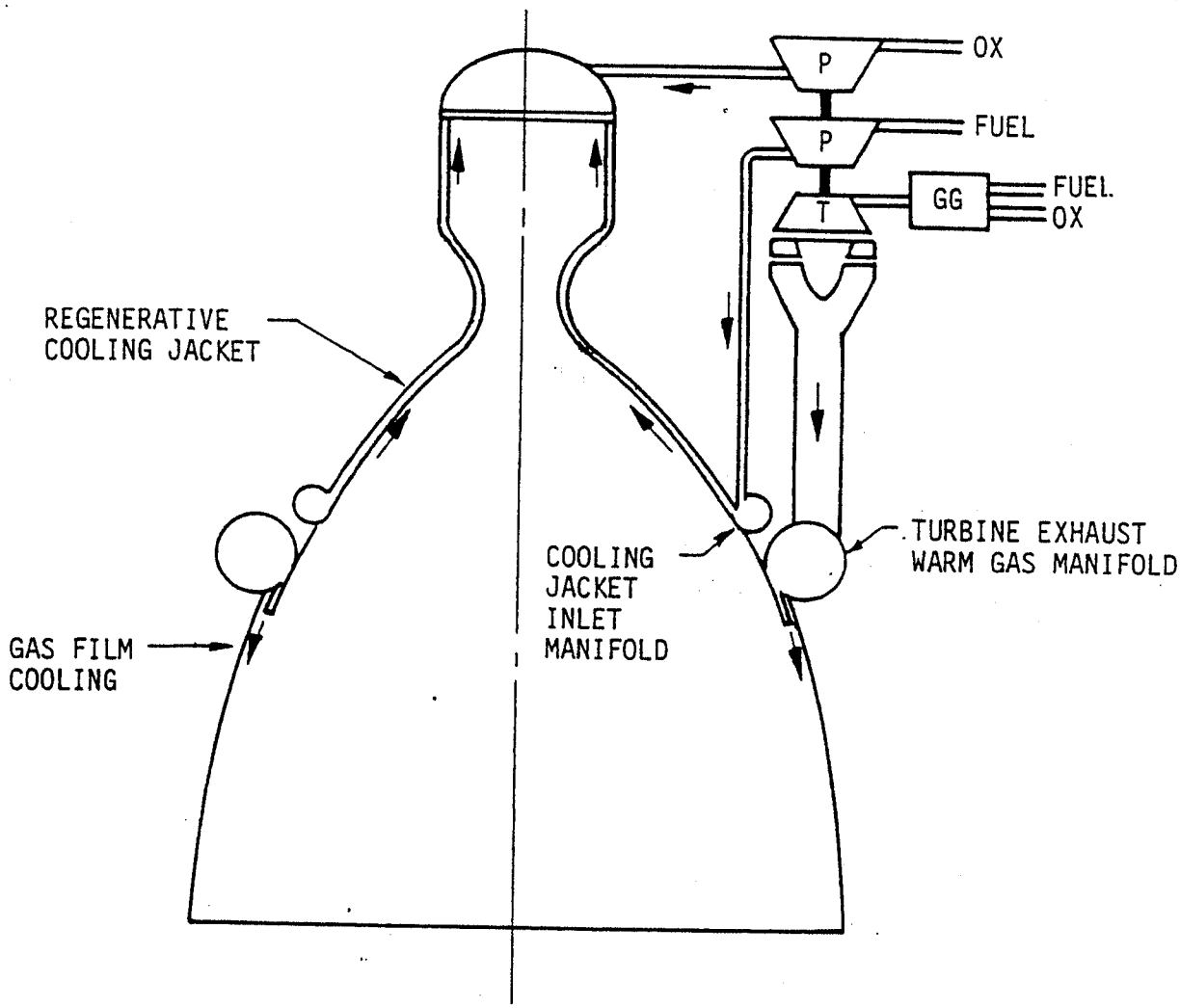

Figure 3.2.4.1. Gas Film-Cooled Nozzle

The performance of a film cooled nozzle is calculated as the weight flow averaged performance of the chamber stream tube and the film coolant stream tube. The chamber stream tube performance is based on the full area ratio of the nozzle whereas the film coolant area ratio is the total area ratio divided by the attach area ratio of the tapered coolant ring. The film coolant performance is also based on the exit temperature and pressure from the turbine as well as the gas generator mixture ratio.

3.3 TCA BARRIER MIXTURE RATIO

The TCA barrier mixture ratio in ELES is a calculated parameter. The barrier mixture ratio in liquid rocket engines is normally governed by the material properties of the chamber and nozzle. Therefore material properties are used in ELES to calculate a compatible barrier mixture ratio consistent with the cooling method or methods used for the chamber and nozzle. When the nozzle requires a lower temperature barrier than that required by the chamber, the lower temperature barrier mixture ratio is chosen for the TCA. Similarly, when the chamber requires a lower temperature barrier than the nozzle, the chamber sets the barrier mixture ratio.

For ablative cooling, the barrier temperature must be constrained to the maximum allowable for the ablative material in use. Silica phenolic, for example, should be used with a barrier temperature no higher than 3900 degrees Rankine.

For regeneratively cooled chambers, the gas wall temperature must be held at or below that which leaves sufficient structural properties for the pressure loads. In ELES,, the gas wall temperature is held constant and the barrier temperature is allowed to vary. It is preferable to run the barrier at the core mixture ratio in order to obtain better performance. If such a high temperature barrier creates too high of a heat flux to the wall, and therefore too high a coolant pressure drop, the barrier temperature can be lowered. The barrier temperature is calculated by the equation

$$T_{barrier} = \text{Constant} \times (T_{core} - T_{gas\ wall}) + T_{gas\ wall}.$$

The constant in the above equation equals 1 for equal barrier and core mixture ratios. It is between 0 and 1 for intermediate mixture ratios. A significant advantage of this approach is that the barrier mixture ratio is always related to the core mixture ratio, even when the core mixture ratio is being changed by the optimizer.

The above equation for calculating barrier mixture ratio for regeneratively cooled chambers will also be used for trans-regen chambers. The tradeoff which will indicate the best barrier mixture ratio will include the regenerative pressure drop as well as performance loss due to fluid injection along the chamber wall.

The required barrier temperature for radiation cooled chambers is calculated based on the heat flux from the outside chamber wall to the environment (vehicle, ambient, and other TCAs). ELES estimates the view factors of the TCA, the vehicle, and the ambient environment to themselves and each other. These view factors are used to convert the simultaneous heat flux equations into a fourth order equation for the outside wall temperature of the chamber. The resultant calculation for heat flux is used to determine the barrier temperature and, therefore, the barrier mixture ratio.

The same approach is used in the nozzle for all of the above cooling schemes except for the calculated barrier temperatures, which include the effects of an isentropic expansion

$$(T_1/T_2) = (P_1/P_2)^{(\gamma-1)/\gamma}$$

4.0 ENGINE SIZE/WEIGHT

4.1 ABLATIVE ENGINE WEIGHT MODELS

There are two different models in ELES for calculating the weight of ablative engines. One is a curve-fit of weight data for existing engines and the other is a physical model of major ablative engine components. Ordinarily the physical model will be more accurate and more versatile.

The scope of both engine weight models includes an ablative chamber and nozzle, a fixed nozzle extension, and bipropellant injector and valve, as depicted in the figure below.

4.1.1 CURVE-FIT WEIGHT MODEL FOR ABLATIVE ENGINES

The analytical approach used for the curve-fit model involved adjusting the constants of the engine weight equation to fit operational engine weight data. A least squares, multi-variable optimization routine was employed for this task. This approach was used because of a desire to maximize the use of physical modeling and an abundance of engine weight data without specific component weight breakdowns.

No.	Item
1	Valves
2	Injector
3	Chamber
4	Nozzle
5	Nozzle Extension

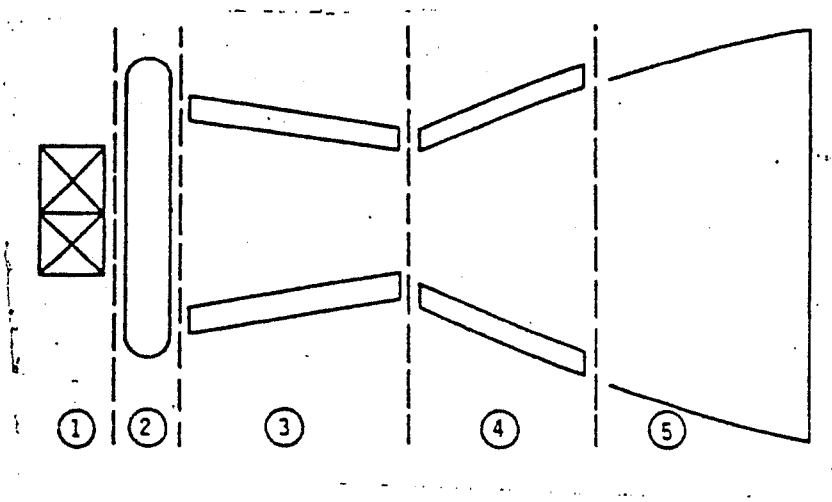

The best fit has been determined to be

$$W_{eng} = \frac{2.817\ F^{1.235}}{P_C^{1.538}} +$$

$$.008171\ T_B^{.2894}\ R_T^{1.424}\ [\ \varepsilon_{tot}^{1.64}\ (\frac{\varepsilon_{att}}{\varepsilon_{tot}})^{3.} + .03864\ L_C^{1.776}\ ] +$$

$$.0005329\ T_B^{1.453} + 34.99,$$

where:

W_{eng}	=	Weight of ablative chamber, nozzle, fixed nozzle extension, bipropellant injector and valves, lbm
F	=	Engine vacuum thrust, lbF
Pc	=	Engine plenum pressure, psia
T_B	=	Total burn duration capability, sec
R_T	=	Throat radius, in.
ε_{tot}	=	Nozzle overall area ratio
ε_{att}	=	Attachment area ratio for nozzle extension
L_C	=	Injector face to throat plane dimension, in.

4.1.2 Physical Engine Weight Model

The physical engine weight model is an option to the curve-fit model, and it should be used where the parameters of interest, (e.g., ε , Pc, etc.) are outside of the curve-fit limits. ELES will warn the user when this occurs.

The major ablative engine components are modeled individually and the total engine weight derived from their sum.

Valve Weight

The valve weight algorithm is a scaling equation which assumes that valve weight is proportional to valve port diameter squared. This assumption is indicated by valve weight data. The calculated diameter is based on the following equation

$$d = \sqrt{\frac{\omega}{21.81\ C_d\ \sqrt{\rho \Delta P}}}$$ where:

ω = weight flow
C_d = pressure coefficient
ρ = fluid density
ΔP = pressure differential

Using the above equation form, the valve weight equation is written as

$$W_{valve} = 1.476 \rho_{matl} \left[\frac{\omega_{ox}}{\sqrt{\rho_{ox}\ \Delta P_{ox}}} + \frac{\omega_{fuel}}{\sqrt{\rho_{fuel} \Delta P_{fuel}}} \right] C_{valve}$$

where:			
	ρ_{matl}	= valve material density	(lb/in^3)
	ω_{ox}	= ox weight flow rate	(lb/sec)
	ω_{fuel}	= fuel weight flow rate	(lb/sec)
	ρ_{ox}	= ox density	($lb/in.^3$)
	ρ_{fuel}	= fuel density	($lb/in.^3$)
	ΔP_{ox}	= ox ΔP across valve	(psi)
	ΔP_{fuel}	= fuel ΔP across valve	(psi)
	C_{valve}	= valve complexity multiplier	(default = 1.0)
	C_d	= .65	

Injector Weight

The injector weight equation is the result of upgrading some existing scaling equations by including material properties and a complexity multiplier. The complexity multiplier can be used to reflect throttling or high-performance capability (e.g., the improved Transtage injector which gets 10 sec of Isp more than the original Transtage injector has a $C_{injector} = 1.6$, and for the throttlable LEM descent engine $C_{injector} = 1.25$).

$$W_{inj} = 0.003\ \rho_{inj}\ A_t\ \varepsilon_c\ (300 + 3771.3\ P_c\ \sqrt{A_t/SY_{inj}})\ C_{injector}$$

where:
- ρ_{inj} = density of injector material (lb/in.^{3})
- A_t = throat area
- ε_c = contraction ratio
- P_c = chamber plenum pressure
- SY_{inj} = yield strength of injector material
- $C_{injector}$ = injector complexity multiplier (default = 1.0)

Nozzle Extension Weight

Nozzle extension weight is based on the surface area of the nozzle extension. This routine begins with surface area calculations which were derived by curve fitting the results of the Aerojet Rao nozzle program. The applicable equations are

SA_{att} = nozzle surface area from the throat to the attach point

$$= r_t^2\ [1.537 + 1.303\ (RATMLR - 1.25)]\varepsilon_{att}^{1.705}$$

$$x\ (0.04558 + 1.678\ EXP(-0.056305\varepsilon_{tot})\ )$$

SA_{tot} = total nozzle surface area

$$r_t^2\ [3.368\ (\varepsilon_{tot} + 10.857)^{1.2606} +$$

$$\varepsilon_{tot}\ (RATMLR - 1.25)\ x\ 10.75]$$

$$t_{noz} = \frac{t_{n\ ref}\ P_c\ r_t}{P_{n\ ref}\ R_{n\ ref}} \geq \text{minimum gauge (default = 0.010)}$$

w_{noz} = nozzle extension weight

$$= (SA_{tot} - SA_{att})\ t_{noz}\ \rho_{noz}$$

where:

A_t	= throat area ($in.^2$)
ϵ_{tot}	= total nozzle area ratio
ϵ_{att}	= attach area ratio
RATMLR	= ratio of nozzle length to minimum length Rao nozzle
r_t	= throat radius (in.)
ρ_{noz}	= nozzle material density ($16_m/in.^3$)
t_{noz}	= effective nozzle thickness (proportional to to $\frac{PR}{SY}$) (in.)
EXP(a)	= 2.7183^a
$t_{n\ ref}$	= reference nozzle thickness (in.) (default = 0.019)
$P_{n\ ref}$	= reference nozzle chamber pressure (psia) (default = 125.0)
$R_{n\ ref}$	= reference nozzle throat radius (in.) (default = 3.74)
$t_{noz\ min}$	= minimum gauge of nozzle (in.) (default = 0.010)

Due to accuracy and applicability constraints of the surface area equations, the following rules are imposed prior to the w_{noz} calculation:

1. If $\epsilon_{tot} < 20$

$$SA_{tot} = SA_{att} (\epsilon_{tot}/\epsilon_{att})^{1.705}$$ (i.e., use SA_{att} eqn form to get SA_{tot})

2. If $\epsilon_{tot} = \epsilon_{att}$ (i.e., no nozzle extension, $w_{noz} = 0$)

$$Sa_{att} = Sa_{tot}$$ (where SA_{tot} has been operated on by the first If statement)

The above conditions should be tested for, and the indicated response should be explicitly followed in order to enhance the accuracy of the procedure.

If a conical nozzle is used in place of a Rao nozzle, the surface area is

$$SA_{att} = \pi(r_t + r_{att}) \sqrt{h_{att}^2 + (r_{att} - r_t)^2}$$

where: $h_{att} = (r_{att} - r_t)/\tan \alpha$

$r_{att} = r_t \sqrt{\varepsilon_{att}}$

α = nozzle half angle, ^{o}

$$SA_{tot} = \pi (r_t + r_{tot}) \sqrt{h_{tot}^2 + (r_{tot} - r_t)^2}$$

where: $h_{tot} = (r_{tot} - r_t)/\tan \alpha$

$r_{tot} = r_t \sqrt{\varepsilon_{tot}}$

The weight calculations are identical to the Rao procedure from this point. The length at a conical nozzle is calculated as

$$L_{noz} = h_{tot}$$

Thrust Chamber Weight

The thrust chamber weight is based on calculation of the volume of an ablative and a structural portion. The thickness of the ablative is sensitive to burn time, chamber pressure, type of ablative, propellant combination, and barrier MR. The user should, therefore, input char depths for ablative materials and propellants other than silica phenolic and N_2O_4/A-50 at some reference chamber pressure/burn time, and the program will calculate thicknesses (based on that input) for any given case. Values for silica phenolic glass wrapped construction are default within ELES.

The thicknesses are calculated using the following definitions

d_{chart} = char depth at throat (in.)
d_{charc} = char depth in chamber (in.)
d_{charn} = char depth in nozzle (in.)

ε_{ref} = reference area ratio for d_{charn}

P_{cref} = reference P_c for char depths (psia)

t_{bref} = reference t_b for char depths (sec)

SF_{abl} = ablative safety factor (default = 1.0)

SF_{str} = structural safety factor (default = 1.0)

SY_{str} = structural yield strength hot (psi)

t_{sref} = reference structural thickness (in.)

P_{sref} = reference P_c for $t_{s\ ref}$ (psia)

r_{sref} = reference chamber radius for $t_{s\ ref}$ (in.)

t_t = throat ablative thickness

$$= a\ P_c^{0.2}\ t_b^{0.77} SF_{abl}$$

where: a = input

or: $a = d_{chart}/(P_{cref}^{0.2}\ t_{bref}^{0.77})$

t_c = chamber ablative thickness

$$= b\ P_c^{0.4}\ t_b^{0.5}\ SF_{abl}$$

where: $b = d_{charc}/(P_{cref}^{0.4} t_{bref}^{0.5})$

or: b = input

t_{att} = ablative thickness at attach area ratio

$$= c t_b^{0.5}\ SF_{abl}\ EXP(-0.0247\ \varepsilon_{att}))$$

where: $c = d_{charn}/(t_{bref}^{0.5} EXP(-0.0247 \varepsilon_{ref}))$

or: c = input

t_s = structural thickness

$$= SF_{str}\ t_{sref}\ P_c\ r_c/(P_{sref}\ r_{sref})$$

or: $t_s = SF_{str} P_c r_c / SY_{str}$

When using the preceding equations to scale thicknesses with default values, it is recommended that safety factors be set equal to 1.0, since the safety factor of the reference chamber is contained in the input reference thickness. When reference thicknesses are calculated, it is recommended that safety factors of 1.25 be applied to silica phenolic ablative and 1.5 be applied to nonmetallic structural materials.

The above thickness equations are also constrained by minimum gauge requirements (i.e., additional input values are $t_{t\ min}$, $t_{c\ min}$, $t_{att\ min}$, $t_{s\ min}$).

The following is a list of the recommended default values to be used with the thrust chamber weight routine.

Default Values:

$d_{chart} = 1.33$
$d_{charc} = 1.02$
$d_{charn} = 0.87$
$\epsilon_{ref} = 7.5$
$P_{cref} = 125.$
$t_{bref} = 500.$
$SF_{abl} = 1.0$
$SF_{str} = 1.0$
$t_{sref} = 0.22$
$P_{sref} = 125.$
$r_{sref} = 5.95$

Once the thickness is known, estimates of material volumes can be made and combined with material densities to calculate weights, using the following method.

V_{abl} = volume of ablative material

$$= XLC\ (r_c + 0.5\ t_c)\ 2\pi\ t_c + XLN\ \frac{(t_c + t_t)}{2}\ \pi\ \left[\ r_c + r_b + \frac{(t_c + t_t)}{2}\ \right]$$

$$+\ SA_{att}\ \left(\ \frac{(t_t + \sqrt{\varepsilon_{att}}\ t_{att}}{(1 + \sqrt{\varepsilon_{att}}}\ \right)$$

V_{str} = volume of structural material

$$= XLC\ (r_c + t_c\ 0.5\ t_s)\ 2\pi\ t_s + XLN\ \pi\ t_s\ \left[\ r_c + r_t + t_c + t_t + t_s\ \right]$$

$$+\ SA_{att}\ t_s\ \left[\ \frac{r_t(\sqrt{\varepsilon_{att}} + 1) + t_t + t_{att}}{r_t\ (\sqrt{\varepsilon_{att}} + 1)}\ \right]$$

W_{chm} = chamber weight

$$= (V_{abl}\ \rho_{abl} + V_{str}\ \rho_{str})\ f_{chm}$$

where:

XLC	= chamber cylindrical length (in.)
XLN	= chamber convergent length (in.)
SA_{att}	= nozzle surface area up to attach point ($in.^2$)
ρ_{abl}	= ablative density ($lb/in.^3$) (default = 0.0632)
ρ_{str}	= structural density ($lb/in.^3$) (default = 0.0632)
f_{chm}	= chamber miscellaneous weight multiplier (default = 1.17)

Total Ablative Engine Weight

Given the weights of the four major components of the engine, the total engine weight is calculated as the sum of their individual weights, plus the miscellaneous weight required to assemble them.

W_{eng} = total engine weight

$= (W_{valve} + W_{injector} + W_{noz\ ext} + W_{chm})\ f_{eng}$

where: f_{eng} = total engine miscellaneous weight multiplier (default = 1.05)

4.2 REGENERATIVELY COOLED CHAMBER WEIGHT

The regeneratively cooled engine weight model is an extension of the physical model developed for ablative engines. The valve, injector, and nozzle extension weight models are taken directly from the ablative model. The ablative chamber and nozzle are replaced with models of milled slot regen cooled chambers and nozzles.

ELES calculates the inside geometry of regen chambers from thrust and performance of the engine. The weight is then a function of required wall thicknesses and milled slot dimensions. The milled slot dimensions are calculated from heat transfer requirements. The wall thicknesses for the liner and closeout are calculated as follows.

The chamber design is a cooled chamber with axial groves cut in chamber liner material for coolant channels which are closed out by electroformed Ni, or other material, such as the OMS (space shuttle orbital maneuvering system) thrust chamber design.

The required closeout thickness to resist chamber pressure (Pc) and coolant pressure (P_{cool}) assuming the hot liner material would take no load would be;

$$t_{closeout} \geq \frac{P_c R_i + P_{cool} h}{F_{ty}}$$

where: R_i = chamber inside radius (in.)
h = coolant channel land height (in.)
F_{ty} = closeout material yield strength at maximum operating temperature (psi)

This would be the total required thickness if there is no elastic followup on the liner thermal growth.

As the hot liner undergoes thermal growth, it is reacted by the cooler closeout material. Thus, thickness to react solely to pressure may not be enough. It is desired to end up with the closeout material worked within its elastic regime, i.e., not allowed to go inelastic. However, the hot liner is not restricted from going into the plastic regime. Thus, an elastic thermal analysis is not desirable, since it would not be realistic, and it would predict an unrealistically high closeout thickness requirement.

A parametric plastic analysis is too rigorous for use in ELES. Therefore, the ELES model is based on results of chamber designs to date, which include the effect of thermal loading and liner plasticity, e.g., OMS, technology engines, and advanced high pressure engines. The total required closeout thicknesses, in each case, were divided by the required closeout thickness to withstand pressure only in order to establish a multiplier (K). This factor is plotted versus chamber pressure (Pc) in Figure 4.2.1.

Using the appropriate value for K, the closeout thickness is calculated as

$$t_{closeout} = \frac{K\,[P_c R_i + P_{cool} h]}{F_{ty}}$$

$$t_{closeout} = K[PcRi + P_{cool}h]/F_{TY\ closeout}$$

$$t_{liner} = w\left(\frac{P_{cool}}{2F_{TY\ liner}}\right)^{\frac{1}{2}}$$

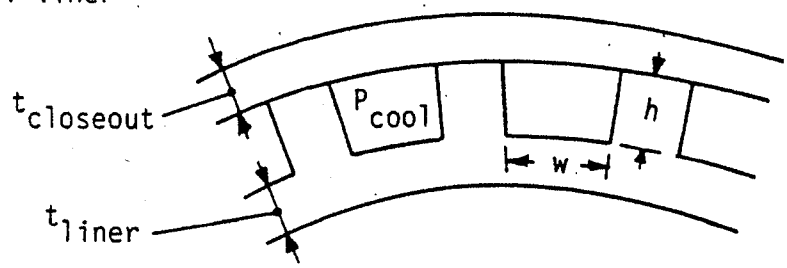

Figure 4.2.1. Chamber Closeout Sizing Constant

The liner thickness is based on the liner strain remaining in the elastic range considering the beam bending loads between lands, which are induced by the differential pressure $\Delta P = Pc - P_{cool}$. The worst condition is shutdown, when $\Delta P = P_{cool}$ and the maximum temperature is still present. The equation used in ELES to calculate liner thickness is

$$t_{liner} = w \left(\frac{P_{cool}}{2 F_{ty}} \right)^{\frac{1}{2}}$$

where
- w = channel width (in.)
- P_{cool} = coolant pressure (psia)
- F_{ty} = liner material yield strength at maximum operating temperature (psi)

The empirical data from which theory is derived includes the effect of hot gas wall liner plasticity, and results are felt to be minimum requirements. Where very thin wall thicknesses are predicted, use a manufacurable thickness, e.g., .030" > t_{liner}.

The theory is based on empirical data for state-of-the-art thrust chamber designs and may not be applicable to designs which employ exotic materials or design concepts.

Having obtained the detailed dimensions and thicknesses of the regen chamber, it is possible to calculate the material volume of the milled chamber and closeout. The chamber weight is then calculated as

$$W_{chamber} = (V_{gw} \ \rho_{gw} + V_c \ \rho_c) \ f_{chm}$$

where:
- V_{gw} = gas wall material volume (including milled lands) (in^3)
- ρ_{gw} = gas wall material density (lb/in^3)
- V_c = closeout material volume (in^3)
- ρ_c = closeout material density (lb/in^3)
- f_{chm} = chamber miscellaneous weight multiplier

The chamber miscellaneous weight multiplier reflects the weight of assembly flanges attachments, etc. (default value = 1.17).

4.3 TRANS-REGEN COOLED CHAMBER WEIGHT

Trans-regen cooled thrust chambers are modeled identically to regenerative chambers, except for the transpiration throat insert. The throat insert is of platelet design and extends between an upstream and downstream area ratio specified by the user.

The weight of the insert is approximated with frustrums of two cones corresponding to an upstream and downstream section. The lengths of the frustrums are calculated, the thickness of the insert is input. The Trans-regen chamber weight is then

$$W_{tr\ cham} = W_{reg\ cham} + \rho_{insert}\, t_{insert}\, SA_{insert}$$

where:

$W_{tr\ cham}$	= weight at trans-regen chamber
$W_{reg\ cham}$	= weight of regenerative chamber
ρ_{insert}	= effective density of platelet throat insert
T_{insert}	= insert thickness
SA_{insert}	= insert surface area

4.4 RADIATION COOLED CHAMBER WEIGHT

The radiation cooled engine weight model is also an extension of the physical model developed for ablative engines. The valve, injector, and nozzle extension are taken directly from the ablative model. The radiation cooled chamber is modeled as a sheet metal cylinder with a convergent/ divergent section. The applicable surface areas are calculated as in the ablative model, however, the chamber wall thickness is calculated by hoop stress.

Although hoop stress of the hot chamber material may be the controlling design criterion, often the design it is controlled by buckling, vibration, exterior over-pressure, etc. This could be considered an area of improvement for ELES despite the good results obtained with the hoop stress model.

Having calculated the chamber wall thickness, the chamber weight is the product of surface area, thickness and density.

4.5 THRUST MOUNT AND GIMBAL SYSTEM WEIGHTS

Because thrust mounts and gimbal system designs are highly varied and geometry dependent, their weight models in ELES are empirical curve fits of existing hardware weights. Both were found to be strong functions of engine thrust. For the thrust mount

W_{tm} = thrust mount weight, including injector-mounted monoball and thrust-spreading structures to aft tank head, (lbm)

$$W_{tm} = \frac{\ell n\ F - 7.509}{.06305} \qquad \text{for } F > 6{,}438 \text{ lbF}$$

$$W_{tm} = 17.\ (F/6438.) + 3. \qquad \text{for } F \leq 6{,}438 \text{ lbF}$$

where: F = engine vacuum delivered thrust (lbF)

For the gimbal system

W_{gim} = complete gimbal actuator system, excluding power supply (head-end gimbal)

$$W_{gim} = \frac{\ell n\ F - 7.447}{.0551} \qquad \text{for } F \geq 5{,}162 \text{ lbF}$$

$$W_{gim} = 15.\ (F/5162.) + 5. \qquad \text{for } F < 5{,}162 \text{ lbF}$$

where: F = engine vacuum delivered thrust (lbF)

If the gimbal system uses a battery powered hydraulic pump to power the gimbal actuators, and that battery power is provided by the stage, then

W_{pow} = power supply (battery) weight

$$W_{pow} = \left(\frac{F}{9600}\right)\left(\frac{t_b}{340}\right)\left(\frac{100}{.006035\ t_b + 18.28}\right)$$

where: F = engine vacuum delivered thrust (lbF)

t_b = total engine burn time (sec)

The above described gimbal actuator/battery model is a thrust vector control weight model consistent with a storable pressure-fed stage. The system is an electric motor-driven hydraulic system. The electric power for running the motor is provided either by the payload or as batteries on-board the stage.

For pump fed engine cycles, the weight penalties of the storage battery and electric motor can be avoided by using more weight-efficient designs. Storable pump-fed cycles can use high pressure pump discharge propellants to drive hydraulic actuators directly. The weight of this system is estimated by deleting the unnecessary components from those in the electric motor-driven hydraulic system. Using N-II hardware data this results in the pump tap-off gimbal system weighing 65% of the electric motor-driven hydraulic system. The equation to model this in ELES is

$$W_{tvc\text{-}prop\text{-}tap} = 0.65\ W_{gim}$$

where: W_{gim} = W_{gim} as defined above

In pump-fed cryogenic application, the pump discharge tap-off method of obtaining hydraulic power is precluded by the nature of the propellants. Shaft power from the turbopump assembly can be tapped, however, and used to drive a hydraulic pump. With this approach, and using N-II hardware data for comparison, it has been determined that shaft-power tap-off system will weigh 80% of the electric motor-driven hydraulic gimbal system. In order to model this ELES uses the equation

$$W_{tvc\text{-}shaft\text{-}tap} = 0.80\ W_{gim}$$

4.6 IGNITION SYSTEMS WEIGHT

Although many liquid propellant combinations are hypergolic (they ignite on contact), many others require an igniter to initiate combustion. Most igniters are similar in shape, function, and weight according to a survey of existing hardware. They consist of small inlet lines, a miniature chamber (.05 in. to 1.0 in.), a spark plug, and wiring (see Figure 4.6.1). Ignition system weight does not seem to correlate well with engine size, thrust, or Pc as shown below;

	SSME	ATLAS	RL-10
weight (lbM)	11	19	7.2
Pc (psia)	3000	707	400
F (1.F)	470K	80K	15K

For this reason, a constant weight of 12.4 lbM will be used for ignition systems in TPAWT. Systems using hypergolic propellants have no ignition system.

4.7 SUPPORT HARDWARE WEIGHT

The support hardware weight is based on a survey of existing engine systems. Support hardware includes items such as:

1. Wiring Harness
2. Instrumentation
3. Miscellaneous brackets and support structure
4. Burst discs, miscellaneous valving
5. Purge system

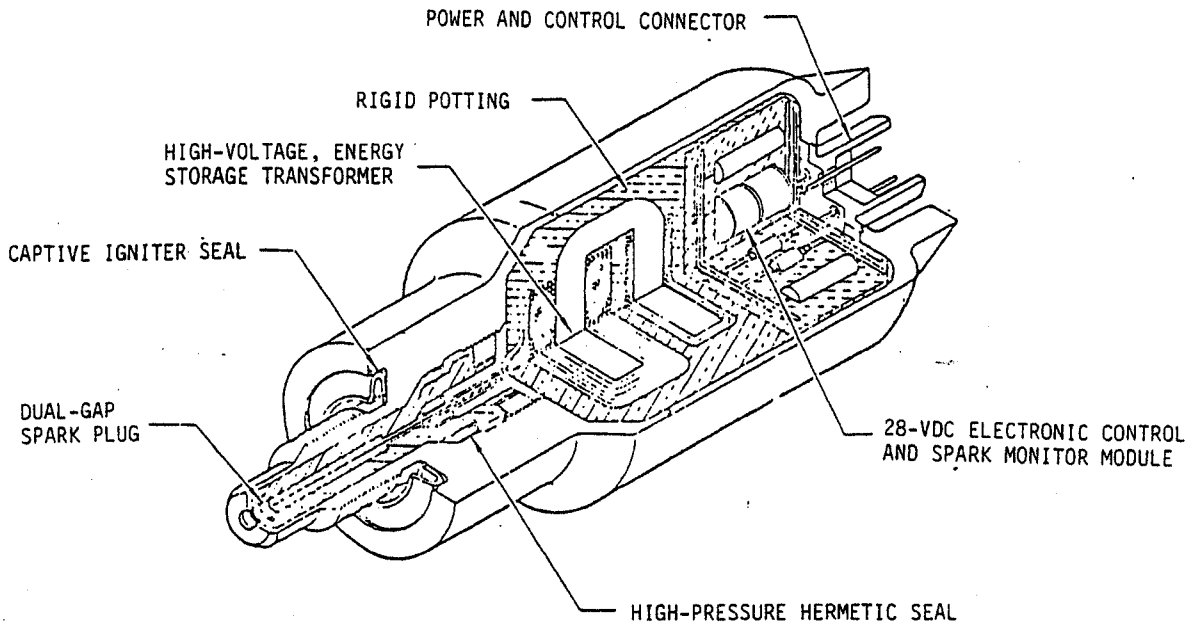

Figure 4.6.1. Integral Spark Igniter

Examination of five existing engine systems yielded the following results:

SSME:	W_{misc}	= 6.5% of $\Sigma W_{components}$
OMS:	W_{misc}	= 8.5%
ASEC:	W_{misc}	= 3.5%
J2:	W_{misc}	= 8.6%
Titan Stage II:	W_{misc}	= 5.4%
Average	W_{misc}	= 6.5% of $\Sigma W_{components}$

The use of a constant percentage is preferable to a complicated physical model because of the myriad design choices and the low relative weights of the individual items. The support hardware weight recommended percentage will therefore be 6.5%.

4.8 EXTENDIBLE/MOVEABLE NOZZLES

In ELES there can be up to three discrete sections of the nozzle; that portion which is integral with the chamber, a nozzle extension which is rigidly attached to the chamber, and a translating or moveable section which does not contribute to the stage length. (see Figure 4.8.1). The third section includes spring actuated translating nozzles, which move along guide-rails into position and gas deployed skirts, which fold inside the main nozzle to be forced into position, at engine ignition.

The function of translating and moveable nozzles is to increase the performance of rocket engines by increasing their expansion area ratio without the stage length penalty normally associated with high area ratio nozzles. The penalty which accompanies moveable nozzles is in the forms of weight, cost and complexity.

The translating nozzle model is a standard, radiation-cooled columbium nozzle. Nontranslating nozzles of this type have been designed and used on ATC production engines such as Apollo SPS, Transtage, Delta, and the Shuttle OMS engine.

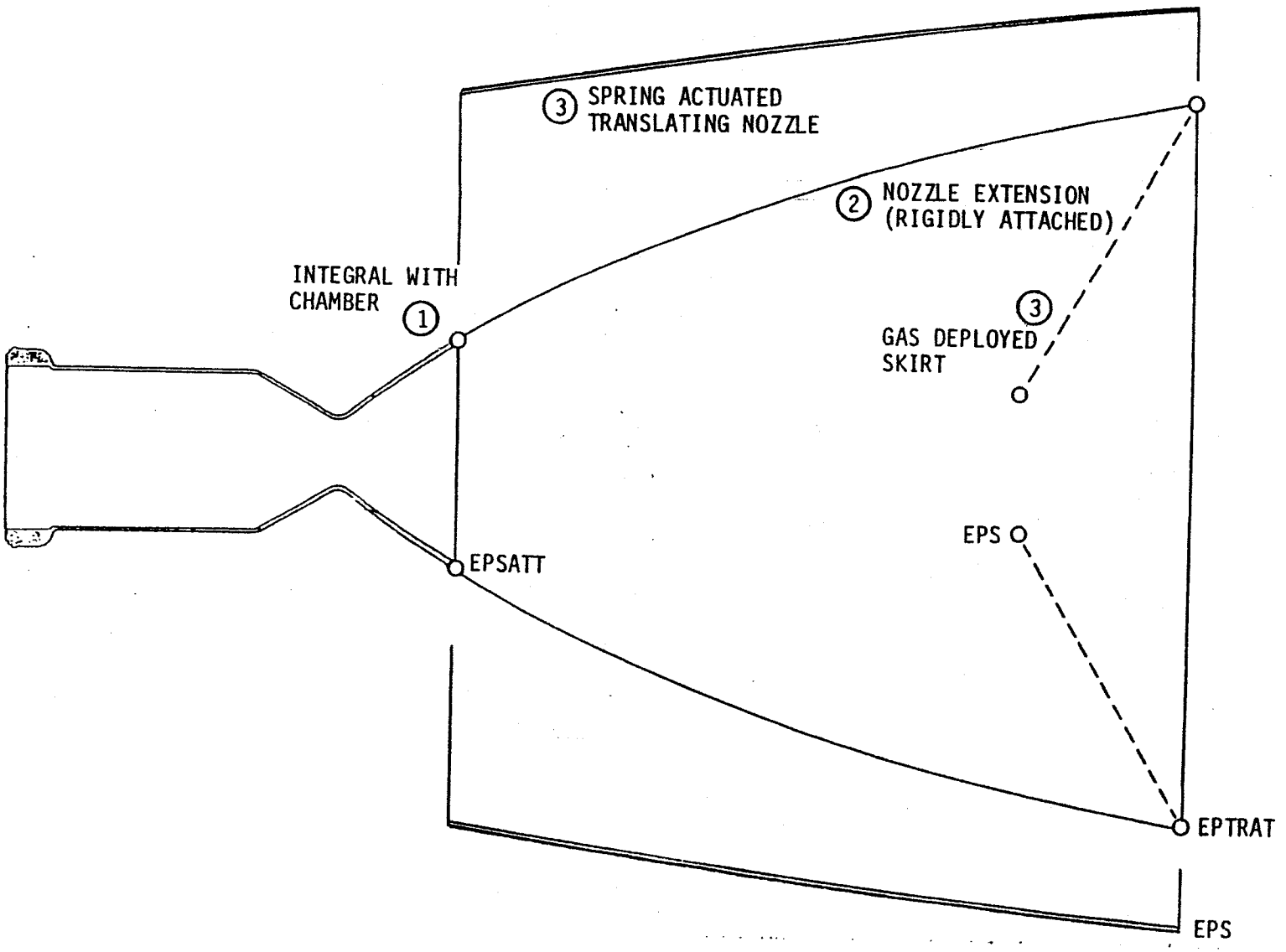

Figure 4.8.1. Extendible/Moveable Nozzles

The coil spring deployment concept (see Figure 4.8.2) is a simple, reliable, and inexpensive method to deploy a nozzle. Production deployment assemblies have the capability of being funcionally acceptance tested. The system uses three guide rails to hold the nozzle in the retracted position, and, during deployment of the nozzle, to guide the nozzle into the extended position. Each guide rail employs two coil spring cartridges, one to start the deployment and one to finish the deployment by forcing the nozzle into the locked and extended position.

EXTENDIBLE NOZZLE WEIGHT ALGORITHM

The extendible nozzle weight algorithm is a physical model of the major nozzle components such as the extendible skirt, guide rails, nozzle flange, nozzle stiffening ring, and tie rods. The nozzle dimensions are calculated from performance requirements and the subcomponent dimensions are scaled from nozzle dimensions. The equations are

$$W_{SKIRT} = SA_{SKIRT}\ t_{SKIRT}\ \rho_{SKIRT}$$

$$W_{rails} = 3\pi\ r^2_{rail}\ \ell_{rail}\ \rho_{rail}$$

$$W_{flange} = SA_{flange}\ t_{flange}\ \rho_{flange}$$

$$W_{ring} = SA_{ring}\ t_{ring}\ \rho_{ring}$$

$$W_{rods} = 6\pi\ r^2_{rod}\ \ell_{rod}\ \rho_{rod}$$

where:
- SA = surface area ($in.^2$)
- t = thickness (in.)
- ρ = density (lb/in^3)
- r = radius (in.)
- ℓ = length (in.)

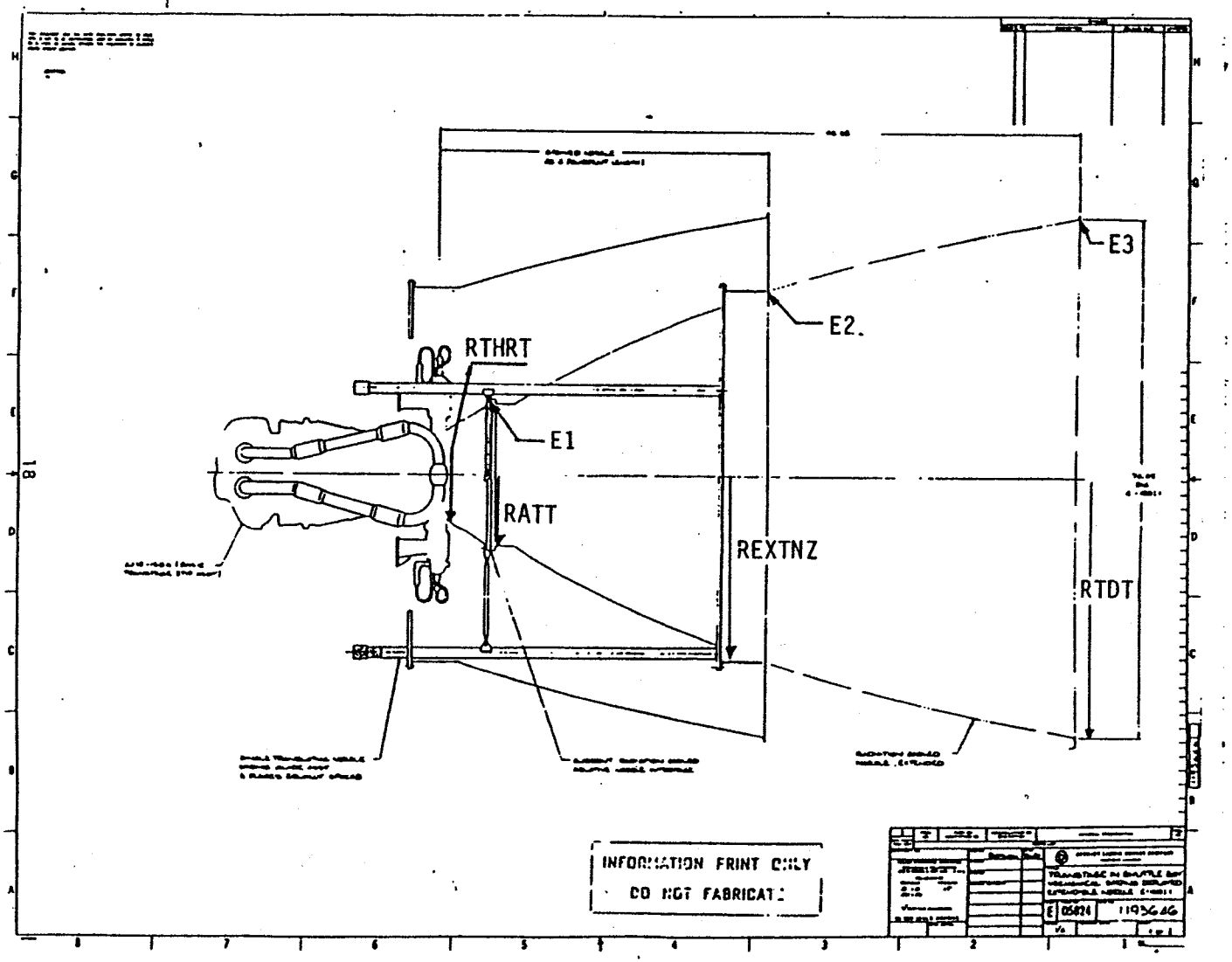

Figure 4.8.2. Transtage Nozzle Design Description

The total extendible nozzle weight is then

$$W_{ex\ noz} = W_{SKIRT} + W_{rails} + W_{flange} + W_{ring} + W_{rods}$$

The analytical model used for the size and weight of a gas deployed skirt (gds) is very simple. It assumes a constant thickness sheet of material attached to the rigid nozzle extension and folded inside it. Although the program does check for deployment clearance, it only outputs a warning message if the clearance requirement is not met. It does not redesign the nozzle. Gas deployed skirts are displayed in the graphical output routines to scale in order to aid the redesign process.

For proper deployment clearance the gds must have a nozzle contour length of less than 90% of the nozzle radius at the attach point.

The weight equation for the gds is

$$W_{gds} = SA_{gds}\ t_{gds}\ \rho_{gds}$$

where:

W_{gds}	= gas deployed skirt weight (lbm)
SA_{gds}	= surface area of gds (in^2)
t_{gds}	= thickness of gds (assumed = 0.020) (in.)
ρ_{gds}	= material density of gds (lb/in^3)

For both translating nozzles and gas deployed skirts the surface area of the skirt itself is provided by the correlations presented in the engine physical weight model.

4.9 TURBOPUMP ASSEMBLY WEIGHTS

The equations which model the weight of turbomachinery in ELES are physical models in the sense that they use the dimensions of the pumps and turbine in order to estimate a material volume and weight. The relationship between the TPA diameter and its length or material fraction are empirically derived. The diameters are calculated in the TPA performance routines.

The main turbopump assembly (TPA) weight is calculated by an equation based on pump and turbine diameters, number of pump and turbine stages, and overall TPA material density. The overall TPA weight is the sum of all pumps and turbines.

$$W_{TPA} = \Sigma W_{pump} + \Sigma W_{turbine} + \Sigma W_{boost\ pump}$$

The equation used to calculate pump weight is

$$W_{pump} = \rho_m \frac{\pi D_p^3}{4} \left(\frac{L}{D}\right)_p f_m$$

where: $\left(\frac{L}{D}\right)_p = (0.7 + 0.3n_p)(47.76/(D_p + 15.7) - 0.36)$

ρ_m = material density (lb/in^3)

D_p = pump tip diameter (in.)

$\left(\frac{L}{D}\right)_p$ = pump length to diameter ratio (-)

n_p = number of pump stages (-)

f_m = pump material fraction (-)

The material fraction in the above equation is

$$f_m = (0.12\ D_p + 0.9)/D_p$$

The expressions for $(\frac{L}{D})_p$ and for f_m are both empirically derived equations based on existing pump hardware. The equation for turbine weight is essentially the same as for pumps with the exception that the length to diameter equation is different.

$$W_{turbine} = \rho_m \frac{\pi D_t^3}{4} (\frac{L}{D})_t f_m$$

where: $(\frac{L}{D})_t = (0.9 + 0.1n_t)\ (47.76/(D_t + 15.7) - 0.36)$

ρ_m = material density (lb/in^3)

D_t = turbine tip diameter (in.)

$(\frac{L}{D})_t$ = turbine length to diameter ratio (-)

n_t = number of turbine stages (-)

f_m = turbine material fraction (-)

Boost pump weights use the same equation as for pumps with the exception, again, of the L/D relationship.

$$W_{boost\ pump} = \rho_m \frac{\pi D_{BP}^3}{4} (\frac{L}{D})_{BP} f_m$$

where: $(\frac{L}{D})_{BP} = 1.3\ (\frac{L}{D})_p$

If a gearbox is used to transmit shaft power from the turbine to the pumps, its weight is included in the TPA weight. Gearbox weight is calculated by an equation based on the horsepower transmitted, gearing ratio, and turbine RPM:

$$W_g = 400 \left[\frac{SH_{pg}}{RPM_g} \frac{(r_s + 1)^3}{r_s} \right]^{.8}$$

where:

SH_{pg} = horsepower of geared pump

RPM_g = speed of geared pump

r_s = turbine to pump speed ratio

W_g = gearbox weight (lb)

4.10 HOT GAS MANIFOLDING

The size and weight of an engine's hot gas manifolding is very much dependent on the engine cycle and the TPA configuration. The table below illustrates various hot gas manifolding schemes -vs- engine cycle and TPA configuration.

	Gearbox	Single Shaft	Series Twin TPA	Parallel Twin TPA
GG Bleed	Axial Duct with either a bleed nozzle or torus exit.	Same as Gearbox	Turbine Interconnect duct plus one axial duct with either a bleed nozzle or torus exit.	Bifurcated GG to turbine ducts plus two axial ducts with either a bleed nozzle or torus exit.
Staged Combustion	Injector Inlet Duct	Same as Gearbox	Turbine interconnect duct plus one injector inlet duct.	Bifurcated PB to turbine ducts plus two injector inlet ducts
Expander	No additional hot gas manifold weight. Picks up heat from REGEN chamber.			
Staged Reaction	Same as Staged Combustion Options.			

The model used in ELES is a "typical" design..The duct diameter is based on an empirically derived average local Mach No. of 0.3. Axial duct length is set at 1.5 x duct diameter. Wall thicknesses are based on hoop stress (Pr/t) at hot operating conditions.

The weight of any given duct, nozzle, or torus segment is calculated as follows:

$$W_{duct} = \pi \, D \, t \, L \, \eta \, C_x$$

where:
- D = diameter (in.)
- t = wall thickness (in.)
- L = length (in.)
- η = duct material density ($lb/in.^3$)
- C_x = Constant times weight (default = 2.5) to account for flanges, bellows, bosses, and attach hardware.

If a bleed nozzle is present, its diameter is set equal to the duct diameter and its length is

$$L_{noz} = \left(\frac{D}{2}\right) \left(\frac{\sqrt{\varepsilon} - 1}{\tan 15^0}\right)$$

where: the area ratio (ε) is 1.05 for first stages and 2.5 for upper stages.

The turbine interconnect duct length is estimated by:

$$L_i = \pi D_c \qquad \text{where } D_c = \text{chamber diameter (in.)}$$

The average torus duct diameter is approximated as 0.65 times main duct diameter, since it tapers considerably as it circles the nozzle. Torus circumference is calculated by:

$$C_T = 4\pi A_t E_{att}$$

where: A_t = engine throat area
E_{att} = torus attach area ratio

4.11 PREBURNER OR GAS GENERATOR

Total GG weight is composed of the GG flange, injector, and cylinder weight. Flange weight is calculated by:

$$W_{flange} = (.00165\ F + .7)\ \left(\frac{100}{P_{gg}}\right)^{.6}$$

where: F = GG thrust (lb)
P_{gg} = GG chamber pressure (psia)

The GG throat area is found via the C* equation and the chamber diameter is determined by assuming a contraction ratio of 12:1. Injector weight is calculated by:

$$W_{inj} = .003\rho_{inj}\ A_t\ C_x\ \left[300 + \frac{3771.3\ P_{gg}\ \sqrt{A_t}}{Sy}\right]$$

where: ρ_{inj} = injector material density (lb/in.^{3})
A_t = GG throat area (in.^{2})
C_x = complexity factor (default = 1)
P_{gg} = GG chamber pressure (psia)
Sy = material yield strength (psia)

The cylinder's thickness is determined by the Pr/t equation while the cylinder's length is based on the concept of typical propellant "stay-time" found in the literature for various propellants. The weight of the cylindrical portion is thus:

$$W_{cyl} = \pi D_{gg} L_{gg} t_{gg} \rho_{cyl}$$

where:
- D_{gg} = GG chamber diameter (in.)
- L_{gg} = GG chamber length (in.)
- t_{gg} = chamber wall thickness (in.)
- ρ_{cyl} = material density ($lb/in.^3$)

The stay-times used to determine L_{gg} are

H_2/O_2 - t_s	= .0025 sec
Storables - t_s	= .005 sec
Lox/HC - t_s	= .008 sec

Chamber volume is thus: $V_c = t_s \omega / \rho_{gas}$

Chamber length is: $L_{gg} = \frac{V_c}{A_c} = \frac{V_c}{A_t CR}$

Although not exact, the stay time approach gives some insight into the time available for mixing, decomposition, and vaporization. The accuracy is consistent with the gas generator/preburner impact on stage weight.

4.12 HEAT EXCHANGER (Autogenous)

The required surface area and tubing length in the heat exchanger are calculated based on propellant temperatures, pressure, and hot gas transport properties. Tubing weight is multiplied by an empirically derived factor to account for the additional weight or brackets, welds, and attach hardware.

The first task is to get the fluid properties of the hot gas and cold liquid at both inlet and outlet conditions. Next, the energy necessary to raise the liquid temperature, vaporize it, and raise the gas temperature to the desired value is approximated as

$$\Delta H = [(T_{sat} - T_{in})\ \overline{C}_{pliq} + \Delta H_{vap} + (T_{out} - T_{sat})\ \overline{C}_{pvap}]\ \omega_{liq}$$

where:
- T_{sat} = saturation temperature of liquid propellant (°R)
- T_{in} = inlet liquid temperature (°R)
- $\overline{C}_{pliq}$ = average liquid heat capacity = $(C_{pin}+C_{psat})/2$ (Btu/lb °R)
- ΔH_{vap} = heat of vaporization (Btu/lb)
- T_{out} = desired outlet temperature (°R)
- $\overline{C}_{pvap}$ = average vapor heat capacity = $(C_{psat}+C_{pout})/2$ (Btu/lb °R)
- ω_{liq} = liquid flow rate (lb/sec)

This energy must be provided by the hot gas. The temperature drop of the hot gas can be calculated as

$$\Delta T_{gas} = \Delta H/(\omega_{gas}\ C_{pgas})$$

where:
- ΔH = energy required to change liquid to ullage gas (Btu/lb)
- ω_{gas} = mass flow rate of hot gas (lb/sec)
- C_{pgas} = heat capacity of hot gas (Btu/lb °R)

After making some approximations for the gas-side and liquid-side heat transfer coefficients, the overall heat transfer coefficient can be calculated as

$$h_t = 1 / (1/h_{liq} + 1/h_{gas})$$

by neglecting the thermal resistance at the metallic tube wall. The overall tube surface area required for heat transfer (A) is a function of the energy required to be transfered, the overall heat transfer coefficient, and the temperature difference between the propellants (log mean temperature).

$$A = \Delta H \, h_t \, / \, \Delta T_{log}$$

where:

$$\Delta T_{log} = \frac{[(T_{gasin} - T_{liqin}) - (T_{gasout} - T_{liqout})]}{\ln [(T_{gasin} - T_{liqin}) / (T_{gasout} - T_{liqout})]}$$

By assuming a nominal tube diameter (3/8 in.) the total length of tubing can be calculated. Assuming a tube wall thickness of .032 in. and a material density of 0.28 lb/in^3 the tube weight can be calculated as

$$W_{tubes} = \pi \, D \, t \, L \, \rho$$

In addition to the tube weight, the heat exchanger housing weight must be calculated. An empirical correlation which includes weight contributions of brackets, baffles, etc., is

$$W_{house} = 5.04 \times D_{man}$$

where: D_{man} = hot gas manifold diameter (in.)

The overall heat exchanger weight (W_{HX}) is then

$$W_{HX} = W_{tubes} + W_{house}$$

A typical autogenous heat exchanger is shown in Figure 4.12.1.

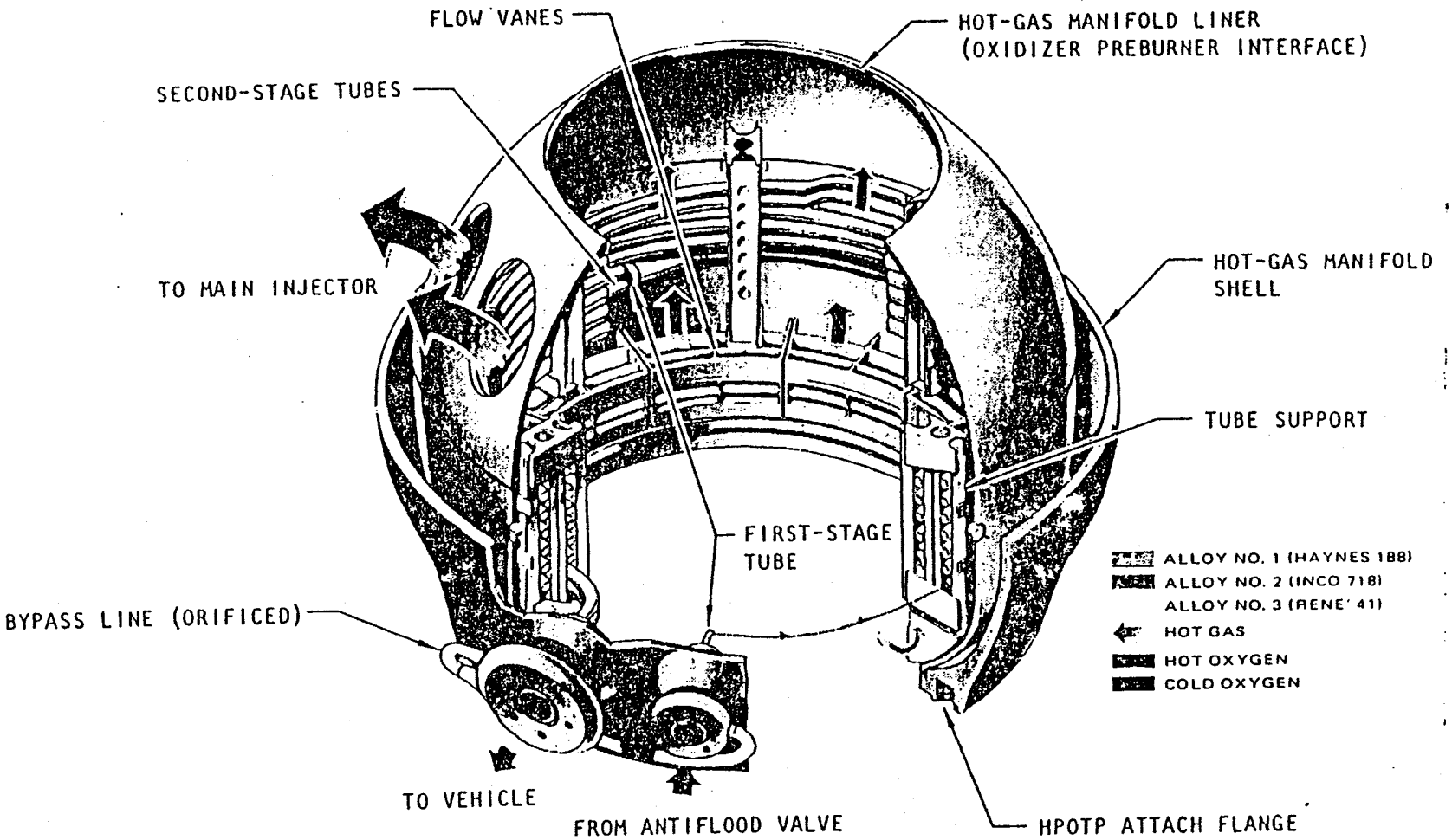

Figure 4.12.1. LOX Tank Pressurization Heat Exchanger

4.13 PROPELLANT LINES DOWNSTREAM OF BOOST PUMP

Propellant line's wall thickness is determined by hoop stress (Pr/t) while the line radius is calculated from the continuity equation using the following flow velocities:

Pump Fed System	= 40 fps
Pressure Fed system	= 20 fps
Hydrogen Fuel	= 200 fps

Main pump discharge line length (see Figure 4.13.1) is estimated as shown below:

$$L = \frac{\pi D_c}{2} + \frac{D_c}{2}$$ (half the circumference + half the chamber diameter)

where: D_c = Chamber Diameter. (in.)

The boost pump discharge line length is estimated as ½ the overall tank length.

Line weight (W_{line}) is calculated by:

$$W_{line} = (2\pi r t L \rho)\ CXWLIN$$

where:
- r = radius (in.)
- t = wall thickness (in.)
- L = length (in.)
- ρ = line material density ($lb/in.^3$)
- CXWLIN = empirically determined constant times the weight (default = 2.5) to account for weight of flanges, bolts, bellows, bosses, insulation, etc.

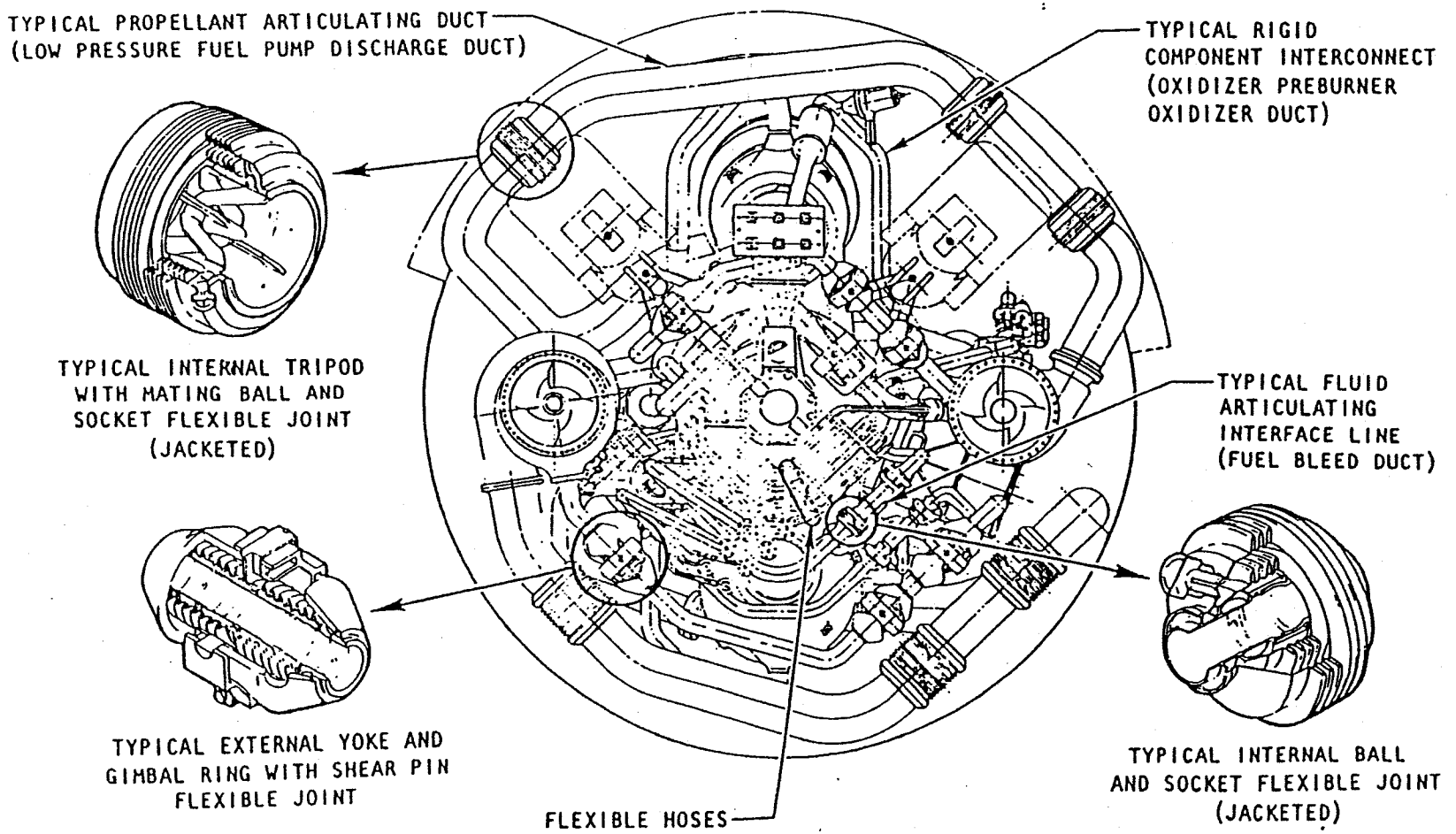

Figure 4.13.1. Typical Propellant Line Configuration

4.14 START SYSTEMS

Size and weight algorithms were developed for four separate start system options. These options are: 1) tank head start, 2) cold gas spin, 3) liquid/pneumatic start tanks, and 4) solid propellant cartridges.

The volumes and dimensions of these systems are based on their containing the mass in one second of rated GG flow at a given pressure, while the wall thickness of the pressure vessels is based on the Pr/t equation.

Valve and control weights are predicted by the following equation:

$$W_{valve} = 1.476 * \rho_v \left[\frac{\omega_v}{\sqrt{\rho_f \Delta P_v}}\right] C_v$$

where:

W_{valve}	=	valve weight (lb)
ρ_v	=	valve material density lb/in.^{3}
ω_v	=	valve flowrate (lb/sec)
ρ_f	=	fluid density (lb/in.^{3})
ΔP_v	=	valve pressure drop (psia)
C_v	=	complexity factor (default = 1)

Various empirically determined multiplying factors are also utilized to account for the additional weight of items such as bellows, bosses, flange, attach hardware etc.

The tank head start system uses the initial pressure in the propellant tanks to spin up the turbo machinery. There is no additional hardware weight for this approach.

The cold gas spin system contains one hydrogen bottle connected through a series of lines and 4 valves to the turbine inlet. Sphere size is based on containing a mass equal to one second of rated turbine flow at twice the nominal inlet pressure. Wall thickness of the sphere is based on a hoop stress calculation ($t = Pr/2\sigma$).

The liquid/pneumatic start system (see Figure 4.14.1) is a self contained and manifolded unit consisting of 2 gas storage vessels, 2 propellant accumulators, and 3 valves. The liquid portion of the accumulator contains the mass in one second of turbine flow. The gaseous volume of the accumulator is three times the liquid volume. The accumulator pressure is twice the turbine inlet pressure. The nitrogen pressure bottle is twice the accumulator pressure and equal in volume.

The solid propellant cartridge start system contains the mass in 0.5 seconds of turbine flow. The grain is a hollow cylinder which burns from both sides.

4.15 ENGINE LENGTH

The engine length is calculated as the sum of the major engine length components

$$L_{eng} = L_{mount} + L_{injff} + L' + L_{noz}$$

where:

L_{eng}	= engine length (in.)
L_{mount}	= length from tank to engine gimbal point (in.)
L_{injff}	= length from injector face to engine gimbal point (in.)
L'	= combustion chamber length (in.)
L_{noz}	= nozzle length (in.)

The mount length (L_{mount}) is a user input. It is the distance from the tank to the engine gimbal point (assuming head-end gimbaling). Ordinarily the default value of 2 inches is appropriate for the gimbal ball mounting bracket; however, if the engine geometry is unusual or the user wishes to adjust the overall engine length, any positive or negative value may be used.

To determine the distance between the engine and the tankage it is necessary to know valve, injector, and mount sizes as well as line routing and component packaging geometry.

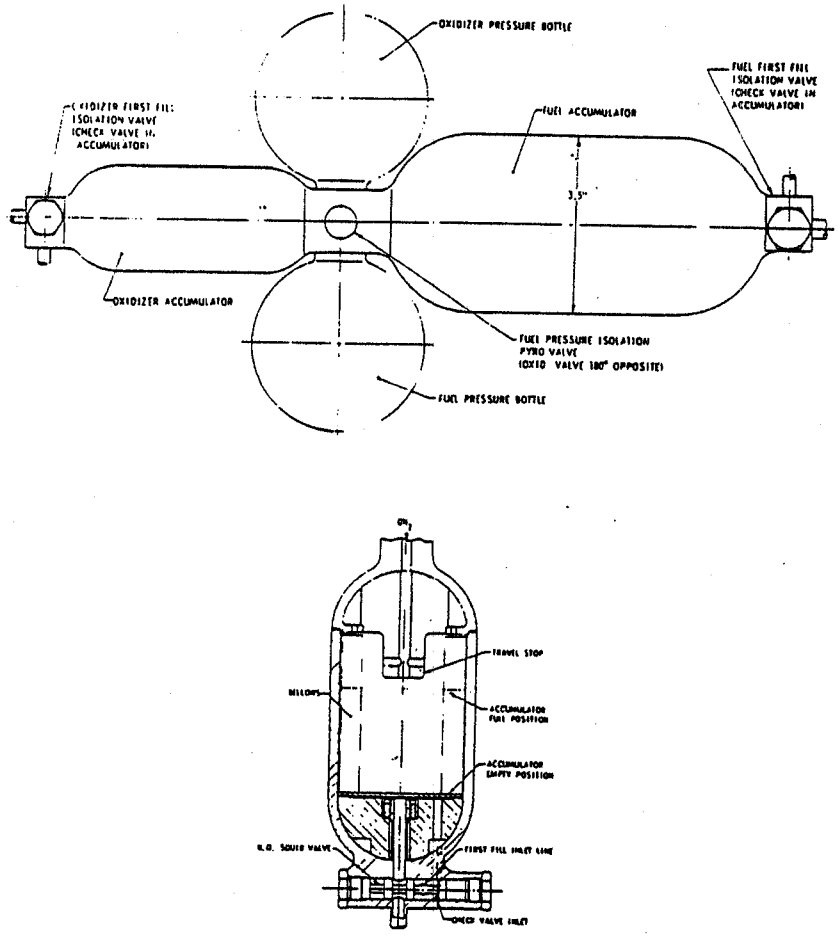

Figure 4.14.1. Typical Liquid/Pneumatic Start System

An alternative to this approach is to curve-fit available data for the distance from the injector face to the gimbal point of the engine. This avoids the many complexities and pitfalls of the first approach.

This second method was employed with the result that

$$L_{injff} = (0.3154\ F^{0.32801} + 2.36)$$

where: F = thrust (lbF)

L_{injff} = length (in.) from the injector face to engine gimbal point

Fifteen engines were used to generate this equation over a thrust range of 100 to 100,000 lbF.

The combustion chamber length (L') is a user input. It is made up of two components, the chamber cylindrical length (XLC) and convergent length (XLN). Ordinarily these values are based on engine performance, cooling, weight, or length considerations.

The nozzle length is calculated based on the nozzle type, expansion area ratio, and throat dimension. The user chooses between Rao and conical nozzles and inputs the desired expansion area ratio. The throat dimension is calculated by the performance routine.

Since for Rao nozzles an input to ELES is the ratio of nozzle length to that of a minimum length Rao, a nozzle length equation as a function of this ratio (RATMLR) was generated. A curve-fit of data presented in CPIA 178* relates minimum length Rao nozzles to Bell Nozzles.

*J. L. Pieper, ICRPG Liquid Propellant Thrust Chamber Performance Evaluation Manual, CPIA No. 178, September 1968.

The length of a minimum length Rao nozzle is related to the length of a 100 percent bell nozzle by the following equation

$$f_{Bell} = \frac{\varepsilon + 1009}{1612.1}$$

where: f_{Bell} = Bell nozzle length fraction
ε = area ratio of minimum length Rao nozzle

From the definition of a 100 percent Bell nozzle length

$$L_{noz\ bell} = R_t\ (\sqrt{\varepsilon} - 1)/.26795$$, it follows that

Therefore:

$$L_{noz\ RAO} = RATMLR\ (\frac{\varepsilon + 1009}{1612.1})\ \frac{R_t\ (\sqrt{\varepsilon} - 1)}{0.26795}$$

where: RATMLR = ratio of nozzle length to length of min length RAO nozzle
ε = area ratio
R_t = throat radius (in.)
L_{noz} = nozzle length (in.)
R_t = throat radius (in.)

For conical nozzles, the nozzle length is simply

$$L_{noz} = (R_{exit} - R_t)/\tan\alpha = R_t\ (\sqrt{\varepsilon} - 1)/\tan\alpha$$

where: α = expansion half angle
R_{exit} = nozzle exit radius

5.0 SHORT ENGINE DESIGNS

5.1 PLUG CLUSTER PERFORMANCE AND BASE PRESSURIZATION

One of the short engine geometries selected for ELES is the plug cluster. The plug cluster is formed from a cluster of modules with Rao or bell-type nozzles extending the full length of the engine as shown in Figure 5.1.1. A central, fluted baseplate is provided and the nested bells are scarfed (see Figure 5.1.2), if desired, for maximum performance and reduced weight. The bells are tilted toward the centerline of the engine at an angle to satisfy the geometry and Prandtl-Meyer expansion criteria. Since the aerodynamics of the flow from each module very closely resemble that for conventional bell nozzles, the JANNAF simplified procedures provide an accurate representation of the performance (providing the base contribution and altitude effects are taken into consideration).

The user-specified engine parameters for a plug cluster refer to a single module of the cluster. The input parameters are module chamber pressure, area ratio, vacuum thrust, mixture ratio, number of modules, and engine diameter. It is with these values that ELES calculates the geometry and flow rates of a single module by the normal performance model. Total plug cluster performance and geometry are then calculated as follows.

User inputs:

P_c	= module chamber pressure (psia)
ε_m	= module area ratio $(De/Dt)^2$
F_{mvac}	= module thrust (lbF)
N_m	= number of modules
D_E	= engine (or vehicle) diameter limit (in.)

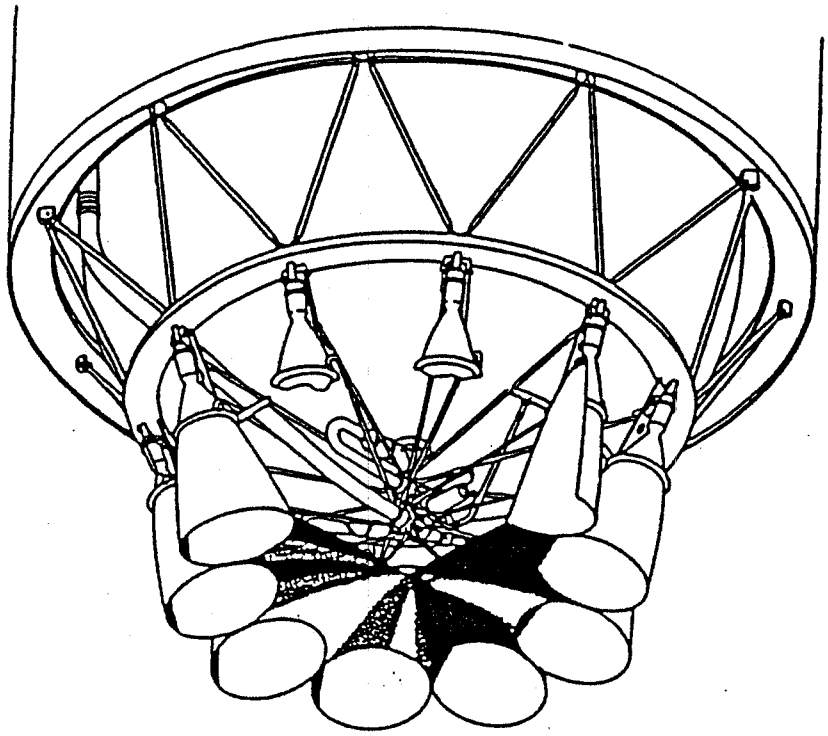

Figure 5.1.1. Clustered Bell Nozzle Concept

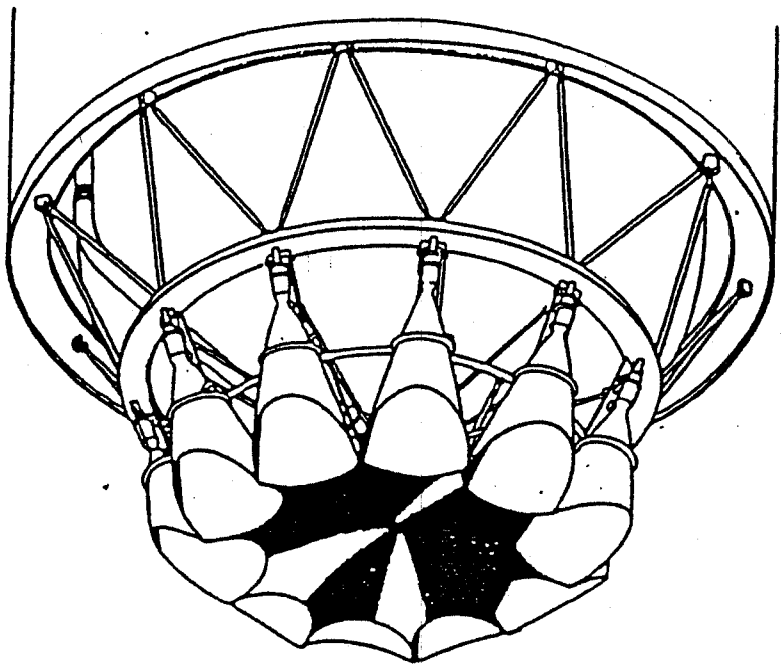

Figure 5.1.2. Scarfed Bell/Plug Cluster Engine Concept

ELES Calculated geometry and flow inputs:

ε_E	= engine area ratio
θ	= module tilt angle (deg)
R_{exit}	= module exit radius (in.)
A_{exit}	= module exit area (in.^{2})
η_m	= module performance loss multiplier
ω_m	= module weight flow (lb/sec)
A_{tm}	= module throat area (in.^{2})
P_a	= ambient pressure (psia)
D_t	= module throat diameter (in.)
D_e	= module exit diameter (in.)

In order to calculate the overall engine area ratio, begin by calculating the angle between modules (ϕ), the radius from the plug cluster center point to the module center point (R_c), and the overall plug cluster radius (R_o).

$$\phi = \frac{2\pi}{N_m}$$

$$R_c = R_{exit} / \sin (\phi/2)$$

$$R_o = R_c + R_{exit} \cos \theta)$$

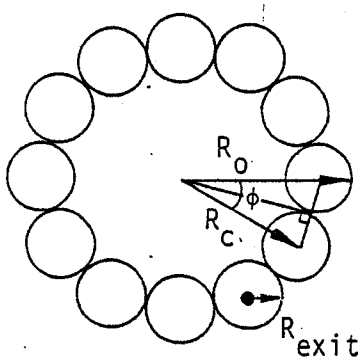

The overall exit area of the plug cluster (A_{Eexit}) can be calculated by adding the area of the triangles which use nozzle center points as vertices, and the portion of the module exit areas not included in the triangles.

$$A_{Eexit} = N_m R_{exit} R_c \cos(\tfrac{\phi}{2}) + N_m (\tfrac{\pi + \phi}{2\pi}) A_{exit} \cos\theta$$

Using the exit area to calculate total expansion area ratio is then

$$\varepsilon_E = A_{Eexit} / N_m A_{tm}$$

$$= \varepsilon_m \left[\frac{1}{\pi \tan(\frac{\phi}{2})} + (\tfrac{\pi + \phi}{2\pi}) \cos\theta \right]$$

The above equation for total area ratio is solved iteratively in ELES, since it is expressed in terms of the module tilt angle (Θ). The value of Θ is calculated by assuming that the gas expands isentropically from the Mach number at the module exit to the Mach number at the cluster exit. Under this assumption, the tilt angle (Θ) is equal to the difference in the corresponding Prandtl angles, at D_E and D_e.

$$\Theta = \nu_E - \nu_M$$

where: ν_E = Prandtl-Meyer angle of plug exit Mach number M_E

$$= \left(\frac{\gamma+1}{\gamma-1}\right)^{\frac{1}{2}} \tan^{-1}\left[\left(\frac{\gamma-1}{\gamma+1}\right)(M_E^2 - 1)\right]^{\frac{1}{2}} - \tan^{-1}(M_E^2 - 1)^{\frac{1}{2}}$$

ν_M = Prandtl-Meyer angle of module exit Mach number M_e

$$= \left(\frac{\gamma+1}{\gamma-1}\right)^{\frac{1}{2}} \tan^{-1}\left[\left(\frac{\gamma-1}{\gamma+1}\right)(M_e^2 - 1)\right]^{\frac{1}{2}} - \tan^{-1}(M_e^2 - 1)^{\frac{1}{2}}$$

and: γ = 1.2 is assumed.

Plug cluster performance is a function of both module performance and base pressurization. The module performance is analyzed by the method described for a normal DeLaval engine. The base pressure is calculated by a base pressure correlation. The overall plug cluster engine thrust (F_{plug}) is then

$$F_{plug} = N_m F_{mvac} C_T + P_B A_{base} C_{base}$$

where:

F_{plug}	= plug cluster thrust (lbF)
N_m	= number of modules
F_{mvac}	= module vacuum thrust (lbF)
C_T	= module thrust efficiency
P_B	= base pressure (psia)
A_{base}	= base area (in^2)
C_{base}	= base thrust efficiency

The contribution to thrust by the modules is degraded by the multiplier C_T. A typical value for C_T is 0.99. The base pressure contribution to the thrust has been correlated to the nozzle separation criteria as

$$\frac{P_B}{P_C} = e^{(0.48 + 0.87 \ln(P_e/P_C))}$$

except when $P_e/P_B \leq 0.27$, then the value of $P_e/P_B = 0.27$

where: P_B = base pressure (psia)
P_C = chamber pressure (psia)
P_e = exit pressure of nozzle having overall area ratio of plug cluster (psia)

After using the above equation to calculate base pressure, the base area is calculated as the difference between the total exit area and the module exit areas.

$$A_{base} = A_{E\ exit} - N_m A_{exit}$$

The constant, C_{base}, is determined empirically as 0.7. There is now enough information to evaluate the equation for plug thrust (F_{plug}).

The nozzle exit pressure (P_e) in the above equations is obtained from a curve-fit of the ideal isentropic expansion equation for constant gamma (γ)

$$1/\epsilon = \left(\frac{\gamma+1}{2}\right) \left(\frac{1}{\gamma-1}\right) \left(\frac{Pe}{Pc}\right)^{(1/\gamma)} \sqrt{\frac{\gamma+1}{\gamma-1} \left[1 - \left(\frac{Pe}{Pc}\right)^{(\gamma-1)/\gamma}\right]}$$

Assuming a constant value of 1.2 for gamma and evaluating the above equation for a large range of expansion ratio (ϵ), a curve-fit can be generated for Pe/Pc in terms of ϵ .

$$(P_e/P_C)^{-1} = P_C / P_e$$

$$= EXP\left[\frac{\ln\epsilon}{.80065} - .87203\ EXP\left\{-[(\epsilon - 1)\ 1.11252]^{.43032} + 1.56518\right\}\right]$$

5.2 PLUG CLUSTER LENGTH

The length of the plug cluster is determined primarily by the length of the modules which form it. In ELES the plug is designed such that there are no gaps between the modules. For modules of less than 200 to 1 area ratio, the tilt angle is less than 12 degrees. The effect of module-tilt on plug cluster length (L_{pc}) will therefore be ignored. The plug cluster length is the same as that of a single engine of the same thrust as one module. Thus

$$L_{pc} = L_{mnoz} + L_{mchm} + L_{miff}$$

where:

$$L_{mnoz} = \left(\frac{\varepsilon_m + 1009}{1612.1}\right) \frac{R_{tm}\ (\varepsilon_{m-1})}{.26795}\ RATMLR_m$$

$$L_{mchm} = XLN_m + XLC_m$$

and:

$$L_{miff} = .3154\ F_{mvac}^{.38201} + 2.36$$

L_{mnoz} = module nozzle length (in.)
L_{mchm} = module chamber length (in.)
L_{miff} = length from module injector face to forward module (in.)
$RATMLR_m$ = module ratio of nozzle length to that of minimum length Rao nozzle (-)
ε_m = module area ratio (-)
R_{tm} = module throat radius (in.)
XLN_m = module convergent chamber section length (in.)
XLC_m = module cylindrical chamber section length (in.)
F_{mvac} = module vacuum thrust (lb)

5.3 PLUS CLUSTER WEIGHT

In the same manner that module parameters are used to calculate plug cluster performance, they are also used to calculate plug cluster weight. The weight of a single module is calculated by the same routines which calculate weight for a single TCA. These routines require module parameters such as area ratio, throat diameter, contraction ratio, chamber length, nozzle type and contour, etc. The weight of the plug cluster is

$$W_{\text{plug cluster}} = N_m W_{MODULE} + SA_{BASE} (t_{BASE} \rho_{BASE} + t_{INSUL} \rho_{INSUL})$$

where:

N_m	= number of modules	(-)
W_{MODULE}	= weight of single module	(lb)
SA_{BASE}	= surface area of base	(in^2)
t_{BASE}	= effective thickness of base	(in.)
ρ_{BASE}	= density of base material	($lb/in.^3$)
t_{INSUL}	= effective thickness of base insulation	(in.)
ρ_{INSUL}	= density of base insulation	(lb/in^3)

5.4 PLUG CLUSTER MOUNT WEIGHT

The plug cluster engine mount can be more complex than that of a single TCA of the same thrust. A measure of that complexity is the number of modules in the cluster. This situation is reflected in the following method of calculating plug cluster mount weight.

$$W_{tmpc} = N_M W_{tmM} + W_{tmb}$$

where:

W_{tmpc} = Weight of plug cluster thrust mount (lbm.)

N_m = number of modules

W_{tmM} = weight of module thrust mount (lbm.)

$= f_{tm}(F_{mvac})$

W_{tmb} = weight of base thrust mount (lbm.)

$= f_{tm}(F_b)$

$f_{tm}(F)$ = thrust mount weight function

$= \frac{\ln F - 7.059}{.06305}$, for: $F \geq 6438$ lbf.

$= 17\ (F/6438) + 3$, for: $F < 6438$ lbf.

F_{mvac} = module vacuum thrust (lbf.)

f_b = base vacuum thrust (lbf)

$= F_{Evac} - N_m F_{mvac}$

F_{Evac} = total plug cluster vacuum thrust (lbf.)

5.5 ANNULAR ENGINE MODEL

An annular engine combustion chamber is designed in such a manner that the throat cross section is at the outer diameter, and the throat flow is aft in a radially inward direction (see Figure 5.5.1). The expansion of the exhaust gases is greatly affected by the ambient pressure such that there are no overexpansion losses. This altitude compensating thrust advantage must be balanced against the disadvantages of the additional weight, complexity, and cooling difficulty of the design.

ELES sizes the annular engine to meet the user-input value of vacuum delivered thrust by neglecting the contribution of base pressurization (the modules of plug clusters are sized by the same criteria). The base pressurization thrust calculation is performed after the annular engine is sized. This approach to the engine design procedure simplifies an otherwise iterative process and results in an engine thrust only slightly greater than the user-input value.

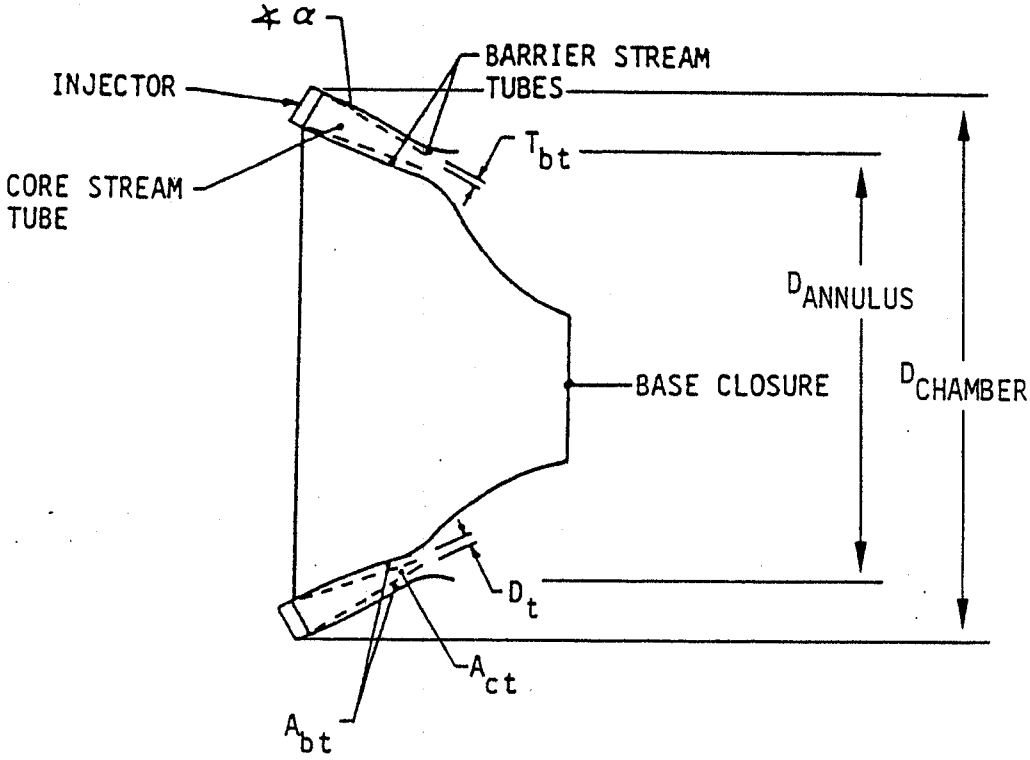

Figure 5.5.1. Annular Engine

The performance calculations for annular engines are conducted in a manner similar to that of internal expanding engines with the added complications that the overall area ratio is not known initially and the barrier stream tube has a different geometry. ELES conducts a thrust analysis to produce an engine design which satisfies the equation

$$F_{VAC} = \frac{Pc\ A_t\ Isp\ g_c\ C_T}{C^*}$$

where:

F_{VAC}	=	annular engine vacuum thrust (lbF)
Pc	=	chamber pressure (psia)
A_t	=	throat area ($in.^2$)
Isp	=	delivered Isp (sec)
g_c	=	gravitational constant ($lbm\text{-}ft/lbF\text{-}sec^2$)
C_T	=	annular engine efficiency (-)
C*	=	characteristic velocity (ft/sec)

The delivered C* in the above equation is dependent on the combustion efficiency, and the Isp is dependent on both the combustion efficiency and the nozzle expansion area ratio and efficiency. Given the overall Isp efficiency and C* efficiency, ELES calculates the total throat area and area ratio of the annular engine by an iterative calculation.

In order to arrive at the overall combustion efficiency, ELES performs a stream tube analysis of the annular engine, for which it must make an initial estimate of combustion efficiency. The initial estimate is improved after the stream tube analysis.

There are three stream tubes of interest in the annular engine; the core stream tube and the barrier tubes on either side of the core. The barrier tube thicknesses at the throat are calculated by a mixing angle from the injector face exactly as in the conventional engine. The flowrates in the different stream tubes are based on the geometry of the engine (see Figure 5.5.1). Mass fluxes through each tube are calculated from

$$\text{Mass Flux} = \frac{\omega}{A_t} = \frac{Pc\ g_c}{C^*}$$

where C* is calculated from the stream tube mixture ratios and combustion efficiencies. The mixture ratio maldistribution efficiency is calculated by mass averaging the stream tube performances. The stream tube flows are much greater than those of conventional design, because the throat circumference is much greater than normal.

The base-pressurization-thrust is calculated for annular engines in much the same manner as for plug cluster engines. Use the correlation

$$P_B/P_C = \text{EXP}\ (0.48 + 0.87\ \ln\ (P_e/P_C)$$

where: P_B = base pressure (psia)
P_C = chamber pressure (psia)

to calculate the base pressure and limit the base pressure by

$$(P_B/P_e)_{max} = 3.7$$

$$F_B = P_B\ A_B\ C_B$$

where: F_B = base pressurization thrust (lbF)
P_B = base pressure (psia)
A_B = base area ($in.^2$)
C_B = base pressure thrust efficiency

The base pressure thrust (F_B) is the product of base pressure, base area and a loss factor (C_B) derived from Aerospike test data.

ANNULAR ENGINE REGEN COOLING

The cooling model considered to be most useful for annular engines is the regen/trans-regen cooling model. Because annular engines must cool a fairly large surface area, and because barrier mixture ratio cooling methods are most costly in terms of performance for annular engines, the regenerative cooling method is the best choice. In addition to the above, the regen model allows expander power cycles to be employed. For these reasons ELES provides regenerative cooling with annular engines.

Modifications were made to the standard ELES regenerative cooling model in order to analyze annular engines. The chamber is treated like a conventional De Laval chamber with a throat diameter corresponding to that of the annulus diameter at the annular engine throat. The heat transfer surface area and number of cooling channels are calculated on that basis and then doubled to account for the inner and outer walls of the annular chamber.

This approach results in a close approximation of both the surface area available for heat transfer and the cross sectional flow area for coolant.

ANNULAR ENGINE WEIGHT CORRELATION

A survey of existing annular engine hardware was conducted in order to develop a weight scaling equation. The equation resulting from that survey is

$$W = W_B \left(\frac{F}{F_B}\right)^{0.892} \left(\frac{P_{cB}}{P_c}\right)^{0.278} \left(\frac{\varepsilon}{\varepsilon_B}\right)^{0.289}$$

The scope of the above equation includes combustion chamber, shroud, nozzle, base closure, thrust mount, gimbal assembly, turbopumps, propellant valves, ducting, hot-gas valves, controls, ignition system, and contingency. Some of those items are modeled separately in ELES, specifically the thrust mount, gimbal assembly, turbopumps and ignition system. Because these weight items are always added in by ELES, the equation is ratioed down to reflect only those components not handled elsewhere. Additionally, in order to allow some influence of combustion chamber length on engine weight, the area ratio used in the equation is a modified area ratio.

$$W = 0.40\, W_B \left(\frac{F}{F_B}\right)^{0.892} \left(\frac{P_{cB}}{P_c}\right)^{0.278} \left(\frac{\varepsilon_M}{\varepsilon_B}\right)^{0.289}$$

where:

W_B = 1030 lbm (baseline engine weight)

F_B = 50,000 lbF (baseline engine thrust)

P_{cB} = 50 psia (baseline engine chamber pressure)

ε_B = 300 (baseline engine area ratio)

ε_M = $\varepsilon \left(D_{chamber}/D_{annulus}\right)^2$
(see Fig. 5.5.1)

6.0 THROTTLING ENGINES

6.1 THROTTLING ENGINE PERFORMANCE

Throttled engine performance can be simulated by using a variable thrust profile which consists of four time intervals. A thrust level can be specified for each time interval. The allowable thrust level can be equal to zero or it can range from ten to one hundred percent of full thrust. Thrust levels outside this range will be reset to full thrust or zero by the code. Optimization of the thrust profile can be accomplished by varying the thrust values and time intervals. Reduced Isp efficiency (caused by throttling) is approximated through tables of throttling efficiency versus thrust fraction.

The throttled thrust level is specified indirectly through the use of a chamber pressure fraction (Pc/Pc_{des}). Pc_{des} is the maximum design operating pressure such that the value of Pc/Pc_{des} is less than or equal to 1.0.

Throttling has been implemented by applying the throttling ratio to the design chamber pressure (Pc). The engine design and sizing is done using this design Pc as if it were an unthrottled engine. The throttling efficiency of the engine must be input by the user as a table of chamber efficiency and nozzle efficiency versus chamber pressure fraction.

The additional weight of a throttlable engine can be accounted for by using the engine weight multiplier or the engine component weight multipliers.

A full analysis of throttling liquid bipropellant thrust chamber performance is not within the scope of ELES, but a brief discussion of the subject follows in order to define the throttling efficiency model. The performance obtained from a throttling engine depends on the dominant loss mechanisms throughout its throttling range. In an engine where propellant mixing is the dominant loss mechanism, it is possible to obtain widely

different $\eta_{throttle}$ vs. Pc/Pc max curves. Such parameters as injection element spray overlap or propellant blowapart characteristics are required to determine the trend of $\eta_{throttle}$ with Pc/Pc max. A comparatively more simple situation would be a vaporization-limited chamber; under this condition throttling performance is more predictable. The following equation is an Aerojet approximation for vaporization-limited throttling efficiency.

$$\eta_{throttle} = \frac{1.0 - (1.0-\eta_{ere\ vap})\ (1.0\ /\ \sqrt{Pc/Pcmax}}{\eta_{ere\ vap}}$$

Notice that the throttling efficiency depends on the energy release efficiency of the unthrottled chamber as well as the degree to which the engine is throttled.

The user is cautioned when inputting $\eta_{throttle}$ vs. Pc/Pc max tables that throttling performance is highly complex and specific to the engine design under consideration. The default $\eta_{throttle}$ vs Pc/Pc max table which follows assumes a vaporization-limited chamber with an energy release efficiency of 0.975 at full chamber pressure. When these assumptions are inconsistent with the case of interest, a new $\eta_{throttle}$ vs. Pc/Pc max table should be used.

Default Vaporization-Limited Throttling Efficiency Table (η_{ere} = 0.975)

$\eta_{throttle}$ (ERETHR)	Pc/Pc max (THRPC)
1.0	1.0
0.997	.8
0.993	.6
0.985	.4
0.968	.2
0.945	.1

When deciding what $\eta_{throttle}$ vs. Pc/Pc max table to input, the following may be of help. The assumption of a vaporization-limited engine is normally good for storable propellant engines. For LOX/hydrocarbon, mixing and vaporization limitations are equally common. If a gas-gas injector is being used then mixing is dominant. In the event that a mixing-limited engine is under investigation, either test data or an analysis of that specific engine will be required.

6.2 WEIGHT OF THROTTLING ENGINES

Engines which throttle are at least as heavy and usually heavier than comparable engines of constant thrust. The greater the degree of throttling, the greater the weight increase. The additional design constraints which accompany a throttling engine are responsible for this weight increase. The control valves will be more complex, the pressure schedule at full thrust will be higher, cooling requirements and combustion stability must both be satisfied over a broader range of conditions, and any turbopump assemblies used will be more complex. A host of other design considerations contribute to the engines' increased weight as well.

The above effects can be accurately quantified only on a case by case basis however the following trends are suggested. Based on engine weight studies done on the first LES contract, the LEM descent engine was about 60% heavier than its predicted weight when using a constant thrust weight model. If that difference is attributed to its 10:1 throttling characteristics, then there is some justification for using a weight multiplying factor of 1.6 on engines which throttle 10:1. It is further suggested that low throttle ratios only slightly affect engine weight (e.g., blow-down systems typically throttle to about 1.5:1 with little impact on weight). Throttle ratios of about 3:1 are considered points of "quantum" changes in the level of design difficulty. These considerations imply an "S" type curve to describe a weight factor vs. throttling ratio relationship. Such a curve is shown below.

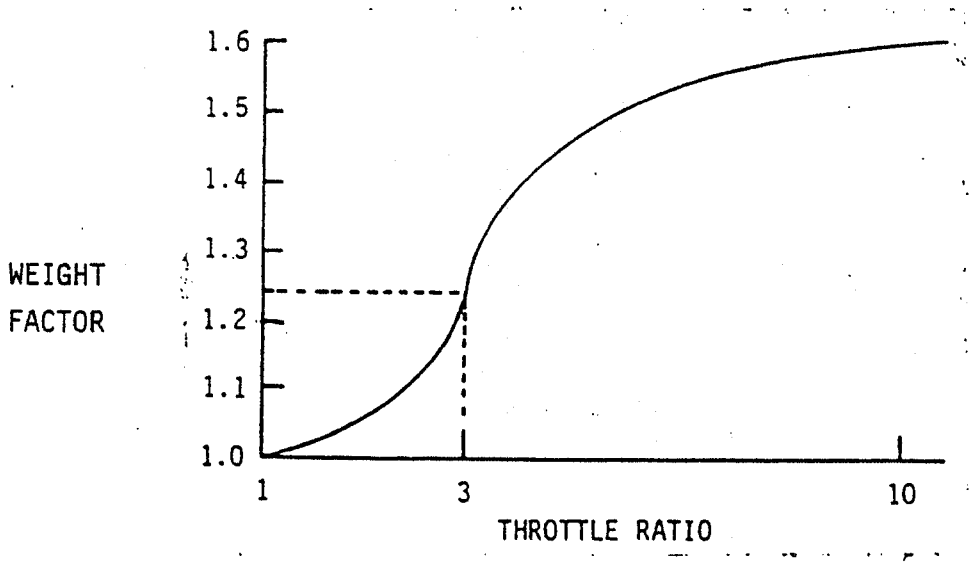

The above curve is suggested for use with ELES. When modeling throttling engines, the input parameter CXWENG should be set equal to that value which corresponds to the throttling ratio under consideration.

6.3 THROTTLING ENGINE PRESSURE SCHEDULE

In a highly simplified analysis of injector requirements for stable operation, there are two major parameters of interest, injector pressure drop and propellant injection velocity. The required injector pressure drop to prevent chug can be calculated from combustion-time-lag analysis. Minimum injection velocity has been empirically determined to be 40 ft/sec. For engines which throttle, the above stability requirements should normally be observed over the whole operating regime (the most difficult condition being the low thrust.)

A parameter in ELES (CHPOPC) is defined as the minimum ratio of injector pressure drop (Δp_j) to chamber pressure (P_c) which can be allowed without chugging. At the low thrust condition, if the ratio of ΔP_j to P_c falls below CHPOPC or the injection velocity falls below 40 ft/sec then ELES will output warning messages to that effect. Methods to correct these conditions include relaxing the throttling requirements, increasing the injector pressure drop, and changing number of orifices on the injector face.

Although CHPOPC has a default value of 0.2, which is a good preliminary estimate, it can easily range from 0.1 to 0.4 or beyond in a real engine design. The impact of this parametric value on the stage pressure schedule can be quite significant.

The method used to calculate ΔP_j at the low thrust condition (ΔP_{jlow}) assumes the equation

$$\Delta P_{jlow} = \Delta P_j (P_{c\ low} / P_c)^2$$

The above equation demonstrates the severe penalty placed on a systems Pressure schedule in a 10:1 throttling environment. ΔP_j must be 10 times ΔP_{jlow} in order to avoid stability problems for the low thrust condition.

Injection velocity is linear with chamber pressure. The injection velocity at the low thrust condition (v_{jlow}) be calculated as

$$v_{jlow} = v_j (P_{c\ low} / P_c)$$

7.0 TANKAGE MODELS

7.1 TANK SIZING PROCEDURE

The tank sizes in ELES for both tandem and non-conventional tank geometries are affected by burned propellant requirements, ullage fractions, acquisition system design, residual propellants, propellant boiloff, and autogenous pressurization. Because of the interdependancy of many of these parameters, it was necessary to devise a scheme within ELES for making simple, fast converging solutions.

The approach taken in these routines is as follows:

1) Calculate weight of each propellant which is burned based on the overall engine mixture ratio.

2) Add to each propellant the weight of autogenous pressurization requirements

3) Calculate the tank free volumes at this point using the propellant densities and ullage fractions.

4) Given this estimate of the free volumes in the tank the propellant residuals and acquisition device volumetric displacement can be calculated.

5) Next the tank surface area is calculated for heat transfer calculations which determine the propellant boiloff.

6) The total tank volume is now calculated as the sum of the above volumes (burnt propellant, ullage, residuals, boil off, autogenous pressurant, and aquisition devices)

The above procedure produces tank volumes which can then be used to determine pressurization requirements. If autogenous pressurization is requested, this step results in an improvement of the initial estimate of autogenous pressurant requirements.

7.2 TANDEM TANK, EXPULSION, AND PRESSURIZATION GEOMETRY

For the tandem tankage model, the lengths and weights of the propellant and pressurization tanks can be obtained from their volumes and geometry. Having established the volumes, this section presents the geometries available to the user and the method by which those geometries are designated. Some bases for choosing a geometry are also included to help the user obtain a more feasible design.

Formulation of the propulsion system size and weight models began with a study of candidate tankage subsystem geometries. Physical mathematical models of tank subcomponents, such as heads, cylinders and lines have been identified. Tankage subsystem models were created by assembling the subcomponent models in various combinations. Cylinders, hemispheres and semioblate spheroids are the major subcomponent geometry models. Separate dome tankage is modeled, having both internal and external propellant lines as well as load carrying and suspended tankage geometries. Figure 7.2.1 depicts the physical geometries which are modeled.

Tanks with bonded rolling bladders are compatible with internal propellant lines, but they provide better design solutions for tanks with nested heads. They can, then, simultaneously provide high expulsion efficiency and small initial ullage fractions. The combination of unused space between separate dome tank heads and a complete oblate spheroid ullage volume in one or both tanks appears to assign such a significant length and weight penalty to a pressure-fed vehicle that it should be considered bad design practice.

The integrated nature of common dome tankage and operational systems data suggest that an important class of such vehicles will feature integration of the pressurization subsystem pressure vessel with the propellant tanks. Figure 7.2.2. depicts two pressurization subsystem geometries that integrate well with common dome tankage: cylindrical, in the forward tank; or spheroidal ahead of and common with the forward tank dome. Notice how bonded rolling bladders are compatible with either style of pressurization geometry, and how the cylinder in the forward tank stiffens the reversed forward dome of the tank. A reversed forward dome may integrate well with certain vehicle front end designs by providing added volume for the payload.

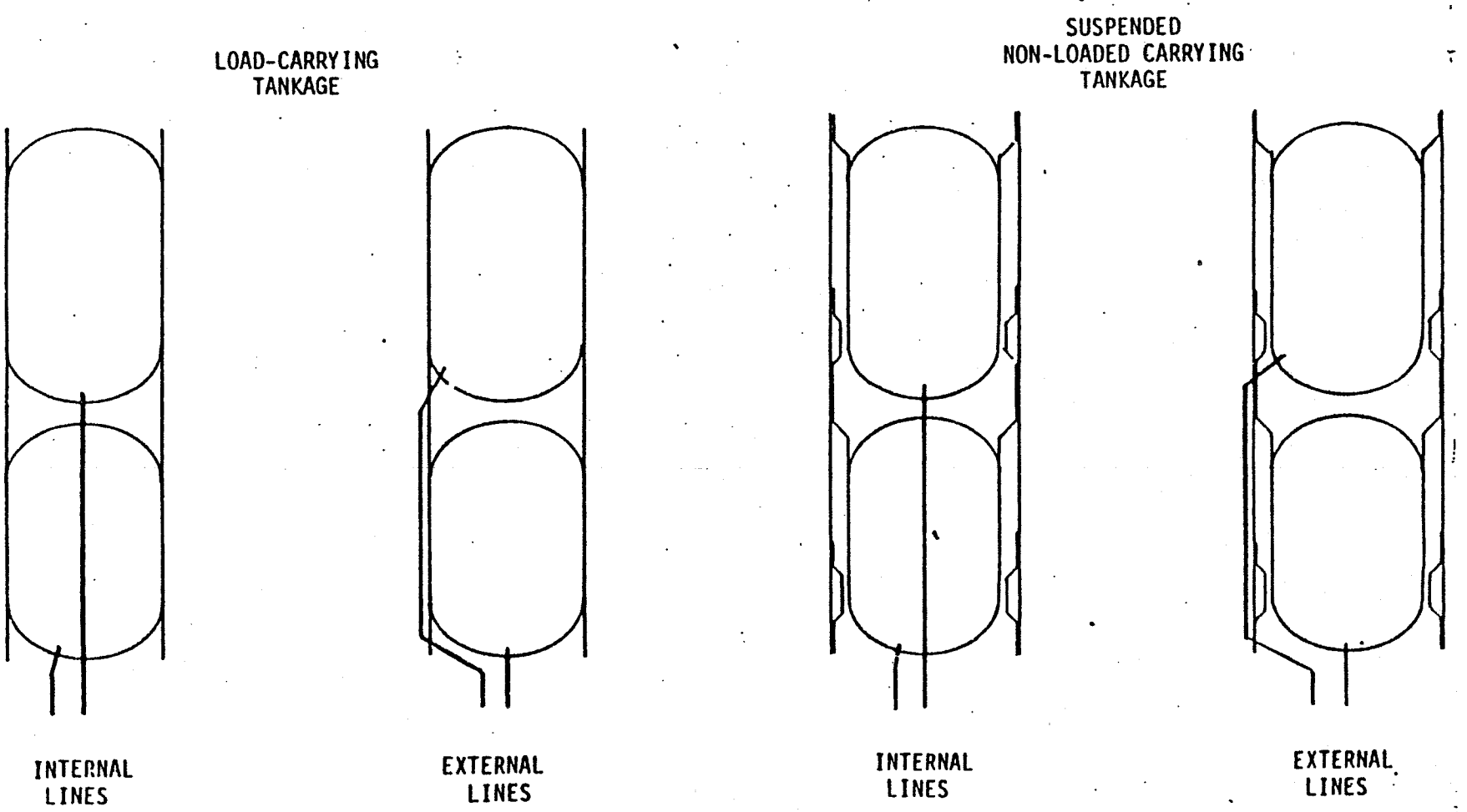

Figure 7.2.1. Separate Dome Tank Schematic

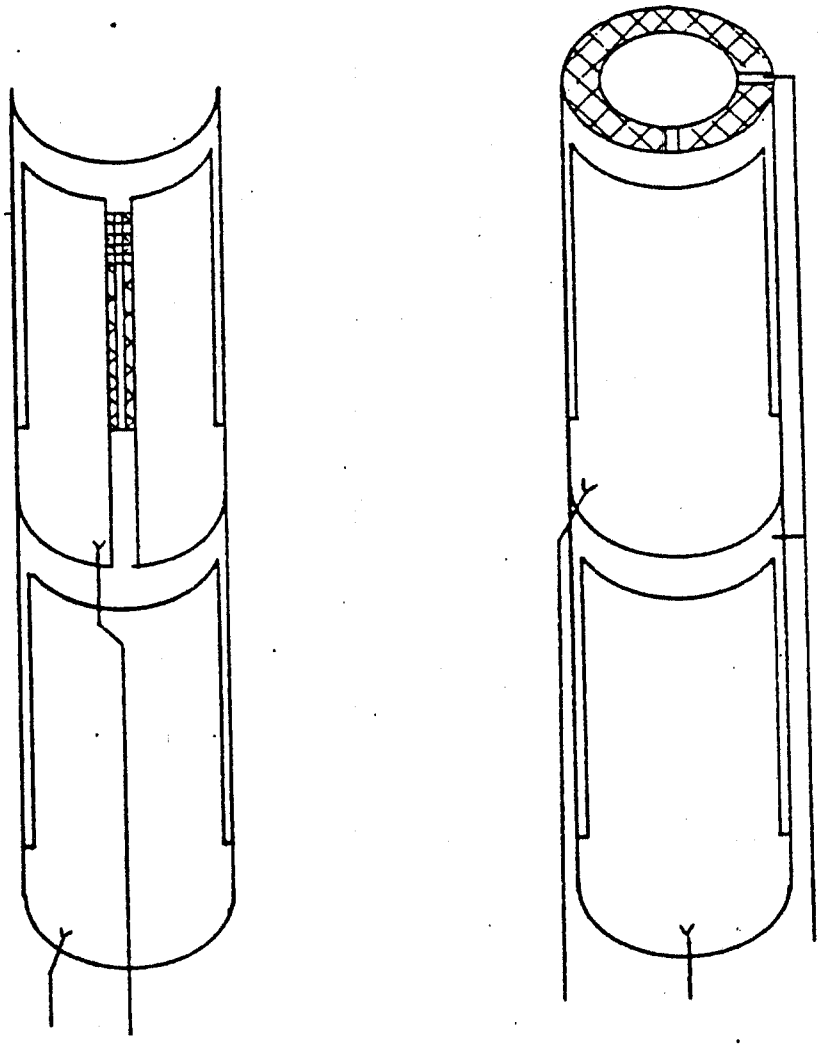

Figure 7.2.2. Common Dome Tank, Integrated Pressurization Options

The major geometric variables for common dome tankage are

- Spheroidal vs Cylindrical vs Non-Integrated Pressurization Vessels
- Bladder vs No Bladder
- Internal vs External Propellant Lines

The twelve remaining designs are depicted schematically in Figures 7.2.3, 7.2.4 and 7.2.5. Table 7.2.1 lists the common set of geometric assumptions underlying the selected design concepts. In concert with Table 7.2.1, Table 7.2.2 lists the tankage geometry flags. Notice that a total of twenty basic tankage/expulsion, pressurization systems are modeled, including those represented in Figure 7.2.1 (with and without bladders) and Figures 7.2.3 through 7.2.5. Other configurations can be modeled by setting geometry flags differently. The user must verify that these configurations are workable.

7.2.1 Tankage Design Assumptions And Geometry Flags

When designing a liquid stage, there are many constraints which dictate its general layout. Some general considerations are included in Table 7.2.1. Once the layout is decided, it can be defined within ELES through the use of stage geometry flags (Table 7.2.2). These flags allow definition of those stages which are diagrammed in the preceding pages as well as many others. The use of flags is straightforward; specify each one to correspond to the local geometry of the stage being investigated.

7.2.2 Tank, Expulsion, And Pressurization Size/Weight

The first step in determining a subsystem weight is to define the scope of weight items within that subsystem. This section itemizes the weight scope of the tankage, pressurization, and expulsion subsystems. It also describes the algorithms required to calculate the size and weight of all scope items. The algorithms are used to calculate volumes, thicknesses, and lengths, as well as weights.

INTERNAL LINES

SPHEROID PRESSURE

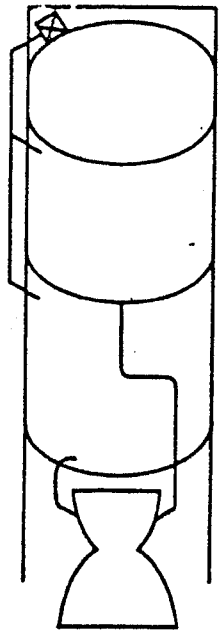

CYLINDRICAL PRESSURE

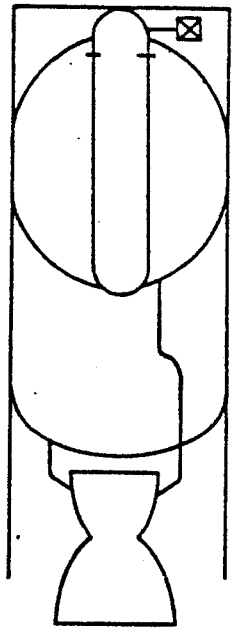

EXTERNAL LINES

SPHEROID PRESSURE

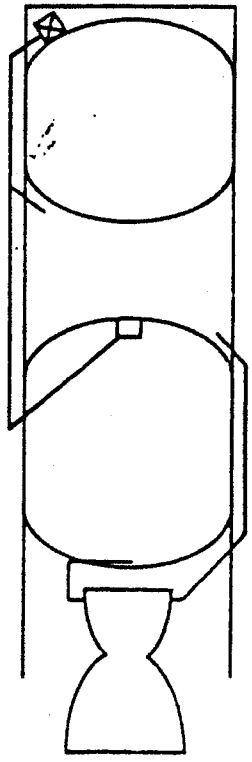

CYLINDRICAL PRESSURE

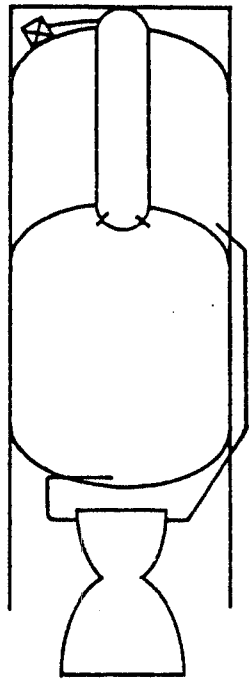

Figure 7.2.3. Common Dome Tanks, Integrated Pressurization, No Bladder

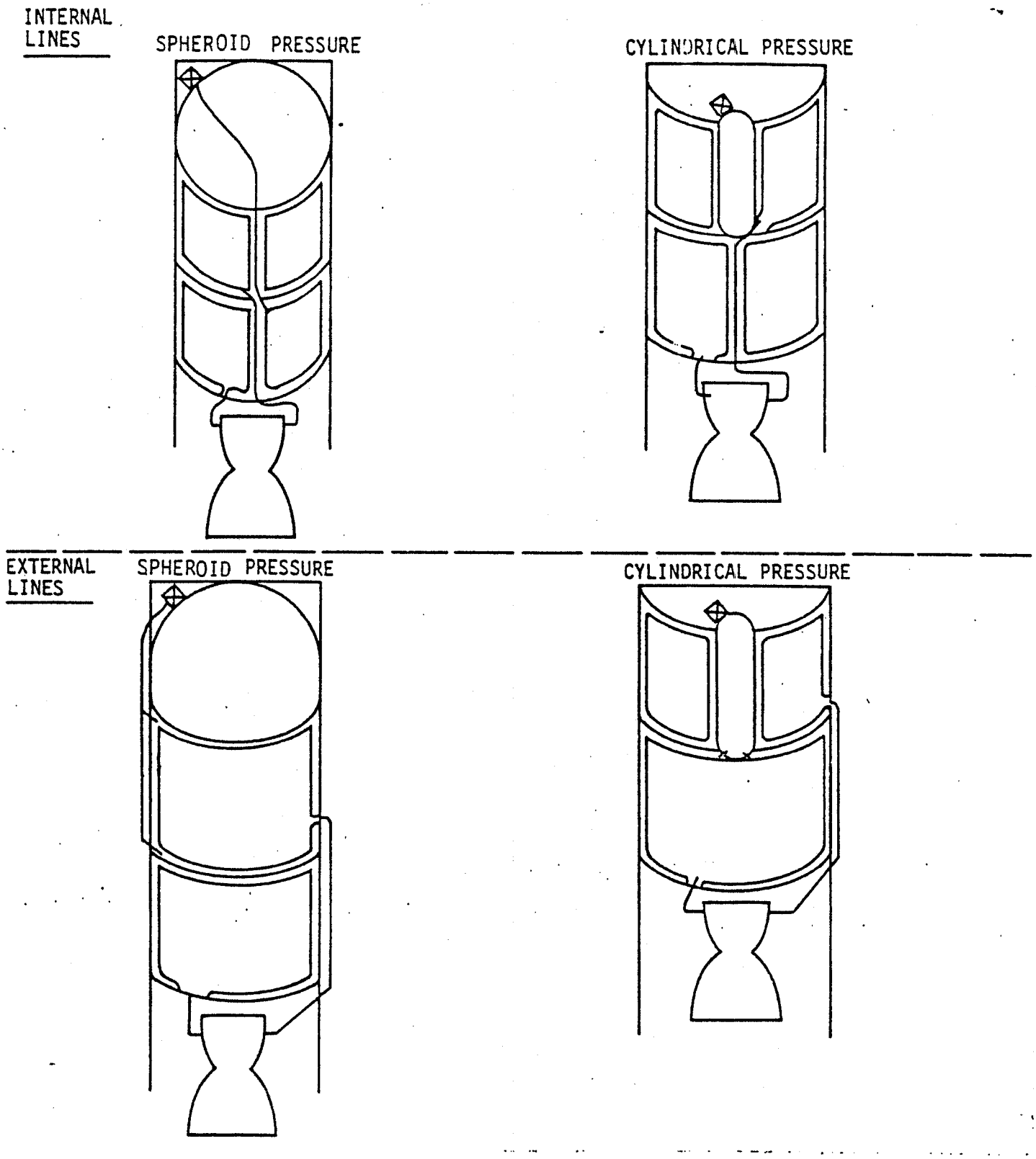

Figure 7.2.4. Common Dome Tanks, Integrated Pressurization, With Bladder

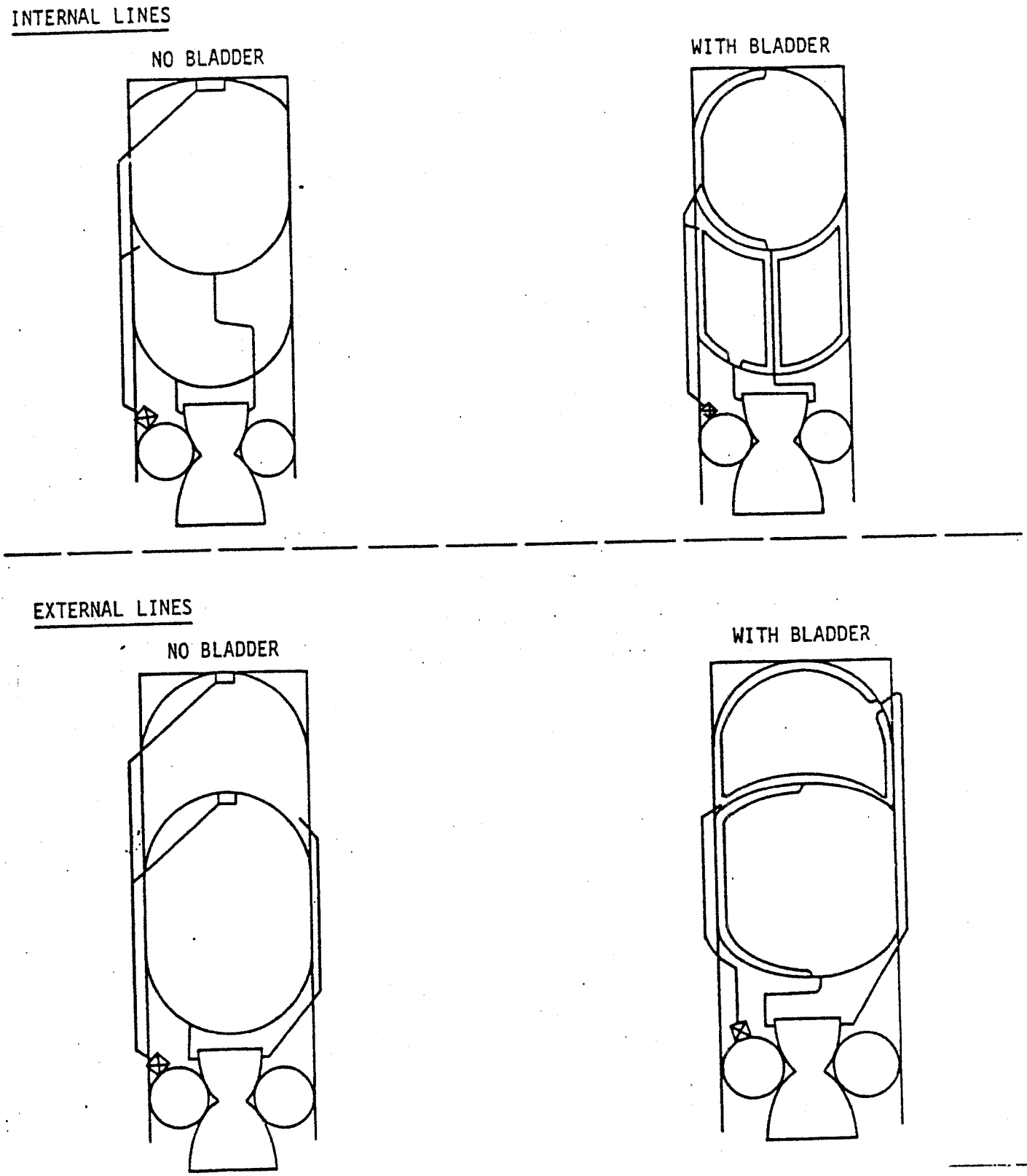

Figure 7.2.5. Common Dome Tanks, Non-Integrated Pressurization

TABLE 7.2.1

ASSUMPTIONS CONTROLLING TANKAGE GEOMETRY

1. Selection of "No Bladder" implies a cold gas pressurization system selection.
2. "Internal Lines" refers to the forward propellant tank line only.
3. All propellant tankage is tandem mounted.
4. A Common Dome tankage selection implies that the stressed external skin of the stage is also common with the tank wall.
5. A Common Dome tankage having "internal lines" implies the common dome is oriented convex aft.
6. Common Dome Tankage having "external lines" implies the common dome is oriented convex forward unless both "bladder" and "integrated pressurization" is also specified.
7. The movable heads of Bonded Rolling Bladders are pressurized from the concave side.
8. Bonded Rolling Bladders are used, when "bladder" specified and tank heads nest.
9. Transverse Collapsing Bladders are used, when "bladder" specified, and tank heads oppose.
10. When Common Dome Tanks, Bladder and Integrated Spheroidal Pressurization geometry are simultaneously specified, the pressurization and propellant tanks must have identical head ellipse ratios.
11. Bladders may be specified in only one of two tanks, if desired.
12. When Common Dome Tanks, Bladder and Integrated Cylindrical Pressurization are simultaneously specified, the forward head is positioned as convex aft, as well as whenever Integrated Spheroidal Pressurization is selected.
13. Propellant Valves will be located forward in the engine bay so that:
    a. The forward tank propellant line is assumed full before firing, and both engine bay (flex) lines are empty.
    b. If "No bladder" is selected, tank and bay lines are assumed empty at burnout.
    c. If "bladder is selected, tank and bay lines are assumed full at burnout.
14. Locate higher vapor pressure propellant on concave side of a common tank dome.

TABLE 7.2.2

TANDEM TANKAGE, EXPULSION, PRESSURIZATION SYSTEM GEOMETRY FLAGS

FWD TNK FWD HD	1 = CONVEX AFT 2 = CONVEX FWD
PRESS GEOM PRESSURIZATION GEOMETRY	0 = NON-INTEGRATED WITH TANKS IN ENG BAY 1 = SUSPENDED FWD OF FWD TANK (SPHEROIDAL) 2 = SPHEROIDAL FWD OF FWD TANK 3 = CYLINDRICAL IN FWD TANK
FWD TNK CYL	1 = MONOCOQUE CONSTRUCTION 2 = SUSPENDED TANK
FWD TNK BLAD	0 = NONE 1 = TRANSVERSE COLLAPSING 2 = BONDED ROLLING, FULL 3 = BONDED ROLLING, HALF
FWD TNK AFT HD	0 = COMMON WITH AFT TANK FWD HEAD 1 = CONVEX AFT 2 = CONVEX FWD
AFT TNK FWD HEAD	1 = CONVEX AFT 2 = CONVEX FWD
AFT TNK CYL	1 = MONOCOQUE CONSTRUCTION 2 = SUSPENDED TANK
AFT TNK BLAD	0 = NONE 1 = TRANSVERSE COLLAPSING 2 = BONDED ROLLING, FULL 3 = BONDED ROLLING, HALF
AFT TNK AFT HD	1 = CONVEX AFT 2 = CONVEX FWD

7.2.2.1 Tankage Pressurization

Pressurization Tank

- Fwd tank pressurization cylinder weight
- Bottle cylindrical section weight
- Bottle head weight
- Bottle head joint reinforcement weight
- Insulation

Lines

- Aft tank bay line
- Fwd tank bay line
- Fwd tank line weight
- Burst diaphram assembly weight
- Gas lines

Pressurant Control Hardware

- Orifice
- Regulator
- Relief valves
- High pressure valve upstream of regulator
- Ignitor

Non-Tank structure

Structural wall
Tank mount weight
Inter-tank cylindrical vehicle sections
Engine bay shroud
Shroud stiffening ring

Propellant Tanks

Aft tank cylindrical weight
Forward Tank cylindrical weight
Tank head joints reinforcement weight
Tank head reversed stiffener weight
Tank head weight

7.2.2.2 Algorithms Required for ELES Tandem Tank Model

ALGORITHM

- Design Stress
- Structural Thickness, Cylinder
- Pressure Thickness, Cylinder
- Tank Head Length
- Tank Head Volume (capacity, not metal)
- Tank Head Thickness (wall, constant)
- Cylindrical Tank Length (General)
- External Pressure Thickness, Cylinder
- Forward Line Dia (Internal)
- Aft Line Dia
- Bay Line Length (Aft & Fwd)
- Cylinder Volume (Capacity)
- Helium Volume, Density & Weight

- Solid Propellant Weight
- Gas Generator Volume
- Bonded Rolling Diaphragm Pressure Drop
- Cylinder Surface Area
- Head Surface Area (hemisphere & ellipsoid)
- Weight of Reversed Head Stiffener
- Weight of Head Joint Reinforcement
- Weight of Propellant Line Burst Disk Assy
- Tank Mount Weight
- Engine Bay Shroud Stiffening Ring Weight
- Cold-Gas Regulator Weight
- Hot-Gas Relief Valve Weight
- Cold-Gas Shutoff Valve Weight
- Hot-Gas Generator Igniter Weight
- Forward Shroud Flange Weight

ALGORITHMS FOR ELES PROPELLANT TANK/PRESSURIZATION

- DESIGN STRESS

OUTPUT: $S = \text{MIN}\left(\frac{SULT}{\eta_{ULT}}, \frac{SYIELD}{\eta_{YIELD}}\right)$ = Design Stress, psi

INPUT:
- SULT = Minimum Ultimate Tensile Strength, psi
- SYIELD = Minimum Tensile Yield Strength, psi
- η_{ULT} = Safety Factor for Ultimate Strength to operating conditions
- η_{YIELD} = Safety Factor for Yield Strength to operating conditions

o THICKNESS OF CYLINDER DUE TO INTERNAL PRESSURE

$P = MAX\ (P_{TANK}$ (from Pressure Schedule), P_{VAPOR} @ $T_{max})$

$$t_{HOOP} = \frac{P\ D}{2\ (S+P)}$$

$$t_{PRESS} = MAX\ (t_{HOOP}, t_{MINGAGE})$$

OUTPUT:
- t_{HOOP} = req'd. pressure vessel thickness due to hoop stress, in.
- t_{PRESS} = practical req'd pressure vessel thickness due to hoop stress, in.

INPUT:
- $t_{MINGAGE}$ = Minimum allowable wall thickness, in.
- P = Max. operating vessel pressure, psia
- D = Outside diameter of vessel, in.
- S = Allowable Design stress, psi
- P_{TANK} = Tank Pressure calculated by Pressure Schedule Subroutine, psia
- P_{VAPOR} = Maximum propellant vapor pressure, defined at Maximum storage temperature, psia.

Propellant Tank Wall Thickness Calculation

The basis for wall thickness calculations are the simple stress and buckling relationships (shown below) applied in concert according to the load combinations, given in Table. 7.2.2.2.1.

Subroutines for Tank Wall Thickness Calculation

$M_{MAX\ CARRY}$ = Maximum Bending Moment applied to a vehicle when the propellant tanks are not pressurized, (in. lbF.)

TABLE 7.2.2.2.1

LOAD COMBINATIONS USED FOR TANK WALL THICKNESS SIZING

Condition	Tank Type: Monocoque	Tank Type: Suspended Tank	Tank Type: Structural Wall
Prelaunch	MAX(HOOP, MINGAGE)	MAX(HOOP, MINGAGE)	MINGAGE
Launch	If net axial tank stress is tensile: MAX(HOOP, MINGAGE) If net axial tank stress is compressive: MAX(LAUNCH, HOOP, MINGAGE)	MAX(HOOP, MINGAGE)	MAX(FRAME, MINGAGE)
Powered Flight and Coast	If both sides of tank remain in tension during Critical Bending Moment Maneuvers: MAX(Tensile Flight, HOOP) (MINGAGE) If one side of tank sees compressive stress during maneuvers: MAX(Compressive Flight) (Tensile Flight) (HOOP, MINGAGE)	MAX(HOOP, MINGAGE) NOTE: Frame is buckling criteria limited from CBM + axial thrust.	MAX(FRAME, MINGAGE)
Transportation	MAX(CARRY, MINGAGE)	MINGAGE	MAX(CARRY, MINGAGE)

Structural Wall

$$t_{STR} = MAX\ (t_{FRAME},\ t_{MIN\ GAGE},\ t_{CARRY}) \qquad \text{(OUTPUT)}$$

$$t_{FRAME} = \left[\frac{2.653}{YMODU}\ \left(\frac{CBM}{D} + \frac{F_v}{4.}\right)\right]^{.5}$$

where:

c_{BM}	= Critical Bending Moment During Flight, in-lbf
F_V	= Vacuum Thrust, lbf
D	= Vehicle O.D., in.
YMODU	= Young's Modulus of Tank Material, psi
t_{FRAME}	= Structural (Axial + Bending) Thickness Required During Flight, in.
t_{CARRY}	= Thickness Required Due to Unpressurized Tank Bending Loads, in.

$$t_{CARRY} = \left[\frac{2.653\ M_{MAXCARRY}}{D\ YMODU}\right]^{.5}, \quad t_{MINGAGE} = INPUT$$

Suspended Tank

$$t_{PRES} = MAX\ (t_{HOOP},\ t_{MINGAGE}) \qquad \text{(OUTPUT)}$$

$$t_{HOOP} = \frac{P*D}{2\ (S + P)}, \qquad t_{MINGAGE} = INPUT$$

Monocoque Tank

$$N_{x1} = F_v - \pi * D^2 * P / 4$$

$$N_{x2} = N_{x1} + \frac{4.*CBM}{D}$$

$$t_{CYL} = MAX\ (t_{HOOP},\ t_{MINGAGE},\ t_{LAUNCH},\ t_{TENSILE\ FLT},\ t_{CARRY})$$

If $N_{x1} < 0$, $t_{LAUNCH} = 0$

If $N_{x2} < 0$, $t_{COMPR.\ FLT} = 0$

$$t_{COMPR\ FLT} = \left[\frac{N_{x2}}{1.508*YMODU}\right]^{.5}$$

If $t_{TENSILE\ FLT} < 0$, $t_{TENSILE\ FLT} = 0$

$$t_{LAUNCH} = \left[\frac{N_{x1}}{1.508*YMODU}\right]^{.5},$$

$$t_{TENSILE\ FLT} = \frac{1}{S}\left[\frac{PD}{4.} + \frac{4.*CBM}{\pi D^2} - \frac{F_v}{\pi D}\right]$$

o CONSTANT TANK HEAD THICKNESS

$$t_{HEAD} = D/((4*S/(P*E)) +2)$$

OUTPUT: Constant Tank Head Thickness, in. = t_{HEAD}

INPUT:
- D = Outside Diameter of Interfacing Cylinder, in.
- S = Allowable Design Stress, psi
- P = Maximum vessel operating pressure, psia
- E = Ellipse Ratio of Head, - (eg. 2, 1.5, etc)
  For Hemisphere E = 1.0

o TANK HEAD LENGTH

$$L_{HEAD} = D/2./E$$

OUTPUT: L_{HEAD} = Overall Head height (length), in.

INPUT:
- D = Outside Diameter of Interfacing Cylinder, in.
- E = Ellipse Ratio of Head

o TANK HEAD VOLUME

$$V_{HEAD} = \pi * d^3 / E / 12$$

OUTPUT: V_{HEAD} = Capacity or Volume of hollow head, $in.^3$

INPUT:
- d = Inside diameter of Interfacing Cylinder, in.
- E = Ellipse Ratio of Head

o TANK HEAD SURFACE AREA (For other than Hemisphere)

$$\varepsilon = (1. - (1./E)^2)$$

$$SA_{HEAD} = (\pi/4)\,(D - t_{head})^2 * \left(1 + \frac{\ln\left(\frac{1+\varepsilon}{1-\varepsilon}\right)}{2*\varepsilon*E^2}\right)$$

OUTPUT: SA_{HEAD} = Mean Surface Area of Head, $in.^2$
INPUT D = Outside Diameter of Interfacing Cylinder, in.
t_{HEAD} = Head Thickness, in.
E = Head Ellipse Ratio

o TANK HEAD SURFACE AREA FOR HEMISPHERE

$$SA_{HEMI} = \pi(D-t_{HEAD})^2/2$$

OUTPUT: SA_{HEMI} = Mean Surface Area of Hemispherical Head, $in.^2$
INPUT: D = Outside Diameter of Interfacing Cylinder, in.
t_{HEAD} = Head Thickness, in.

o CYLINDER SURFACE AREA

$$SA_{CYL} = \pi * (D-t_{CYL})*L_{CYL}$$

OUTPUT: SA_{CYL} = Mean Surface Area of Cylinder, in.
INPUT: D = Outside Diameter of Cylinder, in.
t_{CYL} = Wall Thickness of Cylinder, in.
L_{CYL} = Length of Cylinder, in.

o GENERALIZED FORM FOR A CYLINDRICAL LENGTH CALCULATION

$$L_{CYL} = \frac{V \pm 2*V_{HD}}{(\pi/4)\ (d^2 - f_L d_L^2)}$$

OUTPUT: Cylindrical Length of a Cylindrical Tank with Domed Head, in.

INPUT:
- V = Volume of Tank, $in.^3$
- V_{HD} = Volume within One Head, $in.^3$
- d = Inside Diameter of Tank, in.
- d_L = Outside Diameter of Internal Propellant Line, in.
- f_L = Internal Line Length/Total Aft Tank Lengths

NOTES:
- o Where heads are nested, set $V_{HD} = 0$
- o Where heads oppose in the normal way, the sign of the numerator is negative
- o Where heads oppose convex inward, the sign of the numerator is positive
- o Where the fwd, tank line is external, $f_L = 0$

o VOLUME OF CYLINDER (capacity)

$$V_{CYL} = (\pi/4)*d^2*L_{CYL}$$

OUTPUT: V_{CYL} = Volume of a Hollow Cylinder, $in.^3$

INPUT:
- d = Cylinder Diameter (usually I.D.) in.
- L_{CYL} = Cylindrical Length, in.

o FORWARD TANK PROPELLANT FEED LINE DIAMETER

$$D_{LFWD} = \left[\left[5. + (L_{AFT}+D) *.34*\left(\frac{\rho_{FWD}}{\omega_{FWD}}\right)^{.5}\right] \frac{\omega_{FWD}^2}{4763.*\rho_{FWD}*\Delta P_{LF}}\right]^{.25}$$

OUTPUT: D_{LFWD} = Inside Diameter of Forward Propellant Feed Line, in.

INPUT: L_{AFT} = Length of Fwd Propellant Feed Line

D = Vehicle O.D., in.

ρ_{FWD} = Density of Forward Propellant, lb/in^3

ω_{FWD} = Flow Rate of Forward Propellant, lb/sec

ΔP_{LF} = Pressure Drop in Forward Propellant Feed Line, psi.

Note: Line Length for Fwd Tank Propellant = Aft Tank Cylinder Length plus Vehicle O.D.

- Line length in engine bay = D (for both propellants)

o AFT TANK PROPELLANT FEED LINE DIAMETER

$$D_{LAFT} = \left[\left[3. + .34*D\left(\frac{\rho_{AFT}}{\omega_{AFT}}\right)^{.5}\right] * \frac{\omega_{AFT}^2}{4763.*\rho_{AFT}*\Delta P_{LA}}\right]\Big]^{.25}$$

OUTPUT: D_{LAFT} = Inside Diameter of Aft Propellant Feed Line, in.

INPUT: D = Vehicle O.D., in.

ρ_{AFT} = Density of Aft Propellant, lb./in.^{3}

ω_{AFT} = FLow Rate of Aft Propellant, lb./sec

ΔP_{LA} = Pressure Drop in Aft Propellant Feed Line, psi

o THICKNESS OF CYLINDER DUE TO EXTERNAL PRESSURE

$$t_{EXTP} = \left[\frac{(P_{OUT} - P_{COLD})\, L_{CYL}\, D_{CYL}^{1.5}}{2.49 * YMODU}\right]^{.4}$$

OUTPUT: t_{EXTP} = Cylinder Thickness to Prevent Buckling Due to External Pressure, in.

INPUT: P_{OUT} = Input Value of Max. Expected Ambient Pressure, psia

P_{COLD} = Vapor Pressure of Propellant at T_{COLD} (T_{min}), psia

L_{CYL} = Cylindrical Tank Length, in.

D_{CYL} = Outside Diameter of Tank, in.

YMODU = Youngs Modulus of Elasticity for Tank Material, psi

o TANK HEAD/CYLINDER JOINT REINFORCEMENT WEIGHT

$$t_{reinf} = t_{PRES}\ (1 + \frac{E^2}{4}) - t_{CYL}$$

$$W_{Jt} = 6.664 \times K_J \times \rho_{WALL} * d^{1.5} * t_{reinf} * (t_{PRES})^{.5}$$

Note: (K_J = INPUT, DEFAULT = 1.2)

OUTPUT: W_{Jt} = Joint Reinforcement Weight, lbm.

INPUT: t_{PRES} = Practical Req'd Thickness Due to Hoop Stress, in.

t_{CYL} = Actual Wall Thickness of Cylinder, in.

E = Head Ellipse Ratio

K_J = Weight Multiplier

ρ_{WALL} = Wall Density, lb/in^3

d = Inside Diameter of Tank, in.

o DOME STIFFENER WEIGHT (use when a reversed head is specified. Assume that ellipsoid and hemisphere stiffeners have the same weight).

$$t_{RHS} = D^* (P_t / 1.45 / YMODU_{RHS})^{.5} - t_{HEAD}$$

$$W_{RHS} = 1.57 * K_{RHS} * D^2 * \rho_{RHS} * t_{RHS}$$

OUTPUT: W_{RHS} = Reversed Head Stiffener Weight, lbm (for one tank head)

t_{RHS} = Thickness of the Stiffener, in.

INPUT: D = Outside diameter of tank, in.

P_T = Maximum Tank Pressure, psia

$YMODU_{RHS}$ = Young's Modulus of Stiffener Material, psi

K_{RHS} = Weight Multiplier, - (Default Value = 1.0)

ρ_{RHS} = Density of Stiffener Material, psi

t_{HEAD} = Constant (Normal) Head Thickness, in.

7.2.2.3 Small Weight Items

ω_p - propellant weight flow (lb/sec)
ω_g - gas weight flow (lb/sec)
D_p - propellant line diameter (in.)
W_{bd} - propellant burst diaphragm assy wt. (lb.)
W_{reg} - helium regulator wt. (lb.)
W_{rel} - warm gas relief valve (lb.)
W_{hpv} - high pressure helium valve st. (lb.)
W_{ign} - solid grain ignitor wt. (lb.)

$$W_{bd} = 1.5 \times (D_p)^2$$

$$W_{reg} = 7.07 \times (\omega_g)^{.5}$$

$$W_{rel} = 1.92 \times (\omega_g)^{.5}$$

$$W_{hpv} = 12.9 \times (\omega_g)^{.5}$$

$$W_{ign} = 0.16 \times (\omega_{sg})^{.25}$$

where: (W_{ign}) minimum = .4

TANK MOUNT WEIGHT

The weight of the tank mount is calculated as:

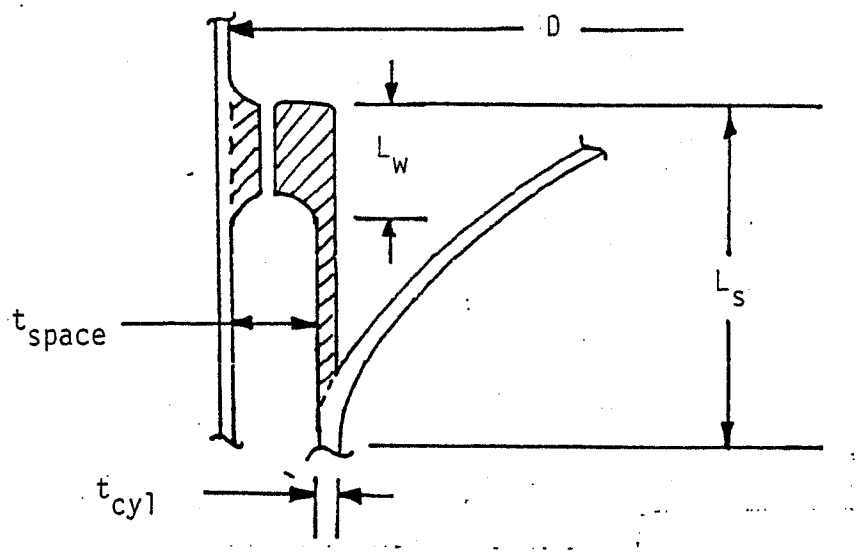

$$W_{tm} = .625\ D\ \rho\ [2\ D\ t_{space}^2 + (D - 2\ t_{space})\ tcyl]$$

$$L_w = D\ t_{space} / 2.5$$

$$L_s = D / 5.0$$

$$t_{space} = \text{Min}\ (t_{space},\ 0.1)$$

ENGINE SHROUD STIFFENING RING WEIGHT

Default values:

W_{essr} = $\pi DLt\rho$ = Weight of the engine shroud stiffening ring, lbm.

where: L = .8 in.

t = .19 in.

Similarly, for the forward shroud flange:

W_{fsf} = $\pi DLt\rho$ = Weight of the forward shroud flange, lbm.

where: L = 1.0 in.

t = .25 in.

7.3 NON-CONVENTIONAL TANKAGE MODEL

An Aerojet non-conventional tankage model has been modified to be compatible with ELES. The model allows up to 15 tanks and 5 engines to be nested into a cylindrical envelope.

In its original form, the tank model created a schematic of the stage on a Tektronix terminal. In order to make the code compatible with a batch environment and to make it more transportable, ELES has been provided with pseudo-Tektronix routines, which accept standard Tektronix commands and execute them on a line printer. Stage schematics are created for non-conventional tankage in this manner (see Figures 7.3.1 through 7.3.3.). (The tandem tankage schematic output also makes use of the pseudo-Tektronix routines.)

Notice that each object is represented by a different character. Tanks use letters A through O. Engines use numbers 1 through 5. The stage envelope is represented by asterisks. The stage summary (see Figure 7.3.4) references tanks and engines by their appropriate character.

For line printers with non-standard lines per row or lines per column, there is provision to input the line printer's characteristics in order to keep the horizontal and vertical scales consistent.

Whereas the tandem tankage model allows use of only CSE tanks (defined as the family of cylindrical tanks with ellipsoidal to hemispherical heads, having zero or non-zero cylindrical length, with the acronym standing for Cylindricall/Spherical/Ellipsoidal), the non-conventional tankage model also encompasses toroids.

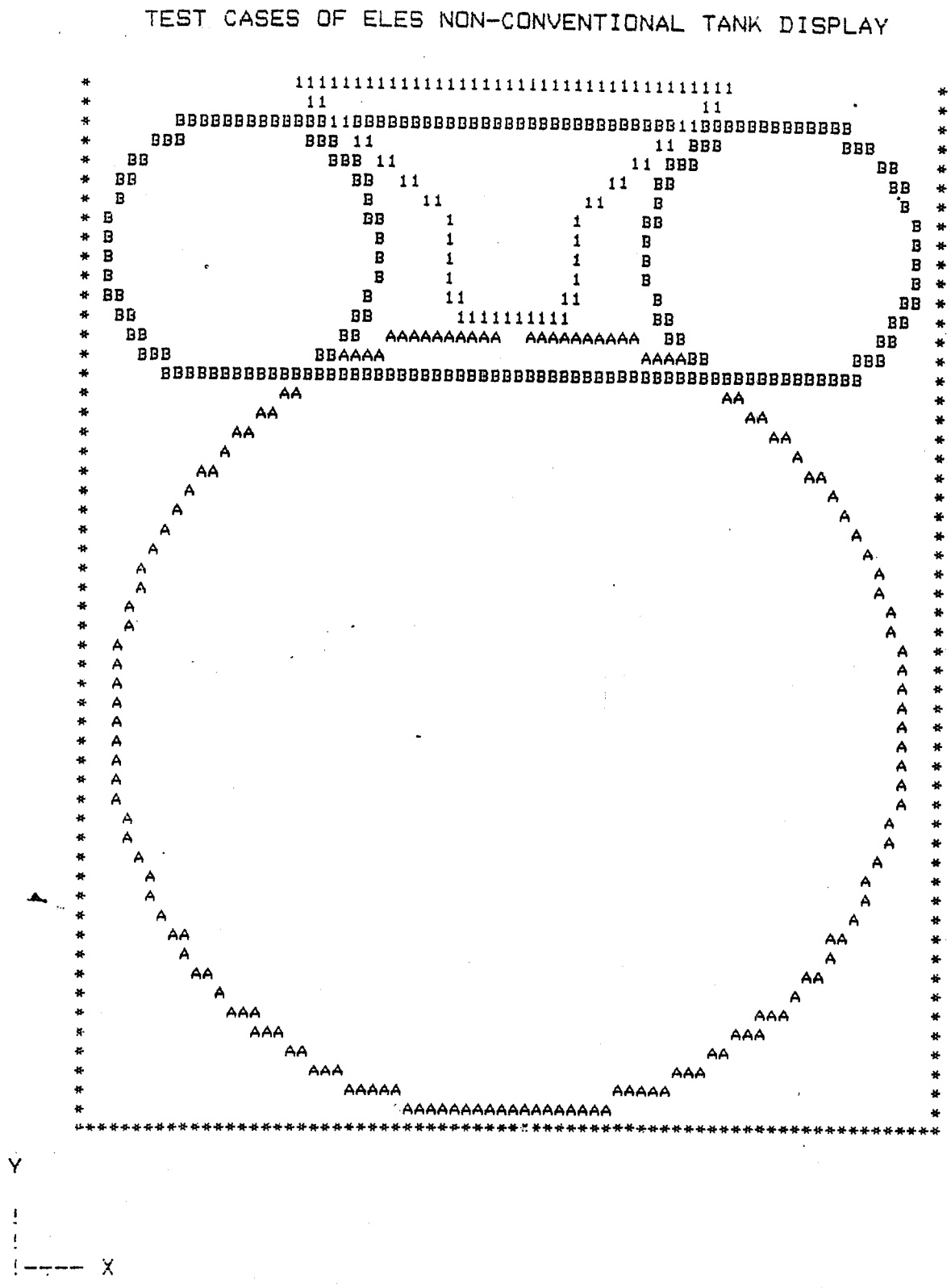

Figure 7.3.1. X-Y View of Stage Schematic

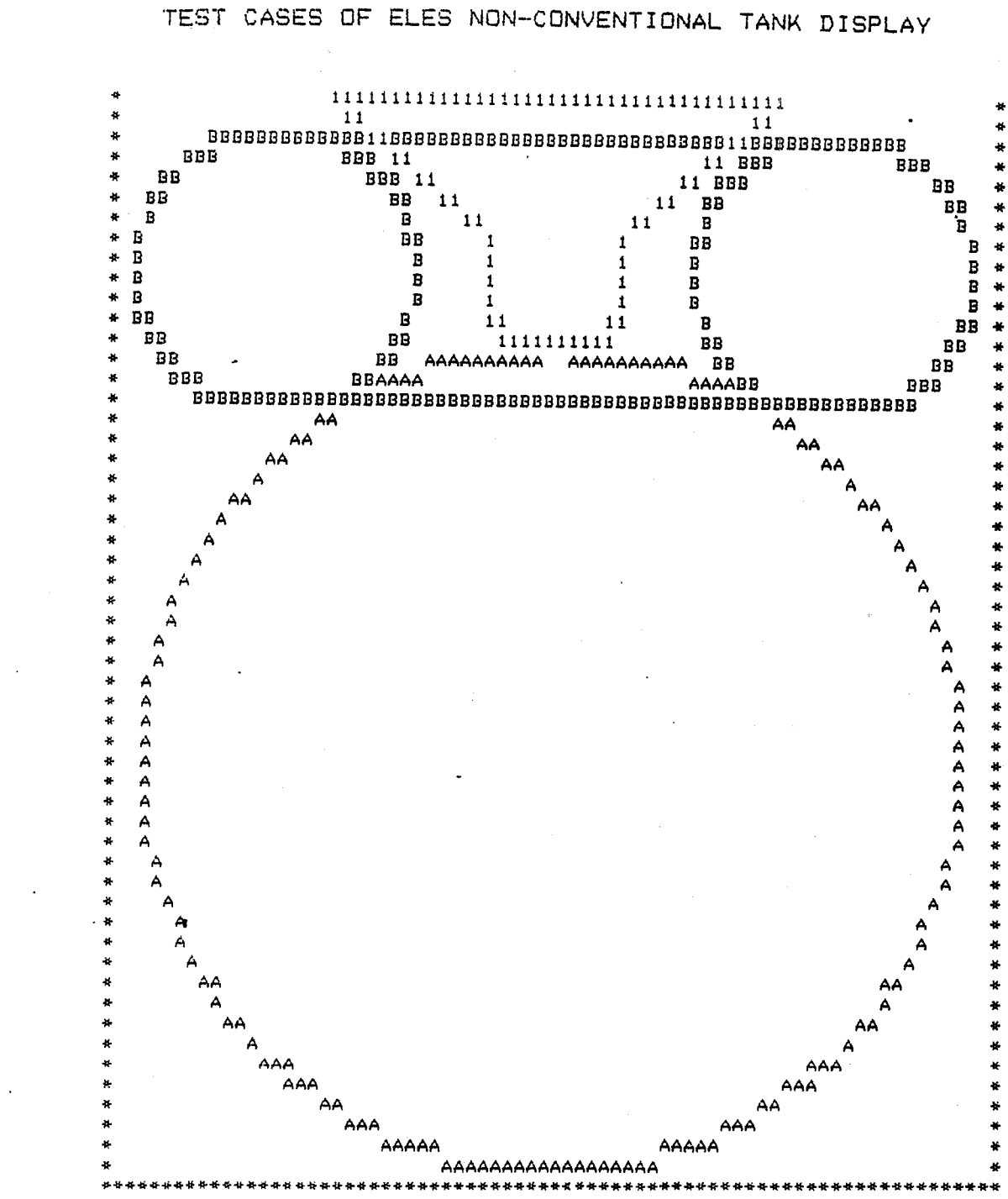

Figure 7.3.2. Y-Z View of Stage Schematic

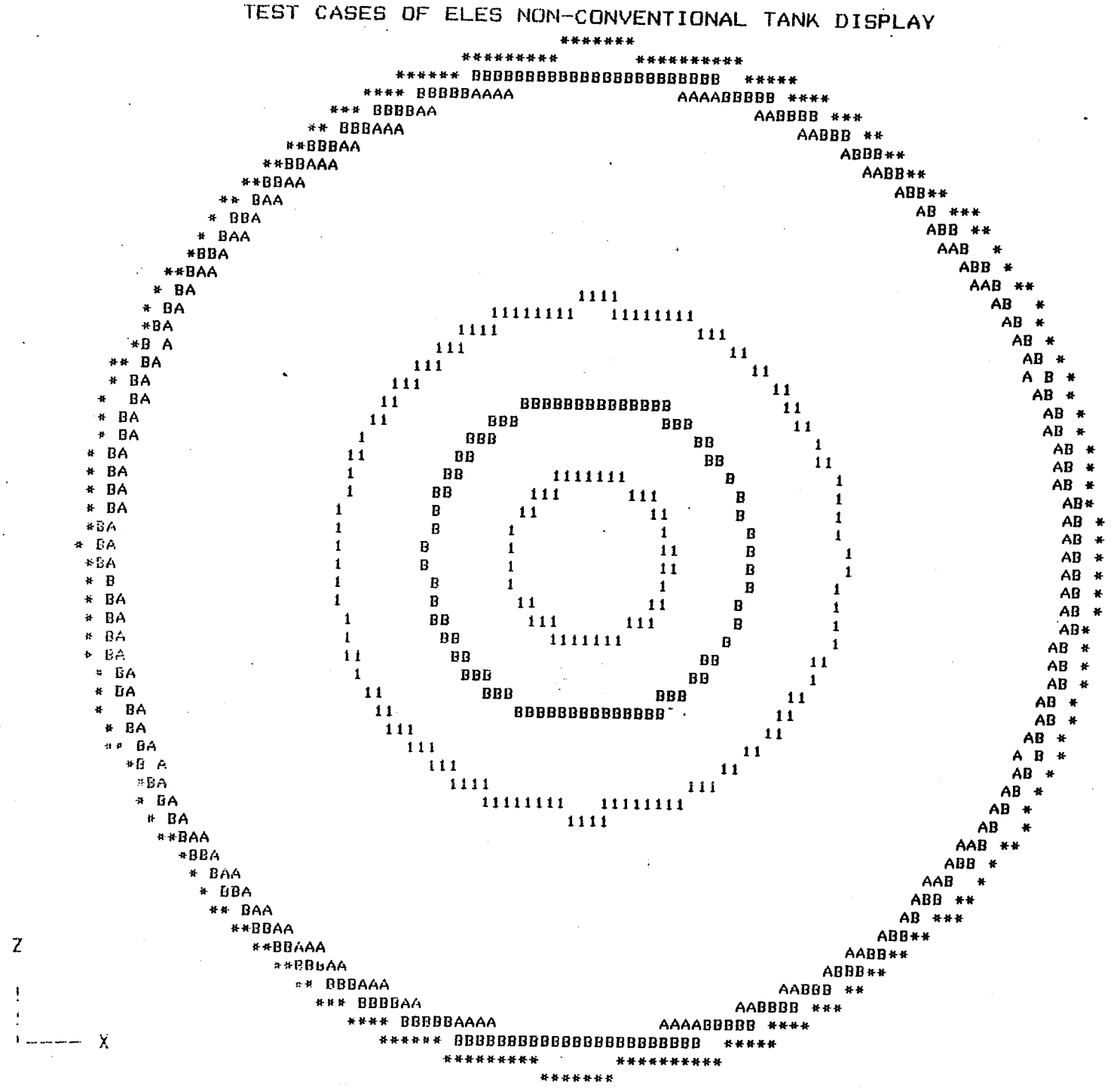

Figure 7.3.3. Z-X View of Stage Schematic

Vehicle Length	123.8	
Vehicle Radius	50.0	
Vehicle Wall Thickness	0.050	
Component Spacing	1.0	
Total Tank Weights	2116.80	
Tank #	A	B
Tank Pressure	500.00	500.00
Material	aluminum	aluminum
Safety Factor	1.500	1.500
Wall Thickness	constant	constant
Volume (x10**-3)	434.89	161.70
Weight	1324.5	792.3
Tank Type	CSE	torus
Inside Radius	47.0	16.0
CSE Ellipse Ratio	1.0	---
CSE Tank Length	94.0	---
Torus Hub Radius	---	32.0
Min Wall Thickness	0.390	0.222
Max Wall Thickness	0.390	0.400
Const Wall Thickness	0.390	0.400
Location of Tank Forward Center Points		
X	0.0	0.0
Y	0.0	0.0
Z	48.4	104.4
Engine #	1	
Chamber Radius	8.0	
Exit Radius	25.0	
Chamber Length	10.0	
Nozzle Length	15.0	
Engines are nested individually		
Location of Injector Dome Center Point		
X	0.0	
Y	0.0	
Z	98.8	

Figure 7.3.4. Stage Summary

7.3.1 Non-Optimum Factor for Actual Non-Conventional Tank Weights

The weight of non-conventional tanks is calculated from an ideal tank weight through the use of a tank non-optimum factor. The term "tank non-optimum factor" (TNOF) is defined as the actual tank mass divided by its ideal tank mass. Included in the actual mass is any required additional material thicknesses for weld lands and fittings over and above the mass of an ideal tank shell consisting of a constant thickness in the dome and cylindrical section. The ideal mass is calculated with wall thicknesses determined by hoop stress using applicable safety factor, or by minimum fabricable gage. Data for actual tanks was obtained to investigate the TNOF variance and trends. A significant amount of scatter exists among the data as can be seen in Figure 7.3.1.1. This is due to the fact that each tank has its own design peculiarities. Actual tank mass is a function of size, but it is also affected by the mounting design, the tank design details and mission requirements. Examples shown on Figure 7.3.1.1 include the shuttle RCS tanks, which were constructed to account for a considerable number of fittings, the GRO tanks, which were designed for various applications of diverse mounting complexities, and the Titan Stage I fuel tanks included feed line conduits through the tank. Considering the data scatter and the reasons for the scatter, it was decided to use more than one value for TNOF. For conventional tanks, which require feedlines, supports, pressurization, and a propellant management device a TNOF of 1.7 is recommended. Tank designs with conduits (to accommodate feed lines for example) running through the tank would require a 2.5 TNOF. Toroidal tank designs of large diameter have not yet been built, except as part of the Russian space program, and detailed designs are not available. From some preliminary design work by Martin Marietta, General Dynamics, and others a TNOF of 2.0 is recommended as a slightly conservative estimate. These approximate values are summarized in Table 7.3.1.1.

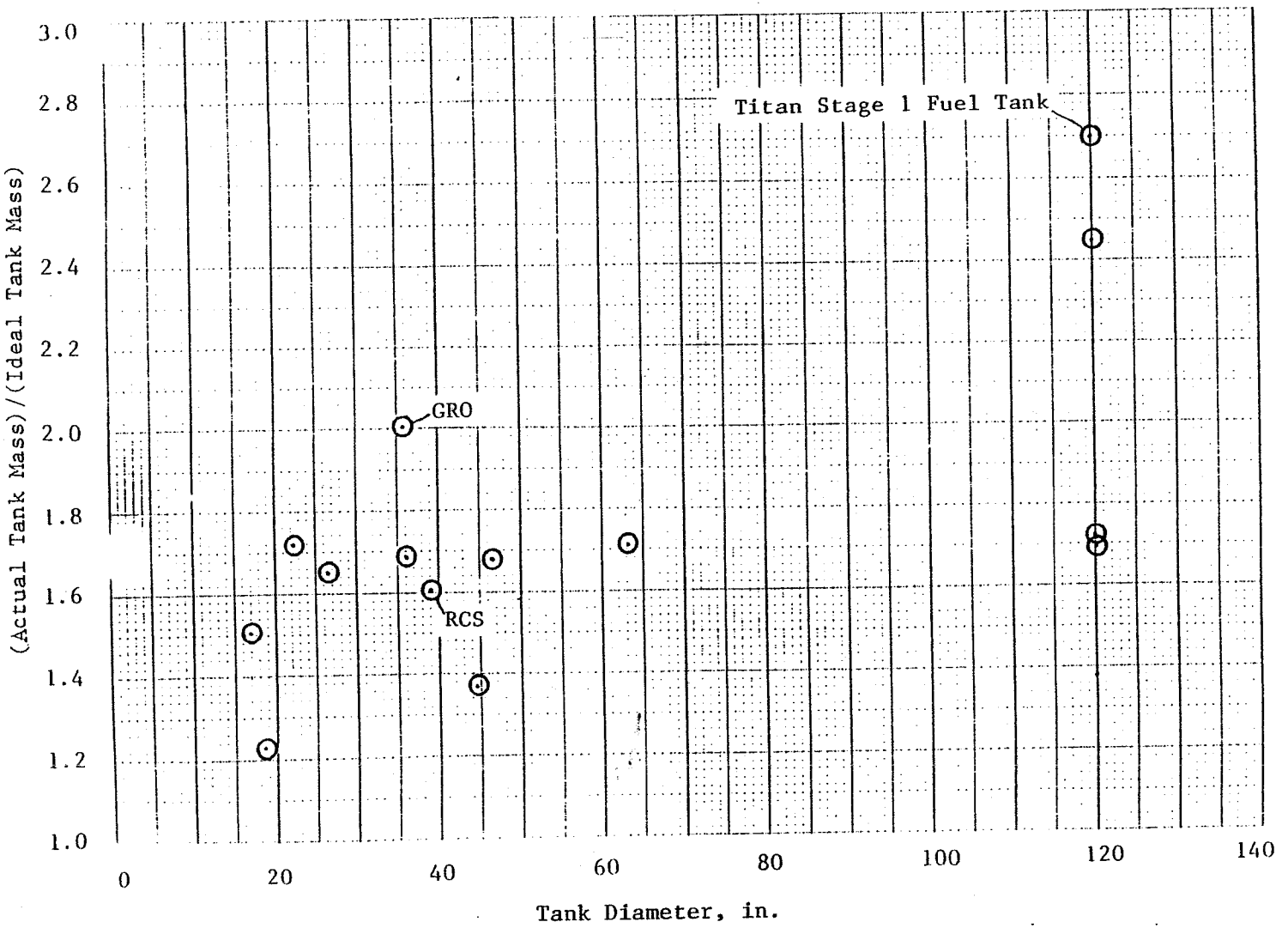

Figure 7.3.1.1. Tank Non-Optimum Factor Versus Tank Diameter

TABLE 7.3.1.1

RECOMMENDED TNOF VALUES

TNOF	APPLICATIONS
1.25	Simple Spherical Tanks
1.7	Conventional CSE Tanks
2.0	Toroidal Tanks
2.5	Tanks With Large Conduits Running Through them

7.4 PROPELLANT ACQUISITION MODELING

Any liquid propulsion system that must start or restart under conditions which do not assure orientation of propellant at the tank outlet (e.g., low-g or adverse acceleration environments), will require a propellant acquisition system. The acquisition system contributes to the mass and performance of the propulsion system. Specifically, the parameters of the propellant acquisition system that must be considered are its mass, the volume the system occupies within the tanks, and the expulsion efficiency of the system or the residual propellant volume. Equations to provide these three parameters for typical propellant acquisition systems have been developed.

Propellant acquisition devices fall into two general categories: positive expulsion devices and propellant orientation devices. Positive expulsion devices use a diaphram, bladder or bellows to push the propellant from the tank. Propellant orientation devices have a variety of designs.

The positive expulsion options in ELES are transverse collapsing bladders and bonded rolling diaphrams. The size and weight of the bladders are easily calculated with physical models, since the geometry is fully defined. The expulsion efficiency is modeled from empirical data (see Section 9.1, "Pressurization Requirements with Bladders")

Propellant orientation devices can take many forms. One type makes use of an auxiliary propulsion system to produce an acceleration that will orient

the propellant over the tank outlet. After the auxiliary system has settled the propellant, the engine being supplied must maintain the orientation of the propellant. If an auxiliary propulsion system is available, the extra propellant required to accomplish propellant settling is the only contribution to the mass of the acquisition system. There is no tank volume penalty and the terminal draining of the tank determines the propellant residuals.

Capillary devices are another type of propellant orientation device. These devices make use of the capillary pressure developed at the pores of a screen, perforated plate or baffle plate to preferentially orient the liquid and exclude gas. Some devices have screen covered channels that can feed propellant to the tank outlet regardless of its orientation. Other devices use screen to form a reservoir at the tank outlet to feed propellant for engine start. Baffles or vanes can orient all or a portion of the propellant over the tank outlet, even when accelerations would normally displace it. Capillary devices are specifically tailored to a particular propulsion system, operating environment, and mission duty cycle, so configurations are many and varied.

The approach to calculating the parameters for propellant orientation devices was established through a survey of the data from acquisition device studies and devices that are being built and flown. The greater credibility of the data for actual hardware was considered. Calculations introducing unnecessary complexity were avoided, such that parameters have an accuracy consistent with the overall accuracy of the computer model.

The basic approach selected was to define the device mass and propellant residuals as a function of the tank volume, and the displacement volume of the device was calculated from the device mass. The data from the survey is plotted in Figures 7.4.1 and 7.4.2.

There are a number of parameters, in addition to tank volume, that influence the mass and residual associated with a particular device, such as:

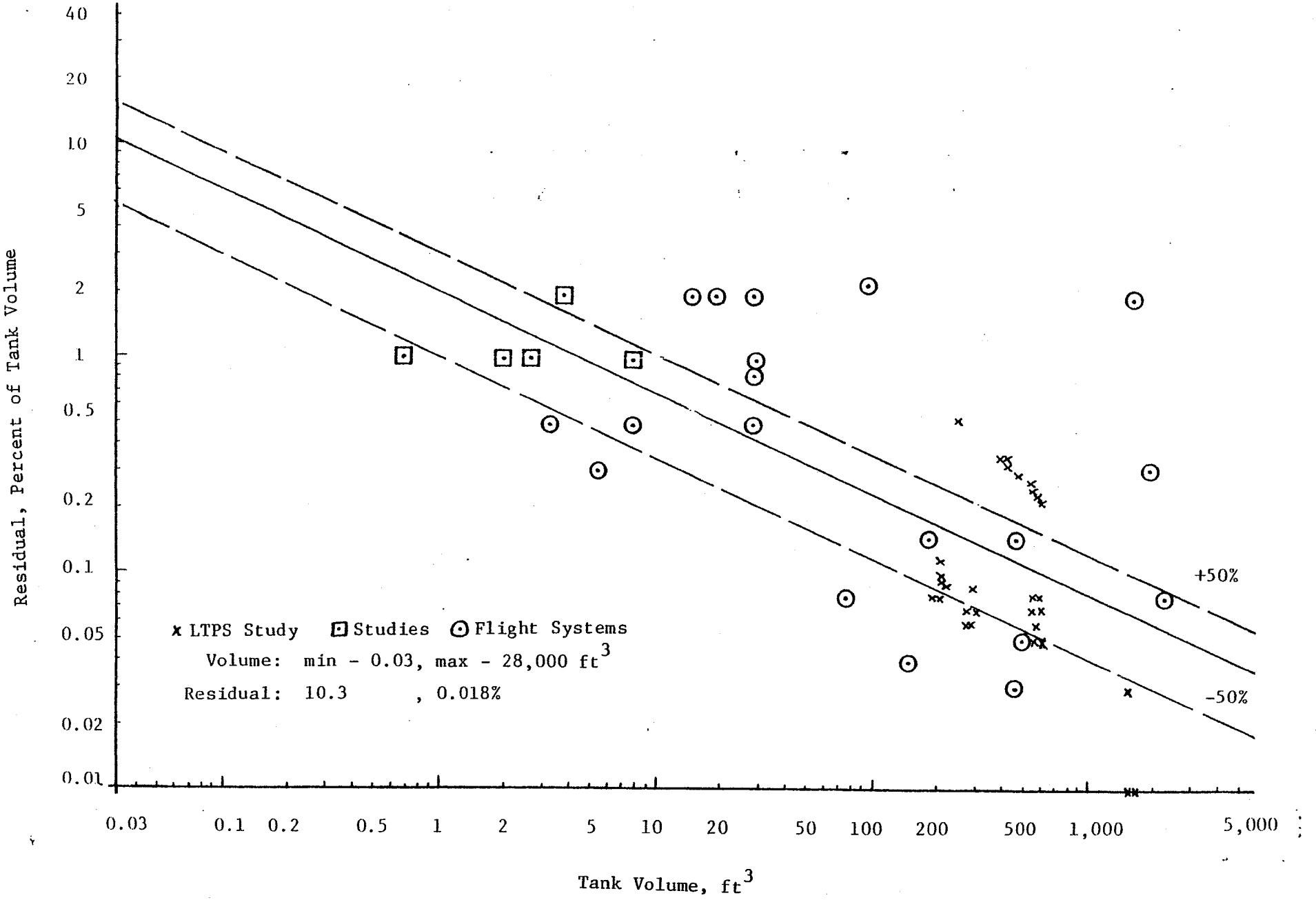

Figure 7.4.1. Tank Residual vs Tank Volume

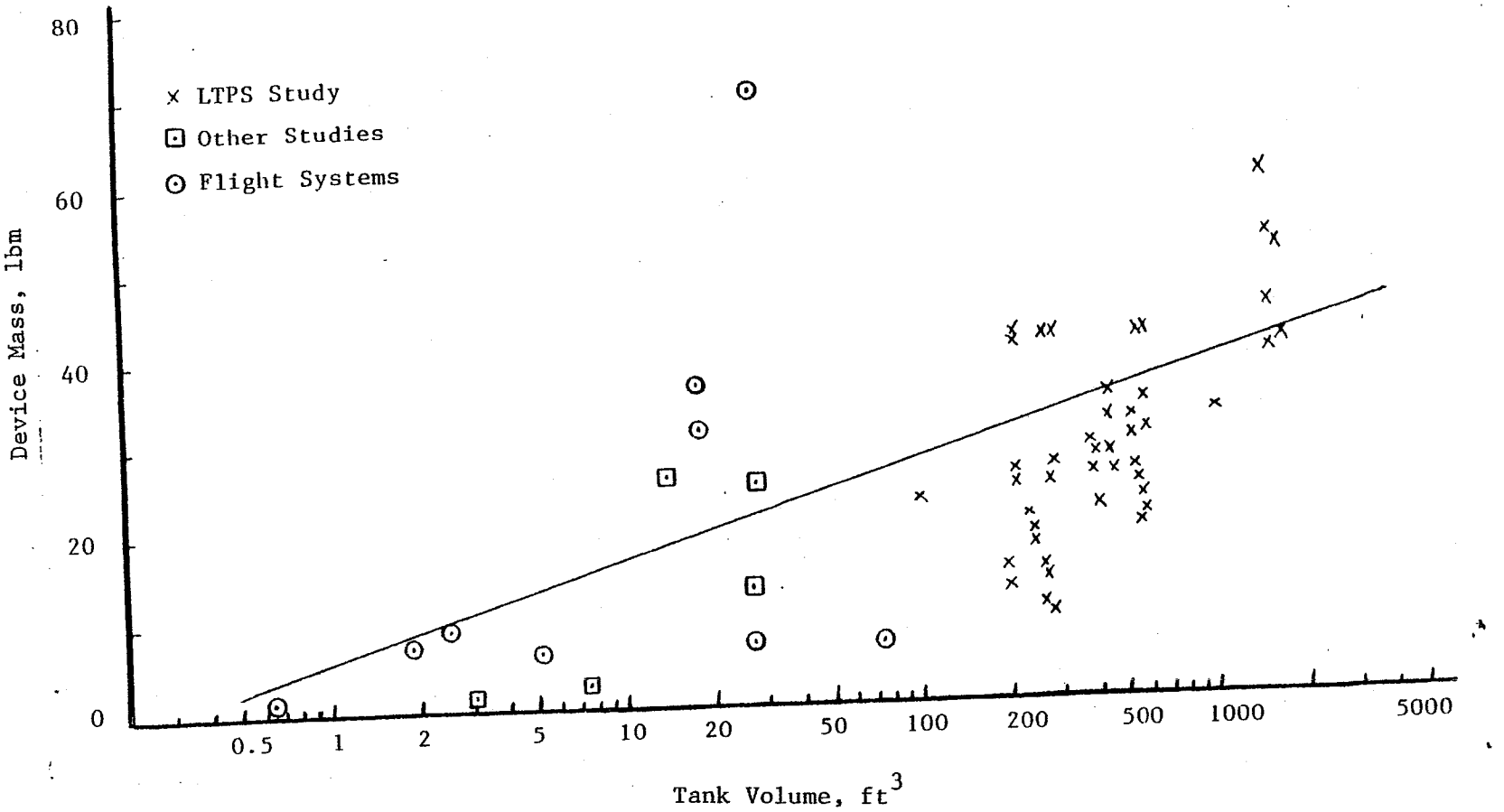

Figure 7.4.2. Propellant Orientation Device Mass Versus Tank Volume

flowrate, acceleration environment, and mission duty cycle. Tank volume is the most dominant variable, because it determines the size of the device, settling distance, and it usually implies a certain range for the other variables mentioned above.

The data assembled in the two figures indicate some definite trends. The device mass increases with tank volume, while the residual propellant, expressed as a percentage of the tank volume, decreases. Curve fits have been derived that yield representative values for the full range of tank volumes.

The expression derived for the residual propellant that can not be expelled by the device is:

$$R = 2 - 0.6 \log_{10} V$$

where: R = residual, percent of tank volume, and V = tank volume, ft^3

This expression is valid between volumes of 0.1 ft^3 to 2000 ft^3. For volumes greater than 2000 ft^3 the residual approaches zero.

The ratio of residual volume to tank volume increases as the tank volume decreases because the dimensions of the device cannot be decreased in proportion to the tank size. The annuli and gaps where liquid can be trapped become a greater portion of the tank volume. Since there is usually no means of actually measuring the residual in flight systems, all the values for residual are analytical predictions and typically are accurate to only one significant digit.

The expression derived for the device mass is:

$$m = 10.7 \log_{10} V + 6$$

where: m = device mass, lbm, and V = tank volume, ft^3

The expression for m is correlated for tank volumes between 0.3 ft^3 and 10,000 ft^3.

Device mass increases with tank volume: values in the range of 10 to 30 ft^3 show that there can be a wide range of variations. The point located on the 70 lbm line of Figure 7.4.2 represents a device that incorporates extensive slosh baffling, and the 7.5 lbm point is a simple device for a communication satellite.

The material volume of the device is derived from the mass as follows:

$$V = \frac{m}{\rho}$$

where: V = device volume, ft^3
m = device mass lbm
ρ = density of device, lbm/ft^3

Mose capillary devices are made of stainless steel, so that density would be the most appropriate (501 lbm/ft^3). Other densities could be input, or for the case of propulsion settling the device volume could be set to zero.

7.5 CRYOGENIC TANK MATERIAL RECOMMENDATION

Martin Marietta Denver Aerospace (MMDA) has completed an extensive cyrogenic tank material survey. General recommendations of the survey include:

1) Aluminum is the first material of choice for cryogenic tanks. Alloy 2219-T87, is inexpensive, available, and easy to work.

2) For weight critical cryogenic programs, titanium is recommended. Choice of alloy is based on temperature regime. However, there are serious propellant compatibility restrictions which apply to its use.

3) Stainless steels are not recommended for cryogenic use even though they have been extensively used in the past. If, however, there is some reason that aluminum is rejected, then stainless steel alloy A-286 and INCONEL 718 are good candidates.

A more complete discussion of MMDA results follows in this section.

Tank Material Property Recommendations (MMDA)

Cryogenic structures used for flight hardware must be "weight limited", therefore they must be fabricated from materials with high strength-to-density ratios both at room temperature and, for cryogenic propellant applications, at sub-zero temperatures. At the same time these materials are required to retain high levels of fracture toughness at all exposure temperatures for "fail-safe" service. Other significant concerns when selecting materials for cryogenic application include availability, cost, machinability and weldability. Certain titanium alloys, aluminum alloys and cold worked stainless steels have been used successfully in fabricating weight limited structures according to state-of-the-art design.

Of the materials investigated, aluminum alloy 2219-T87 has the most favorable properties for cryogenic tank applications. It has a relatively high strength-to-density ratio, good toughness and availability is readily weldable and low in cost. Titanium alloys Ti-6Al-4V and Ti-5Al-2.5Sn also have favorable cryogenic properties. They are high in strength and have good toughness and weldability, but titanium is substantially more expensive than aluminum and also needs a longer procurement time. Titanium is also impact sensitive to liquid fluorine and liquid oxygen. Titanium alloys are recommended in favor of Al 2219-T87 only in the event the program under consideration is extremely weight critical, where cost is not a consideration and the cryogenic propellants are compatible.

Aluminum Alloys

The aluminum alloys 2219-T87 and 5083-0 have been used extensively for major cryogenic applications. Other aluminum alloys considered include 2014-T6, 2024, and 6061.

Aluminum alloy 2014-T6 has relatively high strength at room temperature and at sub-zero temperatures. It retains about the same ductility and notch tensile strength at liquid hydrogen temperature as at room temperature. It is available in all wrought forms and is weldable under controlled conditions.

Alloy 2014-T6 plate was employed in making large welded tanks for the cryogenic propellants (liquid oxygen and liquid hydrogen) used in the Saturn launch vehicle. These tanks were 6.6 m (21 ft. 8 in.) in diameter and were assembled using fusion welding.

Strength and ductility of the welded metal were substantially lower than the same properties of the base metal. Therefore, the welded areas of the tanks were made thicker than the remaining areas of the tank shells, which were milled out to produce a waffle grid pattern or integral ribs. As a result of this design the tanks had high strength and stiffness with minimum weight.

Alloy 2024 has relatively high strength at both room and sub-zero temperatures in the T3 temper (solution treated and cold worked), the T4 temper (solution treated and naturally aged) and the T8 temper (solution treated, cold worked and artificially aged). Fusion welded joints in this alloy are less satisfactory than such joints in alloy 2014. Alloy 2024 is used primarily in aircraft and aerospace structures and is joined by mechanical parts.

Aluminum alloy 5083 is not heat treatable; for maximum toughness, it is used in the annealed (0) condition. It is readily weldable, and the yield strength of the weld metal is nearly equal to that of the base metal. It has excellent toughness and is readily available but is relatively low in strength as compared with alloy 2219-T8.

Aluminum Alloy 6061 is usually used in the T6 temper. It is weldable and may be reheat treated after welding, although this practice is not recommended because it lowers weld ductility. Alloy 6061-T6 has acceptable toughness but is the lowest in strength of the heat-treatable aluminum alloys.

Alloy 2219-T87 has somewhat lower strength than 2014-T6 but better toughness at room and sub-zero temperatures. Alloy 2219 was originally developed for structural applications requiring strength at elevated temperatures. However, because of its favorable properties at cryogenic temperatures, alloy 2219-T87 plate has been used for the liquid oxygen and liquid hydrogen tanks for the space shuttle. These tanks are 8.4 m (27.6 ft) in diameter. The segments of the tanks are joined by fusion welding while assembled in large fixtures. The external tank of the space shuttle contains one liquid oxygen tank and one liquid hydrogen tank joined by an intertank skirt of aluminum alloy 7075-T6 plate. The space shuttle program has provided sufficient testing on the 2219-T87 alloy to permit an evaluation of the design-allowable properties for sheet, plate and weldments.

Of the weldable alloys 2014-T651, 2024-T851, 2219-T87, 5083-0, and 6061-T651, which were evaluated in various heat treated conditions, 2219-T87 has the best combination of strength and fracture toughness both at room temperature and at -196°C (-320°F). Alloys 2014-T6 and 2024-T8 have good tensile strength but have considerably less fracture toughness than 2219-T87 making them more difficult to weld. Alloy 5083-0 has substantially greater toughness than the other alloys but is not heat treatable. Cold working the

alloy substantially reduces ductility, leaving no advantage to its use as compared to alloy 6061-T65. Alloy 6061-T65 has good fracture toughness at room temperature and at -196°C (-320°F), but its yield strength is lower than that of alloy 2219-T87. Therefore, alloy 2219-T87 is recommended as the leading candidate among the aluminum alloys for cryogenic tank applications.

Titanium Alloys

Many of the available titanium alloys have been evaluated at sub-zero temperatures, but service experience at cryogenic temperatures has been gained only for Ti-5Al-2.5Sn and Ti-6Al-4V alloys. These alloys have very high strength-to-density ratios at cryogenic temperatures and have been the preferred alloys for special cryogenic applications.

Among these applications are spherical pressure vessels that are part of the propulsion and reaction-control systems for the Atlas and Centaur rockets, Apollo and Saturn Launch boosters, and the lunar module.

The higher strength of Ti-6Al-4V above -320°F makes this alloy more desirable than Ti-5Al-2.5Sn for cryogenic applications. Titanium Ti-6Al-4V has been used only at a cryogenic range above -320°F. Yield and tensile strength increase with decreasing temperatures while ductility and toughness decrease, giving the alloy unfavorable properties below -320°F. It may be used in the annealed condition or in the solution treated and aged condition, but for maximum toughness in cryogenic applications the annealed condition is usually preferred.

Ti-5Al-2.5Sn has good toughness and ductility throughout the cryogenic temperature range. It has good weldability and is readily available. It has been used for fuel pump impellers for pumping liquid hydrogen. It is usually used in the mill-annealed condition and has 100% alpha microstructure.

There are two precautions that should be emphasized when considering titanium and titanium alloys for service at cryogenic temperatures: 1) titanium and titanium alloys must not be used for transfer or storage of liquid oxygen or fluorine, and 2) titanium must not be used where it will be exposed to air while below the temperature which oxygen will condense on its surfaces. Any abrasion or impact of titanium that is in contact with liquid oxygen or liquid fluorine will cause ignition. Pressure vessels in contact with liquid oxygen in the Appolo launch vehicles were produced from Inconel 718 rather than from Ti-6Al-4V alloy to avoid this problem.

Titanium Ti-Al-4V and Ti-5Al-2.5Sn are recommended for cryogenic weight critical programs. Titanium has a much higher strength-to-density ratio than aluminum and stainless steels but titanium is also substantially more expensive and requires a longer procurement lead time. Cost and incompatibility with liquid oxygen and fluorine are the major restrictions on its use for cryogenic applications.

Stainless Steels

Austenitic stainless steels have been used extensively for cryogenic applications. Yield and tensile strengths of austenitic stainless steel increase substantially as testing temperatures decrease. Some austenitic steels may be fabricated by welding, but often the welding causes a reduction in the corrosion resistance. Strength of austenitic steels can be increased by cold rolling or cold drawing. Cold working at -196°C (-320°F) is more effective in increasing strength than cold working at room temperature. Cold working substantially increases yield and tensile strengths and reduces ductility and notch toughness. These properties must be evaluated for each cryogenic application.

For metallurigically unstable stainless steels such as 301 and 304, plastic deformation at sub-zero temperatures causes partial transformation to martensite which increases strength. Stainless steel types 301 and 310 have

been used in the form of extra-hard cold rolled sheet to provide high strength in such applications as the liquid oxygen and liquid hydrogen tanks for the Atlas and Centaur rockets. Type 304 stainless steel usually is used in the annealed condition for tubing, pipes and valves employed in transfer of cryogens, and for structural components that do not require high strength.

All of the 300 series stainless steel alloys (301, 310, 304L and 321) are work hardened alloys. Only the stabilized grades (304L and 321) have appropriate properties for welding to avoid sensitization and retain corrosion resistance. It is possible to weld non-stablized grades but not without additional welding processes. Alloys 321 and 304L have excellent toughness and can be used throughout the cryogenic range. The most significant drawback to using stainless steel alloys is their low strength to density ratios.

Alloy A-286

Alloy A-286 is a nitrogen strengthened stainless steel. Solution treating and aging A-286 alloys develops good strength with good ductility and notch toughness in the cryogenic range. It is readily weldable and easily obtainable. A-286 has favorable cryogenic properties, however, because it has not been used in cryogenic tank applications, a more extensive research history needs to be established before final selection of this alloy.

Inconel 718

INCONEL nickel-chromium alloy 718 is a high-strength, corrosion-resistant material used at -423° to 1300°F.

INCONEL alloy 718 is used in a wide range of applications because of its good tensile, fatigue, creep and rupture strength properties. INCONEL 718 is used for components in liquid rockets, aircraft turbine engines and cryogenic tanks.

In comparison with other cryogenic materials, INCONEL 718 has a relatively high strength-to-density ratio and good toughness, but it is also very difficult and expensive to machine.

Material Property References

Alloys for Structural Applications at Sub-Zero Temperatures by James E. Campbell: in Metals Handbook, Vol. 3, pg 721 - 772.

Cryogenic Materials Data Handbook, Vol. I and II, by F. R. Schwartzberg, S. H. Osgood, and R. G. Herzog: AFML-TDR-64-280, Martin Marietta Corporation, Denver, August 1978.

Aerospace Structural Handbook, Vol. 2, Department of Defense, AFML-TR, 68, 115, edited by J. Wolf, Mechanical Properties Data Center, Traverse City, Michigan, 1975.

Metal Materials and Elements for Aerospace Vehicle Structures in the Military Standarization Handbook, MIL-HDBK-5C, Vol. 2, Dec. 1979.

INCONEL Alloy 718, Technical Bulletin by Huntington, Alloy Products Division, the International Nickel Company Inc., Huntington West Virginia.

New Data on Aluminum Alloys for Cryogenic Applications, by J. G. Kaufman and E. W. Johnson in Advances in Cryogenic Engineering, edited by K. D. Timmerhaus, Vol. 6, Plenum. Press, 1961, pp 637 - 649.

Handbook on Materials for Superconducting Machinery by K. R. Handby et al: MCIC-HB-04, Metals and Ceramics Information Center, Battlelle Columbus Laboratories, Columbus, OH, January 1977.

Evaluation of Weldments in Austenitic Stainless Steels for Cryogenic Applications by J. M. Wells, W. A. Logsdon and R. Kossowsky in Advances in Cryogenic Engineering, edited by K. D. Timmerhaus et al, Vol. 24, Plenum Press, 1978 pp 150 - 159.

Material compatibility with Space Storable Propellants, Contract No. HF-556439 under NAS7-100, Jet Propulsion laboratory California Institute of Technology, Pasadena, California, March 1982.

7.6 MULTILAYER INSULATION

Insulation systems for cryogenic tanks must achieve maximum thermal performance while satisfying typical spacecraft requirements for handling, storage, launch, and orbital operations. As multilayer insulation (MLI) systems have demonstrated performance levels two orders of magnitude better than other insulations, they are considered the best candidate for cryogenic tank applications. Unfortunately, the installation of MLI blankets on real tanks results in significant performance penalties due to "as installed" effects. For a cryogenic tank application, the MLI system design must provide:

- Minimum outgassing and adequate gas evacuation to achieve low interstitial gas pressures (low gas conduction term)
- Sufficient layer density control to reduce solid conduction heat transfer

Multilayer insulation is a high performance vacuum insulation system that consists of a number of reflective shields in series, each separate from the next to minimize conduction between them. If the vacuum and the separator were perfect, then the heat transfer would be only by radiation and its magnitude would be

$$\dot{Q}/A = \frac{\sigma (T_h^4 - T_c^4)}{(\frac{2}{\varepsilon} - 1)(n - 1)}$$

where:

$\dot{Q}/A$	= heat flux per unit area (Btu/sec in.^{2})
σ	= the Stefan-Boltzman constant (Btu/sec in^2 °R)
ε	= emissivity for the reflectors assuming each the same
n	= the number of reflectors
T_h, T_c	= hot and cold boundary temperatures (°R)

For instance, for a one-inch thick blanket of 60 reflectors, with an emissivity of 0.03, the heat transfer would be 0.035 BTU/hr ft^2 for boundary temperatures of 40 and 530R. This heat flux would be independent of thickness for conductivity-isolated reflectors. For a number of reasons, the actual heat transfer in MLI system is significantly greater, frequently by an order of magnitude or more, and is also very sensitive to layer density.

Materials commonly used as reflectors in MLI systems include mylar or kapton film, coated on one or both sides with aluminum, silver or gold. Film thickness ranges from 0.00015 to 0.001 in. On actual tanks, reflectors will usually be perforated at intervals to facilitate evacuation of the purge gas from between the layers of the insulation blanket.

Several approaches have been used in separating the reflectors. Among these are: 1) crinkling the reflector material to minimize surface contact; 2) a similar approach wherein dimples are formed in the reflector material; 3) the use of knitted netting, such as silk, nylon or dacron, between the reflectors; 4) the use of a matted or fiber material such as fiberglass (Tissuglass or Dexiglass) as the spacer; and 5) bonding of short fibers (flocking) to one side of each reflector. Some of these methods have been tested with good success in ground experiments; however, spacecraft thermal control applications have typically only used double-aluminized mylar shields with dacron net spacers.

In addition to minimizing the solid conduction, gaseous conduction must also be reduced. When the interstitial pressure is reduced below $1x10^{-5}$ Torr, the gas thermal conductivity is reduced to a very low value, about three orders of magnitude lower than its atmospheric conductivity. Figure 7.6.1 shows this effect for a liquid hydrogen test tank. Pumping an insulation system to this pressure may be a lengthy process if the blanket is more than a few layers thick. If any outgassing of the insulation materials (or contaminants) occurs, the steady state interstitial pressure will not reach the required value until the volatile material has been pumped away.

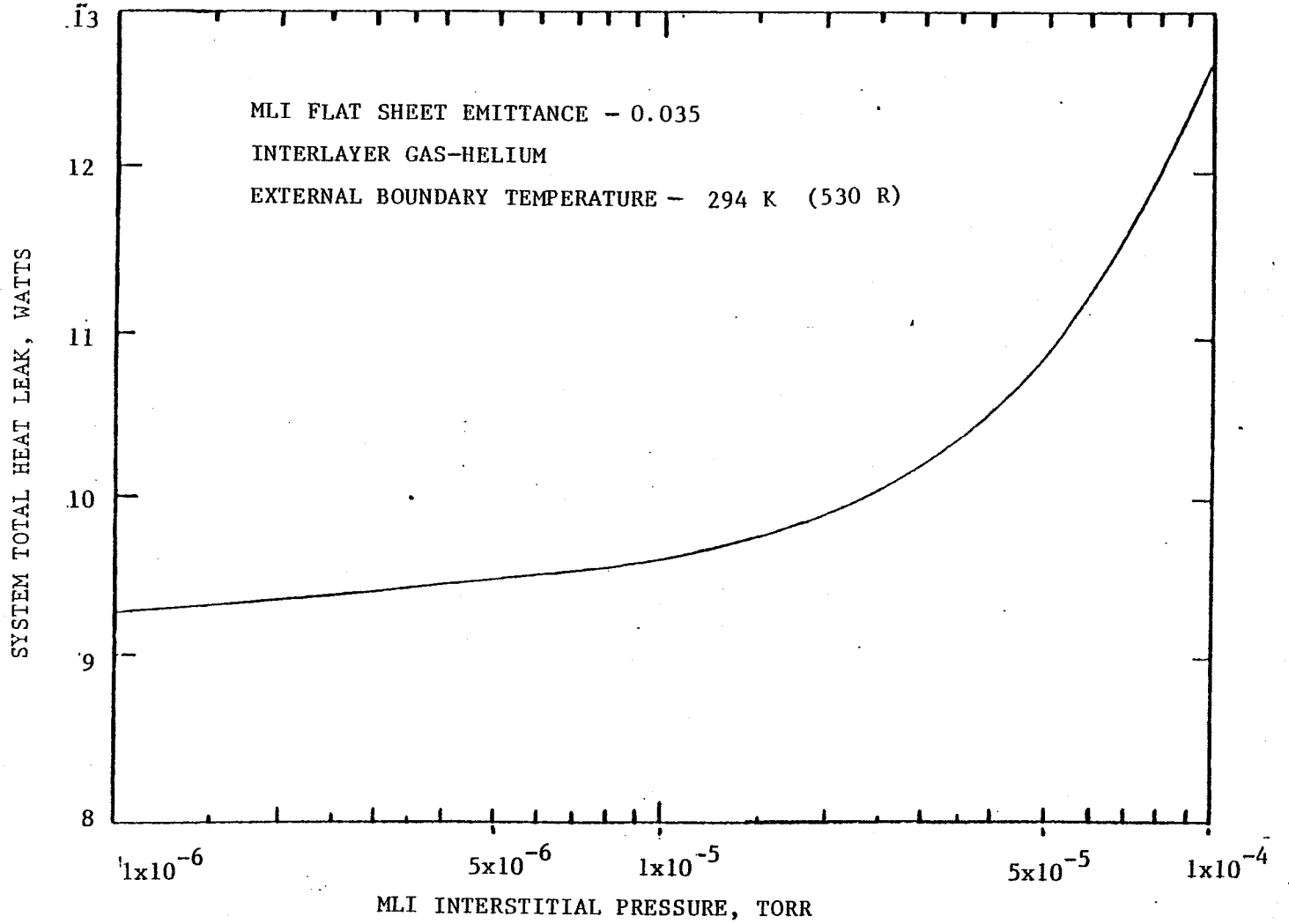

Figure 7.6.1. Effect of Interstitial Pressure on MLI Performance

For cryogenic applications, the heat transfer by solid conduction through the spacers is of major significance. This is especially true for lower temperatures, because the radiant flux, dependent on the fourth power of temperature, is relatively insignificant. Solid conduction between the insulation layers is sensitive to contact pressure, and therefore the thermal conductivity of MLI increases as the layer density increases.

Predicted Ground Hold Thermal Performance

The heat transfer rate through evacuated MLI during ground hold may be determined from the Fourier rate equation for conductive heat transfer using the apparent thermal conductivity k_t of the gas purged through the MLI.

$$\dot{Q} = \frac{k_t A_m (T_h - T_c)}{\Delta X}, \text{ Btu/sec}$$

where: ΔX is the thickness of the insulation in inches T_h and T_c are the temperatures of the warm and cold surfaces of the insulation in °R, and A_m is the mean heat transfer area of the insulation in square inches given by

$$A_m = \frac{A_2 - A_1}{\ln(A_w/A_1)}, \text{ in}^2 \qquad \text{for concentric cylinders}$$

$$A_m = (A_1 A_2)^{\frac{1}{2}}, \text{ in}^2 \qquad \text{for concentric spheres}$$

where: A_1 is the area of the enclosed surface and A_2 is the area of the enclosure. For elliptical heads on cylinders the mean area may be determined from the equation for concentric spheres, and the surface area may be given by

$$A = \tfrac{1}{4} \pi D^2 \left(1 + \frac{1 + \varepsilon^2}{2\varepsilon} \ln \frac{1 + \varepsilon}{1 - \varepsilon}\right)$$

where: D = major diameter of head, in.
$\varepsilon = [1 - (D_1/D)^2]^{\frac{1}{2}}$
D_1 = minor diameter of ellipse, in.

For a standard 2:1 elliptical head $D_1/D = .5$, $\varepsilon = .865$, and the surface area is

$$A = .345 \pi D^2$$

The effective thermal conductivity for a helium and nitrogen purged MLI system may be determined as follows*:

Helium $$k_{eff} = \frac{1}{T_2-T_1} * [.009725974(T_2-T_1) + 4.956035E\text{-}5(T_2^{2.6}-T_1^{2.6}) - 3.116392E\text{-}5(T_2^{2.7}-T_1^{2.7}) + 8.70704E\text{-}7(T_2^{3.0}-T_1^{3.0})]$$

where: k_{eff} is in Btu/h x ft x °R.

Nitrogen

$$k_{eff} = \frac{1}{T_2-T_1} * [-.0043767(_2-T_1) + 2.769053E\text{-}4(T_2^{1.6}-T_1^{1.6})], \text{ Btu/hr ft } ^oR$$

Predicted Space-Hold Thermal Performance

Lockheed Missiles and Space Company has conducted an indepth experimental investigation for MLI performance for both perforated and nonperforated shields. The predicted heat input into the tank attributed to a best data fit of a high performance perforated multilayer insulation may be calculated using the following equation‡:

* King, K., Johns, W.A., "Upgrading and Conversion of Cryogenic Analysis Programs", ESO-55024-2, Martin Marietta Denver Aerospace, July 1982.

‡ Keller, C.W., Cunnington, G.R., Glassford, A. P., "Thermal Performance of Multilayer Insulation", NAS 3-14377, Lockheed Missiles and Space Company, April 1974.

$$\dot{q}_{MLI} = \frac{C_s(\bar{N})^{2.62}T_m}{N_s}(T_h - T_c) + \frac{C_r\,\varepsilon_{TR}}{N_s}(T_h^{4.67} - T_c^{4.67})$$

$$+ \begin{cases} \frac{C_g P}{N_s}(T_h^{.52} - T_c^{.52}) & \text{for } GN_2 \\ \text{or} & \\ \frac{C_g P}{Ns}(T_h^{.26} - T_c^{.26}) & \text{for GHe} \end{cases}$$

for $\bar{N}$ in layers/inch, T in °R, P in Torr and $\dot{q}$ in Btu/h x ft^2. N_s is the total number of radiation shields.

where:	Conduction term:	C_s	$= 6.59 \times 10^{-10}$
	Radiation Term:	C_r	$= 1.44 \times 10^{-11}$
	Interstitial gas pressure:	C_g	$= 3.44 \times 10^{3}$ for GN_2
	Interstitial gas pressure:	C_g	$= 1.33 \times 10^{4}$ for GHe
	Hemispherical emittance:	ε_{TR}	$= .043$
	Temperature of hot boundary:	T_h,	°R
	Temperature of cold boundary:	T_c,	°R
	Mean Temperature:	T_m	$= \frac{T_h + T_c}{2}$, °R
	Pressure:	P,	Torr

The effective thermal conductivity (k_{eff}) may be calculated as follows

$$k_{eff} = \frac{\dot{q}_{MLI} \times \frac{N_s - 1}{LD}}{(T_h - T_c)} \quad , \text{Btu/hr ft } ^\circ R$$

where: $\dot{q}_{MLI}$ = Btu/h x ft^2
N_s = No. of effective radiation shields
LD = Layer density, layers/ft.

A good representative for a high performance unperforated multilayer insulation may be calculated using the following equation

$$\dot{q}_{MLI} = \frac{C_s(\bar{N})^{2.56} T_m}{N_s}(T_h - T_c) + \frac{C_r \varepsilon_{TR}}{N_s}(T_h^{4.67} - T_c^{4.67}) + \frac{C_g P}{N_s}(T_h^{.52} - T_c^{.52}) \quad \text{for } GN_2$$

or

$$+ \frac{C_g P}{N_s}(T_h^{.26} - T_c^{.26}) \quad \text{for GHe}$$

for $\bar{N}$ in layers/inch, T in °R, P in Torr, and $\dot{q}$ in Btu/h x ft^2

where:			
	Conduction Term:	C_s	$= 8.06 \times 10^{-10}$
	Radiation Term:	C_r	$= 1.10 \times 10^{-11}$
	Interstitial Gas Pressure:	C_g	$= 3.44 \times 10^{3}$ for GN_2
	Interstitial Gas Pressure:	C_g	$= 1.33 \times 10^{4}$ for GHe
	Hemispherical emittance:	ε_{TR}	$= .031$

The equations presented are state-of-the-art technology for high performance MLI. They provide a good representation for an MLI concept and are incorporated into the ELES thermal model.

7.7 FOAM INSULATION

The application of foam insulation to cryogenic tanks is state-of-the-art technology. Starting with the Saturn launch vehicles and continuing through the shuttle external tank (ET), material properties and applications techniques have been developed and material performance verified through testing. Based on the results of the experimental investigation* three foam insulation candidates have been selected. The foams all have low weight and good thermal properties. Table 7.7.1 presents the candidate foams and their associated properties.

TABLE 7.7.1 SELECTED FOAM CANDIDATES

Foam	Manufacturer	Density (lb_m/ft^3)	Conductivity (Btu/h-ft-°R)
CPR 488	Upjohn	2.21	$(1.70+.02452T)x10^{-3}$
BX 250A	Stepan	2.21	$(5.393+.01088T)x10^{-3}$
Rohacell 31	Rohm-GMBH	1.79	$(4.338+.02141T)x10^{-3}$

Figure 7.7.1 depicts foam thicknesses for LH_2 and LO_2 tanks resulting from this study. Because of its higher thermal conductivity the Rohacell 31 foam must be thicker than the CPR-488 and the BX-250A foams. Since the thermal conductivities of the CPR-488 and the BX-250A foams are very close at elevated temperatures, the thickness of these foams do not significantly differ for the LO_2 tank. The thermal performance of the CPR-488 is slightly better than that of the BX 250A at lower temperature, as seen by comparing the two foam thermal conductivity curves in Figure 7.7.2.

* Barclay, D.L., "Evaluation of Propellant Tank Insulation Concepts for Low-Thrust Chemical Propulsion Systems", NAS 3-22824, Boeing Aerospace Company, February 1982.

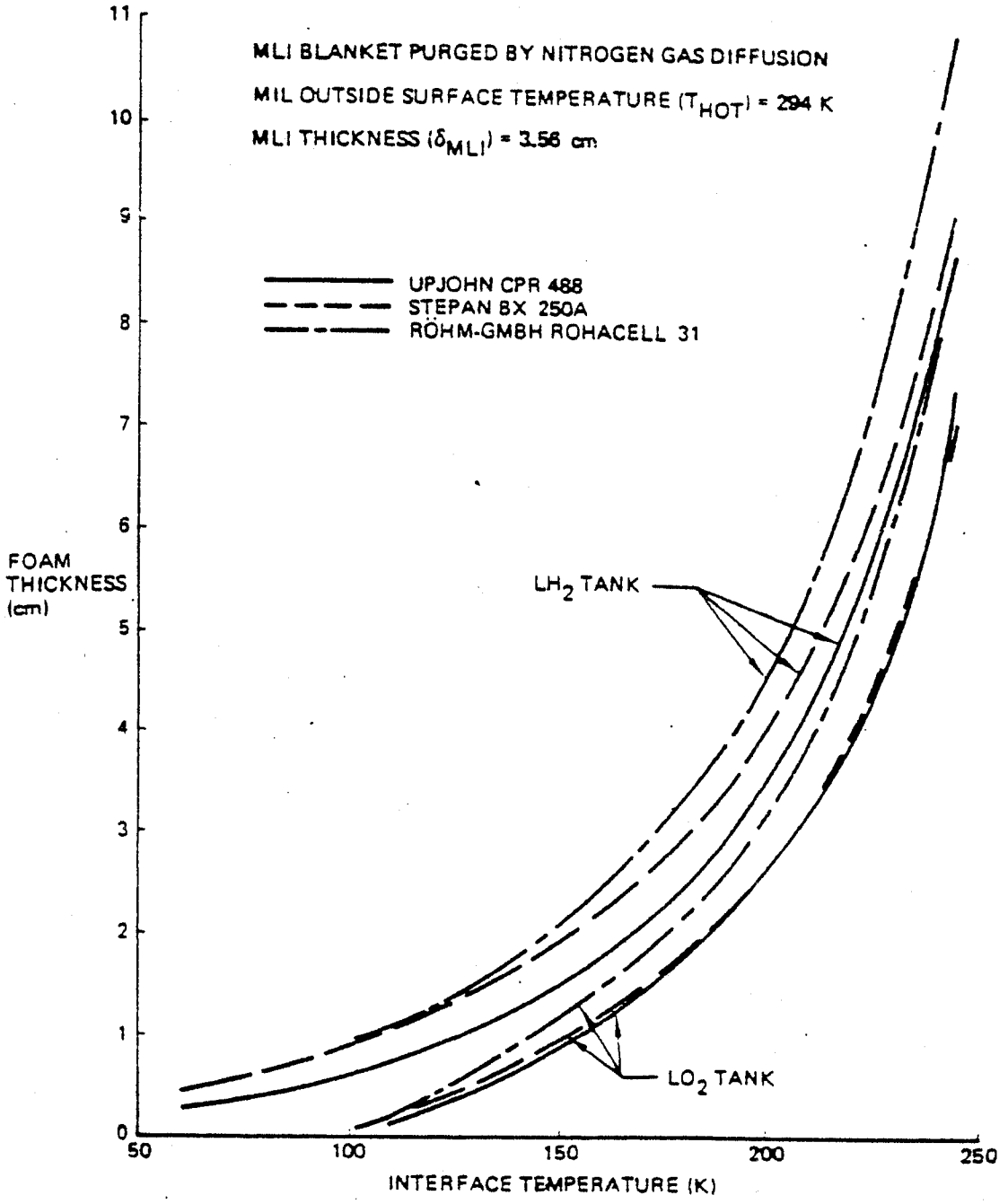

Figure 7.7.1. Foam Thicknesses vs Interface Temperature

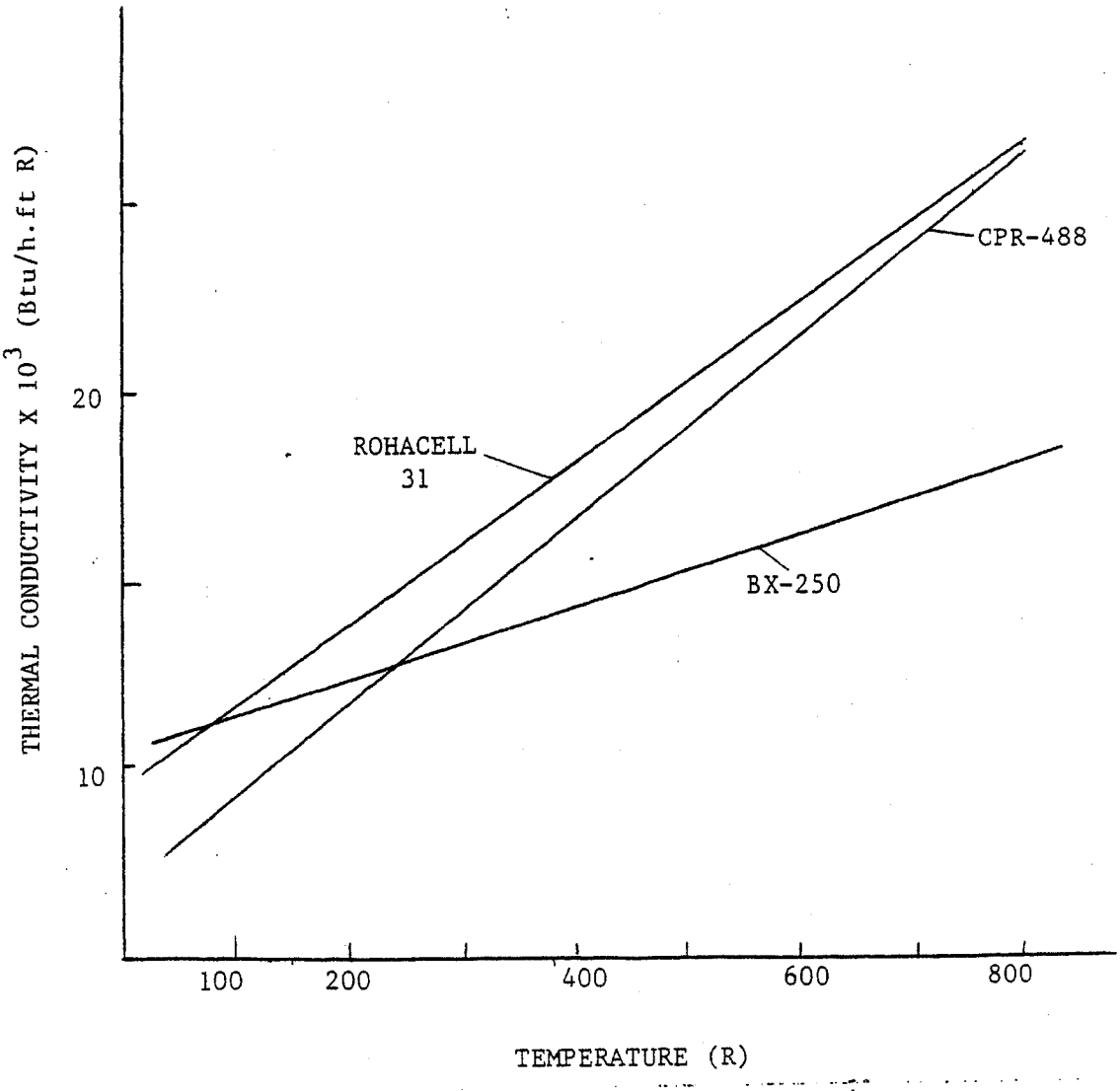

Figure 7.7.2. Thermal Conductivity Curves for Foam Candidates

In addition to a better thermal conductivity at lower temperatures, CPR-488 is also less constrained by design limitations for bonding temperature, heating rate and shear as compared with BX-250A (see Table 7.7.2). Therefore CPR-488 is considered to be the best candidate as a representative for a high performance foam insulation concept.

Table 7.7.2 CPR MAXIMUM DESIGN LIMITS FOR CPR-488 AND BX-250A

Parameter	Maximum Limits	
	CPR-488	BX-250
Bonding Temperature	300°F	200°F
Maximum Heating Rate	No Limit*	4 Btu/ft^2-s
Maximum Shear	2 lb_f/ft^2	1.2 lb_f/ft^2

*actual test limit was 18 Btu/ft^2-s

CPR-488 is a sprayable foam insulation (SOFI) utilized in low heating and low shear applications as compared to ablator usage. Its low density and conductivity is required for minimizing heat leaks and ice/frost formation.

7.8 SUGGESTED INSULATION THICKNESSES

ELES thermal models are set up to allow for any combination of the two insulation concepts (MLI and SOFI). In fact, combinations of any two insulations may be used if the necessary inputs are known. For use of CPR-488 or MLI alone, or a combination of both, the following section provides the necessary information to calculate reasonable thicknesses for use as inputs.

Since CPR-488 is simple to apply and requires no special operations during launch, it is good for tanks that require simple subsystem designs or a minimum of attention. Additionally, stages that will not spend much time outside the atmosphere (> 3 hours) cannot effectively use a high-performance insulation and so CPR-488 would be suggested for this application.

Conversely, MLI provides far superior performance to CPR-488 after the insulation has been evacuated. Since this may take a time period on the order of hours, it is suggested to use MLI either for vehicles that spend more than three hours outside the atmosphere or purely as a radiation shield. Used alone, MLI requires purging with a non-condensable gas that is pumped between the layers to prohibit condensation or freezing of other gases which would result in performance degradation or increased space-evacuation times. For applications on LH_2 tanks gaseous helium is the only option. But, by using an underlayer of CPR-488, the bottom layer of the MLI could be raised to a temperature that is above the liquification temperature of gaseous nitrogen. This would then allow a simpler purge system using nitrogen gas instead of helium.

The following paragraphs explain the approach to calculate insulation thicknesses suggested for use on the tanks if no other values are specified.

MLI alone would generally be used for upper stages of launch vehicles, orbit transfer vehicles or any tanks that are to experience an extended stay outside the atmosphere. From previous studies of cryogenic tanks, equations have been formulated to predict the thickness of insulation that minimizes the total mass of the system. This is achieved by predicting the thickness that produces a minimum mass for the boiloff/insulation, see Figure 7.8.1. A simplified equation was developed and was checked against various propellants and tank shapes and sizes. The equation and results of the comparison are shown in Table 7.8.1. The largest variation between the predicted and actual optimum was for a small LH_2 tank, the difference being 1.3%. Figure 7.8.2 shows the mass of the small LH_2 system as a function of insulation thickness. From this figure it can be seen that the minimum is actually quite flat. This was found to be true for all systems; thus a large variation of the predicted thickness from the actual optimum does not result in a large variation of the total mass.

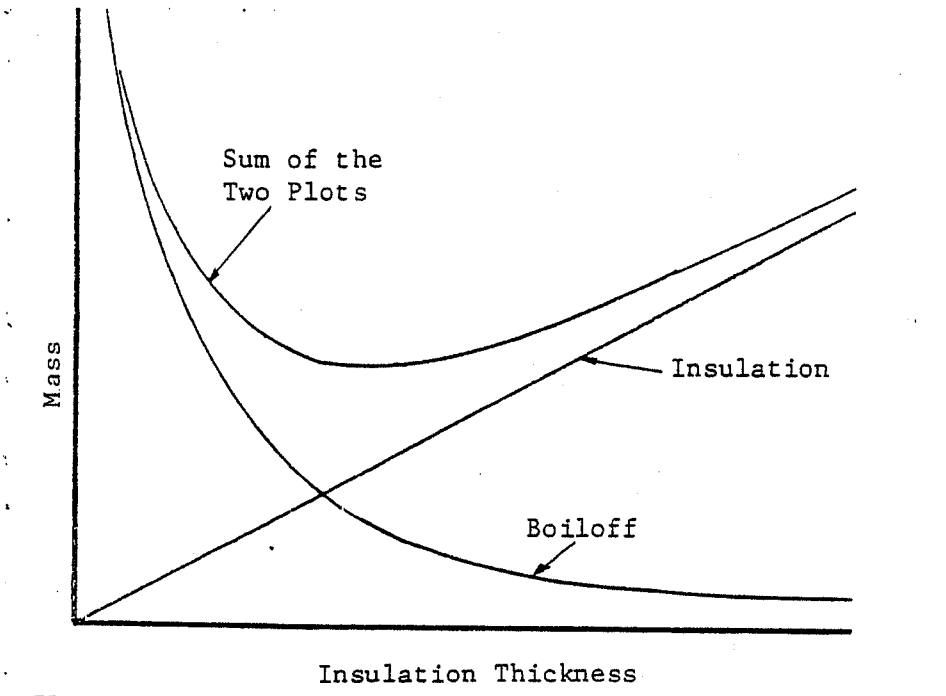

Figure 7.8.1. Effect of Insulation Thickness on System Mass

TABLE 7.8.1

OPTIMUM INSULATION THICKNESS VARIANCES

Propellant	Tank Shape	Diam, in.	L/D	Wet System Mass, lbm	Optimum Thickness, in		Total Mass% Difference,
					Predicted	Actual	
LH_2	Sphere	32	1	333	2.2	2.8	1.3
LF_2	Cylinder/ Spherical Domes	6	3.2	33	0.62	0.8	0
			14.2	131	0.62	0.8	0.2
LO_2	Toroid	30(168)	--	38,080	1.2	0.96	0.02
LH_2	Cylinder/ Elliptical Domes	168	0.95	7,550	1.04	1.04	0.0
LO_2	"	72	1.8	18,525	1.1	0.76	0.05
LCH_4	"	60	2.2	5,120	0.68	0.64	0

$$x' = \left\{ \left[\frac{r^2}{4} + \sqrt{\frac{(k_o \theta_o \Delta T_o + k_g \theta_g DT_g) r^2 v_{fg}}{\rho_I h_{fg} v_g}} \right]^{0.5} - \frac{r}{2} \right\} \times 12 \qquad (1)$$

where:

x' = Predicted optimum insulation thickness; in

k_g = Thermal conductivity of MLI during ground-hold interval; Btu/h-ft-°R

k_o = Thermal conductivity of MLI after evacuation; Btu/h/ft/°R

θ_g, θ_o = Time of effective ground-hold and on-orbit time; h

ΔT_g, ΔT_o = Temperature difference between top and bottom layer of MLI for ground-hold and on-orbit conditions; °R

r = Radius of tank (for toroid use minor radius of torus); ft

ρ = Density of MLI; lbm/ft^3

h_{fg} = Latent heat of vaporization for the propellant; Btu/lbm

v_g, v_{fg} = Specific volume of gas and of change of evaporation; ft^3/lbm.

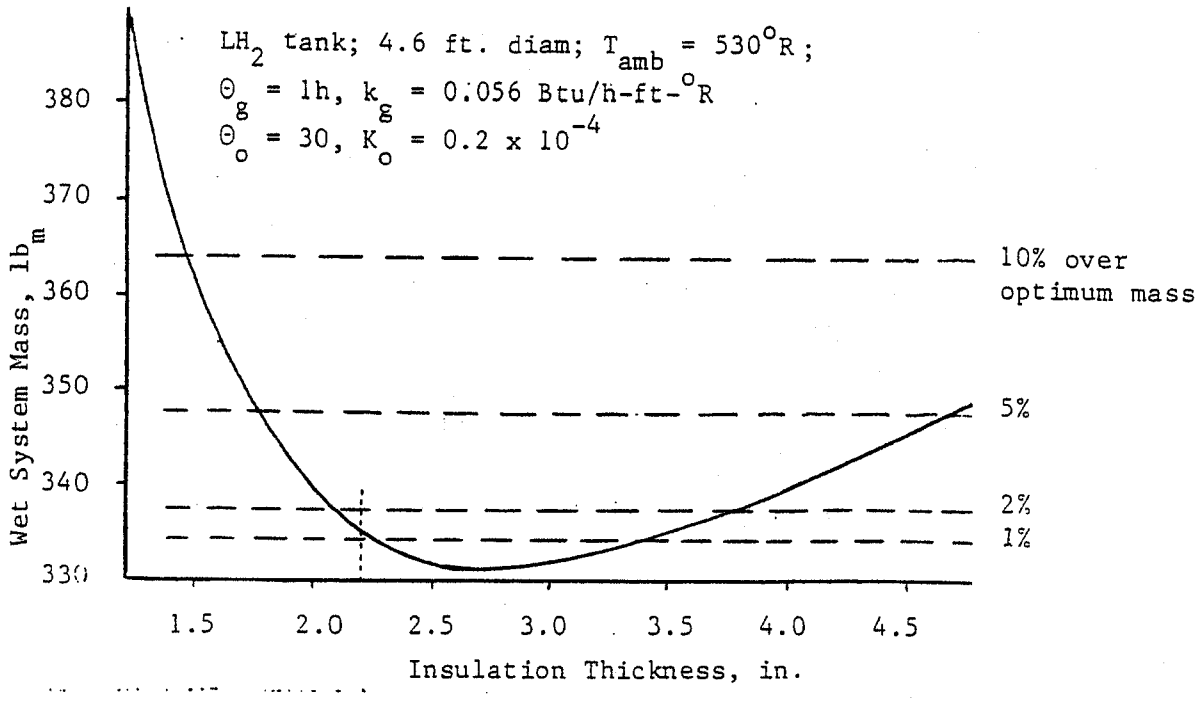

Figure 7.8.2. Variation of Total LH_2 Tank System Mass with Insulation Thickness

No equation currently exists for predicting the optimum thickness of CPR-488 alone.. Rather than deriving a long complex equation to predict how much CPR-488 to use, it was more appropriate to provide a single suggested thickness of one inch for all tanks. This is the thickness recommended for the ET to prohibit ice formation for up to 24 hours. Application techniques for this spray-on foam insulation (SOFI) allow tolerances of ± 0.25 inches, thus negating the accuracy of detailed analysis.

MLI and CPR-488 are often combined. The purpose of placing a layer of SOFI between the tank wall and the MLI is to increase the temperature of the bottom aluminized sheet above that of the liquification temperature of nitrogen. Thus the MLI/CPR-488 interface temperature must be chosen to calculate the insulation thicknesses. Equations to calculate thicknesses are shown below:

$$x'_{MLI} = \left\{\left[\frac{r^2}{4} + \sqrt{\frac{k_o \Theta_o \Delta T_o r^2 v_{fg}}{\rho_I h_{fg} v_g}}\right]^{0.5} - \frac{r}{2}\right\} \times 12 \qquad (2)$$

$$x'_f = x'_{MLI} \left(\frac{k_f}{k_{N_2}}\right) \left(\frac{T_I - T_c}{T_h - T_I}\right) \qquad (3)$$

Where the variables in equation 2 were defined previously in Table 7.8.1 and those in equation 3 are as follows:

x'_f	= Thickness of foam insulation; in
x'_{MLI}	= Thickness of MLI; in
k_f	= Thermal conductivity of the foam; Btu/h-ft-°R
k_{N_2}	= Thermal conductivity of the gaseous nitrogen; Btu/h-ft-°R
T_c, T_h, T_I	= Temperatures at the cold (tank) side, hot exterior of MLI) side, and the MLI/CPR interface; °R

Equation 2 is essentially the same as equation 1 in Table 7.8.1, but this time only the on-orbit component is considered; the CPR takes care of ground-hold concerns. Equation 3 is determined by ratioing the heat leaks to achieve the desired interface temperature.

7.9 PROPELLANT BOILOFF

In order to calculate the amount of propellant boiloff observed for a given total heat leak the following equation was derived. Starting with the continuity equation, energy balance and thermodynamic identities for both the liquid and the gas, the resulting equation provides a boiloff calculation such that

$$M_e = \frac{\tau \dot{q}_{total} v_{fg}}{h_{fg} v_g}$$

where:

M_e	= Mass of propellant that evaporates (lb_m)
τ	= Time (sec)
$\dot{q}_{(total)}$	= Total heat leak (Btu/sec)
v_g	= Specific volume of gas (in^3/lb_m)
v_f	= Specific volume of fluid(in^3/lb_m)
v_{fg}	= $v_g - v_f$ (in^3/lb_m)
h_{fg}	Latent heat of vaporization (Btu/lb_m)

The multiplying factor (v_{fg}/v_g) is the difference between this approach and the more simple method of direct conversion

where: $$M_e = \frac{\tau \dot{q}_{Total}}{h_{fg}}$$

Differences in results from the above equations are most significant for low density liquids such as LH_2 or when a liquid is close to its critical point. For example, results for LH_2 at 25 psia differ by 3.5%, LO_2 and LCH_4 at 30 psia by 1% and LO_2 at 500 psia (P_c = 731 psia) by 26%. Thus at normal operating pressures the difference is small but significant.

7.10 TANKAGE HEAT TRANSFER

ELES calculates the heat flux into propellant tanks under the three scenarios which follow. Because the optimizer requires continuous functions in order to calculate reliable derivative information, the iterative procedures which calculate these heat fluxes are controlled by an iteration loop limit rather than an error or accuracy termination criteria.

The user has the option of using spray on foam insulation (SOFI), or multilayer insulation (MLI) in any combination of thicknesses. The user may input constant thermal conductivities at the existing tank conditions. The MLI may be purged with either helium or nitrogen for both a ground-hold or space-hold condition. Although the equations for MLI thermal conductivity are "hard-wired" into the program, the constants in the equation used to calculate SOFI conductivity are inputs. This allows various foam insulations to be used in the conductivity-calculation mode.

7.10.1 CONSTANT EXTERNAL BOUNDARY TEMPERATURE

The simplest of the heat flux scenarios is the case of a constant external boundary temperature. The calculation is then modeled as a simple composite thermal barrier having one convective heat transfer path and three conductive paths as shown below.

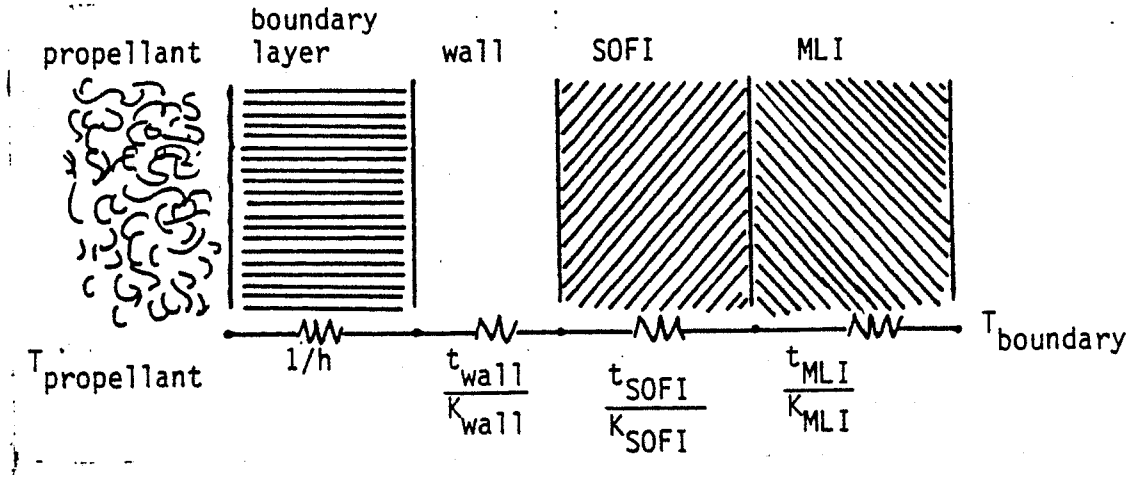

$$q_{\substack{\text{composite}\\ \text{barrier}}} = \frac{(T_{boundary} - T_{propellant})}{(\frac{1}{h} + \frac{t_{wall}}{k_{wall}} + \frac{t_{SOFI}}{k_{SOFI}} + \frac{t_{MLI}}{k_{MLI}})}$$

The solution to this composite thermal barrier is made iterative by the fact that the thermal conductivities and the heat transfer coefficient are functions of temperature.

In parallel with this heat path are the heat loads presented by tank penetrations, lines, struts, and common domes. It has been considered that these loads can be decoupled from the composite barrier equations and included in the form

$$q_{total} = q_{composite} + q_{struts} + q_{penetrations} + q_{common\ dome}$$

The heat load due to tank struts is based on a curve fit of heat leak data for actual tank hardware. Two different curves are presented; one for heat leaks involving hydrogen, and one for heat leaks involving other cryogens (see Figure 7.10.1.1). The equations which fit that data are

$$Q_{strut} = 0.2\ M_{prop}^{0.56} \quad \text{for hydrogen}$$
$$Q_{strut} = 0.04\ M_{prop}^{0.48} \quad \text{for other cryogens}$$

where: Q_{strut} = heat leak through struts (Btu/hr)
M_{prop} = total mass of propellant in tank (lbm)

Because the data applies to tanks with design accelerations of 6 g's, the equation can be further manipulated to include acceleration effects. Assuming that the strut heat leak is directly proportional to acceleration

$$Q_{strut} = a\ (g/6)\ M_{prop}^{b}$$

where: a = empirical constant
g = g load on tank
b = empirical constant

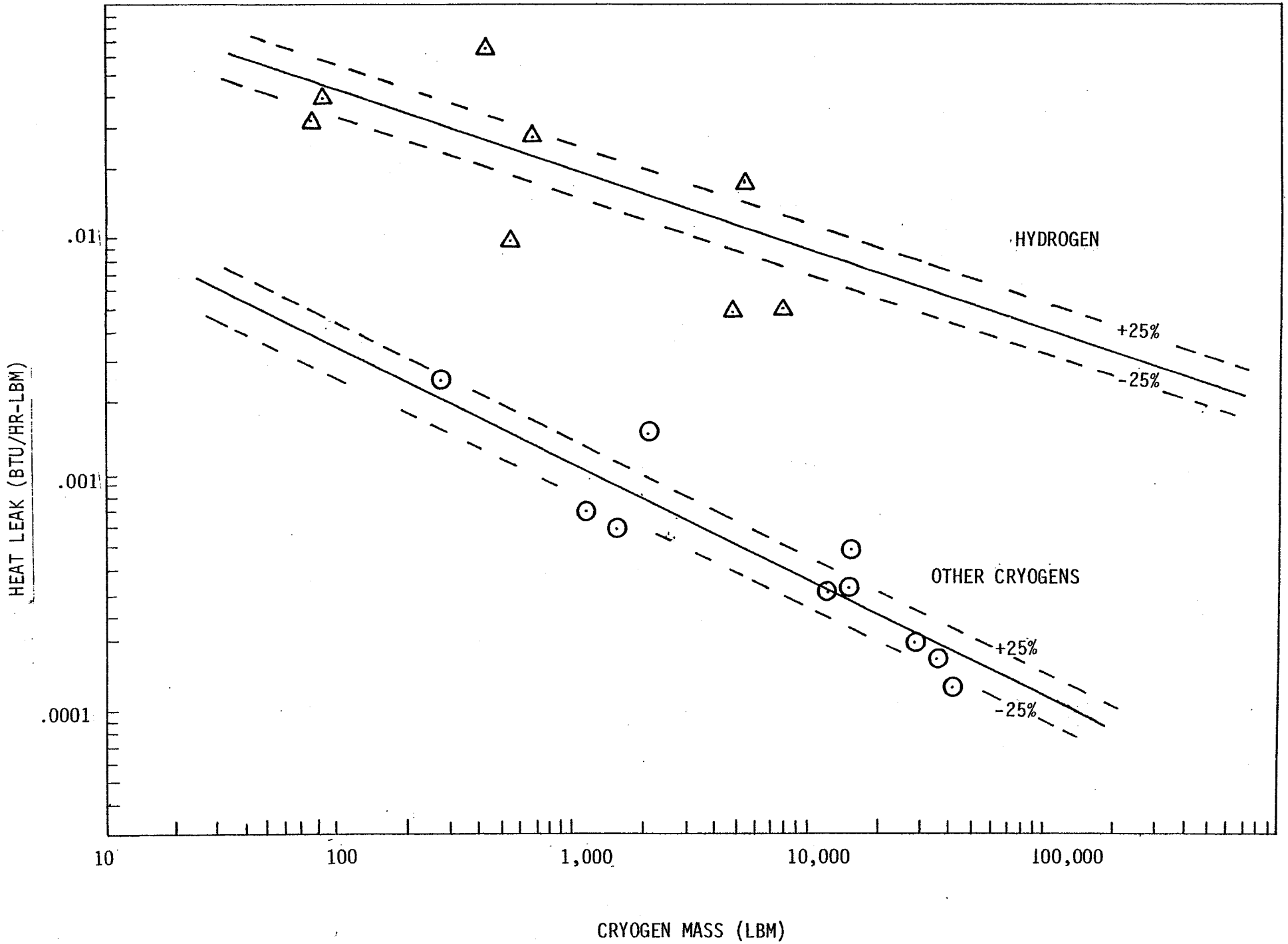

Figure 7.10.1.1. Heat Leak through Fiberglass Supports

Similar to the heat leak through struts, the heat leak through lines, instrumentation, and other penetrations has been based on curve fits of empirical data for existing hardware. (see Figure 7.10.1.2). The equations which fit that data are

$$Q_{pen} = 0.161\ M_{prop}^{0.512} \quad \text{for hydrogen}$$
$$Q_{pen} = 0.0103\ M_{prop}^{0.512} \quad \text{for other cryogens}$$

where: Q_{pen} = heat leak due to tank penetrations (Btu/hr)
M_{prop} = total mas of propellant in tank (lbm)

The heat leak due to common dome construction is based on a thermal model. The use of a common dome membrane between two propellants will result in an exchange of heat between the two liquids. It will not change the net heat loading from the environment but will change the amount of heat that is absorbed by each propellant, and calculation of this amount of heat exchanged depends on the construction of the common dome arrangement and the propellants on either side.

Various approaches to thermally isolate the two propellants exist. Due to the widest range of applicability for this program and availability of data, the approach of the Centaur was chosen. This approach uses concentric domes that are separated by a layer of fiberglass insulation and a gap that is cryopumped by the low temperature of the LH_2. Since combinations other than LO_2/LH_2 and LF_2/LH_2 are to be modeled an adjustment has been added to account for this.

Thermal analyses of the concentric bulkhead used in the Centaur have been performed to provide an effective thermal conductance for this design. For inclusion in the thermal model, ELES will use the value of 0.039 Btu/h-ft^2-°R as a heat leak rate per unit area for either LH_2 fueled combinations. The total heat conducted into the lower temperature liquid and away from the warmer propellant is simply

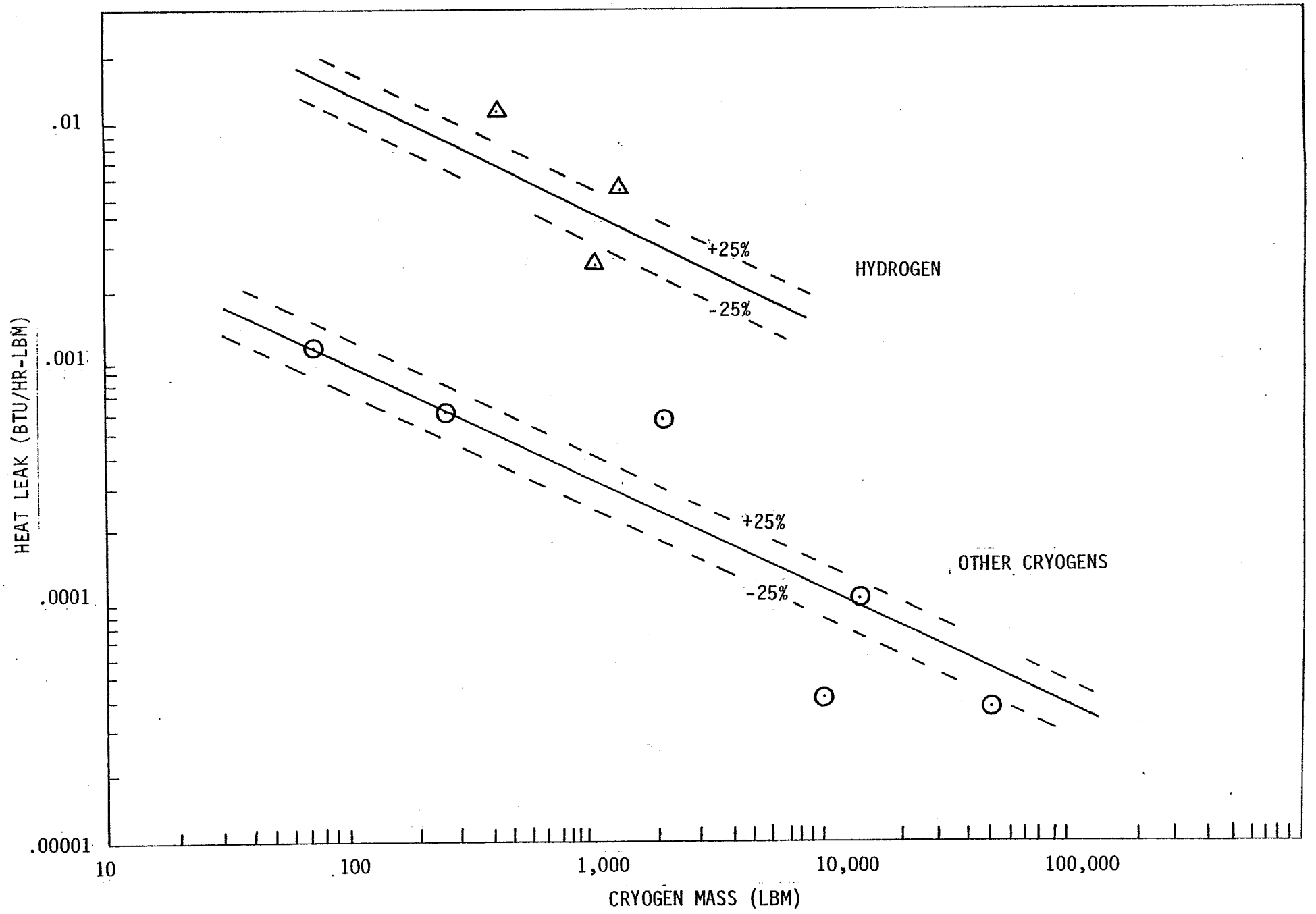

Figure 7.10.1.2. Heat Leak through Lines and Instruments

$$q_{\text{Common dome}} = (0.039)(A_D)(\Delta T_p), \text{ Btu/h}$$

where:

A_D = Dome conduction surface area (ft^2)

ΔT_p = Temperature difference between the LO_2 (LF_2) and LH_2 (°R)

The value for the effective conductance corresponds to a typical measured heating rate through the intermediate bulkhead of 710 Btu/h.

When propellant combinations not using LH_2 as fuel are used, the gap will not be cryopumped, and therefore the effective thermal resistance will be degraded by the presence of the gaseous nitrogen. The other possible combinations will not have as critical a thermal condition as LH_2 presents, or as large a tank surface area. Thus, a degradation is not so critical. To accomodate this increase in the conductance we will assume that the gaseous nitrogen is at the temperature of the coldest propellant. Using this assumption, a thermal conductivity is calculated, and this is divided by the thickness of the layer of gaseous nitrogen.

$$\text{Thermal Conductance} = 1/\text{Thermal Resistance} = kA/\Delta x$$

and

$$\text{Conductance/Unit Area} = k/\Delta x$$

Total Effective Conductance/Unit Area = $(12k/\Delta x + 0.039)$; Btu/h-ft^2-°R

where:

k = Thermal conductivity of N_2 as a function of temperature; Btu/h-ft-°R

$$k_{(T_2-T_1)} = \frac{1}{T_2-T_1}\left[2.76905(T_2^{1.6} - T_1^{1.6})\ 10^{-4} - 0.0043767(T_2-T_1)\right]$$

Δx = Thickness of N_2 layer; 0.02 inches for a pressurized tank

Therefore, the general equation to compute the total heat transfer from the warmer to the colder propellant is

$$q_{\text{common dome}} = (12k/\Delta x + 0.039)(A_D)(\Delta T_p)$$

where: k = 0 if LH_2 is the fuel.

7.10.2 **Tankage Radiant Heat Loads**

The heat flux scenario involving an incident radiant heat flux onto the stage is built largely upon the work done on the simple composite conduction heat flux scenario. The difference between the two is the fact that the external boundary temperature is a variable in the radiant heat flux problem. After solving for the boundary temperature, the two problems are identical. The boundary temperature is calculated by performing a heat balance on the surface of the tank at steady state.

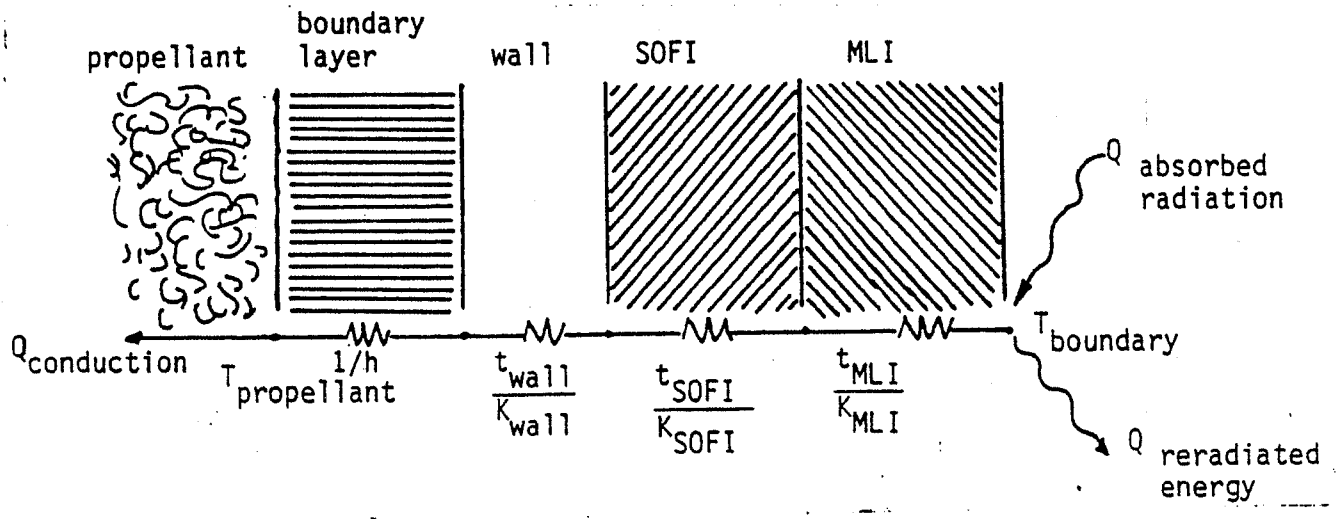

$$Q_{\text{absorbed radiation}} = Q_{\text{reradiated energy}} + Q_{\text{conduction}} \qquad (1)$$

Each of the terms in the above steady state energy balance can be expanded as

$$Q_{\text{reradiated energy}} = \sigma \, \varepsilon_v \, T_v^4 \, A_v$$

$$Q_{\text{conduction}} = q_{\text{conduction}} \, A_v$$

$$Q_{\text{absorbed radiation}} = Q_{\substack{\text{direct} \\ \text{solar}}} + Q_{\substack{\text{reflected} \\ \text{solar}}} + Q_{\substack{\text{earth} \\ \text{radiated}}}$$

Each term in the absorbed radiation term is expressed as

$$Q_{\text{direct}} = \alpha_v \, A_{vs} \, f_s \, C_s$$

$$Q_{\text{reflected solar}} = \alpha_v \, A_{ve} \, f_e \, a_e \, C_s \, (Re/Rv)^2$$

$$Q_{\text{earth radiated}} = \alpha_v \, A_{ve} \, C_e \, (Re/Rv)^2$$

where:
- Q = heat flow (Btu/sec)
- σ = Stephan-Boltzmann constant = 3.302 E-15 Btu/sec-in.^{2} °R^4
- ε = emissivity
- T = temperature (°R)
- A = area (total or cross sectional) (in.^{2})
- q = heat flux (Btu/in.^{2}-sec)
- α = absorbtivity
- f = fraction of time exposed to radiation source
- a = albedo (a_e = 0.39)
- C = radiation constant (Btu/in.^{2}-sec)
- R = radius

subscripts:
- v = vehicle
- s = sun
- e = earth

By combining these equations back into the form of equation (1) and by assuming that the vehicle cross sectional area presented to the earth (A_{ve}) equals that presented to the sun (A_{vs}), one obtains the following:

$$\alpha_v A_{vs}\left(f_s C_s + f_e a_e C_s (Re/Rv)^2 + C_e (Re/Rv)^2\right) = \sigma \varepsilon_v T_v^4 A_v + q_{conduction} A_v$$

The vehicle external temperature can be directly expressed as

$$T_v = \left[\left(\frac{\alpha_v A_{vs}}{\sigma \varepsilon_v A_v}\right)\left(f_s C_s + f_e a_e C_s (Re/Rv)^2 + C_e (Re/Rv)^2\right) - \left(\frac{q_{conduction}}{\sigma \varepsilon_v}\right)\right]^{1/4} \qquad (2)$$

It is equation (2) which is solved in ELES for the boundary temperature. Since the conduction heat flux into the tank is a function of the vehicle external boundary temperature, the solution is iterative.

The values of the constants in the equation (2) are

f_e = 0.5
a_e = 0.39
C_s = 8.28 E-4 Btu/sec-in.^{2}
C_e = 1.46 E-4 Btu/sec-in.^{2}
σ = 3.302 E-15 Btu/sec,in.^{2} °R^4

One parameter of interest in the above equation is the fraction of time a vehicle spends in direct sunlight (f_s). The user inputs which determine this are the orbital radius (Rv) and the orbit-plane-angle with the earth-sun vector (γ). These inputs are used to calculate the vehicles maximum distance above the earth-sun vector (S) as follows:

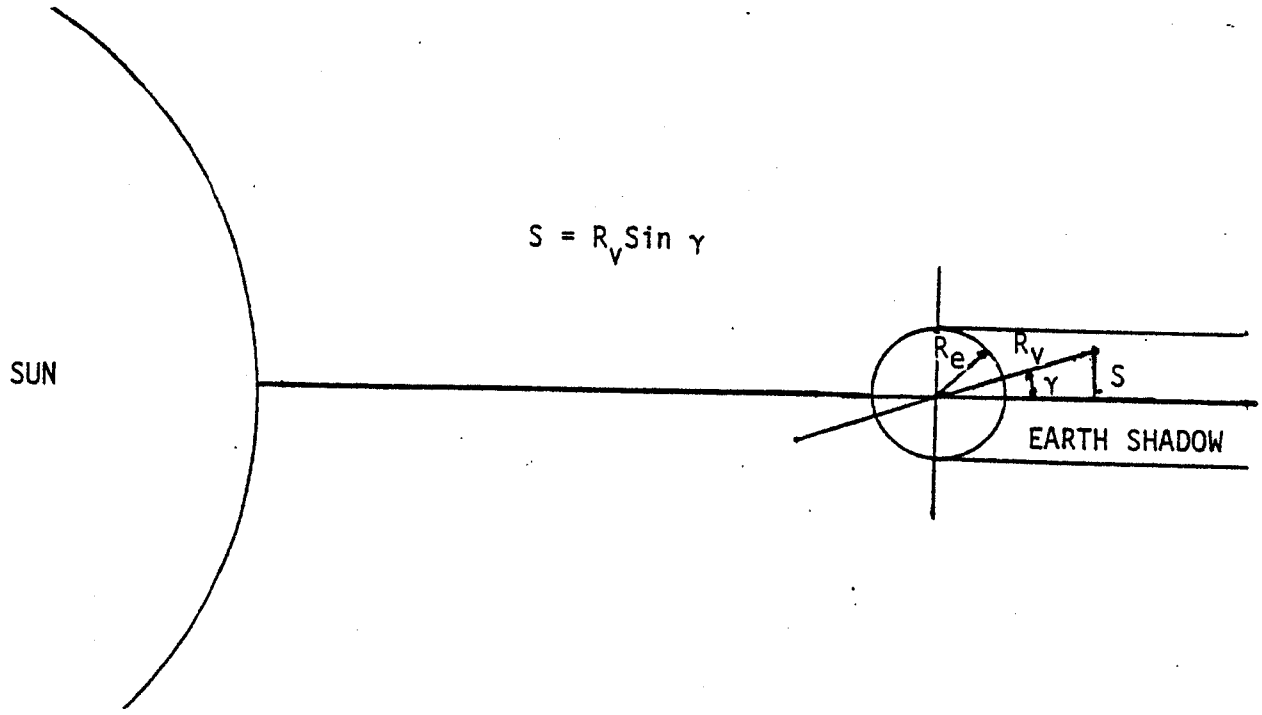

If the value of S is greater than the earth's radius, then the vehicle spends all its time in direct sunlight and $f_s = 1.0$. If S is less than Re then it can be shown by projecting the orbit onto the plane perpendicular to the earth-sun vector that

$$f_s = 1.0 - \left(\frac{1}{\pi}\right) \text{ARCSIN}\left(\left[\frac{\left(Re/Rv\right)^2 - \text{Sin}^2\gamma}{1 - \text{Sin}^2\gamma}\right]^{\frac{1}{2}}\right)$$

Also in equation (2) ELES assumes that the ratio (A_{VS}/A_V) of the vehicle radiation-exposed cross sectional area to the total surface area is approximated as (1/3.5). This corresponds to a cylindrical tank with hemispherical ends in which the tank length equals twice the tank diameter. For a sphere $(A_{VS}/A_V) = 1/4$. For an infinite cylinder $(A_{VS}/A_V) = 1/\pi$. The error introduced by the above approximation can only affect the calculation of T_V by as much as 3 percent.

7.10.3 Ground Hold Ice Layer Heat Transfer

For ground hold ice layer heat transfer the heat transfer rate at incipient ice formation was chosen as the worst-case heat transfer rate for cryogenic tanks. When ice formation is a possibility, it is illegal to

specify MLI insulation, since ice will form between the layers and "short" the thermal circuit. Spray-on foam insulation or no insulation are the only legal choices for ground hold ice heat transfer.

Assuming that the surface temperature of the insulation is held constant by the phase change equilibrium of water, the steady-state rate of heat transfer can be calculated as

$$q_{cond} = k\,(T_{eq} - T_p) / t$$

where:

q_{cond}	= heat flux (Btu/in.^{2}-sec)
k	= tank wall thermal conductivity (Btu/in.-sec °R)
T_{eq}	= water equilibrium temperature (°R)
T_p	= propellant temperature (°R)
t	= insulation thickness (in.)

In order to determine if the rate of mass transfer of water to the insulation surface can support that heat flux with its heats of condensation and freezing, it is necessary to conduct a mass transfer rate calculation. Assuming forced convection around a cylinder, the mass transfer coefficient can be obtained by analogy with heat transfer correlation as

$$Nu_m = 0.683\, R_e^{0.466}\, S_c^{1/3}$$

$$h_m = \left(\frac{c\, D_{AB}}{D}\right) 0.683\, R_e^{0.466}\, S_c^{1/3}$$

$$\simeq \left[\frac{1.95E\text{-}7\ (vD)^{0.466}}{D}\right] \frac{\text{lb mole}}{\text{sec}}$$

where:

Nu_m	= mass transfer Nusselt number
Re	= Reynolds number
Sc	= Schmidt number
v	= velocity (in./sec)
D	= diameter (in.)
c	= total molar concentration (lb mole/in.^{3})
D_{AB}	= diffusivity of water in air (in.^{2}/sec)

Using the above equation for the mass transfer coefficient, the mass transfer rate can be calculated from

$$W = \frac{h_m A (X_o - X_\infty)}{(1 - X_\infty)}$$

where:
- W = molar flux of water (lb moles/sec)
- h_m = mass transfer coefficient (lb moles/in.^{2}-sec)
- A = surface area (in.^{2})
- X_o = mole fraction of water at surface
- X_∞ = mole fraction of water in ambient air

The maximum heat transfer due to ice formation is then calculated as

$$q_{max} = W (\Delta H_c + \Delta H_f) / A$$

where:
- q_{max} = maximum heat flux (Btu/in.^{2}-sec)
- ΔH_c = heat of condensation of water (Btu/lb mole)
- ΔH_f = heat of freezing of water (Btu/lb mole)
- A = surface area (in.^{2})

The actual heat transfer rate at incipient ice formation is then the minimum of q_{cond} or q_{max}.

The use of the above mass transfer equations requires the availability of water concentrations at the surface and in ambient air. The mole fraction of water at the ice surface is assumed to be the vapor pressure of ice at 0°C divided by one atmosphere, or 0.005. The concentration of water in ambient air is taken from the psychrametric charts as a function of ambient temperature and relative humidity (see Figure 7.10.3.1).

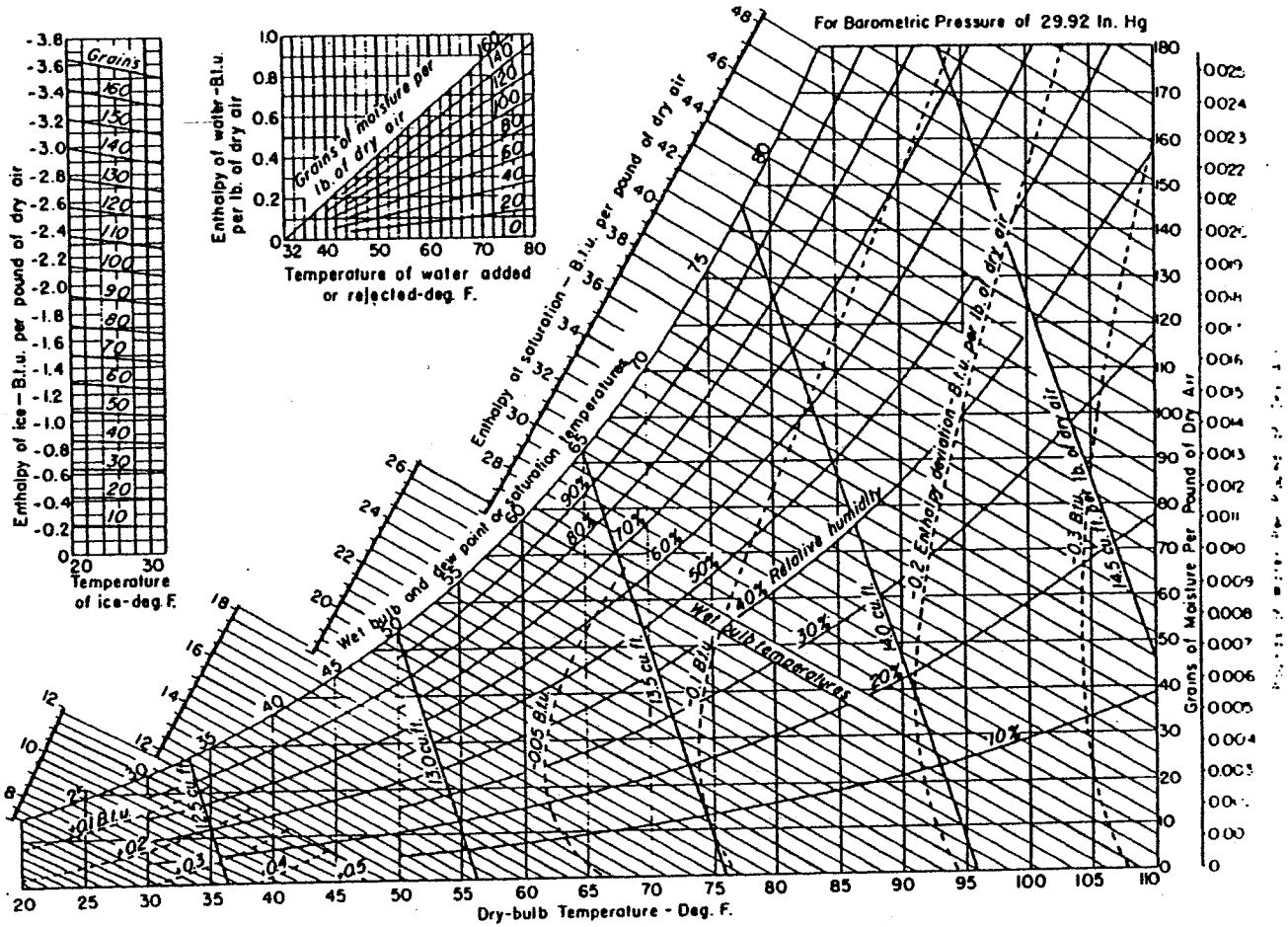

Figure 7.10.3.1. Psychrometric Chart

8.0 PROPELLANT PRESSURE/TEMPERATURE/FLOWRATE SCHEDULES

In order to accommodate the various engine power cycles in ELES, a standard propellant flow schedule was made. At key points within the schedule, the propellant pressure, temperature, and flowrate are determined in order to allow easy interface with the many routines in ELES. The nomenclature used in ELES for the three schedules is shown in Figures 8.1 through 8.3.

The general pressure/flowrate schedule is displayed graphically in Figure 8.4. In order to accommodate all of the power cycles available there are more flow paths in the diagram than can be used with any one cycle. The general diagram can be more easily understood if each of the cycles are examined individually.

The simplest of the power cycles is the pressure fed cycle (shown schematically in Figure 8.5). This cycle is driven strictly by the pressure in the propellant tanks, which may be provided by high pressure stored gas or a solid gas generator. Although the engines associated with pressure fed cycles are typically low pressure ablatively cooled engines, there is no inherent limitation against high pressure and/or regeneratively cooled designs.

The pressure fed flow schematic (Figure 8.6) reflects the simplicity of the cycle. It shows no autogenous nor turbine-related flowrates. Either oxidizer or fuel may be used as regenerative coolant with some regen jacket bypass flow and transpiration cooling.

The gas generator bleed cycle (shown schematically in Figure 8.7) uses small amounts of fuel and oxidizer to feed a gas generator, which drives a turbine. The turbine exhaust is dumped overboard either through a bleed nozzle or into the main engine nozzle for cooling. Although there is a performance loss associated with dumping the turbine exhaust, this cycle has the advantage of low pump discharge pressures required to achieve a given chamber pressure.

WDTKOF, WDTKOO - fuel and ox tank outlet flowrates
WDPMPF, WDPMPO - fuel and ox pump flowrates
WDVLVF, WDVLVO - fuel and ox biprop valve flowrates
WDREGF, WDREGO - fuel and ox regen cooling flowrates
WDTANF, WDTANO - fuel and ox transpiration cooling flowrates
WDBYPF, WDBYPO - fuel and ox turbine bypass flowrates
WDINJF, WDINJO - fuel and ox injector flowrates
WDBYRF, WDBYRO - fuel and ox gas generator/preburner inlet flowrates
WDTROF, WDTROO - fuel and ox turbine outlet flowrates
WDAUTF, WDAUTO - fuel and ox autogenous pressurization flowrates
WDTURB - turbine flowrate
WDBLNZ - gas generator bleed nozzle flowrate

Figure 8.1. Flowrate Schedule Nomenclature

- Feed Temperatures

TULLOX, TULLFL - Propellant tank ullage gas temperature
TPNOMO, TPNOMF - Nominal propellant temperature in propellant tank
TBPOXO, TBPFLO - boost pump outlet temperature
TOXPIN, TFLPIN - main pump inlet temperature
TVLVOX, TVLVFL - main pump outlet temperature
TVLVOO, TVLVFO - bipropellant valve outlet temperature
TREGOO, TREGFO - regen jacket outlet temperature
TINJOX, TINJFL - injector inlet temperature
TFACOX, TFACFL - temperature at injection
TC - combustion temperature

- Feed Temperature Differentials

DTBPOX, DTBPFL - boost pump ΔT
DTLNOX, DTLNFL - feed line ΔT
DTPMPO, DTPMPF - main pump ΔT
DTVLVO, DTVLVF - bipropellant valve ΔT
DTREGO, DTREGF - regen jacket ΔT
DTIJOX, DTIJFL - injector ΔT

- TPA Temperatures and Temperature Differentials

TTURBI - turbine inlet temperature
TTURBO - turbine outlet temperature
DTTURB - turbine ΔT

Figure 8.2. Temperature Schedule Nomenclature

- Feed Pressures

PULLOX, PULLFL - propellant tank ullage pressure for ox and fuel
PPRPOX, PPRPFL - propellant pressure for ox and fuel
PBPOXO, PBPFLO - boost pump outlet pressure for ox and fuel
POXPIN, PFLPIN - main pump inlet pressure for ox and fuel
PVLVOX, PVLVFL - bipropellant valve inlet pressure for ox and fuel
PVLVOO, PVLVFO - bipropellant valve outlet pressure for ox and fuel
PREGOO, PREGFO - regen jacket outlet pressure for ox and fuel
PINJOX, PINJFL - injector inlet pressure for ox and fuel
PCFACE - injector face pressure in chamber

- Feed Pressure Differentials

DPBLOX, DPBLFL - ox and fuel bladder ΔP
DPBPOX, DPBPFL - ox and fuel boost pump ΔP
DPLNOX, DPLNFL - ox and fuel feed line ΔP
DPPMPO, DPPMPF - ox and fuel main pump ΔP
DPVLVO, DPVLVF - ox and fuel bipropellant valve ΔP
DPREGO, DPREGF - ox and fuel regen jacket ΔP
DPIJOX, DPIJFL - ox and fuel injector ΔP

- TPA Pressures and Pressure Differentials

PBINJO, PBINJF - gas generator/preburner inlet pressure
PTURBI - turbine inlet pressure
PTURBO - turbine outlet pressure
DPGGPB - gas generator/preburner ΔP
DPTURB - turbine ΔP

Figure 8.3. Pressure Schedule Nomenclature

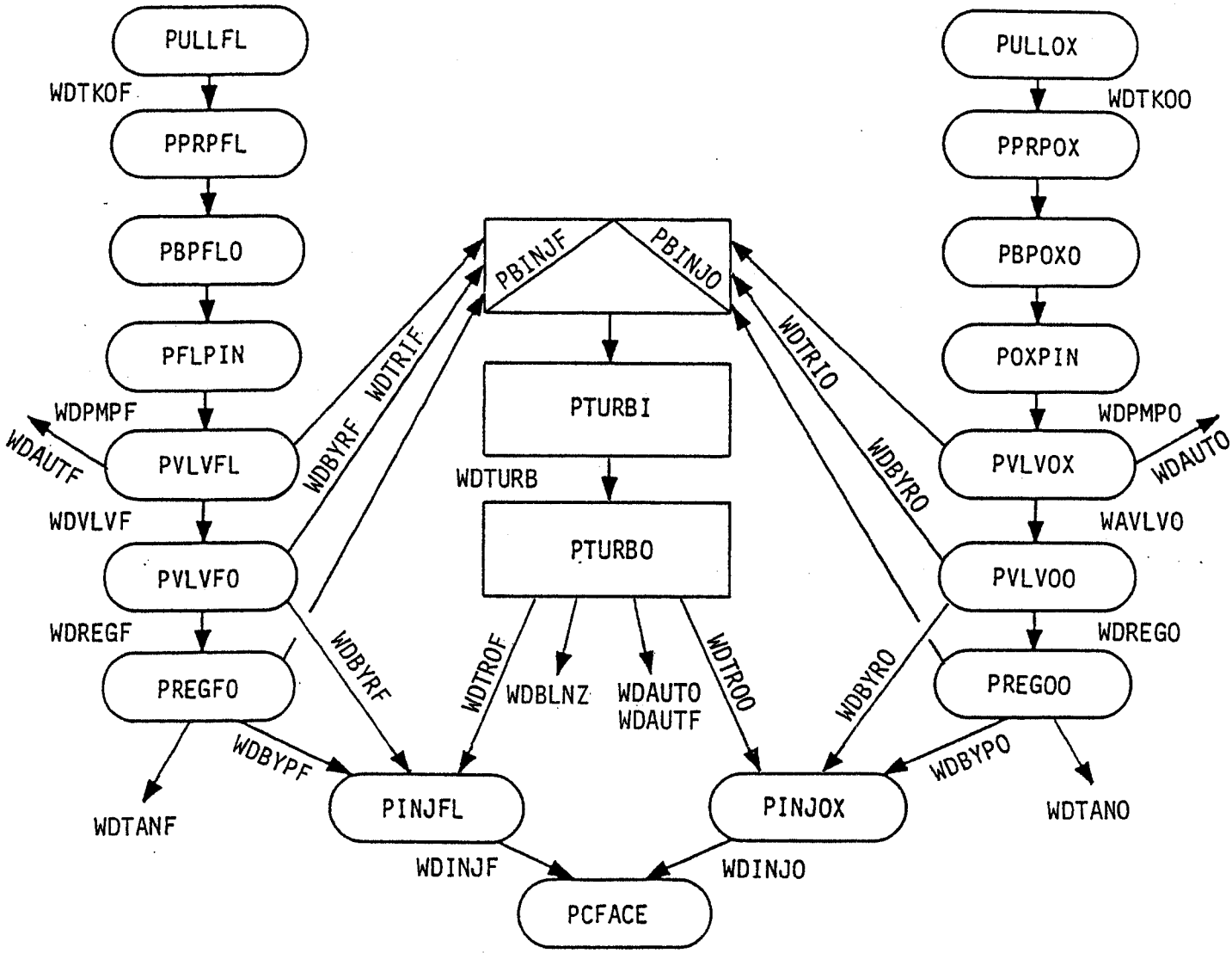

Figure 8.4. General Flowrate Schedule

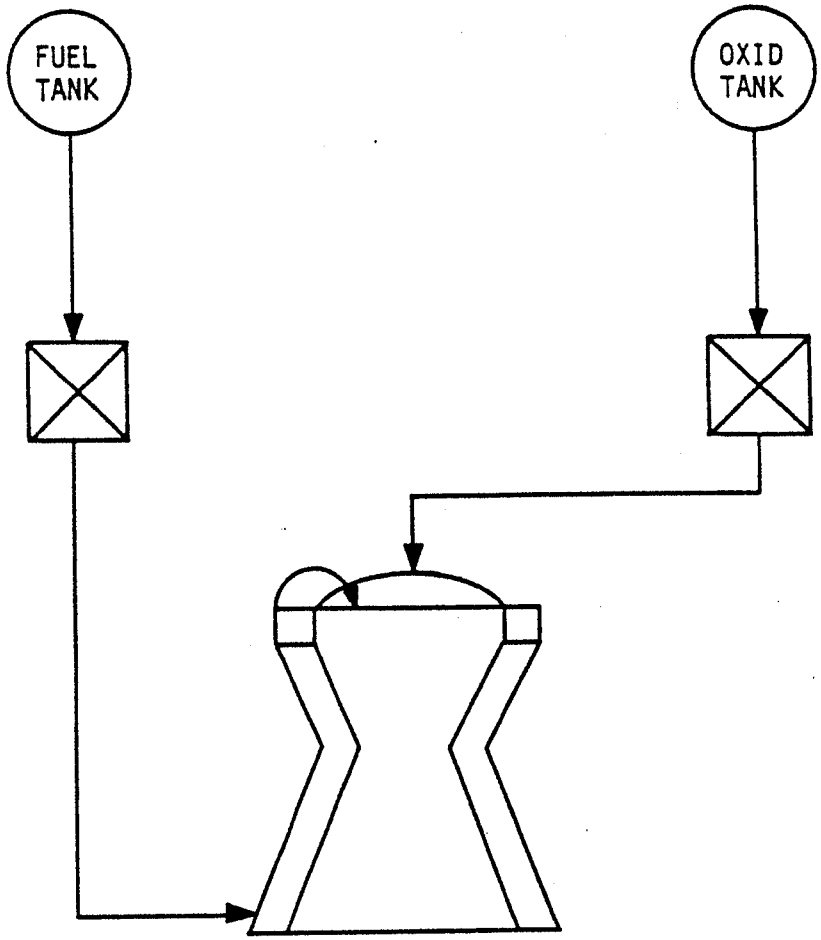

Figure 8.5. Representative Pressure-Fed Engine Schematic

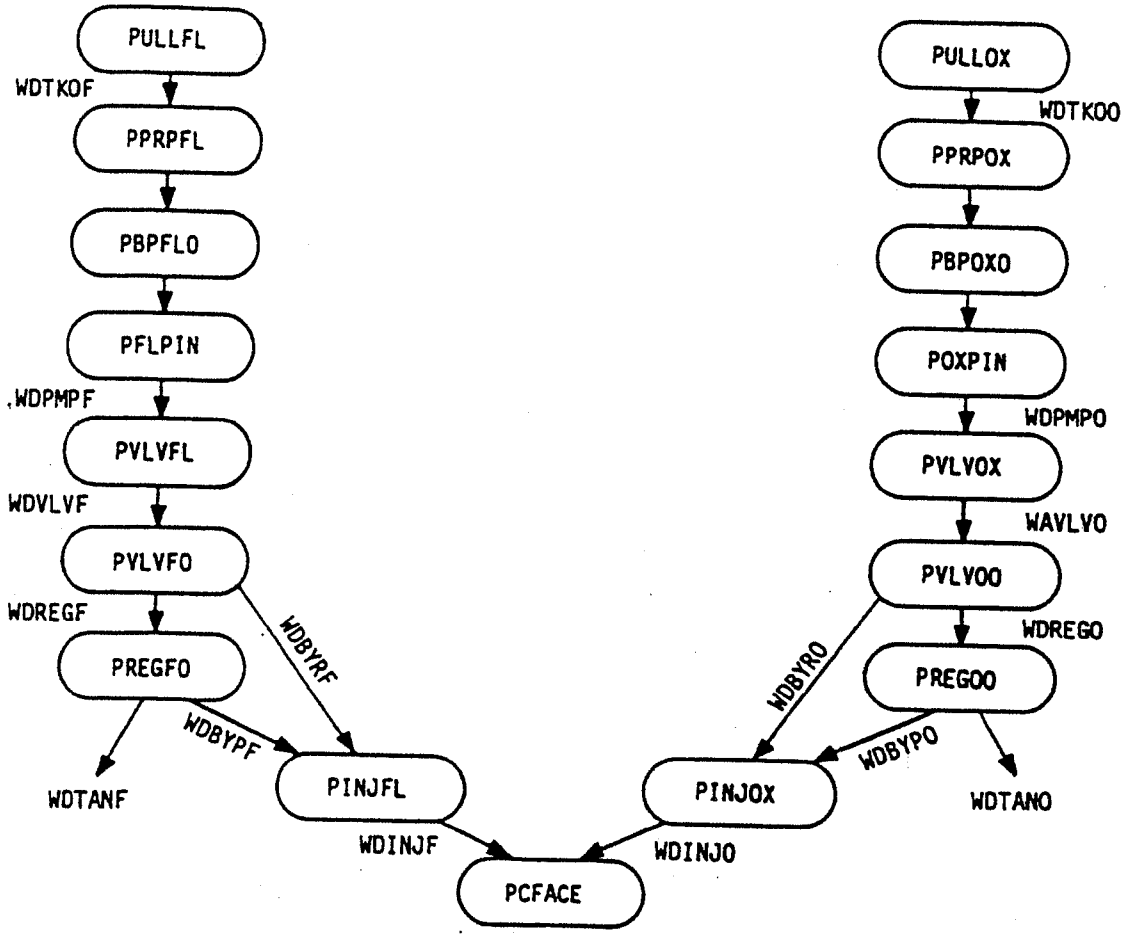

Figure 8.6. Pressure-Fed Flowrate Schedule

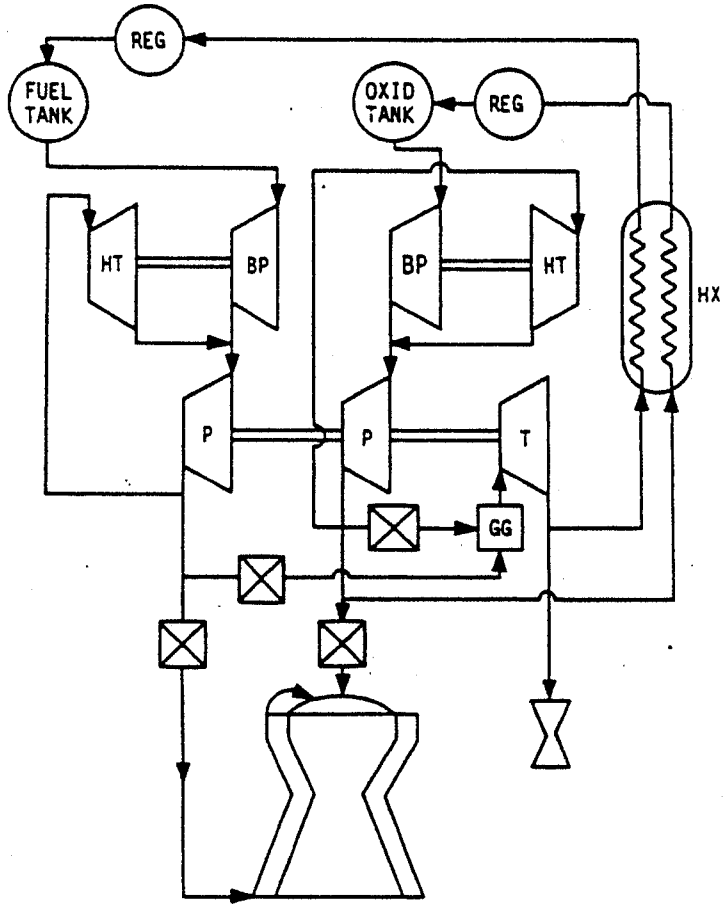

Figure 8.7. Representative Gas Generator Bleed Cycle Schematic

The ELES flow schedule associated with the gas generator bleed cycle is shown in Figure 8.8. This cycle introduces autogenous pressurization and turbine flowrates. Notice that the autogenous pressurant for the fuel tank is taken from the ruel rich gas generator exhaust, while the oxidizer pressurant is taken from upstream of the biprop valve and heat exchanged to raise its temperature.

The staged combustion cycle (representative schematic in Figure 8.9) is a closed cycle. Unlike the gas generator bleed cycle, the staged combustion cycle uses the turbine exhaust as propellant for injection into the main combustor. Although this results in higher pump discharge pressures, it also avoids the performance loss associated with discarding propellant.

The ELES flow schedule for the staged combustion cycle is shown in Figure 8.10. It is the first example where the regen jacket bypass flow can be used as the preburner feed flow. When the regen jacket is fuel-cooled and partial regen jacket bypass is used, that option can be invoked.

The expander cycle (schematic in Figure 8.11) uses the propellant enthalpy gained in regen-cooling the chamber to drive the turbine. Hydrogen is used almost exclusively in that application due to its superior cooling and turbine-drive properties.

The expander cycle flow schedule is shown in Figure 8.12. Notice that the expander cycle cannot use regen bypass for turbine feed since the enthalpy which drives the turbine is acquired in the regen jacket.

The staged reaction cycle (schematic in Figure 8.13) is similar to the staged combustion cycle, except that only the fuel is gasified to drive a turbine. The fuel must therefore be a monopropellant and flow through a monopropellant gas generator upstream of the turbine.

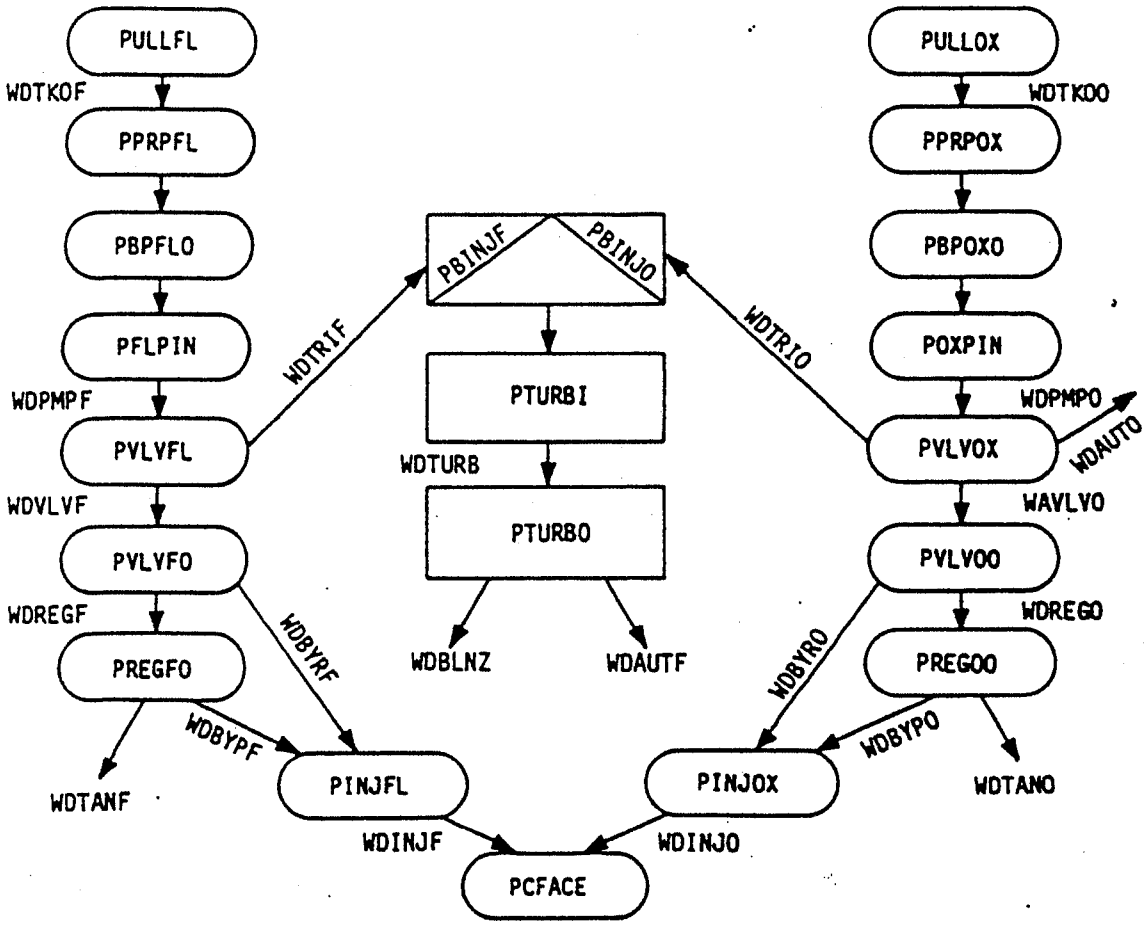

Figure 8.8. General Gas Generator Bleed Flowrate Schedule

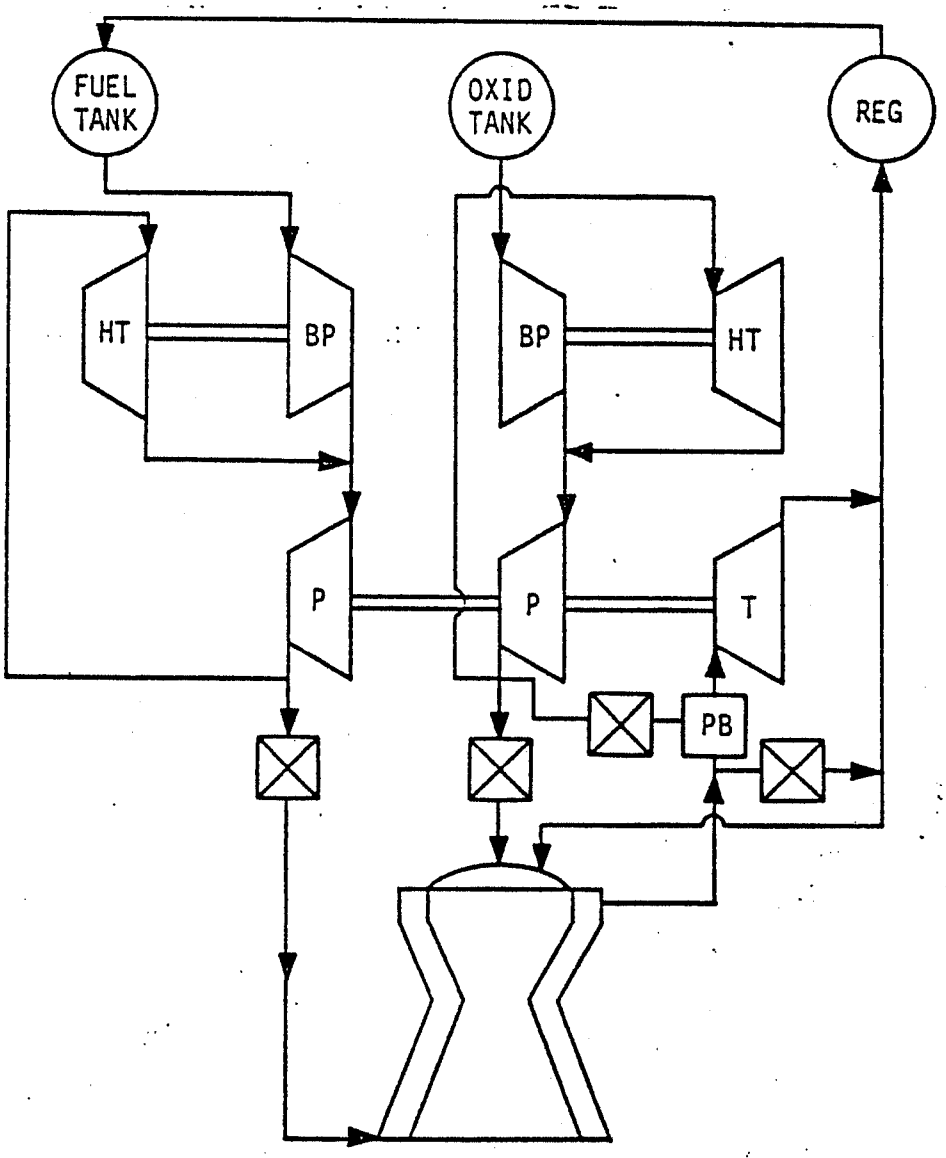

Figure 8.9. Single Fuel Rich Preburner with Regen Cooling and Autogenous Tank Pressurization

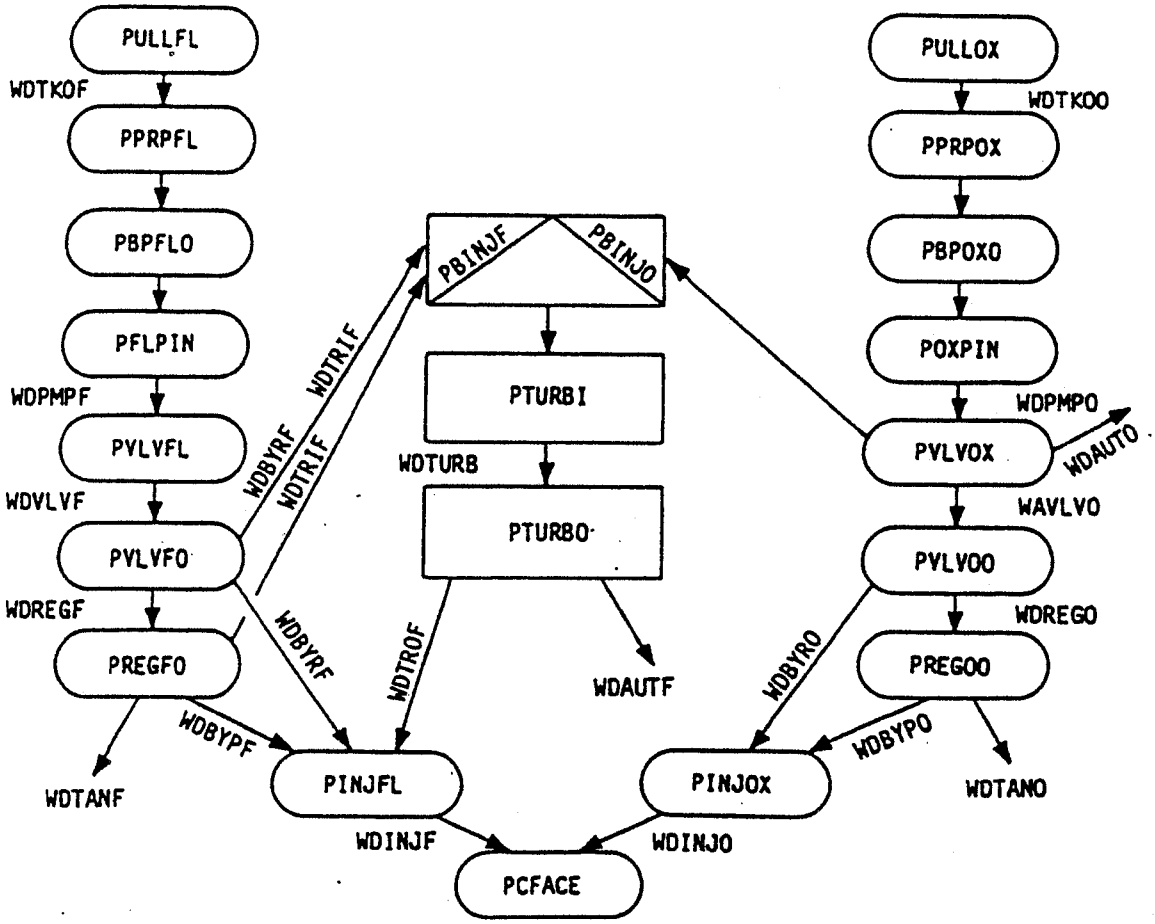

Figure 8.10. General Fuel-Rich Preburner Staged Combustion Flowrate Schedule

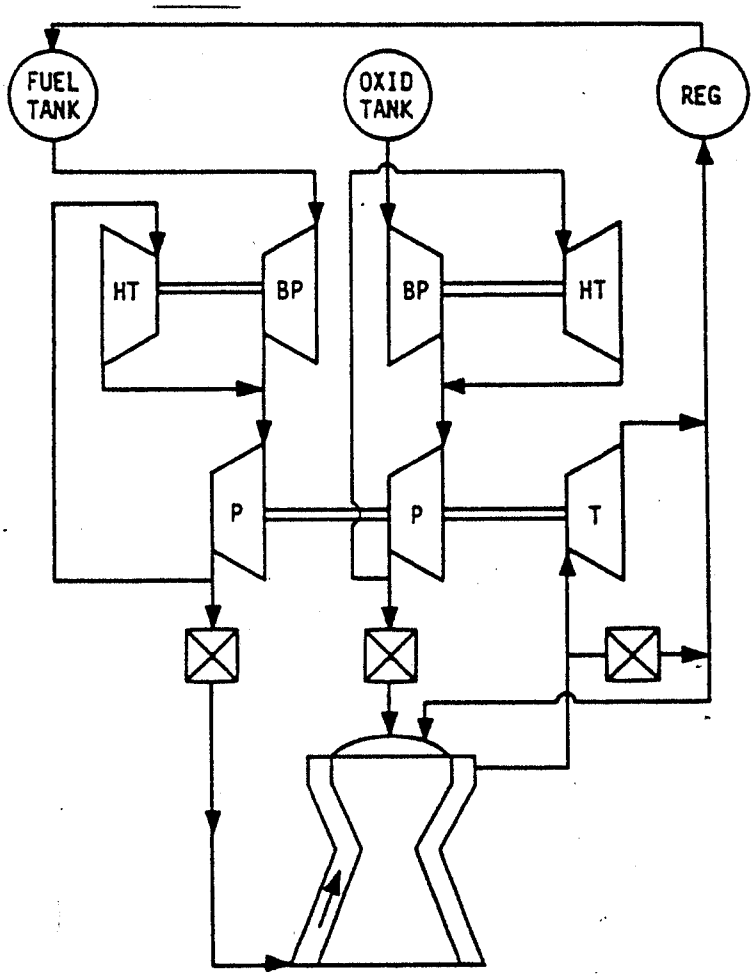

Figure 8.11. Fuel Expander Cycle Schematic

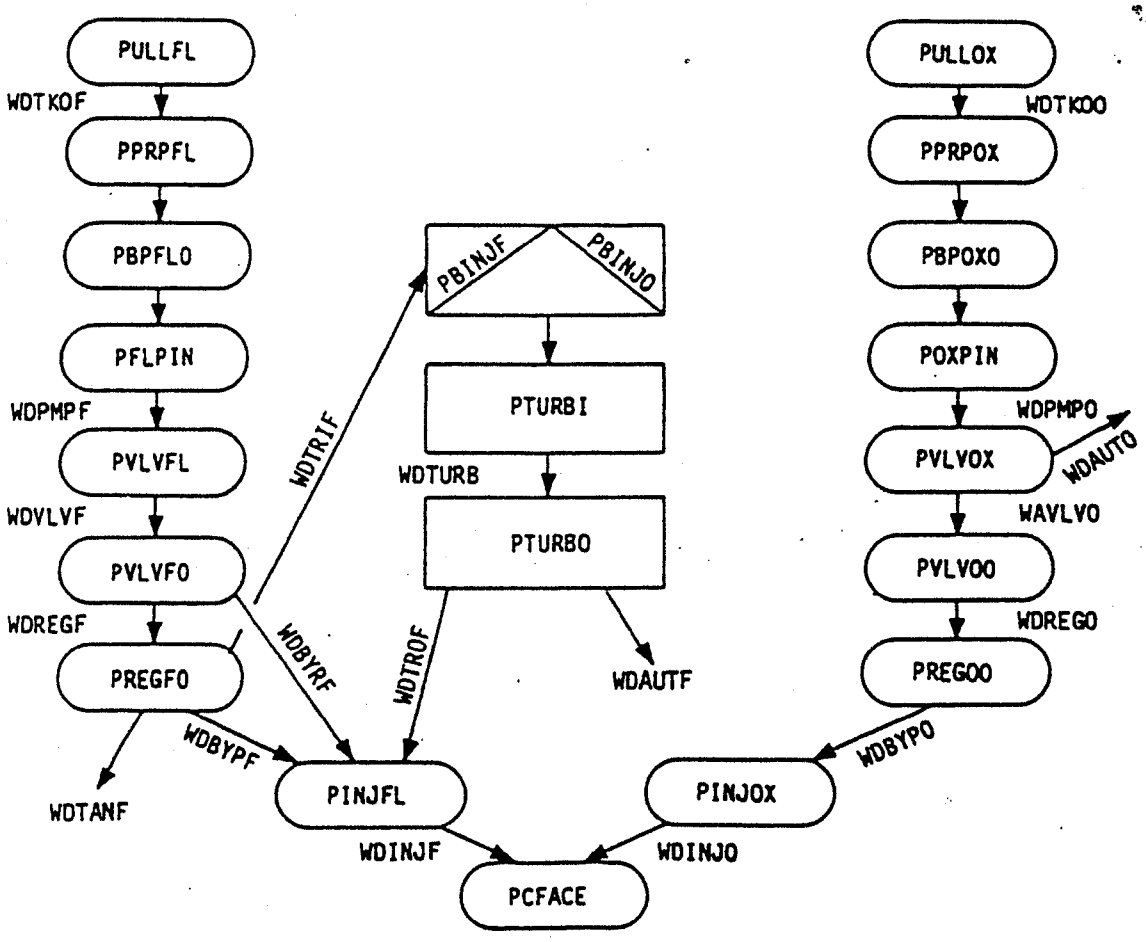

Figure 8.12. General Fuel Expander Flowrate Schedule

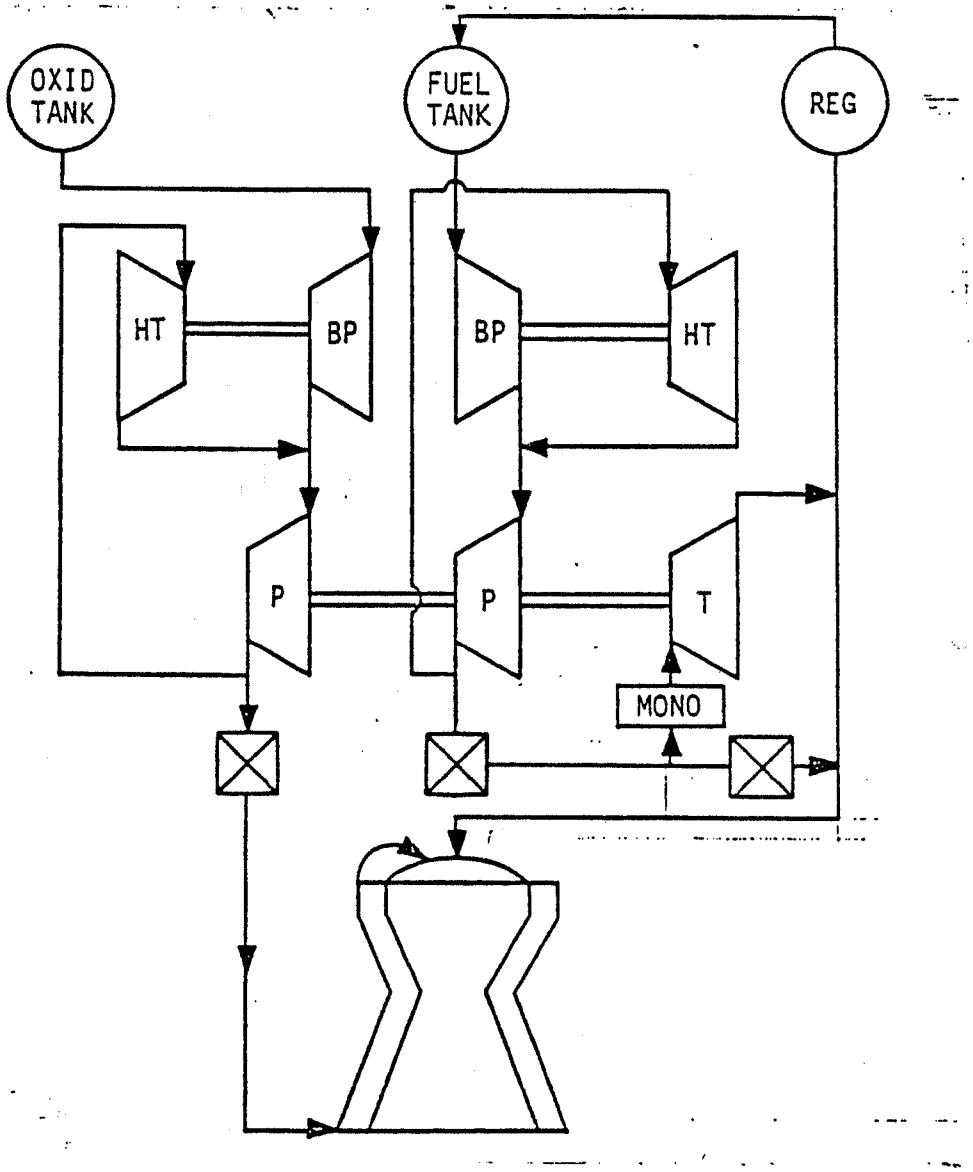

Figure 8.13. Staged Reaction Cycle with Autogenous Tank Pressurization

The staged reaction flow schedule is shown in Figure 8.14. Like the staged combustion cycle, the staged reaction cycle can use regen jacket bypass flow as turbine feed. This option facilitates reduction of the pump discharge pressure; however, the chamber cooling requirement and the TPA power balance requirements must still be met.

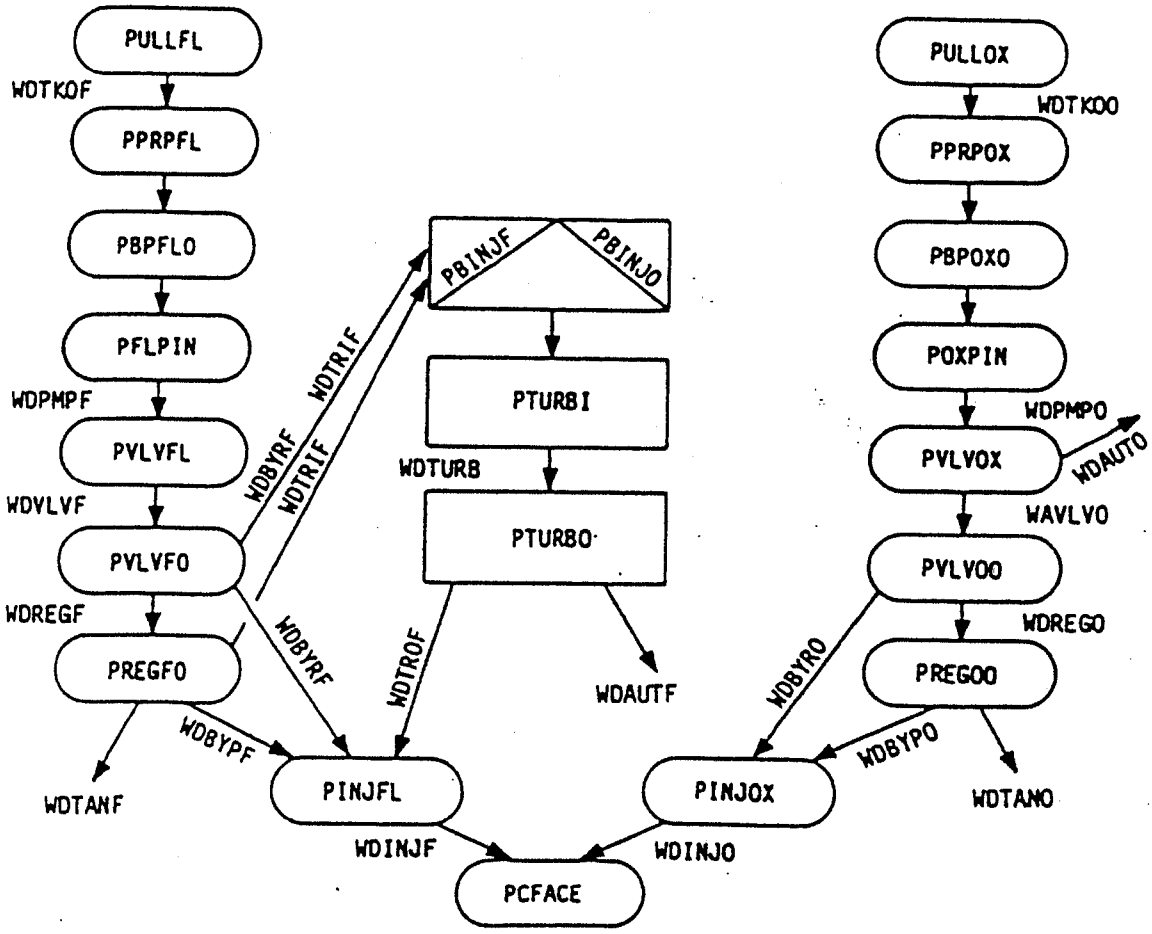

Figure 8.14. Staged Reaction Flowrate Schedule

9.0 PROPELLANT TANK PRESURIZATION

9.1 PRESSURIZATION REQUIREMENTS WITH BLADDERS

The amount of pressurant required to expel the propellant tanks contents is calculated based on the ullage pressure of each propellant tank. The ullage pressure is equal to the required propellant pressure plus the pressure drop across the propellant acquisition device. For tanks with no acquisition device or with surface tension acquisition the pressure drop is negligable. When metallic bladders are used, the pressure drop is calculated with Aerojet emperical equations.

For bonded rolling bladders without center bodies the pressure drop is correlated with the equation.

$$\Delta P_B = mt + b$$

Where: ΔP_B = pressure drop across bladder (psi)
t = bladder thickness (in)
m,b = correlation constants

For a stainless steel 304-L bonded rolling bladder:

$$m = \frac{12000.9}{(R_o - 1.0717)} - 174.03$$

$$b = \frac{-71.549}{(R_o - .97536)} - .37$$

Where: R_o = Maximum bladder radius, in.

$$R_o/t_o \leq 250$$

For aluminum alloy 1100-O bonded rolling bladder:

$$m = \frac{2861}{(R_o - 1.082)} - 43.3$$

$$b = \frac{-17.97}{(R_o - 1.064)} + .01$$

Where: $R_o/t_o \leq 215$

The above correlations correspond to an expulsion efficiency of 0.99.

The total pressure loss across a bonded rolling bladder, having a centerbody within the tank, is calculated as follows:

$$\Delta P_t = \frac{\Delta P_o R_o^2 + \Delta P_1 R_1^2}{R^2_o - R_1^2}$$

Where:
- R_o = bladder outside radius
- R_1 = Center body radius, in.
- ΔP_o = ΔP across a bladder of R_o and thickness t_o, psi
- ΔP_1 = ΔP across a bladder of R_1 and thickness t_1, psi
- ΔP_t = total ΔP across the rolling bladder with a center body, psi

Note: The minimum value of R_1 will be 1.5 inches.

The pressure loss across a moving transverse collapsing bladder constructed of aluminum alloy 1100 is calculated as follows:

$\Delta P_{TB} = 25 - 2\,(D - 2)$ for $2 \leq D \leq 10$ inches

$\Delta P_{TB} = 4e^{-(D\,-10)/2} + 5$ for D>10 inches

Where: D = Tank Inside Diameter, in.

ΔP_{TB} = Pressure loss across moving transverse collapsing bladder of 1100 Al, psi

Let: Bladder thickness = R/215. = D/430, in.

Use of stainless steel is not permitted for the transverse bladder.

The tank expulsion efficiency for the transverse bladder shall be calculated as:

$ee = .948 + .004125\ (D - 2)$ for $2 \leq D \leq 10$ inches

$ee = .99 - .009e^{-.458(D-10)}$ for $D > 10$ inches

Where ee = Tank expulsion efficiency for transverse collapsing bladder of 1100 Al

9.2 COLD GAS PRESSURIZATION OF STORABLE PROPELLANTS

The cold gas pressurization routine assumes helium gas to be expanded from a storage bottle into the propellant tanks. The thermodynamic cooling of the expanding helium is offset by vehicle-aerodynamic heating, radiant heating from the engine, and by convective heat transfer with the tankage and propellants. These heating effects are modeled though the use of a polytropic expansion coefficient* in order to obtain a pressurant temperature. The polytropic coefficient is a function of time and must be based on data or analysis for the vehicle and mission under consideration. The default polytropic coefficient applies to the N-II Delta which is an upper stage with storable propellants. Once the temperature of the pressurant is established, the amount of pressurant required can be obtained from the pressure volume temperature (PVT) properties of helium. To account for non-ideal behavior a curve-fit of the compressibility of helium gas is included in the routine.

*Marks' Standard Handbook for Mechanical Engineers, 8th Edition, pages 4-19

Cold Gas Pressurization Requirements Routine

Inputs: (Some inputs are computer-generated)

T_{min} = Minimum operating temperature (i.e. minimum initial cold gas temperature) (°R)

T_{max} = Maximum operating temperature (i.e. maximum initial cold gas temperature) (°R)

$P_{bi\ max}$ = Maximum initial bottle pressure (psia)

$P_{bf\ min}$ = Minimum final bottle pressure (psia)

$P_{Tf\ ox}$ = Ox tank final pressure (psia)

$P_{Tf\ fuel}$ = Fuel tank final pressure (psia)

V_{ox} = Ox tank volume (in^3)

V_{fuel} = Fuel tank volume (in^3)

t_b = Burn time (sec)

γ_o = γ_{poly} @ time = ∞ (dimensionless)

t' = time at which $\gamma_{poly} = 1.1$ (sec)

γ_{isen} = Isentropic ratio of specific heats (-)

1. Given the above inputs, the first step is to calculate the polytropic gamma (γ_{poly}) using the following empirical equation forms (documentation of the γ_{poly} derivation procedure follows the discussion of the pressurization requirements routine).

$$\gamma_{poly} = \gamma_{isen} - \left(\frac{\gamma_{isen} - 1.1}{t'}\right) t_b \qquad \text{for } 0 \le t_b < t'$$

$$\gamma_{poly} = \gamma_o + (1.1 - \gamma_o)\ EXP\ (-a\ (t_b - t')) \qquad \text{for } t_b > t'$$

Where: $a = \dfrac{\gamma_{isen} - 1.1}{t'\ (1.1 - \gamma_o)}$

2. Assuming operation at initial temperature T_{min} calculate initial bottle pressure:

$$P_{bi\ min} = \frac{T_{min}}{T_{max}} P_{bi\ max}$$

The final temperatures of the pressurant gas in the bottle and tanks is:

$$T = T_{min} \left(\frac{P}{P_{bi\ min}}\right)^{((\gamma_{poly} - 1)/\gamma_{poly})}$$

Where: $T = T_{fb}$, T_{fox}, and T_{ffuel}
$P = P_{bf\ min}$, P_{Tfox}, and P_{Tffuel} respectively

3. Using these values for T and P, it is possible to generate compressibility factors Z_{fb}, Z_{fox}, and $Z_{f\ fuel}$ from the curve fit equation:

$$Z = 1 + P \left(\frac{0.023232}{T + 58.45} - 0.00000481\right)$$

4. The weight of pressurant gas for the conditions W_{fox} and W_{ffuel} can be calculated from (where M = molecular weight of gas, and R = universal gas constant)

$$W_{gs} = PVM/RTZ$$

5. Using the weight of gas in propellant tanks, the volume it occupied in the storage bottle can be calculated from

$$V_{gs} = (W_{fox} + W_{ffuel})\ R\ T_{min}\ Z_{min}/P_{bi\ min}\ M$$

6. Calculate the residual bottle gas weight when the propellant tanks are expelled of propellant.

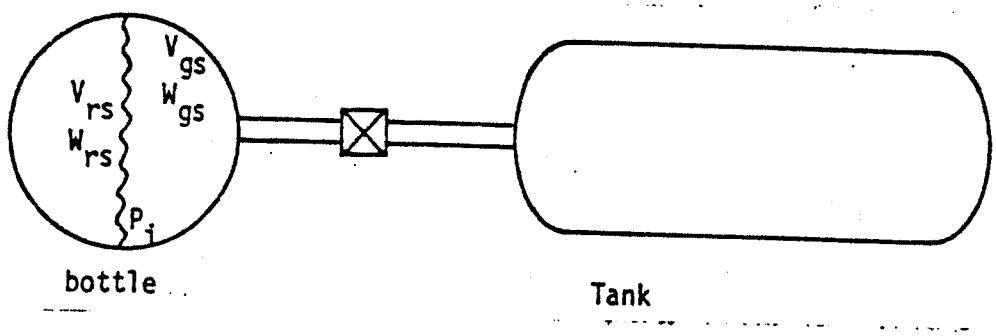

Starting with equations:

$$V_b = V_{gs} + V_{rs}$$

$$V_{rs} = W_{rs}\ R\ T_i\ Z_i/P_iM$$

$$V_b = W_{rs}\ R\ T_f\ Z_f/P_fM$$

V_b = bottle volume

V_{gs} = stored volume of expelled gas

V_{rs} = stored volume of residual gas

W_{rs} = weight of residual gas

Then by substitution:

$$W_{rs} = \frac{Vgs}{\left(\frac{T_f\ Z_f}{P_f} - \frac{T_i\ Z_i}{P_i}\right)\left(\frac{R}{M}\right)}$$

Where subscripts: i = initial bottle condition (T_{min}, P_{bimin})
f = final bottle condition (T_{fb}, P_{bfmin})

7. Total gas weight:

$$W_T = W_{rs} + W_{gs}$$

8. Bottle volume is then:

$$V_b = W_T \, RT_{min} \, Z_{min}/P_{bmin} \, M$$

The curve-fit of compressibility is used to enhance run time over the iterative solution required to use the more standard Beattie-Bridgeman equation. The compressibilities calculated by the curve-fit are well within the 10% of that predicted by Beattie-Bridgeman over the range of interest (200 - 600°R and 100 - 10,000 psia) for helium.

Pressure and temperature data vs. time were collected for the Delta F helium pressurization system and analyzed to determine polytropic gamma vs. time as defined in the following equation:

$$T = T_o \left(\frac{P}{P_o}\right)^{(\gamma-1)/\gamma}$$

Where: T, P = temperature and pressure
T_o, P_o = initial T and P

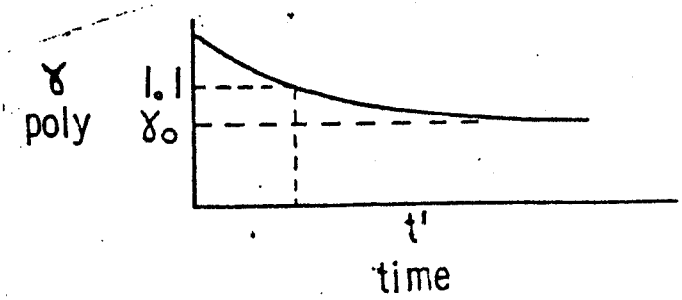

The resulting plot of γ_{poly} vs. time is considered to be the baseline case in the absence of aero heating. An approximating curve for this plot is the following:

$$\gamma_{poly} = \gamma_{isen} - t\left(\frac{\gamma_{isen} - 1.1}{t'}\right) \qquad \text{for } 0 \leq t \leq t'$$

$$\gamma_{poly} = \gamma_o + (1.1 - \gamma_o)e^{-a(t-t')} \qquad \text{for } t \geq t'$$

Where: $$a = \frac{(\gamma_{isen} - 1.1)}{t'(1.1 - \gamma_o)}$$

γ_{isen} = isentropic gamma (ratio of specific heats)
t' = time at which $\gamma_{poly} = 1.1$
γ_{poly} = polytropic gamma (ratio of specific heats)
t = time

For Delta F $\gamma_{isen} = 1.66$, $t' = 240$ sec, $\gamma_o = 1.0$, $a = .02333$. Continuing the analysis for Aerobee 150 data, it is noted that aeroheating gives a much steeper slope for γ_{poly} vs. time, and that γ_o is between 1.0 and 0.0.

It is evident that an in depth aerodynamic heating analysis is required to determine t' and γ_o values for vehicles with varying amounts of aeroheating.

Required User Inputs

T_{min} - Minimum operating temperature

T_{max} - Maximum operating temperature

P_{bimax} - Maximum initial bottle pressure

P_{bfmin} - Minimum final bottle pressure

t' - Time at which $\gamma_{poly} = 1.1$

γ_o - γ_{poly} at $t = \infty$

9.2.1 Helium Compressibility Factor Curve Fit

A standard equation of state used with Helium is the *Beattie-Bridgeman equation defined as follows:

$$P = \frac{RT}{\bar{\upsilon}^2}(1 - e)(\bar{\upsilon} + B) - \frac{A}{\bar{\upsilon}^2}$$

Where: $A = Ao\left(1 - \frac{a}{\bar{\upsilon}}\right)$

$B = Bo\left(1 - \frac{b}{\bar{\upsilon}}\right)$

$e = c/\bar{\upsilon} T^3$

A compressibility factor (Z) is defined by the equation:

$$P\bar{\upsilon} = RTZ$$

Combining this definition with that of Beattie-Bridgeman and plugging in constants for Helium gives the following expression for compressibility of Helium.

$$Z_{BB} = \frac{1}{\bar{\upsilon}}\left(1 - \frac{3730}{\bar{\upsilon} T^3}\right)\left(\frac{}{\upsilon} + .224\right) - (.5172 - .4955/\bar{\upsilon})\frac{1}{\bar{\upsilon} T}$$

ATC has curve fit the compressibility of Helium from physical data with the following result:

$$Z_{fit} = 1 + P\left(\frac{.023232}{T + 58.45} - .00000481\right)$$

*Holman, J.P., Thermodynamics 2nd ed., McGraw Hill, p. 211

Unlike the Beattie-Bridgeman equation which requires an iterative solution for compressibility factor, the ATC curve-fit can be evaluated directly. Its accuracy, as compared to the standard Beattie-Bridgeman, is shown in the following table.

TEMP °R	PRESSURE PSIA	Z BB	Z FIT	Z_{BB}/Z_{FIT}
200	1192	1.111	1.101	1.009
200	4917	1.375	1.418	0.970
200	8408	1.567	1.715	0.914
460	504	1.022	1.02	1.002
460	1767	1.074	1.071	1.003
460	6041	1.224	1.242	0.986
600	658	1.022	1.020	1.002
600	2305	1.074	1.070	1.004
600	4931	1.149	1.150	0.999
600	7879	1.224	1.240	0.987

9.3 SOLID PROPELLANT GAS GENERATOR

The solid gas generator routine allows the use of any solid propellant for which the user has sufficient data. The routine accounts for heat transfer, burn rate variation, and condensibles in the combustion gas.

It is the responsibility of the user to justify the amount of heat transferred from the hot gas to its surroundings. The mechanism for including the results of a heat transfer analysis in the simulation is an exponential pressurant temperature decay curve. This differs from the polytropic expansion coefficient used in the cold gas routine, because the combustion products are not well modeled by a polytropic expansion coefficient. According to the polytropic expansion equation.

$$T = T_{GG} \quad \left(\frac{P}{P_{GG}}\right)^{(\gamma_{poly}-1)/\gamma_{poly}}$$

the lowest obtainable temperature is:

$$T = T_{gg} \ (p/p_{gg}) \quad \text{For} \quad \gamma_{poly} \to \infty$$

Since the combustion products temperature can drop below such a value, this is not a good model for the solid gas generator system.

The inputs which define the solid propellant and the pressurization task are shown below.

SOLID PROPELLANT GAS GENERATOR INPUTS

(Some Inputs are Computer Generated)

Default Values[1]

540	T_{ref}	reference temp for c	(°R)
3932	c*	solid grain characteristic velocity	(ft/sec)
0.095	c	burn rate coeff @ T_{ref}	(in./sec)
0.64	n	burn rate exponent	(-)
0.0036	π_{PK}	temp sensitivity of P_c	($°R^{-1}$)
0.0013	σ	temp sensitivity of burn rate	($°R^{-1}$)
0.056	ρ_{sg}	solid grain density	($lb/in.^3$)
395	T_{min}	min operating temp	(°R)
620	T_{max}	Max operating temp	(°R)
	P_{min}	gas generator min operating pressure @ T_{min}	(psia)
	P_{PT}	propellant tank pressure	(psia)
	V_{PT}	volume of propellant tank	($in.^3$)
	t_b	burn time	(sec)
1.27	γ_{isen}	combustion products ratio of specific heats	(-)
19.0	M	combustion products molecular weight	(-)
2590	T_{GG}	combustion products temperature	(°R)
1.25	C_{des}	design complexity multiplier	(-)
1.5	b	multiplier on T_{min} to calculate T_{eq}	(-)
100	t_d	time at which temp decays by 0.75 x (T_{isen} - T_{eq}) °R	(sec)
0.2662	f_{H_2O}	molar fraction of water in combustion products	(-)
3.0	$(A_p/A_t)min$	port to throat minimum area ratio	(-)

[1]assuming TAL-8 solid propellant

The starting point for the solid gas generator model is the ideal gas equation.

$$W_{pbo} = \text{pressurant weight @ burnout} = \frac{P_{PT}\ V_{PT} M}{R\ T_{bo}}$$

To account for burning rate changes over the design temperature range, increase the pressurant requirement by the ratio (r_{max}/r_{min}) = (maximum burn rate/minimum burn rate). Next, multiply by a design complexity factor (C_{des}) to account for delivered flowrate being greater than demand flowrate. For example, a "perfect" design gives $c_{des} = 1.0$, and off-design operation increases the value of C_{des} (default = 1.25). It also accounts for use of pressure control vent valves which need not close completely. Finally, multiply by the condensibles multiplier (C_{cond}) to allow for replacement of condensed species with uncondensed gas.

The following equation is the result of the above procedure.

$$W_{sg} = W_{pbo}\ C_{des}\ C_{cond}\ (r_{max}/r_{min}) = [\text{solid grain weight}]$$

$$V_{sg} = W_{sg}/\ \rho_{sg} = [\text{solid grain volume}]$$

In order to follow the above method, the values for T_{bo}, C_{cond}, r_{min}, and r_{max} must be determined. This is accomplished as shown in the following equations.

The gas generator is designed to deliver some minimum pressure (p_{min}) at a minimum operating temperature (T_{min}). The burn rate under these conditions is:

$$r_{min} = c\ p_{min}^{n}\ e^{\sigma(T_{min} - T_{ref})}$$

When designed to meet a minimum pressure at a minimum temperature, the maximum pressure (P_{max}) will be:

$$P_{max} = p_{min} e^{\pi_{PK}\ (T_{max} - T_{min})}$$

The burn rate at that condition (r_{max}) is then

$$r_{max} = c\ P_{max}^{n}\ e^{\sigma(T_{max} - T_{ref})}$$

Having established the minimum and maximum burn rates, it remains to calculate the gas temperature at burn out (T_{bo}) and the condensibles multiplier (C_{cond}). The burn out temperature is calculated by assuming a temperature vs. time curve of the following form.

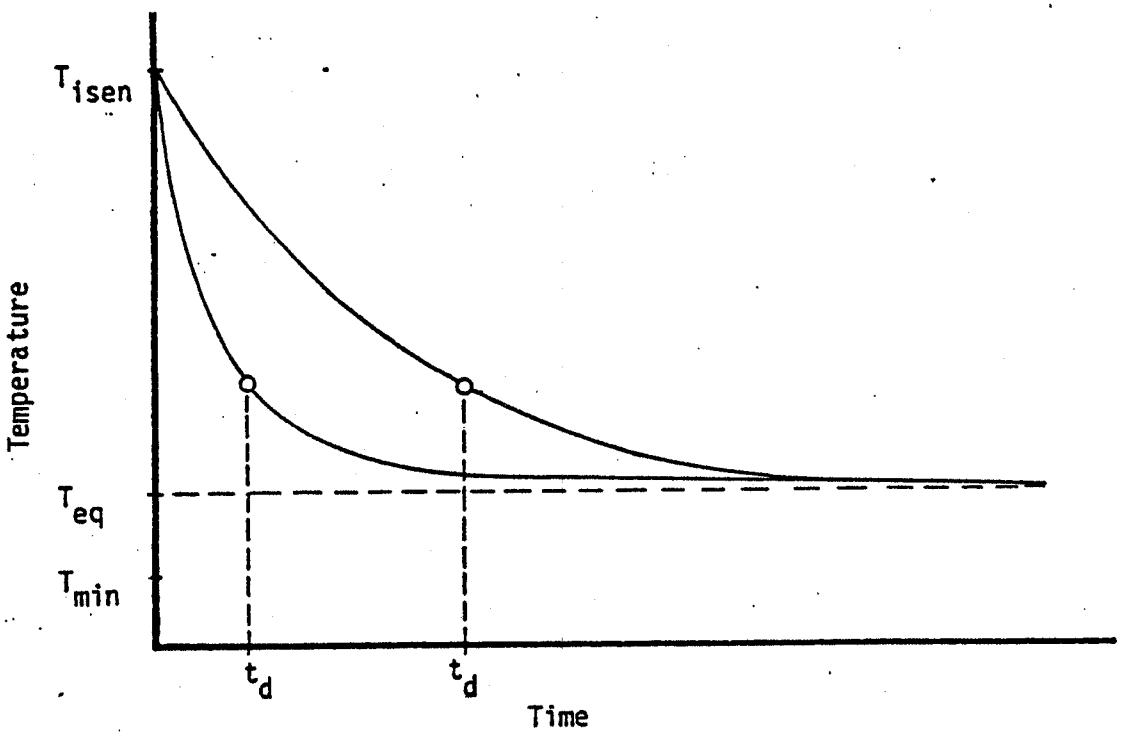

The temperature of the gas at time zero is equal to that of a simple isentropic expansion (ie no heat transfer).

$$T_{isen} = T_{GG}\ \left(\frac{P_{PT}}{P_{min}}\right)^{(\gamma_{isen}-1)/\gamma_{isen}}$$

Assume an exponential decay of gas temperature to an equilibrium value. The user input the equilibrium temperature and the time (t_d), at which it reaches 75% of the distance to that value. (Notice above how the choice of t_d changes the character of the curve.)

Then: $T = T_{eq} + (T_{isen} - T_{eq})e^{-at}$

Where: $a = \frac{1.3863}{t_d} = \frac{-\ln (1 - 0.75)}{t_d}$

The program calculates T_{eq} from:

$$T_{eq} = b \times T_{min},$$

Where: (default) b = 1.5

Using the above definitions the temperature at burnout is calculated as:

$T_{bo} = T_{eq} + (T_{isen} - T_{eq})\ e^{-at_b}$ = pressurant temp @ burnout

The condensibles multiplier is calculated assuming water to be the major condensible species. The partial pressure of water vapor in the propellant tank is calculated as:

P_{vw} = Water vapor partial pressure in combustion products in propellant tank

$= f_{H_2O}\ P_{PT}$

The amount of water vapor which can remain in the pressurant gas is the saturation pressure which corresponds to the gas temperature. At burnout, that gas temperature (T_{bo}) can be used to calculate the burnout saturation pressure of water vapor by using the following curve-fit of saturated steam P vs. T data.

$$P_{vbo} = [0.0078164\ (T_{bo} - 444.1)]^{4.6674} \quad \text{For } T_{bo} \geq 660°R$$

$$= [0.0042071\ (T_{bo} - 323.6)]^{7.0321} \quad \text{For } T_{bo} < 660°R$$

By comparing the actual partial pressure at water vapor (P_{vw}) with the maximum allowable saturation pressure (P_{vbo}) the value of the condensible multiplier (C_{cond}) can be determined.

If $P_{vw} \leq P_{vbo}$, then $C_{cond} = 1.0$ (no condensation)

If $P_{vw} > P_{vbo}$, then $C_{cond} > 1.0$ (condensation)

If condensation occurs, then C_{cond} can be calculated by first calculating the allowable mole fraction of water vapor in the combustion gas (f_{allow}).

$$f_{allow} = P_{vbo}/P_{PT} = \text{allowable mole fraction of condensibles in pressurant gas}$$

The total number of moles in the gas phase after condensation (n) can be calculated as:

$$n = P_{PT}\ V_{PT}/R\ T_{bo} = \text{ideal \# moles at burnout}$$

Finally the equation for C_{cond} is:

$$C_{cond} = \frac{n}{1 + f_{allow} - f_{H_2O}}$$

Where: f_{H_2O} is the actual mole fraction of water in the combustion gas and f_{H_2O} is greater than f_{allow}.

9.4 PRESSURIZATION OF CRYOGENIC TANKS

Variations in heat and mass transfer during the pressurization of cryogenic tanks have profound effects on the quantity of pressurant required. Three approaches to mathematical pressurization models are, (1) analytical, (2) numerical, and (3) empirical. An analytical solution to pressurization requirements for cryogenic tanks is preferred, however, the existing analytic solutions are obtained by making highly restrictive simplifying assumptions. Often the use of the analytical results are iterative in nature *. Finite-difference numerical methods give very good agreement with test data, but the amount of code and run time are in excess of that compatible with ELES **. Epstein, et al, developed a detailed computer model using finite-difference procedures to solve the heat, mass, and transport equations within the tank. The model includes the effects of gas composition, velocity, and gas, liquid, and wall temperatures. Gas mixing, mass diffusion, interfacial mass transfer, external tank insulation, and liquid sloshing are also included. It is this model which Epstein used to develop an empirical pressurization model‡.

* Arpaci, V.S., Clark, J.A. and Winer, W.O., "Dynamic Response of Fluid and Wall Temperatures During Pressurized Discharge of a Liquid from a Container", Advances in cryogenic Engineering, Volume 6, Plenum Press, New York (1961) Page 310.

** Epstein, M., Georgius, H.K. and Anderson, R.E., "A Generalized Propellant Tank-Pressurization Analysis", Advances in Cryogenic Engineering, Volume 10B, Plenum Press, New York (1965), Page 290.

‡ Epstein, M. and Anderson, R.E., "An Equation for the Prediction of Cryogenic Pressurant Requirements of Axisymmertric Propellant Tanks", Advances in Cryogenic Engineering, Volume 13, New York (1968), Page 207.

The empirical Epstein equation has been shown to agree with the detailed finite-difference model to within 7 percent. When compared to test data, the Epstein equation agrees within 12 percent. This equation is used to predict the pressurant requirements in the Cryogenic Third Stage (CTS) computer code at Aerojet Expulsion tests of supercritical hydrogen have validated the Epstein equation in the regime. The supercritical hydrogen expulsion also fell within the 12 percent accuracy band of the Epstein equation.

The empirical equation is small, fast running, and sufficiently accurate for preliminary design calculations. The form of the equation is:

$$\frac{\omega_p}{\omega_p^o} = \left(\left(\frac{T_o}{T_s} - 1\right)\left[1 - \exp\left(-p_1 C^{p_2}\right)\right]\left[1 - \exp\left(-p_3 S^{p_4}\right)\right] + 1\right)$$

$$\times \exp\left[-p_5 \left(\frac{1}{1+C}\right)^{p_6} \left(\frac{S}{1+S}\right)^{p_7} Q^{p_8}\right]$$

Where: $\omega_p^o = \rho_G{}^o \Delta V$

$$C = \frac{(\rho c_p^o\, t)_w}{(\rho c_p)_G^o} \left(\frac{T_s}{T_o}\right)$$

$$S = \frac{h_c \theta_T}{(\rho c_p)_G^o} \left(\frac{T_s}{T_o}\right)$$

$$Q = \frac{\dot{q} \theta_T}{(\rho c_p)_G^o \, DT_o}$$

Constants and variable definitions are:

Pressurant	Propellant	p_1	p_2	p_3	p_4	p_5	p_6	p_7	p_8
H_2, He	H_2	0.330	0.281	4.26	0.857	1.50	0.312	0.160	0.986
O_2, N_2, He	O_2	0.775	0.209	3.57	0.790	0.755	0.271	0.236	0.895
N_2, He	N_2	"	"	"	"	"	"	"	"
F_2, He	F_2	"	"	"	"	"	"	"	"

C = ratio of wall-to-gas effective thermal capacity

c_p = specific heat at constant pressure

D = equivalent tank diameter. (Diameter of a cylindrical tank having same total volume and wall surface area as tank under investigation)

h_c = gas-to-tank-wall-free-convection heat transfer coefficient. (Calculated at film temperature equal to $(T_o + T_s)/2$ and temperature difference equal to $T_o - T_s$)

p = tank pressure during liquid expulsion

$p_1 \ldots p_8$ = fitted constants in Epstein equation

$\dot{q}$ = heat flux from ambient to tank wall, per surface area of wall

Q = ratio of total ambient heat input to effective thermal capacitance of gas

S = modified Stanton number. (Velocity term is equivalent to tank diameter divided by outflow time)

t_w = wall thickness

T_o = pressurant inlet temperature

T_s = saturation temperature of propellant at initial tank pressure. (Equivalent to the initial wall temperature)

ω_p = total pressurant mass

ω_p° = total pressurant mass under conditions of zero heat and mass transfer

$\omega_p/\omega_p^{\circ}$ = collapse factor

ΔV = expelled liquid volume

Θ_T = total liquid outflow time

ρ = density

Subscripts: G refers to gas
W refers to wall

Superscript: O refers to variables at a temperature equal to inlet pressurant temperature and a pressure equal to tank pressure during expulsion

The Epstein correlation was developed using data and computer runs for ranges of input given below. The accuracy of using the equation outside that range is undocumented.

RANGES OF VARIABLES COVERED IN COMPUTER PROGRAM

Variable	Range
Spherical tank diameter	5-30 ft
Ellipsoidal tank diameter	5-30 ft
Cylindrical tank diameter	4-35 ft
Wall thickness	0.1-1 in
Ratio of pressurant inlet temperature to propellant saturation temperature	2-15
Total outflow time	200-500 sec
Ambient heat flow	0-10,000 Btu/ft^2-hr

The computer program used to generate the correlation coefficients was run in the above ranges. Note that the applicable range is also the range of interest for most cryogenic vehicles and that the equation's boundary conditions are satisfied (i.e., with no heat transfer the collapse factor equals unity or with infinite heat transfer the collapse factor equals T_o/T_s, its maximum possible value).

9.5 AUTOGENOUS PRESSURIZATION

Autogenous pressurization has an advantage over helium pressurization when the additional weight of the evaporated propellants is less than that of the helium storage vessel. This occurs in a pump fed stage with low NPSH requirements. The Epstein equation described for the helium pressurization of cryogenic tanks, can account for pressurant collapse with autogenous pressurization, and it will predict cryogenic pressurization requirements.

Although the Epstein equation was not derived with storable propellants in mind, ELES uses it to calculate the collapse ratio of storable autogenous pressurants. Heat transfer coefficients, gas temperatures, and fluid properties are consistent with the storable propellants in use.

The autogenous model evaporates the propellants in heat exchangers located downstream of the turbine of pump-fed stages. Autogenous pressurization for pressure-fed stages is not allowed.

10.0 TURBOPUMP ASSEMBLY

The purpose of the turbopump assembly (TPA) model is to establish accurate turbomachinery size, weight, and performance characteristics for: 1) Gas Generator bleed cycle, 2) Staged Combustion Cycle 3) Staged Reaction Cycle, and 4) Expander Cycle. ELES can evaluate any of the above mentioned cycles while using any of the following turbomachine configurations:

1) Single turbine driving a gearbox which powers 2 pumps on separate shafts
2) Single turbine driving 2 pumps on a common shaft
3) Twin TPA's, series drive fluid flow
4) Twin TPA's, parallel drive fluid flow

ELES checks the necessity for pump or turbine staging, and it also allows the user to include boost pumps on either propellant circuit. Maximum allowable pump tip speeds and turbine blade root stresses are checked to avoid unrealistic designs. Pump head coefficients and pump and turbine efficiencies are calculated from tables included in the program. If turbine blade height drops below 0.3", ELES designs a partial admission turbine.

The propellant pumps are designed by first establishing the pump speed by the equation

$$N = \frac{S_s \, NPSH^{0.75}}{\sqrt{Q}}$$

where:
- N = pump speed (RPM)
- S_s = suction specific speed
- $NPSH$ = net positive suction head (ft)
- Q = volumetric flowrate (gpm)

$$N\sqrt{Q} = S_s \, NPSH^{0.75} = N_s \, H^{0.75}$$

$$S_s = \frac{N_s \, H^{0.75}}{NPSH^{0.75}}$$

If the TPA uses a single shaft configuration, both pumps are set to the lesser of the two RPM's so as not to exceed the maximum suction specific speed. If the pumps specific speed(s) (N_s) falls below 800, staging becomes necessary. The total head rise across the pump is divided by the number of stages until the specific speed rises above 800. The equation used for calculating N_s is:

$$N_s = \frac{N \sqrt{Q}}{H^{0.75}}$$

where: N_s = specific speed
H = pump head rise (ft)

Pump diameter is calculated as

$$D = u / 60 \pi N$$

where: $u = \sqrt{gH / \psi}$ = impeller discharge tipspeed (ft/sec)
g = acceleration due to gravity (ft/sec)
ψ = pump stage head coefficient (-)
π = 3.14159... (-)
N = pump speed (rpm)
D = impeller diameter (ft)

The pump stage head coefficient is taken from a curve of head coefficient vs. specific speed. There is a different curve for main pumps and boost pumps (see Figure 10.1).

If the boost pump option is selected, pump staging is generally not allowed. An exception to this rule is when the fuel is hydrogen and the pump tip speed exceeds 2000 fps. Staging reduces the tip diameter and thus the tip speed. Tip speed is calculated as follows:

- MAIN PUMP AND BOOST PUMP HEAD COEFFICIENTS ARE TAKEN FROM CURVES OF HEAD COEFFICIENT VS. SPECIFIC SPEED

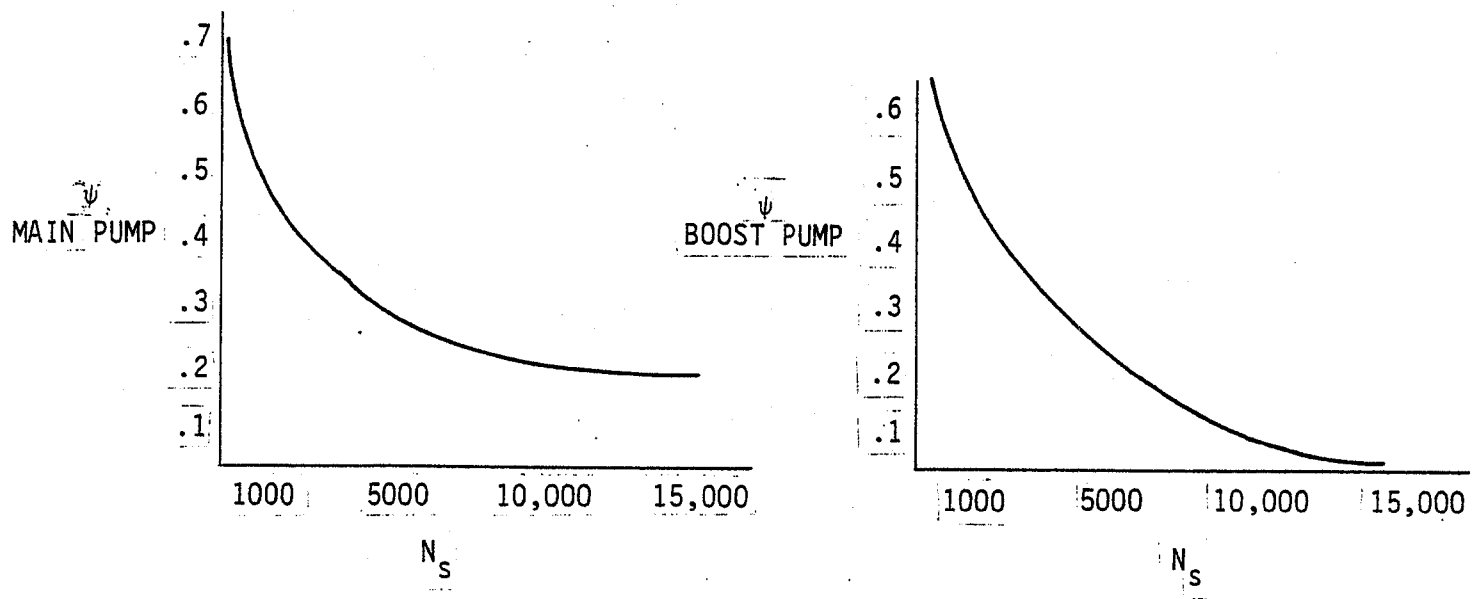

Figure 10.1. Pump Head Coefficient

$$u = DN/229$$

where: u = tip speed (ft/sec)
D = tip diameter (in)
N = pump speed (rpm)

In order to calculate the required pump horsepower, it is necessary to know pump efficiency. Main pump efficiency is determined by interpolation of a table containing pump efficiency vs. specific speed (see Figure 10.2). The efficiency thus found is then modified by a diameter correction factor which is calculated as shown below:

$$\eta_p = C_D \eta_p$$
$$C_D = \text{MIN}\ (0.75\ D^{0.14874},\ 1.0)$$

where: η_p = pump efficiency
D = pump diameter
C_D = diameter correction factor

The pump horsepower requirement is then calculated as:

$$HP = \frac{\omega\ H}{550\ \eta_p}$$

where: HP = pump horsepower (hp)
ω = pump flowrate (lb/sec)
H = pump head rise (ft)
η_p = pump efficiency (-)

Boost pump horse power requirements are calculated by the same procedure, except that the boost pump efficiency vs. specific speed is a different curve.

If the boost pump option is selected for either propellant circuit, the net positive suction head (NPSH) of the main pump must be calculated based on the boost pump discharge pressure. As a default condition the boost pump

- MAIN PUMP AND BOOST PUMP EFFICIENCY IS TAKEN FROM PLOTS OF EFFICIENCY VS. SPECIFIC SPEED AND IS THEREAFTER MODIFIED BY A DIAMETER CORRECTION FACTOR

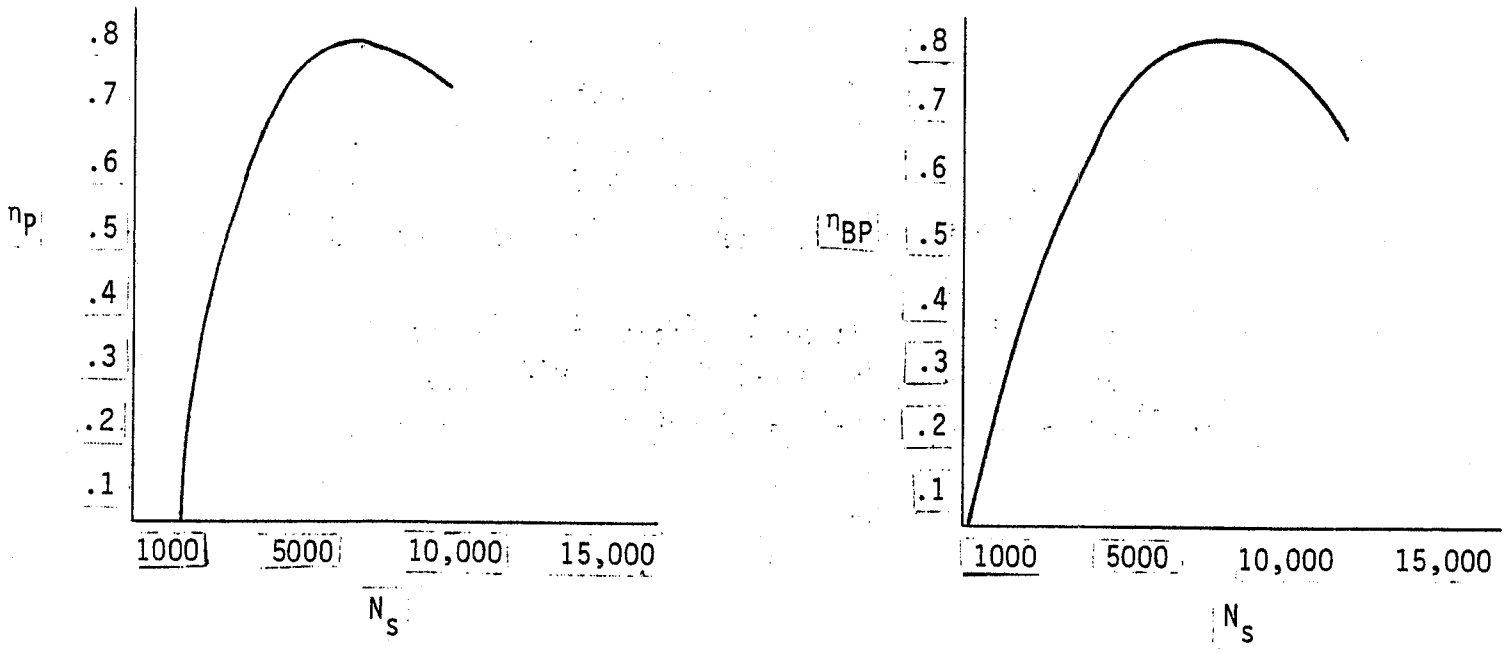

Figure 10.2. Pump Efficiency

provides 4.64% of the total head rise. The main pump NPSH is therefore 4.64% of the total head rise. The main pump attributes are then calculated using that NPSH.

If the TPA configuration utilizes a gearbox or twin TPA's then all of the oxidizer and fuel pump calculations are independent of each other. In the case of the single shaft TPA the main pump RPM is set to the lesser of the two RPM's so as not to exceed the suction specific speed limit. As might be imagined, this can result in some unlikely designs when only one circuit utilizes a boost pump while using a single shaft TPA. In fact, if the circuit utilizing a boost pump is forced to slow down to the speed of the other circuit, the boost pump head rise can become a negative number. If this occurs, the boost pump head rise is set to 1 ft. and the program proceeds. A warning message is printed regarding the inadvisability of such a design.

When all of the pump horsepower requirements are summed together, the amount of power needed from the turbine is known, and the turbine design calculations can proceed By assuming a nominal value of 0.4 for the ratio of turbine blade tangential velocity to isentropic spouting velocity (u/C_o), the turbine efficiency can be derived from the Aerojet curve in Figure 10.3 (initially assume 100% admission).

The isentropic spouting velocity can be calculated as

$$C_o = \sqrt{2gJh_t}$$

where: g = acceleration due to gravity ft/sec^2

J = conversion factor 778 ft lbf/Btu

h_t = total enthalpy Btu/lbm

$$= C_p T_{in} \left(1 - \left(P_{out} / P_{in}\right)^{\frac{\gamma-1}{\gamma}}\right)$$

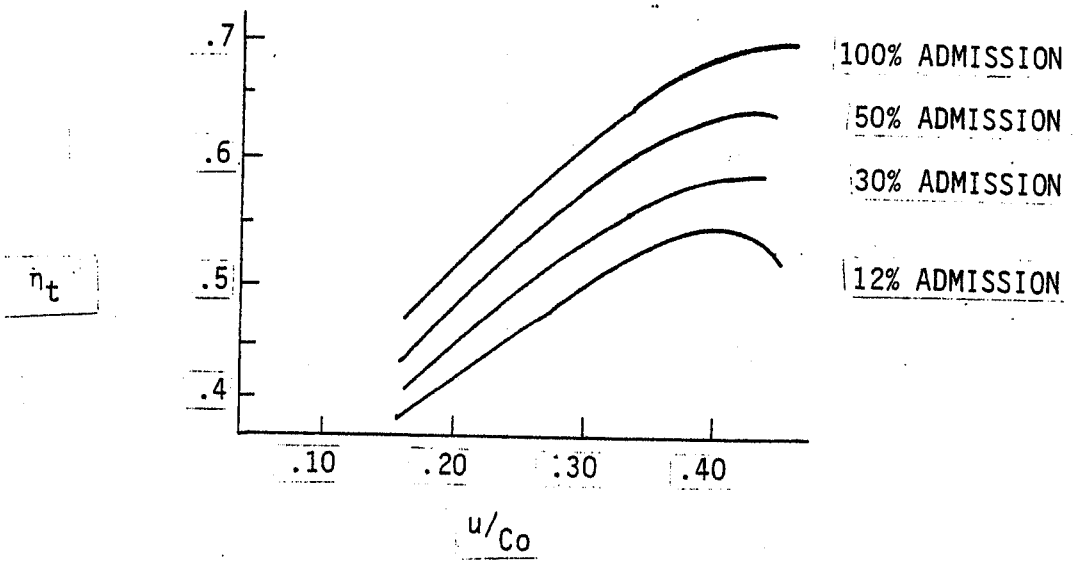

Figure 10.3. Turbine Efficiency vs Tangential Velocity/Isentropic Spouting Velocity (u/Co)

C_p = constant pressure specific heat (Btu/lbm°R)
T_{in} = turbine gas inlet temperature (°R)
P_{out} = turbine outlet pressure (psia)
P_{in} = turbine inlet pressure (psia)
γ = ratio of specific heats

In the case of twin TPA configurations, an isentropic spouting velocity (C_o) is determined for each circuit based on the fraction of total horsepower in each circuit.

$$C_{o\ ox} = \sqrt{2gJh_{ox}}$$

$$C_{o\ fuel} = \sqrt{2gJh_{fuel}}$$

Using the values for u/C_o and C_o, the tangential velocity (u) can be easily calculated. The turbine diameter is then calculated as:

$$D_t = 720\ u/\ \pi\ N$$

where: D_t = turbine diameter (in)
u = tangential velocity (ft/sec)
N = turbine speed (rpm)

Having done an initial sizing of the turbine, ELES then checks the turbine for staging, partial admission, and blade root stress limitations. The staging check begins with a calculation of turbine inlet mach number.

$$N_{mach} = C_o \Big/ \sqrt{\frac{\gamma g R\, T_{in}}{12\, M}}$$

where:
- γ = ratio of specific heats
- g = acceleration due to gravity (ft/sec^2)
- R = universal gas constant (lb_f ft/lbmole °R)
- T_{in} = Turbine gas inlet temperature (°R)
- M = turbine gas molecular wt.
- C_o = isentropic spouting velocity (ft/sec)

If N_{mach} is greater than 1.7 then the turbine is set to a two stage configuration. In addition to the mach number staging criteria the turbine will also be staged if its specific speed (N_s) falls below 100. The same equation as shown earlier for specific speed applies.

$$N_s = \frac{N\sqrt{Q}}{H^{0.75}}$$

If the turbine is staged for either reason, the new isentropic spouting velocity must be calculated as:

$$C_o = \sqrt{\tfrac{1}{2}}\, C_O$$

(assumes a two stage turbine)

The earlier assumption of a 100% admission turbine will now be examined by calculating the turbine blade height. The blade height is calculated from the equations

$$h = \frac{A_{ann}}{\pi\, D_t}$$

$$A_{ann} = \frac{\omega_t}{12\, C_a\, \rho_e}$$

$$C_a = C_o \sin 20°$$

$$\rho_e = \frac{\rho_{out}\, M}{R\, T_{in} \left(\frac{P_{out}}{P_{in}}\right)^{(\gamma-1)/\gamma}}$$

where:

h = turbine blade height (in)

A_{ann} = turbine inlet annulus area (in^2)

D_t = turbine diameter (in)

ω_t = turbine gas flowrate (lb_m/sec)

C_a = absolute fluid velocity (ft/sec)

ρ_e = turbine gas density (lb/in^3)

P_{out} = turbine exit pressure (psia)

M = turbine gas molecular wt

R = universal gas constant (lb_f in/lb_{mole} °R)

T_{in} = turbine gas inlet temperature (°R)

P_{in} = turbine inlet pressure (psia)

If the turbine blades are less than 0.3 inches in height, it is necessary to redesign the turbine to partial admission. Although ELES allows the design of partial admission turbines which are multi-staged, a more practical design would be a re-entry turbine. Coding for the design of a re-entry turbine, however, is not included.

A new turbine efficiency is determined based on the fraction of partial admission (see Figure 10.3). The partial admission fraction is determined from:

$$FADMIS = A_{ann} / .3\pi D_t$$

The turbine gas flowrate (ω_t used in the above equations) is obtained by one of several methods, depending on the power cycle under consideration. For gas generator bleed cycles the pressure ratio across the turbine is fixed and the flowrate varies. The remainder of the pump fed cycles are closed cycles wherein the turbine flowrate is fixed and the pressure ratio must be iteratively calculated.

The gas generator flowrate is calculated as

$$\omega_{gg} = \frac{0.707\ (hp_{mp} + 2.2\ hp_{bp})\ 1.05}{\eta_t\ h_t} \quad (lbm/sec)$$

where: hp_{mp} = main pump horsepower requirements (hp)
hp_{bp} = boost pump horsepower requirements (hp)
η_t = turbine efficiency
h_t = total enthalpy (previously defined) (Btu/lbm)

The above factor of 2.2 on the boost pump horsepower requirement accounts for a 10% line loss and a 50% hydraulic turbine efficiency. The factor of 1.05 on all horsepower requirements accounts for bearing, seal, and other mechanical losses. If the TPA design is parallel flow twin turbines, two flowrates are calculated (one for each turbine).

If the turbine efficiency is updated as a result of partial admission, the gas generator flowrate is updated.

The last design check made on the turbine is the blade root stress limit. The material properties of the turbine blades are taken from Aerojet general guidelines. The alternating stress is calculated as a function of temperature with

$$\sigma_{alt} = 36760 - 6.37 * T_{in}$$

where: σ_{alt} = alternating stress (psi)
T_{in} = turbine inlet temp (°R)

The ultimate and yield strengths of the turbine blades are input by the user, but if the inlet temperature is greater than 1940°R, they are degraded by the equations

$$\sigma_u = \sigma_u - 170\ (T_{in} - 1940)$$

$$\sigma_y = \sigma_y - 170\ (T_{in} - 1940)$$

where: σ_u = ultimate strength (psi)
σ_y = yield strength (psi)

The maximum allowable blade stress (σ_{allow}) is then calculated as the minimum of σ_u / 1.4 or σ_y / 1.1.

The maximum endurance stress (σ_{es}) is calculated as σ_{alt} / 1.33 so that the mean blade root centrifugal stress limit (σ_{mbrsl}) based on a modified Goodman diagram is

$$\sigma_{mbrsl} = \frac{(\sigma_{allow} - \sigma_{es})}{(1 - \sigma_{es} / \sigma_u)}$$

Finally, the design blade root centrifugal stress (σ_{des}) is calculated by assuming a 20% overspeed, 5% centrifugal stress, and 10% gas bending stress as:

$$\sigma_{des} = \sigma_{mbrsl} / 1.6632$$

Once σ_{des} is known, the maximum turbine speed (N_{max}) can be calculated.

$$N_{max} = 1000 \sqrt{\frac{\sigma_{des}}{4.52\ \rho_t\ A_{ann}}}$$

where: ρ_t = blade material density (lb/in^3)
A_{ann} = annular area (in^2)
σ_{des} = design blade root centrifugal stress (psi)
N_{max} = maximum turbine speed (rpm)

If the previously calculated turbine speed (N) is greater than the maximum allowable speed (N_{max}) then N is set to N_{max}. TPA designs which have the turbine and a pump on the same shaft will require also setting the pump speed to N_{max} and redesigning the whole system. If a gearbox is used then only the turbine must be redesigned.

A gas generator bleed cycle TPA design is completed at this point and the weight flow through the turbine has been calculated. The other pump fed cycles, however, began by assuming a turbine pressure ratio for a known weight flow and must now test the accuracy of the pressure ratio assumption. If the pressure ratio needs to be adjusted then the previous TPA design process will be iterated until sufficient accuracy is attained.

The parameter which determines whether or not the cycle is balanced is the ratio of the required pump horsepower divided by the delivered turbine horsepower. If the power ratio (r_{pow}) is approximately equal to 1.0, then the cycle is balanced. If r_{pow} falls outside the tolerance band around 1.0 (ELES uses 0.97 to 1.03) then the turbine pressure ratio is adjusted.

ELES calculates the next trial value of pressure ratio (r_p) by the equation

$$r_p = \left(\frac{T_{in}}{T_{in} - \Delta T}\right)^{\left(\frac{\gamma}{\gamma-1}\right)}$$

where:
- r_p = turbine pressure ratio
- T_{in} = turbine inlet temperature (°R)
- ΔT = calculated temperature drop across turbine (°R)
- γ = ratio of specific heats

In the above equation, ΔT is calculated as

$$\Delta T = 550\ HP\ /\ (778\ \eta_t\ \omega_t\ C_p)$$

where: HP = pump horsepower (hp)
η_t = turbine efficiency (-)
ω_t = turbine mass flowrate (lb/sec)
C_p = turbine gas heat capacity (Btu/lb °R)

For single turbine designs the above equation uses the sum of pump horsepowers for HP and uses the single turbine efficiency and flowrate. For series turbines each pump/turbine pair is calculated separately, and the total ΔT is the sum of the individual ΔT's. . Parallel turbines use the maximum of the individual ΔT's.

ELES uses the latest value of pressure ratio (r_p) to redesign the TPA and check for power balance. If unsuccessful, it will recalculate r_p and try again. The process ends with either a balanced cycle or a maximum iteration error. ELES warns the user of the latter occurance.

If the cycle under consideration is a gas generator bleed cycle, then the turbine exhaust must be included as an engine performance loss. The method used by ELES is to mass average the Isp of the main TCA and the gas generator bleed nozzle. The equation for mass averaging the Isp is

$$Isp_{overall} = (\omega_{TCA}\ Isp_{TCA} + \omega_{gg}\ Isp_{gg})\ /\ (\omega_{TCA} + \omega_{gg})$$

where: $Isp_{overall}$ = overall engine specific impulse (sec)
ω_{TCA} = TCA flowrate (lb/sec)
Isp_{TCA} = TCA specific impulse (sec)
ω_{gg} = gas generator flowrate (lb/sec)
Isp_{gg} = gas generator specific impulse (sec)

The gas generator Isp is calculated as

$$Isp_{gg} = 0.9\ Isp_{ODEgg} / \left[\left(\frac{P_{in}}{P_{out}}\right)^{(\gamma-1)/2\gamma}\right]$$

where: Isp_{ODEgg} = the ideal one dimensional equilibrium Isp of the gas generator (sec)

P_{in} = turbine inlet pressure (psia)

P_{out} = turbine outlet pressure (psia)

γ = turbine gas ratio of specific heats (-)

The gas generator ideal performance (Isp_{ODEgg}) is taken from the ELES tables of Isp using the appropriate values of chamber pressure, area ratio, and mixture ratio. The above equation approximates the turbine exhaust Isp by assuming a 90% efficient ODE performance to be degraded by the square root of the ratio of outlet to inlet temperature. That temperature ratio has been approximated with the equation

$$T_{out}/T_{in} = \left(\frac{P_{out}}{P_{in}}\right)^{\frac{\gamma-1}{\gamma}}$$

The justification for this approach is that ideal isentropic performance equations predict Isp to vary as the square root of exhaust temperature divided by molecular weight. If molecular weight is assumed constant, the above equations result.

11.0 PROPELLANT PROPERTIES

The properties of the propellants in ELES are required over an extremely wide range in order to service the regenerative cooling logic, autogenous pressurization model, component design logic, tankage heat transfer, engine performance, pump design, and turbine design models. The fluid properties are required for both liquid and gas phases.

The approach taken in ELES to obtain these values is to start with a known value of the fluid property at some reference point, and scale that value to some other condition based on empirical or theoretical correlations. The majority of the correlations are based on the theory of corresponding states, which assumes that those properties dependent on intermolecular forces are related to the critical properties in the same way for all compounds. The result is that propellants which did not have extensive experimental properties data available can be analyzed with approximate values using a minimum of data. Another benefit is the reduction in computer space required, since properties data for each propellant can be calculated from a single data base. (Exceptions to this approach are hydrogen and helium which require their own specific data base.)

Propellant vapor pressure is calculated based on the Riedel-Plank-Miller* vapor pressure equations:

$$\ln Pvpr = \frac{G}{Tr}\left[1 - Tr^2 + k\,(3 + Tr)\,(1 - Tr)^3\right]$$

where

$$G = 0.4835 + 0.4605\,h$$

$$h = Tbr\left(\frac{\ln Pc}{1 - Tbr}\right)$$

$$k = \frac{h/G - (1 + Tbr)}{(3 + Tbr)\,(1 - Tbr)^2}$$

Pvpr = reduced vapor pressure
Tr = reduced temperature**
Tbr = reduced boiling point temperature
Pc = critical pressure (atm)

* "The properties of gases and liquids" 3rd Ed., Reid-Prausnitz-Sherwood P. 190.
** Reduced Temperature = Temperature/Critical Temperature.

Typical results of this equation are shown in Figure 11.1 along with several other vapor pressure correlations.

The Riedel-Plank Miller vapor pressure correlation is used by ELES to calculate the acentric factor of each propellant. The acentric factor was originally proposed in order to represent the non-sphericity of a molecule. At present time, it is widely used as a parameter which measures the complexity of a molecule with respect to both its geometry and polarity. It is defined as:

$$\omega = -\log_{10} P_{vpr\ (Tr = 0.7)} - 1.0$$

ω = acentric factor

$P_{vpr\ (Tr = 0.7)}$ = reduced vapor pressure at reduced temperature = 0.7

Correlations using the acentric factor are not recommended for use with quantum fluids such as He and H_2. For normal fluids, however, the acentric factor is often used to correlate fluid properties.

Fluid densities in ELES are calculated based on compressibility factors. Compressibility is a correction term applied to the ideal gas law to yield:

$$PV = nRTZ$$

P = pressure
V = volume
n = number of moles
R = universal gas constant
T = temperature
Z = compressibility constant

$$P_{vp_r} = f(T_{b_r}, T_r, P_c)$$

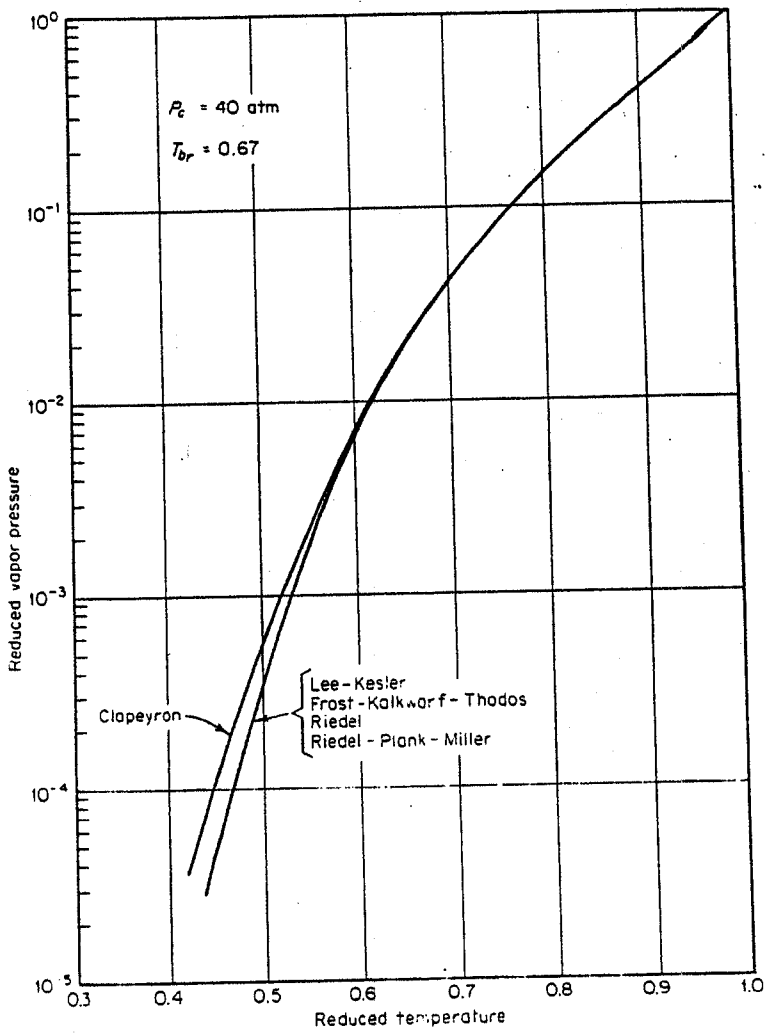

Figure 11.1. Reduced Vapor-Pressure Correlations

A typical compressibility curve for a fluid with a critical compres-

In ELES, the acentric factor is applied to a compressibility factor correlation. The result is to generalize beyond the correlations which assume a specific critical compressibility. Compressibility is calculated from*:

$$Z = Z^{(0)} + \omega Z^{(1)}$$

where $Z^{(0)}$ and $Z^{(1)}$ are derived from table look ups as functions of reduced temperature and pressure.

The acentric factor is similarly used in ELES to calculate the heat capacity difference from that of an ideal gas by the equation**:

$$Cp - Cp^0 = (Cp)^{(0)} + \omega (Cp)^{(1)}$$

Cp	=	heat capacity
Cp^0	=	ideal gas heat capacity
$(Cp)^{(0)}$, $(Cp)^{(1)}$	=	correction factors
ω	=	acentric factor

Tables of $(Cp)^0$ and $(Cp)^{(1)}$ verses Tr and Pr are used to calculate $Cp-Cp^0$. A typical plot of heat capacity correction from ideal gas for a fluid of a specific acentric factor is shown in Figure 11.3.

The ideal heat capacity (Cp^0) is a strong function of the number and type of chemical bonds within the molecule. The internal vibrational and rotational energies of a molecule contribute to the heat capacity as well as

* The Properties of Gases and Liquids" 3rd ed., Reid-Prausnitz-Sherwood p. 31.

** The Properties of Gases and Liquids" 3rd ed., Reid-Prausnitz-Sherwood p. 140.

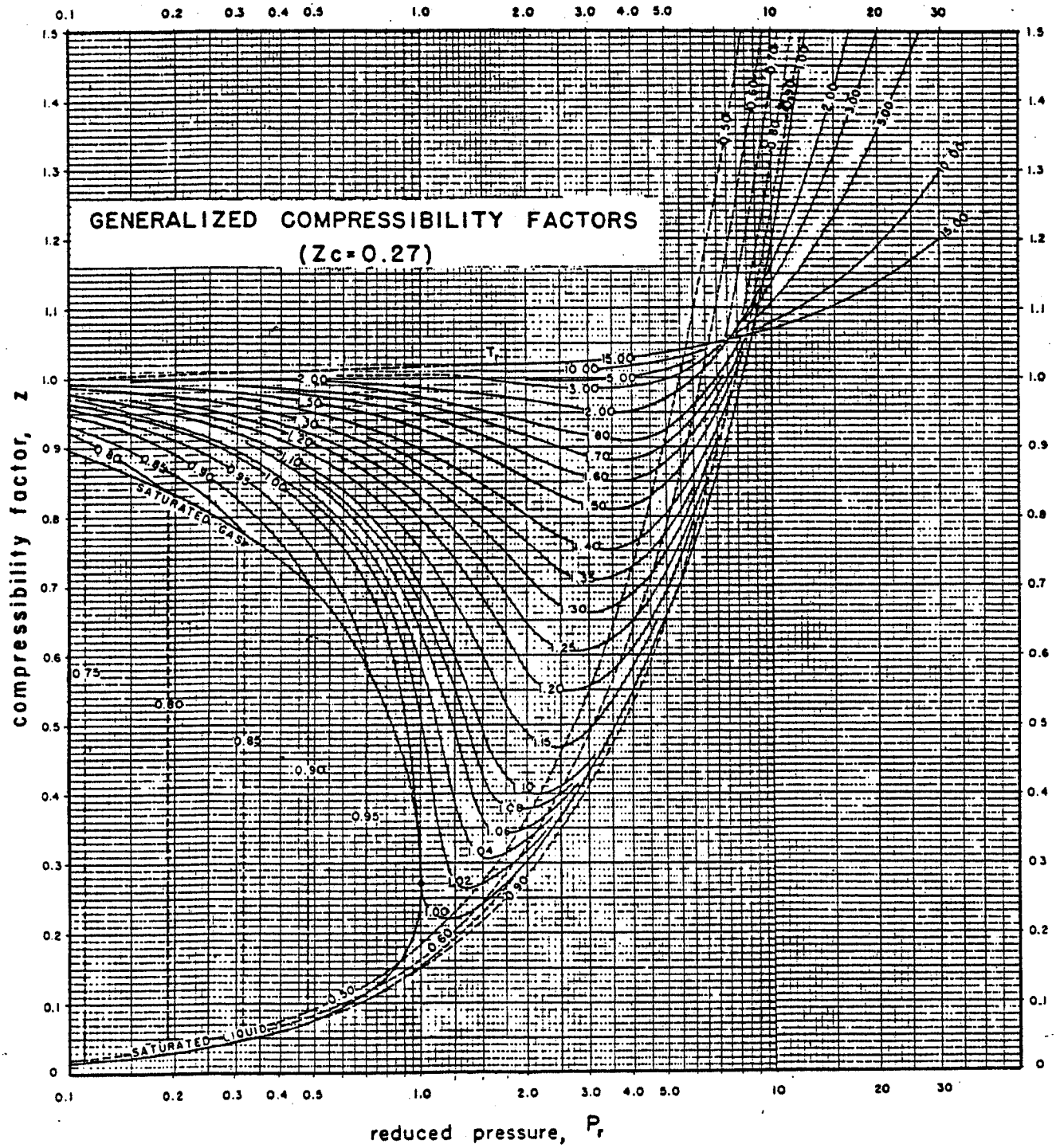

Figure 11.2. Generalized Compressibility Factors (Z_c = 0.27)

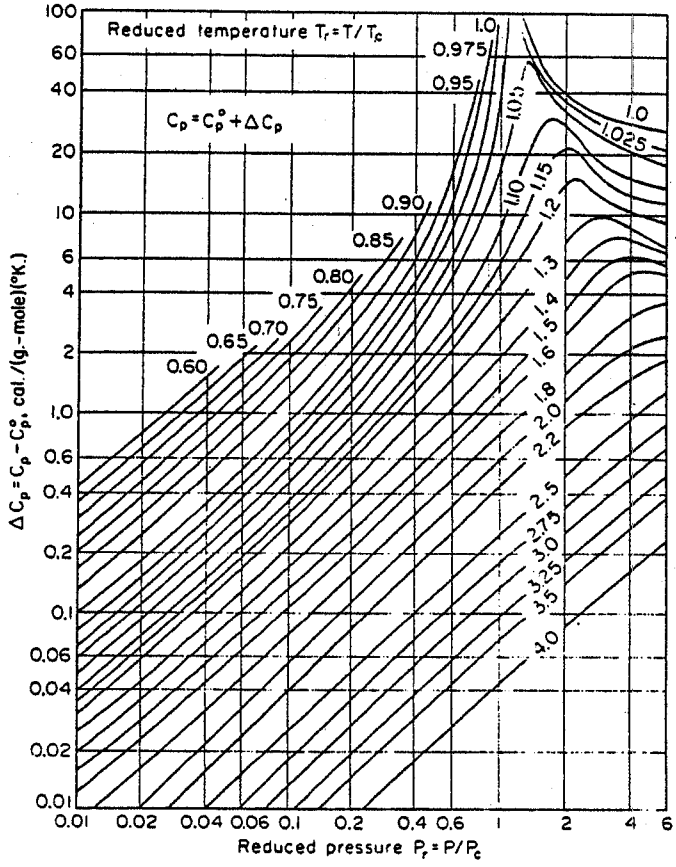

Figure 11.3. Isothermal Pressure Correction to the Molar Heat Capacity of Gases

the more classical translational and external rotational energies. Theoretical methods used to calculate ideal heat capacity are based on extensive spectroscopic data. Empirical chemical bond contribution methods are also available if sufficient information is known concerning the molecule or mixture of molecules in question.

The results of these analyses are often presented in the form of an equation.

$$Cp^0 = A + BT + CT^2 + DT^3$$

Cp^0	=	ideal gas heat capacity
T	=	absolute temperature
A,B,C,D	=	empirical constants

ELES uses a similar equation for determining Cp^0, except that reduced temperatures are used.

$$Cp^0 = A' + B'Tr + C'Tr^2 + D'Tr^3$$

where $A' = A$

$B' = BTc$

$C' = CTc^2$

$D' = DTc^3$

Tr = reduced temperature = T/Tc

Tc = critical temperature

The thermal conductivity calculations in ELES are based on the reduced thermal conductivity graph shown in Figure 11.4*. Given a reference thermal conductivity at a specific temperature and pressure, the graph can be used to calculate the thermal conductivity at some other point.

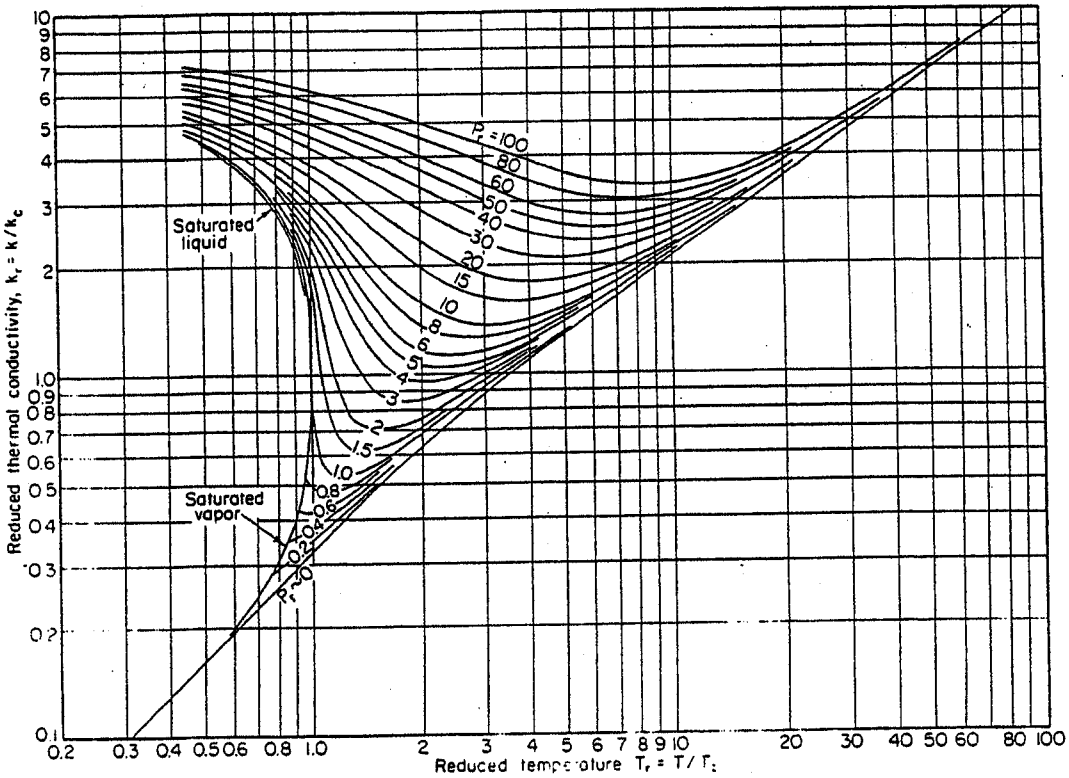

Figure 11.4. Reduced Thermal Conductivity Correlation for the Diatomic Gases

Fluid viscosity is handled in an exactly analogous manner as thermal conductivity. A graph of generalized reduced viscosity* has been tabulated, and ELES interpolates the value of reduced viscosity for a specific reduced temperature and pressure (see Figure 11.5). Viscosity is scaled from an input reference point in this manner.

Liquid surface tension is scaled from a reference point based on the Hakim equation**. The form of the Hakim equation is:

$$\sigma = Pc^{2/3} Tc^{1/3} Qp \left(\frac{1 - Tr}{.4}\right)^m$$

where: σ = surface tension (dyn/cm)
Pc = critical pressure (atm)
Tc = critical temperature (°K)
Qp = $.1574 + .359\ \omega - 1.769 \times 13.69\ x^2 - .51\ \omega^2 + 1.298\ \omega x$
m = $1.21 + .538\ \omega - 14.61\ x - 32.07\ x^2 - 1.65\ \omega^2 + 22.03\ \omega x$
x = $\log_{10} Pvpr_{(Tr = .6)} + 1.7\ \omega + 1.552$
ω = acentric factor
Tr = reduced temperature

The latent heat of vaporization decreases with temperature and is zero at the critical point. Typical data are shown below in Figure 11.6. The shapes of these curves agree with most other enthalpy-of-vaporization data.

* "The Properties of Gases and Liquids" 3rd ed., Reid-Prausnitz Sherwood p. 422.

** "The Properties of Gases and Liquids" 3rd ed., Reid-Prausnitz Sherwood p. 608.

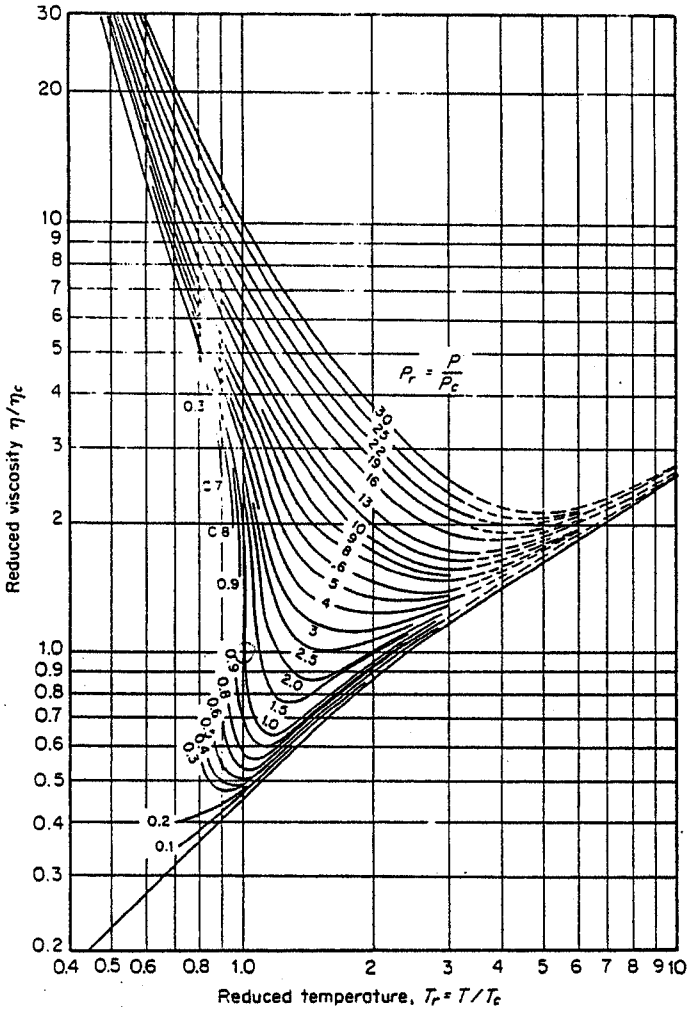

Figure 11.5. Generalized Reduced Viscosities

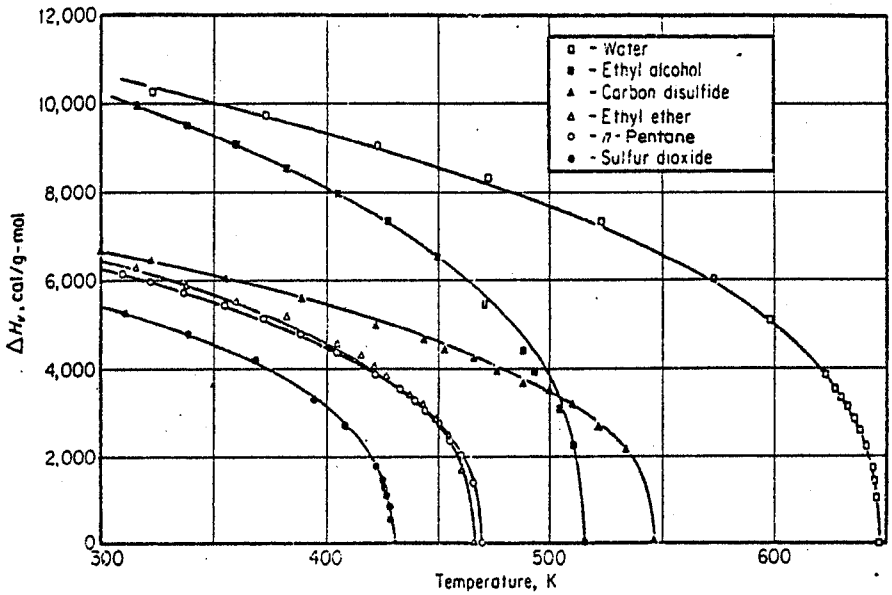

Figure 11.6. Enthalpies of Vaporization

A widely used correlation between ΔH_v and T is the Watson relation*:

$$\Delta H_{v2} = \Delta H_{v1} \left(\frac{1 - Tr2}{1 - Tr1}\right)^n$$

where subscripts 1 and 2 refer to temperatures 1 and 2. A good average value for n is 0.38; for parahydrogen however n = 0.237.

ELES uses the above equation to scale ΔH_v from a reference value at the normal boiling point.

The library of nine propellant combinations in ELES includes the following:

1) N_2O_4/MMH
2) MON-25/MHF-3
3) ClF_5/MHF-3
4) MON-25/60% MHF-3 + 40% Al
5) LO_2/LH_2
6) LO_2/RP-1
7) LO_2/CH_4
8) LF_2/LH_2
9) LF_2/N_2H_4

The physical properties of the propellants used in the above combinations are shown in Tables 11.1 and 11.2. The methods previously described for scaling fluid properties use the information in these tables to predict properties at other conditions.

* "The Properties of Gases and Liquids" 3rd ed., Reid-Prausnitz Sherwood p. 210.

TABLE 11.1

LIQUID PROPELLANT CONSTANTS

Propellant	Tc	Pc	Tb	M	$Hv_{(NBP)}$	A'	B'	C'	D'
MMH	1053	1195	650	46.07	376.9	8.82	27	-12.0	-.7
N_2O_4	776.5	1440	529.8	92.016	178.2	7.9	19.23	-5.018	0
N_2H_4	1175	2131	697.3	32.048	583	3.89	23.2	-9.818	1.666
MHF_3	1077	1373	653	43.41	370.2	7.73	26.5	-11.7	-.4
ClF_5	749.4	771	467.3	130.44	76.04	.31	44.3	-18.33	0
MON-25	747	2100	510	60.7	181.2	7.54	14.53	-3.77	0
LO_2	278	730.6	162.3	32	91.62	6.903	-.058	.046	.00253
LH_2	60	188	36.5	2.016	195.3	6.952	-.0153	.00106	-7.7E-6
RP-1	1218	315	890	172	125	-12.957	159.4	-110.5	29.7
CH_4	343	673.3	201.4	16.04	121.87	4.75	4.116	.356	-.106
LF_2	259	808.5	155	38	71.5	6.115	.8438	-.0867	.00202

Tc = Critical Temperature (°R)
Pc = Critical Pressure (psia)
Tb = Normal Boiling Point (°R)
M = Molecular Weight (lb/lbmole)
$Hv_{(NBP)}$ = Latent Heat of Vaporization (Btu/lb)
A' = Ideal Gas Heat Capacity Constant
B' = Ideal Gas Heat Capacity Constant
C' = Ideal Gas Heat Capacity Constant
D' = Ideal Gas Heat Capacity Constant
Cp^0 = Ideal Gas Heat Capacity (Btu/lbmole °R)

$$Cp^0 = A' + B' Tr + C' Tr^2 + D' Tr^3$$

TABLE 11.2

LIQUID PROPELLANT REFERENCE PROPERTIES

Propellant	T_{ref}	P_{ref}	ρ_{ref}	μ_{ref}	k_{ref}	Cp_{ref}	σ_{ref}
MMH	530	14.7	.0315	4.42E-5	3.317E-6	.7	1.932E-4
N_2O_4	530	14.7	.05177	2.22E-5	1.758E-6	.378	1.433E-4
N_2H_4	530	14.7	.03626	5.113E-5	6.55E-6	.7351	3.794E-4
MHF_3	530	14.7	.03212	4.53E-5	3.69E-6	.7196	2.042E-4
ClF_5	530	14.7	.06417	1.83E-5	2.569E-6	.298	8.8E-5
MON-25	530	14.7	.049	2.225E-5	1.758E-6	.336	1.433E-4
LO_2	160	14.7	.04697	1.117E-5	2.049E-6	.405	7.83E-5
LH_2	40	14.7	.00249	6.25E-7	1.523E-6	2.75	9.2E-7
RP-1	560	14.7	.0285	7.0E-5	1.8E-6	.49	2.77E-4
CH_4	170	15	.01614	9.167E-6	2.778E-6	.791	7.45E-7
LF_2	160	14.7	.05275	1.333E-5	3.63E-6	.368	7.08E-5

T_{ref} = Reference Temperature (°R)

P_{ref} = Reference Pressure (psia)

ρ_{ref} = Density at T_{ref}, P_{ref} ($lb/in.^3$)

μ_{ref} = Viscosity at T_{ref}, P_{ref} (lb/in. sec)

k_{ref} = Thermal Conductivity at T_{ref}, P_{ref} (Btu/in. sec °R)

Cp_{ref} = Heat Capacity at T_{ref}, P_{ref} (Btu/lb °R)

σ_{ref} = Surface Tension at T_{ref}, P_{ref} (lb/in.)

12.0 STAGE SIZE/WEIGHT

Having defined the size/weight algorithms for all currently possible subsystems on board the propulsion stage, the overall size/weight of the stage is obtained by choosing subsystems and summing their lengths and weights. The following tables document the possible contributing size and weight items for each stage. These items have been described by algorithms in the preceding sections.

Stage Weight Scope

Propellant (burned and residual)
Pressurant (helium, solid propellant, or autogenous)
Forward Propellant Tank
Aft Propellant Tank
Pressure Tank
Pressure Tank Insulation
Propellant Lines
Pressurant Lines
Burst Diaphram Assemblies
Pressurant Control Hardware (regulator, igniter, orifices, etc.)
Structural Wall
Skirts (forward and aft)
Skirt Stiffening Ring
Tank Mounts
Reverse Dome Stiffeners
Expulsion/Acquisition System
Bipropellant Valve
Injector
Thrust Chamber
Extendable Nozzle or Gas Deployed Skirt
Thrust Mount
Gimbal System (actuators and power supply)
Turbopump Assembly
TPA Start System
Boost Pumps
Gas Generator/Preburner
Hot Gas Manifolding
Autogenous Heat Exchanger
Tank Insulation
Thrust Chamber Igniter
Propellant Boiloff

Stage Length Scope

Forward Skirt
Pressurization Tank(s)
Propellant Tanks
Gimbal Mount
Injector Face to Gimbal Point
Chamber Length
Nozzle Length
Aft Skirt

13.0 WARNING MESSAGES

There are a number of warning messages output by ELES. The objective of these messages is to alert the user to potential problems in the stage design or situations outside of normal engineering practice. The following is a list of the warning messages currently output by ELES.

1) Injector element to throat angle outside recommended limits (2 to 2.5 degrees)

2) Cold gas pressure bottle outside recommended limits (100 to 10,000 psia)

3) Vehicle operating temperature range outside recommended limits (-65 to 145°F)

4) Simplified ablative engine weight model called with correlating parameter out of range

5) Injector element density outside recommended range (1 to 30 elements/in.^{2})

6) Injector orifice size below recommended minimum (0.020 in. diameter)

7) Nozzle contour outside recommended range

8) Contraction ratio outside recommended range (1.5 to 4)

9) Nozzle exit diameter larger than stage diameter

10) Vapor pressure of propellant at maximum operating temperature is greater than the pressure required by feed system requirements (i.e., vapor pressure designs tanks)

11) Carry moment designs structural wall

12) Material minimum gauge designs tank or structural wall

13) Tank volume increased due to geometry constraint

14) Tank centerbody designed by bonded rolling diaphram constraint

15) Tank head ellipse ratio outside recommended range

16) Pressurant tank pressure less than propellant tank requirement

17) Pump tip speed exceeds 2000 ft/sec

18) Power balance iteration limit exceeded without coverging on a solution

19) Power balance cannot be achieved for current values of input

20) Multi-staged partial admission turbine used whereas a re-entry turbine is a better design.

21) Propellant injection velocity below minimum acceptable value (40 ft/sec)

22) Pressure drop across injector does not satisfy chug stability requirement at low throttled condition

23) Non-regen propellant used as autogenous pressurant in expander cycle

24) Multi layer insulation used in ground hold ice heat transfer scenario

25) Turbine inlet temperature is too high for materials of construction

26) Gas deployed skirt will not fit engine geometry

14.0 REFERENCES

1. Coats, D. E., et al, "A Computer Program for the Prediction of Solid Propellant Rocket Motor Performance," Vol. I, AFRPL-TR-75-36 Ultrasystems, Inc., July 1975.

2. Nickerson, G. R., et al, "A Computer Program for the Prediction of Solid Propellant Rocket Motor Performance," Vol. I, AFRPL-TR-79 to be issued, SEA, Inc., May 1980.

3. Final Report, Contract AF04(611) 11205, AFRPL-TR-66-231, Aerojet General Corporation, September 1966.

4. Ablative Response of a Silica Phenolic to Simulated Propellant Rocket Engine Operating Conditions, NASA Report, Aerotherm Corporation.

5. Experimental and Theoretical Analysis of Ablative Material Response in a Liquid Propellant Rocket Engine, NASA Report, Aerotherm Corporation.

6. Schmidt, D. L., Ablative Plastics and Elastomers in Chemical Propulsion Environments, Technical Report AFML-TR-65-4, April 1965.

7. Advanced Rocket Design Section Memoranda, Notes, Files, etc., Aerojet TechSystems Company.

8. Corning, G., Weight Prediction Method for Space Tug, Report P-1027, Institute for Defense Analysis, Arlington, Virginia, June 1974.

9. Arnold, C. S., and Rhoden, M., Prepackaged Liquid Bipropellant Rocket Parametric Design Computer Program, Report RK-TR-65-3, U.S. Army Missile Command Redstone Arsenal, Alabama, May 1965.

10. Lemke, D. E., Propulsion System General Weight Model, Contract 9450-5-1, ALRC, July 1967.

11. Ewen, R. L. and Evensen, H. M., Liquid Rocket Engine Self-Cooled Combustion Chambers, NASA SP-8124.

12. Huzell, K. K., and Huang, D. H., Design of Liquid Propellant Rocket Engines, 2nd Edition, NASA SP-125, 1971.

13. Hyde, J. C., and Gill, G. S., Liquid Rocket Engine Nozzles, NASA SP-8120, July 1976.

14. Lee, J. C., and Ramirez, P., Pressurization Systems for Liquid Rockets, NASA SP-8112, October 1975.

15. Wagner, W. A., Liquid Rocket Metal Tanks and Tank Components, NASA SP-8088, May 1974.

16. MacConochie, I. O. and Klich, P. J., Techniques for the Determination of Mass Properties of Earth-to-Orbit Transportation Systems, NASA Technical Memorandum No. 78661, June 1978.

17. Glatt, C. R., WATTS - A Computer Program for Weights Analyses of Advanced Transportation Systems, NASA CR-2420, September 1974.

18. Barclay, D. L., Evaluation of Propellant Tank Insulation Concetps for Low-Thrust Chemical Propulsion Systems, NAS 3-22824, Boeing Aerospace Company, February 1982.

19. Keller, C. W., Cunnington, G. R., Glassford, A. P., Thermal Performance of Multilayer Insulation, NAS 3-14377, Lockheed Missiles and Space Company, April 1974.

20. King, K., Johs, W. A., Upgrading and Conversion of Cryogenic Analysis Programs, ESO-55024-2, Martin Marietta Denver Aerospace, July 1982.

21. Rohsenow, W. M., Hartnett, J. P., Handbook of Heat Transfer, McGraw-Hill, 1973.

22. Siebenhaar, A., TURBO - Version 1 User Manual, internal Aerojet Liquid Rocket Company document, 1981.

23. NASA, Liquid Rocket Engine Centrifugal Flow Turbopumps, NASA SP-8109, December 1973.

24. NASA, Turbopump Systems for Liquid Rocket Engines, NASA SP-8107, August 1974.

25. Arpaci, V. S., Clark, J. A. and Winer, W. O., "Dynamic Response of Fluid and Wall Temperatures during Pressurized Discharge of a Liquid from a Container," Advances in Cryogenic Engineering, Volume 6, Plenum Press, New York (1961) Page 310.

26. Epstein, M., Georgius, H. K. and Anderson, R. E., "A Generalized Propellant Tank-Pressurization Analysis," Advances in Cryogenic Engineering, Volume 10B, Plenum press, New York (1965), Page 290.

27. Epstein, M. and Anderson, R. E., "An Equation for the Prediction of Cryogenic Pressurant Requirements for Axisymmetric Propellant Tanks," Advances in Cryogenic Engineering, Volume 13, New York (1968), Page 207.

28. Klassen, H. A., Cold-Air Investigation of Effects of Partial Admission on Performance of 3.75-inch Mean-Diameter Single Stage Axial-Flow Turbine, NASA TN D-4700, August 1968.

29. Reid-Prausnitz-Sherwood, The Properties of Gases and Liquids, 3rd Ed.

30. Perry, R. H., Chilton, C. H., Chemical Engineer's Handbook 5th Ed, McGraw-Hill, 1973.

31. Pieper, J. L., ICRPG Liquid Propellant Thrust Chamber Performance Evaluation Manual, CPIA No. 178, September 1968.

32. Nickerson, C. R. et al., The Two-Dimensional Kinetic (TDK) Rocket Nozzle Analysis Reference Computer Program, December 1973.

33. JANNAF Liquid Rocket Engine Performance Prediction and Evaluation Manual, CPIA Publication No. 246, April 1975.

15.0 GLOSSARY OF TERMS

-A-

ablation. process in which thermal energy is expended by a sacrificial loss of material. In the process, heat is absorbed, blocked, dissipated, and/or generated by mechanisms that include phase transitions (melting, vaporization, and sublimation); mass transfer into the boundary layer; convection in the liquid layer (if one exists); radiant-energy transport; conduction into the solid body; chemical reactions; and erosion

ablative cooling. reduction of the heat transferred from hot combustion products to a nozzle or chamber wall by ablation of material on the wall

ablative material. material designed or formulated so as to dissipate incident heat by degrading through the process of ablation

accelerometer. an instrument, usually a transducer, that measures change in velocity, or measures the gravitational forces capable of imparting a change in velocity

acoustic absorber. an array of acoustic resonators distributed along the wall of a combustion chamber, designed to prevent oscillatory combustion by increasing damping in the engine system

action time. interval from attainment of a specified initial fraction of maximum thrust or pressure level to attainment of a specified final fraction of maximum thrust or pressure level

actuation time. elapsed time from receipt of signal to first motion of the device being actuated

actuator. device that converts hydraulic, pneumatic, electrical, or potential energy into mechanical motion

adiabatic. term applied to a thermodynamic process in which heat is neither added to nor removed from the system involved; when the process is reversible, it is called isentropic

adiabatic wall. in a thermodynamic system, a boundary that is a perfect heat insulator (neither emits nor absorbs heat); in boundary-layer theory, the wall condition in which the temperature gradient at the wall is zero

adiabatic wall temperature. steady-state temperature of the wall of a combustion chamber or nozzle when there is not heat transfer between the wall and the exhaust gas; also called recovery temperature

aerodynamic heating. heating of a body by the friction generated by high-velocity air or other gas passing over the body surfaces

aerodynamic performance. portion of the nozzle performance due to nozzle divergence efficiency (the degree of perfection of the nozzle contour)

aerodynamic throat area. effective flow area of the nozzle throat; the effective flow area is less than the geometric flow area because the flow is not uniform

aerospike nozzle. annular nozzle that allows the gas to expand from one surface - a centerbody spike - to ambient pressure

allowable load (or stress). load that, if exceeded, produces failure of the structural element under consideration. Failure may be defined as buckling, yielding, ultimate, or fatigue failure, whichever condition prevents the component from performing its intended function. Allowable load is sometimes referred to as criterion load or stress; allowable stress is equivalent to material strength

altitude engine. rocket engine that is designed to operate at high-altitude conditions (see sea-level engine)

ambient. term referring to a condition or state (e.g., temperature, pressure) of the environment surrounding a component or system

anisotropy. condition in a material in which properties are not the same in all directions; observed or measured properties change when the axis of observation or test is changed

annular nozzle. nozzle with an annular throat formed by an outer wall and a centerbody wall

anti-slosh baffle. device provided in a tank to damp liquid motion; can take many forms including flat ring, truncated cone, and vane

anti-vortex baffle. radial vane attached to inner tank wall adjacent to the inlet to engine feedline to inhibit fluid vortexing at the inlet

area ratio. ratio of the geometric flow area of the nozzle exit to the geometric flow area of the nozzle throat; also called expansion area ratio or simply expansion ratio

aspect ratio. 1. ratio of width to height in a rectangular flow passage; 2. ratio of blade height to chord length; 3. ratio of width to depth in a rectangular combustion chamber

autoignition. self-ignition or spontaneous combustion of propellant

axial deflection. elongation or compression along the longitudinal axis

baffle. partitioning device (plate, wall, screen) used to deflect, check, or interrupt fluid motion; used, for example, in a combustion chamber for stabilizing combustion, or in a tank for preventing slosh

ball valve. rotary-action valve incorporating a ball with a flow passage that rotates to align the flow passage with the mating upstream and downstream lines

bandwidth. limits of variation of a regulated variable (e.g., pressure) above and below its desired value

barrier cooling. use of controlled mixture ratio near the wall of a combustion chamber to provide film of low-temperature gases to reduce the severity of gas-side heating of the chamber

base. 1. configuration of a plug nozzle in the plane of truncation; 2. portion of a blade (or vane) that forms the attachment to the rotor (or vane support)

base cavity. the opening in the base of a plug nozzle

base pressure. static pressure in the base cavity of a plug nozzle

bearing (rolling-element). a mechanical device, usually consisting of two integral concentric channels with rolling elements (e.g., spheres or cylinders) confined between them, used to support and position a rotating shaft with as little friction as possible

Beattie Bridgeman. an equation of state which is considered accurate for helium

bed reactor. term for a gas generator design in which the combustion chamber is nearly filled with a solid material that assists decomposition by either catalytic or thermal action

bell nozzle. nozzle with a circular opening for a throat and an axisymmetric contoured wall downstream of the throat that gives the nozzle a characteristic bell shape

bell nozzle length. the length of a bell nozzle is often approximated as that of a 15° half angle cone.

$$L = \frac{R_t \left(\sqrt{\varepsilon} - 1\right)}{\tan \alpha}$$

bipropellant valve. valve incorporating both fuel and oxidizer valving units driven by a common actuator

blade. 1. one of a set of slat-like objects rigidly fixed to a rotatable shaft, each slat being carefully shaped as an airfoil such that (a) rotation of the shaft in a fluid creates a flow of fluid, or (b) fluid flow impinging on the blades rotates the shaft; 2. a flat plate used to adjust flow in a blade valve

bleed. 1. continuous flow of gas through a pilot valve. 2. to remove or draw off fluid from a system

blowdown system. a closed propellant/pressurant system that decays in ullage pressure level as propellant is consumed and ullage volume thereby is increased

boattail. aft (rear) end of a rocket that contains the propulsion system and its interface with vehicle tankage

booster. the first or basic separable self-propelled section (stage) in a rocket vehicle having two or more such sections

boss. thickened protuberance in the wall of a duct or tank for the purpose of allowing attachment of components or connection of other lines or instruments

boundary layer. in fluid flow, the film of fluid next to a bounding surface such as the combustion chamber wall or nozzle wall; its thickness usually is taken as the radial distance from the surface to the point at which fluid velocity reaches 99 percent of freestream velocity

boundary-layer trip. discontinuity or local turbulence in the boundary layer generated by a protrusion from the surface in contact with the boundary layer; tripping usually increases the severity of the thermal environment

BRD (Bonded Rolling Diaphram). a type of positive expulsion device in a propellant tank which has been successfully tested at high G loads with high expulsion efficiency.

brittle failure. rupture of structural material that is not preceded by appreciable deformation of the material

bulkhead. structural membrane perpendicular to the axis of the structure containing it; usually used in a rocket vehicle to physically separate two fluids contained in a single tank

burn rate. literally, the rate at which a solid propellant burns, i.e., rate of recession of a burning propellant surface, perpendicular to that surface, at a specified pressure and grain temperature; in grain design, the rate at which the web decreases in thickness during motor operation

burning surface. all surface of a solid-propellant grain that is not restricted from burning at any given time during propellant combustion

burn time. for a solid propellant, the interval from attainment of a specified initial fraction of maximum thrust or pressure level to web burnout

burst disk. passive physical barrier in a fluid system that blocks the flow of fluid until ruptured by fluid pressure

burst pressure. fluid pressure at which a pressurized component will rupture

burst test. pressure test of a coamponent to rupture to determine whether the component can withstand the calculated burst pressure

butterfly valve. valve constructed to close off or throttle flow by rotation of a circular disk around a transverse axis within the flow passage

-C-

capacity (pump). volume of liquid pumped per unit time

captive firing. test firing of a propulsion system, in which the engine is operated at full or partial thrust while restrained in a test stand; the system is completely instrumented, and data to verify design and demonstrate performance are obtained

case. 1. the structural envelope for the solid propellant in a solid rocket motor; 2. the outer portion of metallic materials

case bonding. cementing of the solid propellant to the motor case through the insulation by use of a thin layer of adhesive (the liner)

case hardening. infiltration of a metallic surface with carbon so that the outer portion of the material (case) is made harder than the inner portion (core)

casing. the part of the pump housing that surrounds the impeller

cavitating venturi. convergent-divergent constriction in a line that produces cavitation at its throat; because of the cavitation effects, flow of the liquid in the line is a function only of pressure upstream of the constriction even though the downstream pressure varies

cavitation. formation and instantaneous collapse of vapor bubbles in a flowing liquid whenever the static pressure becomes less than the fluid vapor pressure

chamber. see combustion chamber

chamber plenum. the portion of the TCA combustion chamber where the total pressure (static + dynamic) equals that of the throat

chamber pressure. stagnation pressure of the exhaust gases in a combustion chamber

channel construction. use of machined grooves in the wall of the nozzle or chamber to form coolant passages

char. rigid, porous material remaining after severe thermal degradation of an organic material; also refers to any solid residue formed by thermal degradation of a material

characteristic length. ratio of combustion chamber volume to nozzle throat area

characteristic velocity. ratio of effective exhaust velocity to thrust coefficient; also called characteristic exhaust velocity

chatter. uncontrolled rapid seating and unseating of a flow-control device, usually at low-flow conditions

check valve. flow-control device that allows flow in one direction only

chevron seal. term for a set of seals having a V-shaped cross section loaded by mechanical or fluid wedging action

chilldown. cooling of all or part of a cryogenic engine system from ambient temperature to cryogenic temperature by circulating cryogenic fluid through the system prior to engine start

choked flow. flow condition in a flow passage such that flowrate through or upstream of the passage cannot be increased by a reduction of pressure downstream of the passage

chord. straight line connecting the ends of an arc; usually, the line joining the leading and trailing edges of an airfoil

chugging. low-frequency oscillatory combustion; in a fluid system, the oscillations are hydraulically coupled to the propellant feed system

circumferential seal. seal, composed of a continuous ring or of one or more split or segmented rings, whose sealing surface is parallel to the centerline of the flow passage (also called radial seal)

clean room. a delimited space in which dust, temperature, and humidity are controlled as necessary for the fabrication and/or assembly of critical components

clearance seal. seal that limits the leakage between a rotating or reciprocating shaft and a stationary housing by controlling the annular clearance between the two

closed loop. term applied to an electrical or mechanical system in which the output is compared with the input command signal, and any discrepency between the two results in corrective action by the system elements.

coaxial injector. type of injector in which on propellant surrounds the other at each injection point

coined groove. narrow channel or depression stamped in a burst disk to provide localized thinning of material in a desired pattern

coking. deposition of a solid residue by a material when it is burned or distilled

cold flow. 1. term applied to a test of an engine or all or part of an engine system, in which fluid is flowed through the test configuration without the engine being started; term also is applied to tests of model fluid systems; 2. permanent deformation of material caused by a compressive load that is less than the load necessary to yield the material; some time is required to obtain cold flow

combustion chamber. portion of a rocket engine in which propellants are burned

combustion stabilization device. contrivance in the combustion chamber that reduces or eliminates oscillatory combustion by reducing the coupling of the oscillations with the driving combustion processes or by increasing the damping inherent in the engine system

compressibility factor (Z). ratio of ideal-gas density to real-gas density - an additional term in the ideal gas law which accounts for non-idealities of the particular gas under consideration

contraction ratio. ratio of the area of the combustion chamber at its maximum diameter to the area of the throat

controller. device that converts an input signal from the controlled variable (temperature, pressure, level, or flowrate) to a valve actuator input (pneumatic, hydraulic, electrical, or mechanical) to vary the valve position to provide the required correction of the controlled variable

coolant tube. relatively small-diameter thin-wall conduit attached to or forming the wall of a regeneratively cooled combustion chamber or nozzle and carrying propellant to cool the wall

coupling. mechanical device that fastens together two parts of a turbopump shaft or connects the shaft to other components of the turbopump; also a separable connector in a fluid system line or duct

cracking. 1. thermal decomposition of heavy (complex) hydrocarbons into lighter and simpler hydrocarbons and other products; 2. opening of a flow-control device to allow flow of fluid

cracking pressure. effective differential pressure above which a flow-control device (e.g., a valve) will open and allow flow of fluid

creep. permanent deformation of material caused by a tensile or compressive load that is less than the load necessary to yield the material; some time is required to obtain creep

creep strength. degree to which a given material resists creep; also, the maximum load at which a given material will not exhibit a significant amount of creep

crevice corrosion. corrosion that occurs in a narrow, relatively deep opening where two similar surfaces meet and trap a reactive fluid that acts as an electrolyte; corrosion occurs because of the concentration gradient of the reactive species established within the trapped fluid

critical crack size. crack or flaw size in a pressure vessle at or above which the crack, at a specified stress level, will grow and become unstable (i.e., will lead to brittle failure)

critical flow capacity. point in the performance of a tank-pressurization heat exchanger at which pressurant volumetric flowrate is at a maximum and an increase in pressurant produces a decrease in volumetric rate

critical speed. shaft rotational speed at which frequency of a rotor/stator system coincides with a possible forcing frequency

cryogenic. fluids or conditions at low temperatures, usually at or below -150°C (123K)

cryogenic propellant. propellant that is liquid only at temperatures below -150°C (123K)

cryogenic seal. seal that must function effectively at temperatures below -150°C (123K)

cryopump. to reduce pressure in a cavity by condensing confined vapors and gases on extremely cold (cryogenic) surfaces

cycle life. number of times a unit may be operated (e.g., opened and closed) and still perform within acceptable limits

debond. localized failure of adhesive at the interface of two components cemented together

deep-space vacuum. term applied to pressure less than 10^{-11} mm Hg (1.1333×10^{-13} N/cm^2)

deflagration. burning process in which large quantities of gas and energy are released rapidly. In a deflagration, the reaction front advances at less than sonic velocity and gaseous products move away from unreacted material; a deflagration may, but need not, be an explosion

design allowables. precise accepted values of material mechanical properties for use in design and analysis

design bust pressure. maximum limit pressure multiplied by the ultimate factor of safety

design load (or pressure). product of the limit load (or pressure) and the design safety factor

design margin. term for the difference between the capability of a component to perform and the specified use requirement; e.g., if an expulsion device's cycle life under full working pressure and dynamic environments exceeds mission requirements by 100,000 cycles, then the device has a design margin of 100,000 cycles

design safety factor. arbitrary multiplier greater than 1 applied in structural design to account for design uncertainties such as slight variations in material properties, fabrication quality, load magnitude, and load distributions within the structure; the safety factor may be based on yield, buckling, or ultimate strength or on fatigue life

design stress. the stress, in any structural element, that results from the application of the design laod or combination of design loads, whichever condition results in the highest stress

design ultimate load. limit load multiplied by the ultimate design safety factor

design yield load. limit load multiplied by the yield design safety factor

detonation. explosion characterized by propagation of the reaction front within the reacting medium at supersonic velocity and by motion of reaction products in same direction as reaction-front movement

diaphragm. 1. thin membrane that can be used as a seal to prevent fluid leakage or as an actuator to transform an applied pressure to linear force; 2. positive expulsion device used to expel propellant from a tank in zero-g condition

diffusion bonding. method of joining two metals, wherein temperature and pressure create intermolecular bonds.

diluent. fluid (often excess fuel) added to the exhaust gas to cool the gas below the temperature resulting from chemically balanced combustion; also, any substance added to a material to attenuate one or more properties of the material

discharge coefficient. ratio of the actual flowrate to the ideal flowrate, calculated on the basis of one-dimensional inviscid flow

dissociation. separation of a compound into chemically simpler components

divergence angle. see half-angle

divergence efficiency. ratio of thrust calculated for the actual nozzle contour (potential flow) to the thrust of an ideal-flow nozzle

DN. index to bearing speed capability; the product of bearing bore in millimeters (D) and shaft speed in revolutions per minute (N)

dome manifold. manifold that spans the back of the injector

doublet. injector orifice pattern consisting of one or more pairs of orifices that produce converging streams

downcomer. 1. axial feed passage from the rear of the injector; 2. vertical feedline that conveys fluid from a higher to a lower location on a vehicle; 3. coolant tube in which coolant flows in the same direction as exhaust gas

drag pump. pump whose rotor consists of a disk with many short radial blades. The flow enters radially and is carried within the blade passages around the disk and is discharged radially through a port

dynamic seal. mechanical device used to minimize leakage of fluid from the flow-stream region of a fluid-system component when there is relative motion of the sealing interfaces

dump cooling. method of reducing heat transfer by flowing the nozzle coolant turbine exhaust gas down the nozzle coolant passages and discharging the gas at the exit, expansion at the exit being used to increase performance

E-D nozzle. short term for expansion-deflection nozzle, which has an annular throat that discharges exhaust gas with a radial outward component

effective heat of ablation. figure of merit for a given material subjected to steady-state heating conditions and undergoing steady-state ablation; the quantity represents the heat dissipated per unit mass of ablated material under specified conditions

efficiency. ratio of energy output to energy input

elastic limit. maximum stress that can be appalied to a body without producing permanent deformation

engine. see rocket engine

entry. region of the thrust chamber where the contour of the chamber converges to the nozzle throat

envelope. external boundary defining the limits on the dimensions of the component, subsystem, or system

Enzian-plate injector. type of injector that produces atomization by impingement of a jet on a solid plate

equilibrium composition. chemical composition that the exhaust gas would attain if given sufficient time for reactants to achieve chemical balance

erosion. wearing away of surface material by the action of moving liquids or gases; may be accelerated by presence of suspended solid particles and in some cases by corrosive action of the fluid

exhaust plume. hot gas ejected from the thrust chamber of a rocket engine; the plume expands as the vehicle ascends, thus exposing the engine and vehicle to greater radiative area

exit. aft end of the divergent portion of a nozzle, the plane at which the exhaust gases leave the nozzle; also called exit plane

exit pressure. pressure of the exhaust gas at the nozzle exit

expansion geometry. contour of the nozzle from throat to exit plane

expansion ratio. see area ratio

explosion. very rapid chemical reaction or change of state in a material involving production of a large volume of gas and resulting in rupture of the material container (if present) and generation of a shock wave in surrounding medium

explosive valve. valve having a small explosive charge that when detonated provides high-pressure gas to change valve position (also known as a squib valve)

expulsion efficiency. index of the ability of an expulsion device to expel the liquid from a tank; the ratio of expelled volume to loaded volume

external expansion. expansion of the exhaust gases from the nozzle throat directly without a controlled-expansion wall

fabricability. capability of being fabricated into a desired configuration and size without loss of properties

face seal. seal whose sealing surface is perpendicular to the centerline of the flow passage; generally, a face seal prevents leakage of fluids along rotating shafts by a means of a stationary primary-seal ring that bears against the face of a mating ring mounted on a shaft. Axial pressure maintains the contact between seal ring and mating ring. Also called face-contact seal.

fatigue life. number of cycles of stress, under a stated test condition, that can be sustained by a material prior to failure

fillet. material faired into the angle formed by the junction of two surfaces, primarily to relieve stress concentration at the junction

film cooling. technique for reducing heat transfer to the gas-side wall of a combustion chamber or nozzle by maintaining a thin layer (film) of cooling fluid over the surface. The film may be self-generated by thermally induced phase change in the surface material, or fluid may be injected through holes or slots in the surface or through a porous surface

filter. device in a fluid system that limits size and amount of particulate contamination in the system downstream of itself

finite-element method. comnputer-based technique for structural or hydrodynamic analysis, in which the structure or flow system is divided into many small segments (called elements), for which a matrix of coefficients of algebraic equations is set up and solved for values of the desired parameter (stress, strain, velocity, etc.)

flexible joint. (flexible section). nonrigid connector such as metal bellows, flexible hose, or ball-joint assembly that joins two duct sections and permits relative motion between the ducts in one or more planes; includes both the flexible member and the restraint linkage

flow coefficient. in a pump, ratio of axial absolute fluid velocity to rotor tangential velocity (blade tip speed); in a flow-control device, volumetric flowrate at specified pressure drop across the device

flow separation (separate flow). detachment of the flow from the wall of the flow passage

fluid-cooled. term applied to a chamber or nozzle whose walls are cooled by fluid supplied from an external source, as in regenerative cooling, transpiration cooling, or film cooling

fluid-film bearing. type of bearing wherein separation of the bearing and journal depends on the shearing of a lubricating film in the clearance between parts; viscous forces within the fluid support the bearing load

free stream. 1. length of the jet from the orifice exit to the point of impingement on another jet or a surface; 2. the central flow region in a flow passage, where flow is unimpeded by any constraints

frozen composition. exhaust-gas chemical composition that does not change during expansion in the nozzle

fuel. liquid or solid material used to supply thermal energy by chemical reaction (combustion) with an oxidizer

gas generator. assemblage of parts similar to a small rocket engine, in which propellant is burned to provide hot exhaust gases to (1) drive the turbine in the turbopump assembly of a rocket vehicle, or (2) pressurize liquid propellants, or (3) provide thrust by exhausting through a nozzle

GDS (Gas Deployed Skirt). a nozzle extension which is tucked inside the main nozzle and is deployed by the combustion products at ignition

gimbal. to incline freely in any direction from a fixed support (i.e., a pivot point)

gimbal ring. circular structural member of a gimballed joint to which the yokes or clevises of the joint are attached, so that the joint can be angled in any direction

half-angle. angle between the nozzle center line and a line parallel to the inner surface of the nozzle exit cone, also called divergence angle

hard vacuum. term appalied to pressure less than 10^{-8}mm Hg (1.333×10^{-10} N/cm^2)

head or headrise. increase in fluid pressure supplied by a pump; the difference between pressure at the pump inlet and pressure at pump discharge, fluid pressure being expressed as equivalent height (in feet) of a fluid column

head coefficient. measure of headrise related to impeller discharge tip speed

heat-affected zone (HAZ). the region of material affected by the heat of welding or brazing

heater blanket. electrical heater in sheet form wrapped around all or a portion of a cryogenic component (e.g., an actuator) to prevent the temperature within the component from falling below a stated operating minimum

heat of ablation. total of the incident heat that an ablative material dissipates per unit mass ablated. See effective heat of ablation

heat-sink chamber. combustion chamber in which the heat capacity of the chamber wall limits wall temperature (effective for short-duration firing)

heat soak. increase in temperature in rocket-engine components after firing has ceased, the result of heat transfer through contiguous parts when no active cooling exists

heat-transfer coefficient. analytically or empirically determined parameter that expresses the rate of heat transfer per unit area per unit temperature difference between two substances

high-cycle fatigue. life-cycle capability determined by the elastic strain range; generally greater than 10^4 cycles

hot-core injector. injector that produces a central hot-gas combustion region surrounded by a "cold" fuel sheath

hot fire. term applied to a test of an engine system in which the engine is started (ignited) and operated while performance of the system and its components is observed and measured; period of operation need not be full operational duration

hot-gas valve. valve that controls the flow of hot gases, opening at low power levels but restricting the flow at mainstage; it operates at temperatures in excess of 200°F (366K) and as high as 1000°F (811K) or higher

hot streaking. stratification of burning gases in a combustion chamber into longitudinal zones of high-temperature gases that do not break up and mix with cooler gases; term derives from the localized heat marks visible on the chamber wall after firing has ended

housing. physical structure that forms the containing envelope for an assembly

hub-tip ratio. ratio of radius of pump rotor at blade hub to radius of rotor at blade tip

hydraulic. 1. operated, moved, or affected by liquid used to transmit energy; 2. a system or device using a liquid as the operating fluid

hydrogen embrittlement. decrease in a metal's tensile strength, notched tensile strength, fatigue strength, resistance to crack growth, and especially ductility as a result of absorption by the metal of newly formed gaseous hydrogen

hydrostatic bearing. fluid-film bearing wherein the pressure required to maintain separation of the surfaces is externally supplied.

hydrostatic pressure. fluid pressure due to gravitational force

hydrostatic seal. seal that incorporates features that maintain an interfacial film thickness by means of pressure provided with either an external source or by the pressure differential across the seal

hypergolic ignition. ignition that involves no external energy source, but results entirely from the spontaneous reaction of two materials when they are brought into contact; materials may be two liquids or a liquid inpinging on a solid

hypergolic propellants. propellants that ignite spontaneously when mixed with each other

ideal nozzle. nozzle that when analyzed on the basis of one-dimensional point-source flow provides theoretically perfect performance for a given area ratio

ideal velocity. speed that a rocket vehicle could achieve if free of drag and gravity

igniter. device that can, in a controlled and predictable manner, induce self-sustaining combustion of propellants in the combujstion chamber of a rocket engine or motor

ignition. attainment of self-sustaining combustion of propellants in a rocket engine or motor

ignition delay. in solid rocket motors, time period from the moment of arrival of the thermal energy from the igniter at the propellant grain surface until an exothermic gas-phase reaction is self-sustaining (i.e., the propellant is burning); in liquid rocket engines, the time from the initial contact of fuel and oxidizer until a measurable pressure is generated

impeller. disk with curving radial ribs (blades) or spiralled screw that rotates within a casing and accelerates fluid in the flow passage outwardly into a collector or into flow passages of a following stage

impulse. product of average thrust and the time during which it acts; mathematically, the integral of the thrust-time function over a definite time interval

impulse stage. stage in a pump or turbine in which there is no change in static pressure across the rotor

incidence angle. angle between inlet-fluid direction and the tangent to the blade mean camber line at the leading edge of the blade

inducer. an auxiliary pump with a spiral impeller, mounted at the inlet of a main pump, whose function is to raise the fluid pressure at the inlet by an amount sufficient to preclude cavitation in the main pump

inert gas. gas that will not react with other materials

inert weight. weight of all rocket vehicle parts that do not produce thrust

injector. device in a liquid rocket engine that atomizes and mixes fuel and oxidizer to produce efficient and stable combustion

insulation (thermal). material applied to a surface to prevent or reduce heat transfer to or from that surface

interface. region of mating (common boundary) between interconnected elements

internal expansion. gas expansion within a controlled expansion wall or shroud

isentropic. a reversible adiabatic process

isotropy. condition in a material in which properties are the same in all directions

iterative. proceeding in a step-by-step repetitive manner

Joule-Thomas effect. the change in gas temperature with gas pressure as the gas expands through a throttling device

kinematics. study of motion exclusive of the influences of mass and force

kinetic performance. that portion of the nozzle performance that depends on the equilibrium state of the chemically reacting system during gas expansion

laminar flow. fluid flow in which the motion of the fluid is smooth and regular, and there is no crossflow between adjacent streamlines

land. the actual sealing surface of the part that mates with a seal

launch vehicle. the combination of booster, upper stages, and spacecraft (or other payload) adapter making up the total rocket at time of launch; the spacecraft or payload itself is not regarded as part of the launch vehicle

Lewis number. dimensionless parameter, the ratio of mass diffusivity to thermal diffusivity

liftoff. term designating the instant of vhicle flight at which vehicle contact with all holddown and support divices is terminated; also called "first motion" of the vehicle

limit load (or pressure). maximum expected load (or pressure) on a structure that will occur under the specified conditions of operation, with allowance for statistical variation

line (or duct). enclosed passageway (usually circular in cross section with relatively thin walls) that conveys fluid under pressure

linear characteristic. straight-line relation between valve flow and valving element stroke at a constant value of pressure drop

liner. 1. thin layer of adhesive specifically used to bond solid propellant to the motor case or to the insulation; 2. ablative material used to line the inner wall of the combustion chamber or nozzle to reduce heat transfer to the wall

liquid length. distance along chamber wall over which film coolant remains in liquid state

load factor. ratio of vehicle thrust to its overall mass

lockup. the no-flow condition when a pressure regulator is kept closed in response to downstream pressure being at or above the regulator setpoint

lockwire. 1. flexible slender rod or thread of material (usually metal) that is passed through matching holes in two (rotating) parts so as to fasten them together securely; 2. to fasten securely in place by means of a wire

lumped mass. concept in (shaft) dynamic analysis wherein a mass is treated as if it were concentrated at a point

-M-

Mach number. ratio of the velocity of fluid flow to the velocity of sound in the fluid

mainstage. attainment of 90 percent or more of the steady-state rated thrust level of a raocket engine

main valve. valve, usually located just upstream of the thrust chamber injector, that controls flow of propellant to injector

manifold. fluid-flow enclosure that distributes the flow in a desired manner from an inlet or inlets to an outlet or outlets

margin of safety. fraction by which the allowable load or stress exceeds the design load or stress

mass flux. mass flowrate through a given area expressed as the ratio of mass flowrate to flow area

mass ratio. 1. ratio of usable-propellant mass to vehicle total launch mass; 2. ratio of vehicle initial mass to vehicle final (burnout) mass

mass-transfer cooling. cooling technique characterized by an energy-comsuming expenditure of mass (solid, liquid, or gas)

method of characteristics. technique for facilitating the solution of a set of partial differential equations by the use of lines or surfaces that are at all points tangent to characteristic directions determined by certain specified linear combinations of the equations; method often is used in nozzle design

minimum length RAO nozzle. a RAO contoured nozzle which is as short as it can be before experiencing gas flow separation, i.e., the divergence angle all along the contour is at it maximum value without gas flow separation.

mission duty cycle. total propulsion system requirement for a scheduled number of operations over the total elapsed mission time

mixture ratio. mass flowrate of oxidizer divided by mass flowrate of fuel

monocoque. term appalied to a structure in which the stressed outer skin carries all or a major portion of the torsional and bending stresses

monopropellant. liquid propellant that decomposes exothermally to produce hot gas; e.g., hydrogen peroxide, and hydrazine

net positive suction head (NPSH). the difference, at the pump inlet, between the head due to total fluid pressure and the head due to propellant vapor pressure, expressed in feet of the propellant being pumped; this is the head available to suppress cavitation in the pump

nonequilibrium composition. exhaust gas chemical composition resulting from incomplete chemical reaction of the products of combustion in the exhaust gas

nonpositive-displacement pump. pump in which the fluid pressure is raised by alternately adding to and then diffusing the kinetic energy of the fluid; examples of this type of pump are the axial-flow,. Barske, centrifugal-flow, drag, Pitot, and Tesla

normally closed valve. powered valve that returns to a closed position on shutoff or on failure of the actuating energy or signal

normally open valve. powered valve that returns to an open position on shutoff or on failure of the actuating energy or signal

"normal" propellants. bipropellants that derive thermal energy primarily from oxidizer-fuel reactions; see "energetic" propellants

nozzle. 1. carefully shaped aft portion of the thrust chamber that controls the expansion of the exhaust products so that the thermal energy produced in the combustion chamber is efficiently converted into kinetic energy, thereby imparting thrust to the vehicle; 2. convergent passage in a pump or turbine that directs fluid into or leads it away from the impeller or turbine wheel

nozzle extension. nozzle structure that is added to the main nozzle in order to increase expansion area ratio or provide a change in nozzle construction

NPSH. net positive suction head

nucleate boiling. formation and breaking away of bubbles from active bubble sites (nuclei) on a submerged heated surface; the rising bubbles stir the liquid so that heat transfer from the surface to the liquid is much greater than that due to normal convection

Nusselt number. dimensionless parameter expressing the ratio of convective heat transfer to conductive heat transfer

O/F. ratio of mass flowrate of oxidizer to mass flowrate of fuel at the time of combustion

OFO triplet. an injector element consisting of three orifices; two oxidizer orifices which impinge on one fuel orifice.

oil canning. flexing of unsupported sheet metal

on-off. term referring to a system or device in which full-stroke actuation or deactuation occurs in response to input signals

open loop. term referring to an electrical or mechanical system in which the response of the output to the input is scheduled or preset; there is no feedback of the output for comparison and corrective adjustment

operating pressure. nominal pressure to which the fluid-system components are subjected under steady-state conditions in service operations

operational pressure transients. rises in operating pressure (due to water hammer, rapid startup, or shutdown) with sufficient duration to be felt as loads on the system or structure

oscillatory combustion. unstable combustion in the rocket engine or motor, characterized by pressure oscillations in either transverse or axial modes

outgassing. release of gas from a material when it is exposed to an ambient pressure lower than the vapor pressure of the gas; generallay refers to the gradual release of gas from enclosed surfaces when an enclosure is vacuum pumped

overexpansion. expansion of nozzle exhaust gas to a pressure lower than the ambient pressure

oxidizer. material whose main function is to supply oxygen or other oxidizing materials for deflagration of a solid propellant or combustion of a liquid fuel

payload penalty. extent to which the weight of a given component in any part of the vehicle decreases the weight allowable for the useful load (usually the spacecraft) that the vehicle carries

phase. solid, liquid, or gaseous homogeneous form existing as a distinct part of a heterogeneous system

pintle valve. flow-control device utilizing a translating tapered shaft (pintle) to change flow area through an orifice or flow passage

pitch. 1. angular motion of a vehicle about a lateral axis passing through its midpoint or center of gravity and perpendicular to the longitudinal axis; 2. distance between corresponding points on adjacent teeth of a gear or on adjacent blades on a turbine wheel, as measured along a prescribed arc, the pitchline

plastic deformation. permanent distortion of material under applied stress great enough to strain the material beyond its elastic limit; also called plastic flow, permanent strain, and permanent distortion

plug nozzle. annular nozzle that discharges exhaust gas with a radial inward component; a truncated aerospike

pneumatic. operated, moved, or effected by gas used to transmit energy

pogo. term for feed-system-coupled longitudinal oscillations of a rocket vehicle; named after motion of a pogo stick

poison. any material that interferes with catalytic action

polytropic gamma (γ_{poly}). the use of a polytropic gamma is a method by which heat transfer can be included in a gas expansion process. Its use requires empirical data or engineering estimates of the heat transfer environment under consideration.

popping. sudden, short-duration surges of pressure in a combustion chamber

Prandtl-Meyer angle. angle through which supersonic flow may turn during expansion in the nozzle

Prandtl number. dimensionless parameter expressing the ratio of momentum diffusivity to thermal diffusivity

preflight. occuring before vehicle liftoff

preload. the mechanical load appalied to components in an assembly at the time of assembly to ensure dimensional accuracy and proper operation; bolt or nut torque, and spring force, for example, are means for providing preload

prepressurization. sequence of operations that increases the ullage pressure to the desired level some time before the main sequence of propellant flow and engine firing; in launch vehicles, prepressurization occurs prior to liftoff

pressurant. gas that provides ullage pressure in a propellant tank

pressure fed. term for a propulsion system in which tank ullage pressure expels the propellants from the tanks and into the combustion chamber of the engine; cf. pump fed

pressure overshoot. maximum or relative-maximum point that occurs on the pressure-time curve, as in ullage pressurization or engine ignition

pressure ratio. 1. ratio of combustion chamber pressure to ambient pressure; 2. ratios of turbine inlet pressure to turbine outlet pressure

pressure recovery. conversion of velocity head to pressure head in a fluid system

pressure regulator. pressure control valve that varies the volumetric flow-rate through itself in response to a downstream pressure signal so as to maintain the downstream pressure nearly constant

pressurization system. the set of fluid-system components that provides and maintains a controlled gas pressure in the ullage space of space vehicle propellant tanks

proof pressure. pressure that a pressurized component must sustain and still function satisfactorily; proof pressure is the maximumn limit pressure multiplied by the proof-test safety factor and is the reference from which the pressure levels for acceptance testing are established

proof test. pressure test to prove the structural integrity of a component or assembly without exceeding allowable stresses or producing any permanent deformation

propellant. material carried in a rocket vehicle that releases energy during combustion and thus provides thrust to the vehicle

propulsion system. vehicle system that includes the engines, tanks, lines, and all associated equipment necessary to provide the propulsive force as specified for the vehicle

pump. machine for transferring mechanical energy from an external source to the fluid flowing through it, the increased energy being used to lift the fluid or increase the fluid pressure

pump fed. term for a propulsion system that incorporates a pump that delivers propellant to the combustion chamber at a pressure greater than the tank ullage pressure; cf. pressure fed

purge. gas flow used to clear a volume (e.g., a manifold) of propellant or combustion products

pyrolysis. chemical decomposition of a material by heat

race (or raceway). track or channel in a bearing in which the rolling elements ride

radiation cooling. cooling of a combustion chamber or nozzle in which heat loss by radiation balances heat gained from the combustion products, and the chamber or nozzle wall thereby operates in thermal equilibrium

ramping. opening or closing of a valve at a controlled rate to achieve a desired flow-vs-time relation

RAO nozzle. an optimum thrust nozzle contour which is mathematically derived through the calculus of variation

Rayleigh flow. steady frictionless flow in a constant area duct with heat being added or removed.

Rayleigh line loss. total pressure loss in combustor gases caused by heat addition at a Mach number greater than zero, i.e., the mechanism which results in a higher total pressure at the injector face than that of the chamber plenum and throat.

reaction. 1. term in pump and turbine design for the ratio of static headrise in the stage; 2. response of a vehicle to the thrust of the vehicle engines; 3. chemical activity between substances (e.g., propellant and contacting surfaces)

recovery temperature. see adiabatic wall temperature

redundant. incorporating multiple identical components to achieve increased reliability

redundant design. design in which more than one unit is available for the performance of a given function, so that failure of a unit will not cause failure of the system or abort the mission

regenerative cooling. cooling of the wall of a combustion chamber or nozzle by circulating a propellant, usually fuel, in coolant passages in or wrapped around the outer surface of the wall to be cooled

regression. erosion of the surface of a material

regression analysis. statistical technique based on the method of least squares for establishing a mathematical representation of empirical data

regulator. flow-control device that adjusts the pressure and controls the flow of fluid to meet the demands of a liquid-propellant rocket system

reliability. the probability that a system, subsystem, or component will perform its required functions under defined conditions at a designated time and for a specified operating period

relief valve. pressure-relieving device that opens automatically when a predetermined pressure is reached

repeatability. capability of a component or assembly to operate in the same way and in the same time each time it is actuated

repressurization. sequence of operations during vehicle flight that utilizes an on-board pressurant supply to restore the ullage pressure to the desired level after a burn period

response time. in a flow-control device, the interval from receipt of signal to completion of the commanded action, a total comprised of electrical delay plus pneumatic or hydraulic control system delay plus travel time for the movable element

retro rocket. small rocket engine used to produce a retarding thrust or force on the vehicle so as to reduce vehicle velocity

reverse-flow design. design of a gas generator that produces turbulent mixing and largely prevents hot streaking by forcing the flow to stagnate and then reverse its direction

reverse transition. change from a turbulent to a laminar boundary layer as a result of flow acceleration (laminarization)

Reynolds number. dimensionless parameter expressing the ratio of the inertial forces to the viscous forces in fluid flow

rise time. interval from first continuous chamber pressure increase to attainment of a specified level of thrust or pressure

rocket engine. the portion of the chemical propulsion system in which combustible materials (propellants) are supplied to a chamber and burned under specified conditions and the thermal energy is converted into kinetic energy, or thrust, to propel the vehicle to which the engine is attached. The term "rocket engine" usually is applied to a machine that burns liquid propellants and therefore requires rather complex systems of tanks, ducts, pumps, flow-control devices, etc.; the term "rocket motor" customarily is applied to a machine that burns solid propellants and therefore is relatively simple, requiring basically only the solid propellant grain within a case, an igniter, and a nozzle.

rocket motor. see rocket engine

root. juncture of blade and rotor hub or a vane and vane support

safe operating pressure. maximum operating pressure allowable without using shields to protect personnel and associated hardware

screech. high-frequencys oscillatory combustion, characterized by shrill noise emanating from the combustion chamber

sea-level engine. rocket engine designed to operate at sea level; i.e., the nozzle flows full at sea-level pressure

self-cooled. term appalied to a combustion chamber or nozzle in which wall temperature is controlled or limited by methods that do not involve flow within the wall of coolant supplied from an external source

self-pressurization. increase of ullage pressure by vaporization or boiloff of contained fluid without the aid of additional pressurant

sensible atmosphere. that part of an atmosphere that offers significant resistance to a body passing through it

sensitivity. measure of relative susceptibility of a propellant to deflagration or detonation under specified conditions

separated flow. flow detached from the wall of the flow passage

servovalve. modulating operator that amplifies a low-power control signal for variable-displacement, closed-loop control of actuator position

shaft. a bar (almost always cylindrical) used to support rotating pieces or to transmit power or motion by rotation

shroud. 1. short extension of the outer wall of a plug nozzle downstream of the throat; 2. continuous covering of the outer surfaces of an impeller or other rotative component

shutoff valve. valve that terminates the flow of fluid; usually a two-way valve that is either fully open or fully closed

sigma. term in statistics: the standard deviation from the mean

spacecraft. separable, self-contained, self-propelled vehicle designed to operate in space either in orbit about earth or in travel to and orbit about another heavenly body; generally is the final stage (useful payload) atop a launch vehicle

specific diameter. parameter in pump design used to relate pump physical size, head, flowrate, and performance

specific impulse. performance index for rocket propellants, equal to the thrust produced by propellant combustion divided by the mass flowrate

specific speed. parameter in pump design used to relate pump rotational speed, head, flowrate, and performance

squib. term for an electroexplosive device

stabilization device. see combustion stabilization device

stage. 1. a separable, self-contained, self-propelled section of a space vehicle; 2. a set of rotor blades and stator vanes in a turbine or an axial-flow pump, or one set of impeller and associated flow passages in a centrifugal-flow pump; 3. the degree of polymerization of a synthetic resin

staged combustion. rocket engine cycle in which propellants are partially burned in a preburner prior to being burned in the combustion chamber

staging. 1. separating a stage or set of stages from a spent stage of a launch vehicle; 2. incorporating two or more stages in a pump or turbine; 3. increasing the molecular weight of a resin without effecting a cure

stagnation. condition in which flowing fluid is brought to rest isentropically

stagnation point. point in a flow field about a body immersed in a flowing fluid at which the fluid particles have zero velocity with respect to the body

stagnation pressure. 1. pressure that a flowing fluid would attain if brought to rest isentropically; 2. pressure of a flowing fluid at a point of zero fluid velocity on a body around which the fluid flows

stagnation temperature. temperature that a flowing fluid would attain if the fluid were brought to rest isentropically from a given flow velocity (same as total temperature); for an ideal gas, the process need only be adiabatic

stay time. average length of time spent within the combustion chamber by each gas molecule or atom involved in the combustion process; also called residence time

steady state. condition of a physical system in which parameters of importance (fluid velocity, temperature, pressure, etc.) do not vary significantly with time; in particular, the condition or state of rocket engine operation in which mass, momentum, volume, and pressure of the combustion products in the thrust chamber do not vary significantly with time

stoichiometric combustion. the burning of fuel and oxidizer in precisely the right proportions required for complete reaction, with no excess of either reactant

streamline. line tangent to the velocity vector at each point in a flowfield; in steady flow, a streamline is the pathline of a fluid element

subcritical. a coined word denoting (1) operation of rotating machinery below a critical speed or (2) fluid maintained at pressures or temperatures below its corresponding critical point

sublimation. phase change of a substance directly from solid to gas (without apparent liquification)

submerged nozzle. nozzle configuration in which the nozzle entry, throat, and part or all of the nozzle exit cone are cantilevered into the combustion chamber

suction specific speed. index to pump suction performance relating rotational speed and flowrate to the minimum NPSH at which the pump will delivery specified performance

supercritical. coined word denoting (1) operation of rotating machinery above a critical speed or (2) fluid maintained at pressures or temperatures above its corresponding critical point

super-insulation. high-efficiency laminated-foil insulator used in low temperature applications; thermal conductivity is 1/10 to 1/150 that of common insulating materials

sustainer engine. auxiliary booster engine in a propulsion system that provides thrust after the main booster engines cease firing.

tank. pressure vessel containing propellant or pressurant to be used in a rocket vehicle fluid system

tank components. (1) devices for controlling the behavior of propellants (positioning devices, slosh and vortex suppression devices, baffles, standpipes, expulsion devices); (2) tank insulation

TCA (Thrust Chamber Assembly). the main engine components including the chamber, nozzle, valve, injector, and the hardware required to interface with the thrust mount

thermal cycling. exposure of a component to alternating levels of relatively high and low temperatures

thermal reactor. term for a monopropellant gas-generator design in which the combustion chamber does not contain a catalyst bed, and convection processes are depended on to promote the decomposition reactions

thermodynamic suppression head. an effect, due to a decrease in fluid vapor pressure and in fluid density, that acts to decrease the critical NPSH requirement of a turbopump

throat. portion of a convergent/divergent nozzsle at which cross-sectional area is minimal, the region of transition from subsonic to supersonic flow of exhaust gases

thrust. propulsive force developed by a rocket engine during firing

thrust barrel. structure in the rocket vehicle designed to accept the thrust load from two or more engines; also called thrust structure

thrust chamber. the assembly of injector, combustion chamber, and nozzle

thrust coefficient. ratio of engine thrust to the product of nozzle throat area times nozzle inlet pressure

thrust collector. structure attached to a rocket engine during testing to transmit the engine thrust to thrust-measuring instrument

thrust-time profile. plot of thrust vs time for the firing duration of a rocket engine

thrust-vector control. steering or guidance of vehicle by angular deflection of the rocket engine thrust vector; e.g., by gimballing the engine

total pressure. same as stagnation pressure

total temperature. same as stagnation temperature

transient. condition of a physical system in which parameters of importance (temperature, pressure, fluid velocity, etc.) vary significantly with time; in particular, condition or state of rocket engine operation in which the mass, momentumn, volume, and pressure of the combustion products within the thrust chamber vary significantly with time

transient period. interval from start or ignition to the time when steady-state conditions are reached

transpiration cooling. cooling of a porous inner wall of a combustion chamber or nozzle by flow of coolant fluid through the porous material; the fluid may be supplied from an external source or generated within the material (as in ablation)

tripple point. intersection of the solid/vapor, solid/liquid, and liquid/vapor lines in a phase diagram; at this point, solid, liquid, and vapor phases may coexist in equilibrium

triplet. injector orifice pattern consisting of one or more sets of three orifices that produce streams converging to a point; usually fuel is injected through outer orifices, and oxidizer is injected through the central orifice

tripping. see boundary-layer trip

tube-wall construction. use of parallel metal tubes that carry coolant to form the combustion chamber or nozzle wall

turbine. machine consisting of one or more bladed disks (rotor or turbine wheel) and one or more sets of fixed vanes (stator) inside a casing, so designed that the wheel is turned by incoming fluid (usually hot gas) striking the blades

turbine velocity ratio. ratio of pitchline velocity to isentropic spouting velocity, an index for classifying turbine type and for estimating performance

turbopump. an assembly consisting of one or more pumps driven by a hot-gas turbine

turbopump system. an assembly of components (e.g., propellant pumps, turbine(s), power source) designed to raise the pressure of the propellants received from the vehicle tanks and deliver them to the main thrust chamber at specified pressures and flowrates

turbulence ring. circumferential protuberance in the gas-side wall of a (gas generator) combustion chamber intended to generate turbulent flow and thereby enhance the mixing of burning gases

turbulent flow. fluid flow in which the velocity at a given point fluctuates randomly and irregularly in both magnitude and direction

turndown ratio. ratio of maximum to minimum controlled flowrates of a throttle valve

turning vane. see vane

TVC (Thrust Vector Control). the method by which the total vehicle thrust vector is directed, e.g., gimballing, liquid injection into the nozzle, fins, jet vane control, etc.

two-phase flow. simultaneous flow of gases and solid particles (e.g., condensed metal oxide), or of liquid and vapor

ullage. volume by which a container (tank) falls short of being full of liquid, the empty space being filled with gas

ullage pressure. pressure in the ullage space of a container, either supplied or self-generated

ultimate load (or pressure) load (or pressure) at which catastrophic failaure (general collapse or rupture) of a structure occurs

ultimate stress. stress at which a material fractures or becomes structurally unstable

underexpansion. expansion of the nozzle exhaust gas to a pressure higher than the ambient pressure

upper stage. the second or later self-propelled separable section in a rocket vehicle having two or more such sections

valve. mechanical device by which the flow of fluid may be started, stopped, or regulated by a movable part that opens, closes, or partially obstructs a passageway or port in a containing structure, the valve housing

vane. one of a set of slat-like objects rigidly fixed to a wall or other nonmoving part of a fluid system, each slat being carefully shaped, usually as an airfoil, so as to guide or direct the flow of fluid or create a special kind of flow

vehicle tank. tank that serves both as primary integral structure of a vehicle and as a container of pressurized propellants

velocity head. pressure (i.e., head) of a fluid due to speed of flow, i.e., the difference between total pressure and static pressure

vent-and-relief valve. specialized version of a relief valve wherein the assembly acts as an outlet for ullage vapor during filling of a tank and then performs as a relief valve during operation

vent valve. pressure-relieving shutoff valve that is operated on external command, as contrasted to a relief valve, which opens automatically when pressure reaches a given level

vernier engine. small rocket engine attached to a rocket vehicle to provide low thrust levels for precise control of velocity

virtual mass. mass of fluid near a moving body (e.g., a blade) that moves with the body and thereby increases the effective mass in motion

viscosity. fluid resistance to flow caused by internal molecular attraction

void. air bubble in a cured propellant grain or in rocket motor insulation

volumetric efficiency. measure of the desirability of a given design for an expulsion device: ratio of loaded liquid volume to internal tank volume

volute. spiral-shaped part of a pump casing that collects fluid from the impeller in a single channel of gradually increasing area

warmant passages. passages provided in cryogenic-valve hydraulic actuators to maintain actuator temperatures above specified operating minimums under extended hold conditions

water hammer. literally, the sound of concussion in a conduit when a flowing liquid is suddenly stopped; more generally, the pressure surge in the system that results from such stoppage

whirl. motion of a rotating shaft in a path or orbit about a longitudinal axis different from the axis of rotation; whirl may be forced or self-excited

yaw. angular motion of a vehicle about a vertical axis through its midpoint or center of gravity and perpendicular to the longitudinal axis

yield load. load that must be applied to a structure to cause a permanent deformation of a specified amount

yield stress. stress at which a material exhibits a permanent deformation, usually specified as 0.0020 inch per inch (0.2 percent)

zero-g. term appalied to a condition or state in which the force of gravity is absent